

Université Paris 13, Sorbonne Paris Cité

U.F.R d'Informatique

THÈSE

pour obtenir le grade de

DOCTEUR DE L'UNIVERSITÉ PARIS 13

Discipline : Informatique

présentée et soutenue publiquement

par

Stéphane Dartois

le 9 Octobre 2015

Titre

Random Tensor models: Combinatorics, Geometry, Quantum
Gravity and Integrability.

Directeur de Thèse

Adrian Tanasă

Jury

M. Kontsevitch Maxim, *Président*

M. Duplantier Bertrand, *Rapporteur*

M. Schaeffer Gilles, *Rapporteur*

M. Frederique Bassino, *Examineur*

M. Sportiello Andrea, *Examineur*

M. Rivasseau Vincent, *co-directeur*

M. Tanasă Adrian, *directeur*

LIPN, UMR CNRS 7030
Institut Galilée - Université Paris-Nord,
Sorbonne Paris Cité,
99, avenue Jean-Baptiste Clément
93430 Villetaneuse

Abstract

In this thesis manuscript we explore different facets of random tensor models. These models have been introduced to mimic the incredible successes of random matrix models in physics, mathematics and combinatorics. After giving a very short introduction to few aspects of random matrix models and recalling a physical motivation called Group Field Theory, we start exploring the world of random tensor models and its relation to geometry, quantum gravity and combinatorics. We first define these models in a natural way and discuss their geometry and combinatorics. After these first explorations we start generalizing random matrix methods to random tensors in order to describes the mathematical and physical properties of random tensor models, at least in some specific cases.

Résumé

Dans cette thèse nous explorons différentes facettes des modèles de tenseurs aléatoires. Les modèles de tenseurs aléatoires ont été introduits en physique dans le cadre de l'étude de la gravité quantique. En effet les modèles de matrices aléatoires, qui sont un cas particuliers de modèles de tenseurs, en sont une des origines. Ces modèles de matrices sont connus pour leur riche combinatoire et l'incroyable diversité de leurs propriétés qui les font toucher tous les domaines de l'analyse, la géométrie et des probabilités. De plus leur étude par les physiciens ont prouvé leur efficacité en ce qui concerne l'étude de la gravité quantique à deux dimensions.

Les modèles de tenseurs aléatoires incarnent une généralisation possible des modèles de matrices. Comme leurs cousins, les modèles de matrices, ils posent questions dans les domaines de la combinatoire (comment traiter les cartes combinatoires d dimensionnelles ?), de la géométrie (comment contrôler la géométrie des triangulations générées ?) et de la physique (quelle type d'espace-temps produisent-ils ? Quels sont leurs différentes phases ?). Cette thèse espère établir des pistes ainsi que des techniques d'études de ces modèles.

Dans une première partie nous donnons une vue d'ensemble des modèles de matrices. Puis, nous discutons la combinatoire des triangulations en dimensions supérieures ou égales à trois en nous concentrant sur le cas tri-dimensionnelle (lequel est plus simple à visualiser). Nous définissons ces modèles et étudions certaines de leurs propriétés à l'aide de techniques combinatoires permettant de traiter les cartes d dimensionnelles. Enfin nous nous concentrons sur la généralisation de techniques issues des modèles de matrices dans le cas d'une famille particulières de modèles de tenseurs aléatoires. Ceci culmine avec le dernier chapitre de la thèse donnant des résultats partiels concernant la généralisation de la récurrence topologique de Eynard et Orantin à cette famille de modèles de tenseurs.

To my parents

Remerciements

Cette thèse n'aurait pas été possible sans les nombreux scientifiques que j'ai pu croiser tout au long de mon parcours. Tous ont joué un rôle dans mon apprentissage et m'ont transmis les connaissances et l'enthousiasme nécessaires pour mon début dans les sciences. Aussi j'aimerais qu'ils reçoivent ma reconnaissance. Je pense à mes professeurs à l'université, qui sont trop nombreux pour être tous cités ici mais qui pour certains m'ont particulièrement marqué, parmi eux, Claude Aslangul, Dominique Mouhanna, Redha Mazighi et Sofian Teber. Mes directeurs de stages ont été tout aussi important, merci donc à Aurélien Perera, Raoul Santachiara et Vladimir Dotsenko. J'aimerais aussi remercier les étudiants qui ont croisé mon chemin pendant ces premières années et qui les ont rendues stimulantes intellectuellement (et bien marrantes !). Je pense entre autres à Arnaud, Stéphane et Yasar.

Adrian Tanasă et Vincent Rivasseau ont tous les deux été d'incroyables soutiens pendant ces trois ans. Ils m'ont permis de rentrer dans le monde de la recherche par la grande porte. Leur passion et curiosité pour la combinatoire, la physique autant que pour les mathématiques devrait être une source d'inspiration pour tout les étudiants qui les entourent. Leur indulgence aussi devant mes difficultés à me fixer sur un sujet et m'y tenir a permis que cette thèse se déroule sans encombre malgré ma (trop) forte tendance à m'éparpiller. Leur patience vis-à-vis de ma capacité à fuir tout problème administratif aussi longtemps que possible leur aura sûrement, aussi, été précieuse. Je leur suis reconnaissant pour m'avoir laissé cette chance de travailler dans ce groupe où ma curiosité n'a jamais manqué de matière à travailler. Merci à eux.

Ce groupe doit tout autant à ses autres membres, tous d'excellents et prolifiques scientifiques. J'ai beaucoup appris en travaillant avec eux, que ce soit lors d'un journal club, d'un séminaire, d'une discussion autour d'un café ou d'un projet commun. Dario avec qui j'ai partagé un bureau durant cette fin de thèse. Je pense à Razvan pour notre papier commun et son soutien pour mes recherches de post-docs. Je pense à Robin, la personne grâce à qui la théorie des catégories ne me fait plus vraiment peur, ou alors seulement dans le noir et sans veilleuse. Aussi car il a supporté mes questions de mathématiques sans broncher, que ce soit en algèbre, géométrie, topologie, analyse complexe (et j'en oublie sûrement), quitte parfois, à finir un peu (beaucoup) trop tard le soir. J'espère que nous

aurons l'occasion de (re-)travailler ensemble sur un projet qui fonctionne. Je pense enfin à Valentin pour nos tentatives de faire sortir l'intégrabilité de la forêt dans laquelle elle se cache. Pour son incroyable culture s'étendant de la combinatoire la plus pure aux affres de la gravité quantique, en passant par la physique statistique, la théorie des champs, les modèles de matrices et quantité d'autres sujets.

Je souhaite aussi remercier Bertrand Eynard et Gaëtan Borot. Le premier pour m'avoir introduit dans le monde de la récurrence topologique, ainsi que pour nos rendez-vous matinaux au LPT malgré son agenda surchargé, pour son cours à L'IPhT et pour son appui dans ma recherche de post-docs. Pour ça je lui dois toute ma reconnaissance. Le second pour avoir la patience de répondre à mes innombrables questions (pas toujours très futées) sur son travail. Je souhaiterais aussi citer Roland Van der Veen que j'ai rencontré à Vienne pour m'avoir aidé à comprendre les bases de la géométrie à trois dimensions. Je dois aussi le remercier pour m'avoir prêté ses compétences, nous permettant ainsi d'écrire un algorithme construisant des triangulations colorées idéales de compléments de noeuds, répondant ainsi à une question qui me taraudait. J'aimerais aussi remercier Gérard Duchamp, autant pour sa bonne humeur et sa sympathie que pour sa passion pour le violon.

Je me dois aussi de remercier tous les membres du jury qui me font l'honneur de relire cette thèse. Un remerciement particulier va à Bertrand Duplantier et Gilles Schaeffer qui ont eu la lourde tâche de rapporter ce manuscrit. Je voudrais aussi exprimer ma gratitude à Maxim Kontsevitch pour avoir accepté de présider ce jury, ainsi qu'à Andrea Sportiello et Frederique Bassino pour les, je n'en doute pas, nombreuses questions qui parsèmeront la soutenance (et qui ont parsemé l'avant soutenance).

Je souhaiterais aussi exprimer ma reconnaissance aux étudiants, et aux autres, qui ont traversé mon chemin pendant cette thèse et avec qui j'ai passé d'agréables moments autour de quelques verres et d'un pack de bière, d'une table et d'un bloc de papier, d'un tableau et d'une réserve de craie ou d'un saxophone et une boîte d'anches. Adrien, Etienne, Fabian, Harold, Hermès, Luca, Oliver, Rémi et Rémi, Sylvain, Tatiana, Thibault et Vincent.

Enfin, je voudrais remercier mes parents pour leur soutien indéfectible pendant mes toutes premières années et la suite. Et ce, quitte à me laisser mettre le feu (au sens propre) à la baraque, remplir ma chambre de piles au citron, démonter la moitié des appareils électroniques passant à ma portée ou encore remplir les pièces de livres sur les volcans et de journaux de vulgarisation sans discontinuer dès mes six ans. Ma (plus si) petite soeur aussi. Enfin à Pitinette, qui mérite bien un n -ième délire bien camouflé dans ces pages pour ces deux années Ionescquement absurdes - un type d'absurde bien plus rigolo que la version Kafkaïenne, tu me l'accorderas - et qui ne les a rendues que plus réelles. À toi de le trouver.

Tiens, il est neuf heures. Nous avons mangé de la soupe, du poisson, des pommes de terre au lard, de la salade anglaise. Les enfants ont bu de l'eau anglaise. Nous avons bien mangé, ce soir. C'est parce que nous habitons dans les environs de Londres et que notre nom est Smith.

La Cantatrice Chauve, Eugène Ionesco.

Contents

1	Introduction	12
2	Random Matrices	20
2.1	Introduction to matrix models	20
2.2	Combinatorial problems and matrix models	24
2.2.1	Formal matrix integrals and combinatorics of maps	24
2.2.2	Matrix models as formal power series	28
2.3	Quantum gravity	29
2.4	Intersection theory on the moduli spaces of curves	31
2.4.1	From counting triangulations to Riemann surfaces	31
2.5	Inspiration from matrix models.	36
3	Group Field Theories	37
3.1	Quantum gravity ideas	37
3.1.1	Connection variables for general relativity.	38
3.1.2	Topological BF theory	40
3.2	Group field theory as generating function for spinfoams	42
3.2.1	Implementing gauge symmetry	43
3.3	Concluding remarks	43
4	Tensor Models and Colored Triangulations	45
4.1	Solving geometrical ambiguities: the 3-dimensional case	45
4.1.1	Generating function of dual 2-skeleton.	47
4.2	Graph Encoded Manifold	49
4.2.1	Knot complements.	55
4.3	Random tensor models and colored GFT.	60
4.3.1	Random multi-tensor models.	60
4.3.2	Invariant random tensor model.	61
4.3.3	Comments.	66
4.4	More figures.	67

5	Single Scaling Limit of Tensor Models	69
5.1	1/ N expansion of multi-tensor models	69
5.1.1	Setting the 1/ N expansion	69
5.1.2	Next-to-leading order	72
5.2	Expansion of multi-orientable model	74
5.2.1	Definition of the model	74
5.2.2	Classification of Feynman graphs	76
5.2.3	Combinatorial and topological tools	77
5.2.4	1/ N expansion of m.o. i.i.d. model	81
5.2.5	Leading graphs	83
5.2.6	Next-to-leading order multi-orientable graphs.	88
5.3	Generic 1-tensor model.	89
5.4	Conclusion	90
6	Double Scaling Limit of Tensor Models	92
6.1	Double scaling of matrix models.	92
6.2	Double Scaling of melonic T^4 tensor model.	93
6.2.1	Graphs classification: Pruning and Grafting.	95
6.2.2	Reduction.	99
6.2.3	Cherry Trees	102
6.2.4	Reduced graphs amplitudes	104
6.2.5	Proof of Theorem 9: Bounds.	109
6.2.6	Computation of Cherry Trees	110
6.2.7	The Double Scaling Limit	110
6.3	Further results.	112
7	Matrix Model Representation of Tensor Models	113
7.1	Saddle point technique	113
7.1.1	T^4 melonic tensor models and intermediate field representation.	113
7.1.2	Leading Order 1/ N Computation.	115
7.2	Schwinger-Dyson Equations	117
7.3	Double Scaling revisited.	120
7.4	Bilinear identities	125
7.4.1	Orthogonality Relations	125
7.4.2	Decomposition of matrix models.	128
7.4.3	Decomposition of tensor models.	130
7.4.4	Deformation of Hirota equations.	132
7.5	Remarks.	133

8	Loop Equations for Tensor Models	136
8.1	Schwinger-Dyson equations of generic tensor model.	136
8.2	Loop equations for Hermitian matrix model and topological recursion. . . .	138
8.3	Loop equations for the T^4 model	141
8.3.1	Exact 'disc' and 'cylinder' equations.	141
8.3.2	First term of $1/N$ expansion.	144
8.3.3	Three-dimensional higher degree term	147
8.3.4	The six dimensional case	149
8.4	Remarks	152

Chapter 1

Introduction

This text is an introduction to some aspects of random tensor models. It is not an introduction in the sense that there is already much more advanced material that one could find in the literature. Rather, it is an introduction because the subject is young, and the study presented here raises much more questions than it brings answers. I hope that it opens a line (several lines!) of research for the random tensor models, their combinatorics, physics, and geometry.

Of course, the best way to introduce this text is probably to give some ideas about the problem that led to this embryonic theory. It is known as the problem of *Quantum Gravity*. Until now physicists are aware of four different forces that manifest in nature. They are able to give a satisfying enough description of all of them as long as they limit themselves to the phenomena they can experimentally produce.

Among these forces three of them are particularly well understood. These are the electromagnetic force, the weak force and the strong force. The electromagnetic force is the one that we experiment everyday. It is light, it is the magnet on the fridge, it is the motor in your car (electric or not), it is the cell phone communications and so on... Indeed, this is the force that can be tested with the greatest precision. The reason for which it is so well known is probably that one can observe it at almost any scales of length or energy, especially at human scale. For the other forces we do not have this chance. In fact the theory for it can be traced back to the XIXth century. The incredible work of Maxwell triggered a flood of conceptual progresses in physics as well as new mathematical studies. This work allowed to test the theory and was already quite well-suited in its form to the conceptual revolution later brought by Quantum Mechanics. The clear mathematical apparatus together with the possibility of experimenting this force in a wide range of physical situations is the reason why the theory can be tested up to an accuracy of order 10^{-9} . The two other forces were understood along the lines of what had been developed for the electromagnetic force. In all these three cases, the quantum behaviour of each one

of these forces is successfully described by using Quantum Field Theory (QFT) techniques. Roughly speaking, the physical objects are represented by collection of fields $\{\phi_a\}$ (scalar, vector and so on..) such that each field configuration is weighted by a complex number $e^{iS[\{\phi_a\}]}$ where S is the action of the theory and generally associates a real number to a given field configuration. One usually constructs the partition function (that mimics the configuration integral of probability theory) as the (not always well defined) functional integral of these weights over all field configurations. The partition function is then the generating function of correlation functions between field configurations [Kak93]. From this object one derives physical quantities that can be compared to actual experiments. The correlation functions are interpreted as the quantum amplitudes for the system to switch from one field configuration to another. The square of these quantum amplitudes is interpreted as the more sensible *probability* of switching from one configuration to the other.

The rules of the formalism being (roughly) explained, one has now to compute these amplitudes in order to compare with the experimental behaviour and validate or invalidate the theory. This is where amazing connections with mathematics arose. In his founding works, Richard Feynman was able to interpret the computation of these amplitudes in terms of the combinatorics of quantum events [Fey49, Fey50, Dys49]. This technique was, at that time, highly original and it took the work of Freeman Dyson [Dys49], to allow physicists to understand this technique in their usual mathematical framework. Richard Feynman was able to associate a graph to each event (or family of events) from which one could easily recover the mathematical expressions of the amplitudes from the so-called *Feynman Rules*. The partition function becomes the generating functional of these decorated weighted graphs. From these graphical techniques one can test almost all QFT produced nowadays by thousands of theoretical physicists. But one has to understand that it is not only a mathematical tool to compute amplitudes, it is also a strong guide for the intuition, as these diagrams have a physical interpretation.

Unfortunately there are drawbacks. In fact, the computation of these diagrams give access only to perturbative physics, and the Feynman rules can lead to ill-defined mathematical expressions. Physically it means that one should not only rely on Feynman graphs to understand the physics. One also have to put some more physical input to regularize the problematic expressions. This is done through the process of *renormalization*. Moreover we need to be careful with respect to convergence of the series of graphs. In fact, generically, one can only obtain asymptotic expressions that are valid up to a given order. And if we may prove that there really exists a well-defined function of the physical (renormalized) parameters, computing it explicitly in a non-asymptotic form is still a very big challenge. However, one points out that these problems are also a great source of new ideas in physics and mathematics as they provided the unification of the electromagnetic force and the weak force (by demanding that a renormalization process

exists [Gla61, GSW62, SW64, Wei67, Sal68]), and it gave rise to the combinatorial Connes-Kreimer algebra of renormalization [CK00].

Let us now consider the case of the fourth force, namely gravity. As for the electromagnetic force, one has a pretty good intuitive picture of it. This is due to the fact that it is the second force that shows up at human scale, but this is due to its additive character (no negative masses) and to our living on a big planet. Between object of our size gravity is actually very weak. The study of gravity also comes with its bunch of breakthroughs in physics. Any scientist thinks of the works of Isaac Newton. But one should also think to Le Verrier who was able to analyze the gravitational force in the solar system with enough care so to predict the existence of Neptune. At the philosophical level this has been a very strong argument for the deterministic thought. Then, of course, came the work of Albert Einstein [Ein14b, Ein14a, Ein15] which radically changed our vision of the world we live in. The space (and time) is not a fixed background anymore but becomes dynamical and interacts with its content. Despite the works of these great scientists, the weakness of gravity does not allow one to test it with great accuracy as is the case for the electromagnetic force. Also this weakness prevents gravitational effects to be big at small (length) scales that are experimentally accessible. So indeed one could argue that our current understanding of the physics of gravity is sufficient at the moment and one does not need to deepen its study. However, without dismissing some experimental facts that could contradict this point of view¹, one could argue that physics is not only made of models valid in a certain range, but is also a search for a complete and mathematically coherent description of the world. But if one sticks to this latest idea, one can find several problems in our understanding of gravity.

In fact, although it can be described in a way that is very similar to the other theories², the QFT techniques, at least when applied naively, appear to be failing. In this setting, the theory seems to be not (perturbatively) renormalizable, so that there is no (finite) renormalization scheme allowing to mathematically define the theory. Nevertheless, this may be due to the way one applies the QFT framework. In fact one is, in the naive approach, tempted to consider the flat space as a fixed background state of low energy on which one defines a field that is interpreted as a perturbation of this flat metric space allowing for curved geometry [Fey63]. However one can try to tackle the problems appearing in this framework. It is actually at the source of a lot of different approaches. Some of them are very ambitious, such as string theory, and aim at solving both the problem of quantizing gravity together with unifying it with the other interactions [Pol98]. Some of them restricts to the problem of defining the theory by finding the right renormalization scheme [tH02, Emo06]. But this may well be not sufficient as these kinds of theories keep

¹It may be the case that the problems of dark matter and dark energy are just a manifestation of our lack of understanding of gravity, even at large scales.

²*i.e.* as a $SO(3,1)$ gauge theory.

describing the quantum history of a field (even though this is a perturbation of the metric field) *on* space-time. Hence, alternative approaches are possible, as for examples the ones of Loop Quantum Gravity (LQG) [Rov07], which get rid of a “background” space-time. We can also try to deepen our understanding of quantum mechanics, as is done in Non-Commutative Geometry (NCG), which can be used to rewrite the standard model, or to define a new form of quantization of geometry [Con94, CC12]. But if one relies on the physical interpretation of QFT, one can also consider that a quantum theory of space-time³ should describe the quantum histories *of* space-time. Making connection to the combinatorial interpretation of QFT explained sooner one is tempted to think that quantum histories of space-time should be expressed in combinatorial terms [Riv14]. In this line of research, the generating series of the corresponding combinatorial objects should be interpreted as providing the partition function of the theory.

This is how connections with combinatorics, discrete geometry and probability theory show up. In fact one needs to encode geometry (in the sense of, at least a topological space-manifold? with some distance function), in a way that can be generated by a partition function. Considering the simple case of ribbon graphs, or maps [Sch98, Lan04]. They are graphs drawn on a surface. They provide a decomposition of surface in a way that can be encoded in a generating series. Moreover this generating series can be written as a partition function of a quantum⁴ system. This generating series has an integral representation which is interpreted as a field theory of matrices on a point space. It has a Feynman expansion, each graph representing a geometry. The associated Feynman rules give natural weights for the surfaces⁵, in a way that they can be interpreted as the probability for a given geometry to arise. Thus it provides in a natural way a theory of random two-dimensional geometry. In the continuum limit of this theory the most likely geometry is the one of the sphere \mathbb{S}^2 . It is physically sound that the emergent geometry is not a wild geometry of a surface with very big genus. Also one can cite works about the matrix representation of $c = 1$ Liouville theory [KW10]. This should connect to works in mathematics on random two dimensional geometry such as [Le 14, DMS14] which are expected to coincide in some sense with Liouville quantum gravity [Dup11, DMS14]. The mathematical study of objects such as the Brownian sphere of [Le 14] has been possible thanks to works of combinatorists deepening the study of two dimensional maps by bijective

³and thus of gravity.

⁴Actually statistical. There is a link between statistical field theory that is about statistical physics and quantum field theory which concerns quantum physics. This is technical but can be thought as an analytical continuation. Statistical field theory is really about probability theory on the phase space of the system, each state of the system being weighted by a positive number. On the other hand, quantum physics is a kind of ‘complex’, analytically continued, probability theory on the configuration space, each point of the configuration space being weighted by a complex number. This connection is a rich guide to understand quantum physics as it allows us to think in term of probability theory to get an intuition, although this has a lot of limitations.

⁵And these weights transcribe as discrete Einstein-Hilbert weights for the geometry of the surface.

means [Sch98]. These works allowed to encode planar combinatorial maps in terms of well-labelled trees. Since it is possible to construct a continuous random tree [Ald91, Ald93] by considering Dyck Brownian paths, it is possible to construct a Brownian planar map by considering both a Brownian Dyck path and a Brownian walk on the set of labels. Although this is a different approach to two dimensional random geometry it is expected to be equivalent to the matrix formulation [Dup11, DMS14, DE13]. Of course, the theory in two dimensions is not the theory we expect to apply in our world, but it has to be explored as a tractable example. Although one can find a lot of problems still unsolved (and probably very difficult to solve) for two dimensional geometry (random or not), we already learnt a lot from it and we should now try to also make the first steps toward random geometry in higher dimensions. A good question is how could we start exploring these random geometries in more than two dimensions? One can mention several approaches:

- Restricting to the three dimensional case we could apply what we learnt from two dimensional geometry. By considering Heegaard splitting we would be able to translate three dimensional geometry in term of two dimensional geometry. How could we define such a random geometry? Just pick, at random, a surface S of genus $g \geq 2$ (to avoid unstable cases), and glue the corresponding handlebodies with a random element of the mapping class group of the surface. This kind of approach has been started by Lubotzky, Maher and Wu [LMW14]. Of course, this is full of technical difficulties. One has to define probability on the mapping class group of any surface. Moreover one has to guess the right weights or probability distributions both on the set of surfaces and their mapping class groups. For instance it is not obvious and probably not true that uniform distributions on the mapping class groups will lead to three dimensional emergent gravity. This approach is for instance useful to prove existence theorems. Indeed, if one can build a specific class of objects and a measure on a larger set such that the specific class has strictly positive measure, this proves that the specific class is not empty. This mimics somehow the Cantor argument, in which Cantor proved that transcendental numbers exist by proving that almost all real numbers are transcendental, without being able to show any of them in particular.
- One could also in $3d$ define random knots. For instance in the Petaluma model a knot K is represented as a petal diagram (so to say a graph with one vertex and a certain number of loops, called petals), together with a permutation that encodes how the edges under- and over-cross at the only vertex. Then by randomly picking a petal (by choosing randomly a number of loops) and a permutation on the edges, one obtains a random knot [EHLN14]. After that one could consider constructing the induced random 3-manifolds as being the associated complements of random knots. This has the advantage that we can probably set up a canonical geometry in the generic case, as in fact most knots are hyperbolic and by Mostow theorem there is a unique geometry over hyperbolic knots complements. We then could go a bit further

by defining a random Dehn filling over these complements by picking at random a rational number. However, this is again a very tough subject and connection to gravity is not *a priori* obvious.

- Another tries to extend the set up of matrix models and their connection to both physics and random geometry. This is the approach of random tensor models, which we develop in this thesis. One writes a generating series for triangulations of (pseudo)-manifolds. It is doable in any dimension, at least as long as one restricts to specific classes of triangulations. Moreover, the link to gravity seems more natural as the weights of the random triangulations are not uniform but correspond to an equilateral discretization à la Regge of the Einstein-Hilbert action for gravity on the triangulated (pseudo)-manifold. Indeed the curvature is encoded in the counting of $(d - 2)$ -simplices of the triangulation. This counting can be encoded in the generating series. The cosmological constant term is encoded in the counting of d -simplices. Finally, the diffeomorphism groups volumes collapse to the cardinals of the automorphism groups of the generated triangulations. Therefore all the basic physical ingredients seem to be there in this approach. However the mathematical tools have to be further developed. The starting point is the existence of $1/N$ expansions for tensor models [Gur11b, Gur12a]. However they are not yet geometrically interpretable as easily as the ones of matrix models (for which the $1/N$ expansion is a topological expansion). Hence there are several tracks one could follow. First one should try to interpret the $1/N$ expansion as leading to a new kind of classification of manifolds. But one could also try to extend ideas on combinatorial maps, and understand higher dimensional triangulations by bijective means in such a way as to explore the metric properties of the corresponding random geometry.

In this thesis, we explore the generalization of ideas and structures relevant for matrix models to random tensor models. It is structured as follows,

- Chapter 2 describes matrix models seen as combinatorial objects and physical theories. We also relate some of their uses in mathematics as generating series of intersection numbers of moduli spaces using Strebel graphs. This is again a striking example of the connection between gravity, combinatorics and matrix models as this corresponds to *topological* $2d$ gravity. This chapter motivates the study. In this philosophy matrix models should be seen as a source of ideas for tensor models.
- Chapter 3 shortly discusses another motivation for a study of random tensor models. This concerns spin networks and group field theories that appear naturally in some quantization schemes of gravity. Random tensor models can be seen as toy models of these theories. They have similar combinatorics, but the weighting of graphs used in tensor models is simpler.

- In Chapter 4, we evoke the problem of constructing generating series of triangulations in three and more dimensions. Building integral representations of these series for general triangulations is actually a difficult and very interesting problem, and it is not done in this thesis. Nevertheless it motivates the introduction of colored triangulations as a subset of triangulations that is tractable. We also write an algorithm allowing to construct colored triangulations of knot complements with ideal boundary. It can be used to understand the topology of Feynman graphs contributing to the computation of genus 1 observables.
- Chapter 5 describes the $1/N$ expansion of tensor models. First we explain the colored tensor models setting. Then we relate our contribution to the construction of the $1/N$ expansion of $3d$ tensor models with a richer combinatorics called *multi-orientable* models. These models generate Eulerian 3-maps, these are 2-cells complexes which are not just maps (since they are not cell decomposition of surface), but rather dual 2-skeletons of triangulations. The motivation for this study is the fact that Einstein-Hilbert gravity weights, when computed on a triangulation, depend only on the dual 2-skeleton of the triangulation. We also compute the leading terms in this formalism, and the first sub-dominant term in both colored and multi-orientable models. In particular, we compute the generating series of degree 0 and 1 (or $1/2$ for the multi-orientable model) edge rooted Feynman graphs.
- In chapter 6, we introduce the concept of double scaling. It is concisely introduced for matrix models, and then extensively described for the simplest interacting tensor model (the so-called quadratic melonic model). The double scaling limit of the two points function in dimensions $d = 3, 4, 5$ is derived explicitly, and the contributions of the remaining terms are bounded. This work established the existence of a singular dimension $d = 6$ at which the double scaling limit series is not summable⁶. See also [GS13] for the study of a different model which reached the same conclusions.
- Chapter 7 focuses on the intermediate field representation of the quartic melonic tensor models. This representation allows one to represent the corresponding generating series as multi-matrix integrals rather than a tensor integral. This is useful as it allows us to understand a tensor model by using methods of matrix integration. In this way we compute the saddle point approximation and derive the Schwinger-Dyson equations. We then notice that the melonic phase can be resumed by performing a translation in the matrix variables. Thanks to an idea of Razvan Gurau that I found beautiful, I describe how this allows a new interpretation of the combinatorial techniques introduced in chap. 6. Moreover I take advantage of this representation to derive bilinear identities for these quartic melonic models by using Givental-like decompositions but with a more general Givental operator. These equations are reminiscent of the integrable bilinear Hirota's equations satisfied by matrix models.

⁶It might be Borel summable, but we do not settle this question.

- In Chapter 8 the Schwinger-Dyson equations of a generic 1-tensor model are written and rephrased as the action of a differential operator on the partition function. This is used later to argue that these constraints should lead to several sets of loop equation of the Witt type. Then I explore the loop equations of the quartic melonic tensor model in order to investigate the possibility of extending the *topological recursion* methods to this special case. Although this is not well understood yet, this is one of my two main current interests⁷.

To end this introduction, let us precise some general ideas that you may (or may not find) in this thesis. First, one has to be aware that no definitive theory of quantum gravity in any dimension (even in two!) has yet been fully completed. I prefer to warn the potential adventurous and optimistic reader who would go through this thesis with some hope to find such a definitive theory. But to paraphrase John Baez, this adventurous reader can probably consider this missing theory just as an exercise left for him. Also, how our thesis related to current modern geometry, and in particular to three dimensional geometry, is not clear yet. Nevertheless our recent work (not reviewed in the thesis) indicates that the degree that governs the tensor $1/N$ expansion, although not a topological invariant, can be used to sort out manifolds. It measures some kind of complexity of the geometry, and is very similar (although not identical) to the complexity defined by Matveev in [Mat90].

The bilinear identities derived in Chap. 7 state the question of the integrability properties of, at least, the quartic melonic tensor models. In this line of thought, loop equations and topological recursion techniques should be explored. In fact the topological recursion sets up a lot of structural properties and may allow one to derive explicit connection with problems of algebraic and enumerative geometry.

So to reassure our adventurous reader and maybe compensate a bit for its disappointment, even if tensor models may not be the definitive theory of quantum gravity, they are certainly the source of new mathematical ideas⁸.

⁷with the use of the degree as a filtrating quantity of the set of 3-manifolds and a measure of the complexity.

⁸as it is the case for most contemporary theoretical physics.

Chapter 2

Random Matrices

In this chapter I give a review of matrix models. I especially focus on their applications to $2d$ Quantum Gravity and their combinatorics. A list of references for this chapter is [DFGZJ95, Di 04, LM04, Eyn15b, Zvo97].

The motivation for this presentation is twofold. First, the matrix models are an incarnation of quantum gravity in $2d$ and tensor models can be viewed as their natural generalizations. Secondly, they contain a lot of structures and are at the source of a lot of progresses in mathematics, condensed matter, nuclear physics, statistics and combinatorics. Consequently they should be a source of inspiration for the study of random tensor models. After a generic presentation, I focus on their applications to quantum gravity.

2.1 Introduction to matrix models

Random matrices appear first in physics in the work of Wigner. At that time physicists investigate the rules of nuclear physics by studying the diffusion of a neutron by a nucleus. In these experiments, they discovered there are some resonance values for the energy ϵ_n of the neutron. This is very similar to the diffusion experiment of light by a photon, for certain values of the energy of the photon, it is absorbed and then re-emitted by the electronic cloud of the atom. This can be very well understood in the quantum mechanical description of the atom. So, it is tempting to try to reiterate this success in the case of diffusion of neutrons by the nucleus. Unfortunately, as long as the energy ϵ of the neutron is high enough and the nucleus heavy, the interaction is a very complicated multi-body interaction which is dictated by a large number of variables. It is then impossible to think about giving a complete description of the interaction in term of a quantum Hamiltonian and to solve exactly the associated eigenvalues problem (or at least with accurate enough and well controlled approximations).

Nevertheless, one notices that the situation is clearly analogous to the one of classical

statistical physics. The ideas of Boltzmann were introduced in order to study classical systems with large number of degrees of freedom which were intractable using the methods of classical mechanics. Typically, one considers a system of a large number M of particles whose state is given by a set of M positions and M velocities. Boltzmann then proposed to abandon the classical deterministic viewpoint. In his approach, one assigns a probability $\mathcal{P}(x_i, v_i)$ for the particle i to be in a given state with, say, position and velocity (x_i, v_i) . For the sake of completeness, let us mention that the probability measure is the Boltzmann-Gibbs measure.

The idea was to extend this technique not just to hadrons themselves but to the parameters of the interaction. In fact one can think that if the interactions between the neutron that undergoes diffusion and the hadrons of the nucleus are too complex to be described exactly one can hope that statistically the average interaction can be understood. One can think that there is a most probable "shape" for the interaction and a distribution around this shape. Wigner introduced random matrices in order to quantitatively implement the preceding remark *i.e.* to give a model of a random Hamiltonian. The initial physical problem is thus transformed into the one of finding the distribution of eigenvalues and eigenvectors of a random matrix. However, the matrix has to satisfy some constraints. For example, the Hamiltonian should be Hermitian (as long as one forgets about the finite lifetime of a nuclear energy level). So the random matrices under consideration should be Hermitian as well. The symmetries of the problem can give more and/or different constraints on the random matrices under consideration.

This method is in fact very similar to the ideas behind the birth of statistical physics. In this latter case the system is also too complicated due to a large number of degrees of freedom. One is led to abandon the purely deterministic view. Boltzmann associated a probability measure that gives a probability for each state of the system and then described statistical quantities that can be measured by experimentalists (as the pressure, the temperature...). This is actually a very fruitful approach that revealed the universal behaviour of several classes of systems. Universality means that if one does not change too much the details of the interactions between microscopic degrees of freedom one obtains the same average behaviour of the whole system in the thermodynamic limit.

In the work of Wigner, the behaviour of large size random matrices depends only on the symmetries of the ensemble of random matrices one considers. One has to implement several constraints in order to construct the needed probability measures on the matrices. This is done by setting the following conditions [LM04]:

- Statistical independence: the matrix entries should be independent. For a matrix M of size N

$$\mathcal{P}(M) = \prod_{i,j=1}^N P_{ij}(M_{ij}). \quad (2.1)$$

2.1. INTRODUCTION TO MATRIX MODELS

- Invariance under change of basis. It is indeed a matrix probability law, so it should depend on the linear map represented by the matrix, not just on the array of numbers. For $Q \in GL(N, \mathbb{K})$,

$$\mathcal{P}(QMQ^{-1}) = \mathcal{P}(M). \quad (2.2)$$

\mathbb{K} is a number field. In physical situations $\mathbb{K} = \mathbb{R}$ or \mathbb{C} . This second condition tells us a lot about the form of the probability distribution. In fact a lemma due to Weyl [LM04] states that all the invariants of a matrix of size N can be expressed in term of the traces of the first N powers of the matrix M . Moreover it can be shown that the postulate of statistical independence with the invariance condition implies that \mathcal{P} depends only on the traces of the two first powers of M . If one considers a probability distribution that depends on higher powers of M then the entries of the matrix are no longer statistically independent and thus become correlated.

However, one has to realize that the condition of statistical independence is reminiscent of the application to nuclear physics problems. In fact in this case one considers a system that is governed by a very large number of interactions. We are concerned only by quantities that appear at a statistical level minimizing the information about the system contained in the probability distribution. The postulate of statistical independence is then a way to take into account this constraint. Finally, one notices that this assumption can be derived from information theory. Consider the space of all the probability distributions. The one that minimizes the information functional $I(\mathcal{P}) = - \int dM \log[\mathcal{P}(M)]\mathcal{P}(M)$ satisfy the statistical independence property. In the quantum gravity context for example, there is no reason to impose such a condition and the set of possible probability measures is then much richer.

We now derive the Wigner law for the Gaussian unitary ensemble [LM04]. The partition function of this ensemble is given by

$$Z = \int_{H_N} dM e^{-\frac{N}{2} \text{tr}(M^2)}, \quad (2.3)$$

H_N being the space of $N \times N$ Hermitian matrices. The measure

$$dM = \frac{1}{2^N} (N/\pi)^{N^2/2} \prod_{i=1}^N dM_{ii} \prod_{i < j} d\mathcal{R}M_{ij} d\mathcal{I}M_{ij} \quad (2.4)$$

is such that $Z = 1$ for the Gaussian distribution. One needs to compute the distribution of eigenvalues λ_n , $\rho(x) = \frac{1}{N} \sum_n \langle \delta(x - \lambda_n) \rangle$ with respect to the distribution in the limit $N \rightarrow \infty$ of a large size matrix. To this aim we first re-express Z in eigenvalues variables. This is done by using the following trick: M is a Hermitian matrix and consequently can be

2.1. INTRODUCTION TO MATRIX MODELS

diagonalized by a unitary transformation, *i.e.*, $M = UDU^\dagger$, where D is a diagonal matrix with real eigenvalues $\lambda_1, \dots, \lambda_N$. One then has,

$$\begin{aligned} dM &= d(UDU^\dagger) = dUDU^\dagger + UdDU^\dagger + UDDU^\dagger \\ &= [dUU^\dagger, UDU^\dagger] + UdDU^\dagger. \end{aligned} \quad (2.5)$$

Acting with U^\dagger, U on the measure dM , one has:

$$(U^\dagger dMU)_{ij} = dU_{ij}(\lambda_i - \lambda_j) + \delta_{ij}\lambda. \quad (2.6)$$

Computing the Jacobian J ,

$$J = \left| \frac{\partial M}{\partial U_{ij}} \frac{\partial U_{ij}}{\partial \lambda_j} \right| = \prod_{i < j} (\lambda_i - \lambda_j)^2. \quad (2.7)$$

Then, we get,

$$Z = \frac{\text{Vol}(U(N))}{|\text{Weyl}(U(N))|} \int_{\mathbb{R}^N} \prod_{i=1}^n d\lambda_i \prod_{p < q} (\lambda_p - \lambda_q)^2 \exp\left(-\frac{N}{2} \sum_{j=1}^N \lambda_j^2\right), \quad (2.8)$$

where $|\text{Weyl}(U(N))|$ is the cardinal of the Weyl group of $U(N)$. It is equal to $N!$. Dropping this constant factor, we obtain by definition:

$$Z = \int_{\mathbb{R}^N} \prod_{i=1}^n d\lambda_i e^{-N^2 S(\{\lambda_i\})}. \quad (2.9)$$

One can evaluate this integral by the saddle point technique. We shall not here perform the derivation in full mathematical rigor but this can be done with consequent additional effort, see for instance [Dis03]. Minimizing S with respect to λ_j one gets:

$$0 = \partial_{\lambda_j} S(\{\lambda_i\}) = \frac{\lambda_j}{N} - \frac{1}{N^2} \sum_{i \neq j} \frac{1}{\lambda_j - \lambda_i}. \quad (2.10)$$

Let us introduce the resolvent $W(x) = \frac{1}{N} \sum_{i=1}^N \frac{1}{x - \lambda_i}$. We have the well known relation

$$W(x)^2 = \frac{1}{N^2} \sum_{k,j | k \neq j} \left(\frac{1}{x - \lambda_k} - \frac{1}{x - \lambda_j} \right) \frac{1}{\lambda_k - \lambda_j} - \frac{1}{N} \partial_x W(x). \quad (2.11)$$

Thus using (2.10) it reduces to:

$$W(x)^2 = \frac{2}{N} \sum_k \frac{\lambda_k}{x - \lambda_k} - \frac{1}{N} \partial_x W(x) \quad \Leftrightarrow \quad W(x)^2 = 2xW(x) - 2 - \frac{1}{N} \partial_x W(x). \quad (2.12)$$

2.1. INTRODUCTION TO MATRIX MODELS

When the size N of the matrix becomes large, it reduces to a second order polynomial in W . The solutions writes:

$$W_{\pm} = x \pm \sqrt{x^2 - 2}. \quad (2.13)$$

The resolvent $W(x)$ is the Stieljes transform of the eigenvalue density (see [LM04,Eyn15b]), so one has

$$\rho(x) = -\frac{1}{2i\pi}(W(x+i0) - W(x-i0)), \quad (2.14)$$

hence

$$\rho(x) = \frac{1}{\pi}\sqrt{x^2 - 2}. \quad (2.15)$$

This corresponds to a semi-circle on the upper half-plane. The eigenvalues distribute along this semi-circle. In Wigner original context this semi-circle corresponds to the distribution of resonant energy of the diffused neutron.

2.2 Combinatorial problems and matrix models

This section explain several points. Some of these results are well exposed (especially for combinatorists) in [Zvo97]. Also relevant here are the combinatorial interpretation of Gaussian models [Eyn15b, Pen88, Zvo97], maps counting [IZ80, Zvo97], and links counting [ZZ99, SZ03].

2.2.1 Formal matrix integrals and combinatorics of maps

In this subsection we introduce Feynman graphs. We introduce them step-by-step by considering the following baby problem. We want to compute the integral:

$$I(\lambda) = \int_{-\infty}^{+\infty} \frac{d\phi}{\sqrt{2\pi}} e^{-\frac{1}{2}\phi^2 + \frac{\lambda}{4}\phi^4}, \quad \lambda \in \mathbb{R}_-. \quad (2.16)$$

This integral cannot be computed naively. Still, it is possible to compute it perturbatively in λ . In fact we can factorize the ϕ^2 and the ϕ^4 terms and then expand the second term with respect to λ , this leads to

$$I(\lambda) = \int_{-\infty}^{+\infty} \frac{d\phi}{\sqrt{2\pi}} \sum_{n \geq 0} \frac{\lambda^n}{4^n n!} \phi^{4n} \exp(-\frac{1}{2}\phi^2). \quad (2.17)$$

Exchanging (illegally)¹ the order of the sum and the integral, one can compute the sum term by term using the Gamma function $\Gamma(z) = \int_0^{+\infty} dt \, t^{z-1} e^{-t}$ after a change of variable

¹In fact $\lambda = 0$, around which we made the expansion, is a singular point for this integral as it converges for $\lambda \geq 0$ and diverges for $\lambda < 0$.

2.2. COMBINATORIAL PROBLEMS AND MATRIX MODELS

$\frac{1}{2}\phi^2 \rightarrow t > 0$. Thanks to the property $\Gamma(n + 1/2) = \sqrt{\pi} \frac{(2n-1)!!}{2^n}$,

$$\begin{aligned} I_{asymptotic}(\lambda) &= \sum_{n \geq 0} \frac{\lambda^n}{\sqrt{\pi} n!} \Gamma(2n + \frac{1}{2}) \\ &= \sum_{n \geq 0} \frac{\lambda^n}{n! 4^{2n}} (4n - 1)!! \end{aligned} \quad (2.18)$$

This leads to an asymptotic expansion in λ . However this method of computation misses an important point, namely the combinatorial interpretation of the result. In fact the coefficients of the expansion are related to the number of 4-valent graphs².

Indeed it is possible to compute this integral using Wick's theorem, which computes moments of Gaussian integrals. It states the following:

Theorem 1. *The moments of a Gaussian integral $\langle \phi^{2p} \rangle = \int \frac{d\phi}{\sqrt{2\pi}} \phi^{2p} e^{-\frac{1}{2}\phi^2}$ are given by the number of pairings of the labelled variables ϕ_1, \dots, ϕ_{2p} . This number is*

$$\sharp \text{ pairings} = (2p - 1)!! \quad (2.19)$$

Hence we recover (2.18). But one can index pairings with graphs. Each ϕ^4 is represented as a vertex with labelled half-edges going out of it. This labelling represents the labelling of variables of Wick's theorem. For each pairing of a variable ϕ_j with a variable ϕ_k we match the half-edge j with the half-edge k in order to draw a line of the graph.

After this presentation we introduce the problem of computing perturbatively a matrix integral. Consider the Hermitian matrix integral:

$$Z[t_4] = \int_{H_N} dM \exp\left(-\frac{N}{2} \text{Tr}(M^2) + N \frac{t_4}{4} \text{Tr}(M^4)\right). \quad (2.20)$$

Again this integral should converge at least for $t_4 \in \mathbb{R}_-$. However, we discard the problem of convergence for the moment. Expanding with respect to t_4 :

$$\begin{aligned} Z[t_4] &= \sum_{q \geq 0} N^q \frac{t_4^q}{4^q} \int_{H_N} \text{Tr}(M^4)^q \exp\left(-\frac{N}{2} \text{Tr}(M^2)\right) \\ &= \sum_{q \geq 0} N^q \frac{t_4^q}{4^q} \int_{H_N} \left(\sum_{ijkl} M_{ij} M_{jk} M_{kl} M_{li}\right)^q \exp\left(-\frac{N}{2} \text{Tr}(M^2)\right) \\ &= \sum_{q \geq 0} N^q \frac{t_4^q}{4^q} \langle \text{Tr}(M^4)^q \rangle. \end{aligned} \quad (2.21)$$

²We consider here graphs with loop and multiple edges.

2.2. COMBINATORIAL PROBLEMS AND MATRIX MODELS

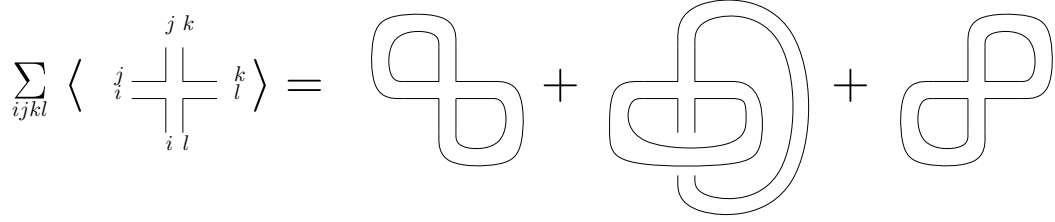


Figure 2.1: Feynman graphs that contribute to the Gaussian expectation value $\langle \text{Tr}(M^4) \rangle$. The leftmost one has three faces, the one at the center has only one face, while the rightmost one has also three faces.

The integrals over H_N are moments of Gaussianly distributed matrix variables. These moments can be computed by Wick's theorem. We compute a simple example of such moments in order to make clearer the rules for computing these integrals. Consider,

$$\begin{aligned}
 \langle \text{Tr}(M^4) \rangle &= \sum_{ijkl} \langle M_{ij} M_{jk} M_{kl} M_{li} \rangle \\
 &= \sum_{ijkl} \langle M_{ij} M_{jk} \rangle \langle M_{kl} M_{li} \rangle + \sum_{ijkl} \langle M_{ij} M_{kl} \rangle \langle M_{jk} M_{li} \rangle \\
 &\quad + \sum_{ijkl} \langle M_{ij} M_{li} \rangle \langle M_{kl} M_{jk} \rangle
 \end{aligned} \tag{2.22}$$

obtained by pairing the random variables. From trivial Gaussian integration we have $\langle M_{ab} M_{cd} \rangle = \left((N \text{Tr}(\cdot))^{-1} \right)_{ab,cd} = \frac{1}{N} \delta_{ad} \delta_{bc}$. Thus, one has,

$$\begin{aligned}
 \langle \text{Tr}(M^4) \rangle &= \frac{1}{N^2} \left(\sum_{ijkl} \delta_{ik} \delta_{jj} \delta_{ki} \delta_{ll} + \sum_{ijkl} \delta_{il} \delta_{jl} \delta_{ji} \delta_{kl} \right. \\
 &\quad \left. + \sum_{ijkl} \delta_{ii} \delta_{jl} \delta_{kk} \delta_{lj} \right) \\
 &= \frac{1}{N^2} (N^3 + N + N^3).
 \end{aligned} \tag{2.23}$$

Again one can index each pairing by a graph. But this time it has double lines in order to keep track of the indices. These graphs are called ribbon graphs. They are dual to quadrangulations of surfaces. One notices an important feature. The weight of the graphs depends on the number of closed circuits. In fact, a factor N comes for each vertex of the graph, a factor $1/N$ comes for each edges and one factor of N comes for each closed circuit (also called faces). In the case we have computed, Fig. 2.1 shows the relevant graphs. That way the power of N associated to a graph is $N^{\#v - \#e + \#f}$. From the relationship to the dual triangulation with V vertices, E edges, F faces we have:

2.2. COMBINATORIAL PROBLEMS AND MATRIX MODELS

- $\sharp v = F$
- $\sharp e = E$
- $\sharp f = V$.

Then $\sharp v - \sharp e + \sharp f = V - E + F = \chi(g) = 2 - 2g$, where $\chi(g)$ and g are respectively the Euler characteristic and the genus of the triangulated surface. Finally,

$$Z[t_4] = \exp(-F) \quad (2.24)$$

$$F[t_4] = \sum_{\mathcal{G} \text{ 4-valent ribbon graphs}} \frac{1}{|Aut(\mathcal{G})|} N^{-\chi(\mathcal{G})} t_4^{\sharp v(\mathcal{G})}. \quad (2.25)$$

Then $F[t_4]$ is the generating function of ribbon graphs of constant valency 4, with t_4 as counting variable for the vertices. Moreover the factor N is a counting variable for the Euler characteristic of the ribbon graphs. Then, with notations derived from combinatorics, we have:

$$\mathbb{T}_{n,g}^4 = \sharp\{\text{Ribbon graphs with } n \text{ vertices and genus } g\} = [N^{2-2g}][t_4^n]F[t_4]. \quad (2.26)$$

To be more specific ribbon graphs are two dimensional combinatorial maps (also called 2-maps). They are defined in the following way,

Definition 1. A 2-map is a triple (H, σ, α) or equivalently (H, σ, ϕ) ,

- H is a set of half-edges (also called “dart”)
- σ is a permutation on H
- α is an involution on H without fixed point
- $\phi = \sigma \circ \alpha$.

This corresponds to the previous figure. Each edge of the ribbon graph (2-map) is cut into two half-edges. The permutation σ defines the *oriented* vertices of the ribbon graph through its cycles while α matches the half-edges to form edges. Finally the cycle of ϕ defines the faces of the ribbon graph. This can be generalized to n -dimensional map (n -maps for short) by using a n -uplet of permutations. n -maps are also called stranded graphs in the tensor models and group field theories literature³.

³Actually, the general stranded graphs such as the m.o. graphs -seen later in this thesis- or even more general ones appearing in the early tensor models literature are only a weak form of n -maps, but these are subtleties...

2.2. COMBINATORIAL PROBLEMS AND MATRIX MODELS

2.2.2 Matrix models as formal power series

Given a field \mathbb{K} we can define:

Definition 2. *The set of formal power series over \mathbb{K} in r variables $\{X_1, \dots, X_r\}$, is the set $\mathbb{K}[[X_1, \dots, X_r]]$ of all sums whose coefficients are indexed by monomials X^α such that:*

$$\left(\sum_{\alpha} b_{\alpha} X^{\alpha}\right) + \left(\sum_{\alpha} c_{\alpha} X^{\alpha}\right) = \sum_{\alpha} (b_{\alpha} + c_{\alpha}) X^{\alpha}, \quad (2.27)$$

and

$$\left(\sum_{\alpha} b_{\alpha} X^{\alpha}\right) \cdot \left(\sum_{\beta} c_{\beta} X^{\beta}\right) = \sum_{\alpha, \beta} b_{\alpha} c_{\beta} X^{\alpha+\beta}. \quad (2.28)$$

Notice that one needs a magma structure on the set of index of monomials to define these operations.

The variables X_r 's here are not evaluated to some value as in fact in general the sums do not converge. We call these variables as before *i.e. counting variables*.

Matrix models in the sense described in the preceding subsection are formal series [Eyn15b, Eyn06]. For instance $\frac{1}{N^2} F[t_4] \in \mathbb{C}[[t_4]][[N^{-2}]]$. From now on we consider $\mathbb{K} = \mathbb{R}$ or \mathbb{C} . In order to introduce the generic Hermitian one matrix model we define

Definition 3. *Set $\mathbb{C}[[\mathbf{i}]] = \mathbb{C}[[\{t_0, \dots, t_i\}]]$ the set of complex formal series in i variables. The set $\mathbb{C}[[\infty]]$ of complex formal series in an infinite number of variables is defined as*

$$\mathbb{C}[[\infty]] = \varinjlim \mathbb{C}[[\mathbf{i}]]. \quad (2.29)$$

We define now the generic Hermitian one matrix model.

Definition 4. *The generic Hermitian one matrix model is defined through the partition function $Z_{1MM}[[\{t_p\}_{p \in \mathbb{N}}]] \in \mathbb{C}[[\infty]]$:*

$$Z_{1MM}[[\{t_p\}_{p \in \mathbb{N}}]] = \int_{\text{formal}} dM \exp\left(-\frac{N}{2} \left(\frac{1}{2} \text{Tr}(M^2) - \sum_{p \geq 0} t_p \text{Tr}(M^p)\right)\right). \quad (2.30)$$

We call $\sum_{p \geq 0} t_p \text{Tr}(M^p) = \text{Tr } V(M)$. We further introduce $F_{1MM}[[\{t_p\}_{p \in \mathbb{N}}]] \in \mathbb{C}[[\infty]]$:

$$F_{1MM}[[\{t_p\}_{p \in \mathbb{N}}]] = -\log Z_{1MM}[[\{t_p\}_{p \in \mathbb{N}}]]. \quad (2.31)$$

Indeed this model leads to a generating series of all cellular decomposition of 2-dimensional surfaces. This can be seen by expanding with respect to all the counting variables:

$$Z_{1MM}[[\{t_p\}_{p \in \mathbb{N}}]] = \sum_{\{k_i\}_{i \in \mathbb{N}}} \int_{H_N} \prod_i \frac{t_i^{k_i}}{k_i!} (N \text{Tr}(M^i))^{k_i} e^{-\frac{N}{2} \text{Tr}(M^2)}. \quad (2.32)$$

2.2. COMBINATORIAL PROBLEMS AND MATRIX MODELS

Each term of the sum is well-defined for a finite number of non-vanishing k_i 's. Each term can be computed with the same technique than before. However, there are a few differences. The ribbon graphs are not of fixed valency⁴ anymore. All values of the valences of the vertices are allowed. A vertex of degree p is weighted by the counting variable t_p . Again taking the logarithm restricts the sum over connected graphs. Thus:

$$F_{1MM}[[\{t_p\}_{p \in \mathbb{N}}]] = \sum_{\mathcal{G} \in \{\text{connected Ribbon graphs}\}} \frac{1}{|Aut(\mathcal{G})|} N^{\chi(\mathcal{G})} \prod_{p \in \mathbb{N}} (pt_p)^{V_p(\mathcal{G})}, \quad (2.33)$$

where $V_p(\mathcal{G})$ is the number of p -valent vertices of \mathcal{G} . F_{1MM} is a generating series for cellular decomposition of surfaces counted with respect to their Euler characteristic and their number of vertices.

2.3 Quantum gravity

One of the main motivation of random matrix models comes from the problem of quantum gravity. We recall here the physical and mathematical motivations for the introduction of matrix models in the study of quantum gravity. In fact, a similar philosophy leads to the introduction of tensor models. Despite the fact that gravity is the most common force in our everyday life⁵, it is still a challenge to understand it at the microscopic level. Indeed none of the current theories gives a description of gravity at the microscopic level which is satisfactory both in the physical and mathematical point of view. However, if one follows the experience gained in the study of other forces, one is tempted to do the following. Considering a n -dimensional oriented (pseudo)-Riemannian manifold (M, g) , the Einstein-Hilbert action is defined as:

$$S_{EH}[M, g] = \int_M R vol_n, \quad (2.34)$$

with R the Ricci scalar, and vol_n the canonical Riemannian volume form. The Euler-Lagrange equations derived from this equation are the Einstein equation for the gravitational field. In order to obtain the microscopic theory, one should quantize this theory. A rather direct approach, very much inspired by the techniques used to (successfully) quantize the other forces, is to attempt to give a meaning to the following 'sum/integral':

$$\mathcal{Z} = \int_{\text{pairs } (M, g)} \exp(-iS_{EH}[M, g]). \quad (2.35)$$

The 'sum' is taken over pairs (M, g) satisfying suitable boundary conditions⁶. One points out several difficulties in establishing such a program. First, one has to understand properly

⁴sometimes called degree in graph theoretic literature.

⁵With, of course the electromagnetic force.

⁶One has to realize that even the meaning of 'suitable' is not at all clear here.

the set of manifolds one wants to sum over. A research direction is to understand the set of topologies of n -dimensional manifolds. This is of course already a very harsh problem. In fact one cannot establish an algorithm to classify topological manifolds of high dimension (*i.e.* $n \geq 5$). Any attempt to classify topology of general manifolds of high dimensions is thus ineffective. However the, *a priori*, interesting case is the 4-dimensional case. But still, one has then to classify the differential and metric structures (as one wants to avoid under- or over-counting of metric structures, one should sum over different metric up to diffeomorphisms). It is well known that classifying geometric structures of 4-dimensional manifolds is also ineffective as it is not possible to find an algorithm allowing such a classification. But one can argue that this direct approach is not necessarily the best one to understand the problem.

In order to improve our understanding of this issue we can limit ourselves to the case of 2-dimensional quantum gravity. In this case we can easily classify the geometry. The topology of 2-dimensional oriented manifold is completely characterized by its homology. Moreover the geometry and metric aspects are also well understood, as in fact they are classified by the moduli spaces $\mathcal{M}_{g,n}$. In the 2-dimensional context one can compute exactly the Einstein-Hilbert action. It can be expressed in terms of the Euler characteristic of the surface:

$$S_{EH}[M, g] = \frac{c^4}{16\pi G} \int_M R(g) vol_2 = \frac{2\pi}{G} \chi(M) \quad \forall g \text{ metric on } M. \quad (2.36)$$

One can even consider the case of non-vanishing cosmological constant Λ .

$$S_{EH}[M, g, \Lambda] = \frac{1}{G} \int_M (R(g) - \Lambda) vol_2 = \frac{1}{G} (2\pi \chi(M) - \Lambda Vol(M)). \quad (2.37)$$

Hence the only dynamical variables of $2d$ gravity are the Euler characteristic and the volume of M . However this is not enough to compute \mathcal{Z} . Since it is heuristically defined as the integral over all pairs (M, g) of the exponential of the Einstein-Hilbert action, one has to compute properly some 'combinatorial' or volume factor taking into account the 'number' of different metrics g on M . One can then argue that it could be given by counting sufficiently refined triangulations of M . In fact, triangulating M with equilateral triangles is always possible. Moreover such a triangulation comes with a canonical metric, which is the graph metric on the triangulation. So to every triangulation of M is associated a metric \tilde{g} , and for sufficiently refined triangulations one hopes that $\tilde{g} \rightarrow g$, for some g on M . So one is tempted to replaced the ' $\int_{(M,g)}$ ' by a sum over triangulations of M with a weight that takes into account the Einstein-Hilbert action of the \tilde{g} on the triangulation. Setting $t_3 = \exp(-a\Lambda)$, $t_{i \neq 3} = 0$ and $N = e^{\frac{2\pi}{G}}$ and recalling that the sum over ribbon graph is a sum over triangulations, in this case one can argue that:

$$\mathcal{Z} = \int_{\text{pairs } (M,g)} \exp(-S_{EH}[M, g]) := \int dM \exp\left(-\frac{N}{2} \text{Tr}(M^2) + t_3 \text{Tr}(M^3)\right). \quad (2.38)$$

2.3. QUANTUM GRAVITY

The integration over Hermitian matrices is here an important feature. This restricts the set of triangulations to the set of *orientable* triangulations of surfaces for which the Einstein-Hilbert action is well-defined⁷. Moreover we comment on the fact that we simplified a bit the problem. Indeed we erased the i in front of S_{EH} . This allows better convergence properties, and simplifies the combinatorial interpretation.

When one thinks about quantum gravity, one may be led to consider string theory. Matrix models are also related to string theory, for almost the same reasons. String theory associates an action (a weight) to every surface as the trajectory of a string evolving in space-time spans a surface. However there is no canonical choice for the action. It is in general constrained by symmetry considerations. It is typically chosen to be invariant under coordinate transformations of the surface. However the coordinates play the role of matter fields on the surfaces and complicate the measure. But one can argue as above that if the target space is zero dimensional, the string theory can be put in a matrix integral form [Wit91, Eyn15b].

2.4 Intersection theory on the moduli spaces of curves

2.4.1 From counting triangulations to Riemann surfaces

This subsection title has been borrowed to Bertrand Eynard. From the preceding consideration, one is led to think more deeply about the space of Riemann surfaces and its relationship with matrix integrals. Technically, a Riemann surface is defined as [Sch07]:

Definition 5. *A Riemann surface is a Hausdorff topological space X with \mathbb{C} as model space. The coordinate patches (U_i, ϕ_i) , i.e. $\phi_i : U_i \rightarrow V_i \subset \mathbb{C}$ are analytic. Moreover the transition functions defined on $U_i \cap U_j$ $\phi_i^{-1} \circ \phi_j$ are analytic.*

The above definition implies that X is 2-dimensional. Moreover, it also implies that it is orientable, as in fact analytic maps preserve orientation. Still one should be aware that every orientable 2-dimensional Riemannian manifold (M, g) can be turn into a Riemann surface. This is done by setting an almost complex structure J as $J_{\mu\nu} = \sqrt{|g^{-1}|} \epsilon_{\mu\rho} g_{\rho\nu}$. A Riemann surface is thus equivalent to the data of a Riemannian 2-dimensional manifold. One is now interested in classifying the possibles metric properties of a surface X . This is done by the moduli spaces of Riemann surfaces that are classifying spaces for these metric properties. In some sense the moduli space $\mathcal{M}_{g,n}$ are the

$$\mathcal{M}_{g,n} = \{\text{analytic isomorphy classes of Riemann surfaces of genus } g\}. \quad (2.39)$$

This set can be given a geometric structure [Sch07].

⁷recall that you need a volume form.

There exists a matrix model that computes the intersection of these spaces. This is the Kontsevitch matrix model [Kon92, Muk06, Eyn15b]. The rough idea is as follows. One can fix a metric on a surface S of genus g by defining a horocyclic quadratic differential (HQD) $\eta \in T^*S^{\otimes 2}$ on it. In local coordinates,

$$\eta = \eta_{z,z} dz \otimes dz. \quad (2.40)$$

It is meromorphic and has poles at n marked points $\{p_1, \dots, p_n\}$ of S . Outside the poles and zeroes, this HQD defines a metric on S which is given by $g = |\eta_{zz}| dz \otimes dz$. Such a differential is not unique, but with further restrictions one can use it to describe $\mathcal{M}_{g,n}$. In fact, the differential is not defined at the marked points, then one can consider it defines a metric over the punctured surface S_n . Moreover, we define the *horizontal trajectories* as the paths γ along which η is real positive, and the *vertical trajectories* as the ones on which η is negative. The behaviour at zeroes of η in centered local coordinates $z = |z|e^{i\theta}$ is of the form $Kz^{n+2}dr \otimes d\theta$ for zeroes of n -th order. Then there are $n+2$ values of θ for which η is real positive. The behaviour at the poles is given in local polar coordinates as $\eta = K'(\frac{dr \otimes dr}{r^2} + d\theta \otimes d\theta)$. These two remarks imply that there are $n+2$ horizontal trajectories adjacent to a zero of order n , and the horizontal trajectories form circles around the poles of η . We consider the Jenkins-Strebel HQD (JS HQD),

Definition 6. • A non-closed horizontal trajectory is a horizontal trajectory starting and ending at a zero of η .

- A Jenkins-Strebel HQD is a HQD whose set of non-closed horizontal trajectory has measure zero.

Moreover we have:

Theorem 2. Set X a connected, compact Riemann surface with $\{z_1, \dots, z_n\}$ marked points. One associates a real number to each of these marked points, $\{p_1, \dots, p_n\}$. Then there exists a unique JS HQD η on $X \setminus \{z_1, \dots, z_n\}$ such that the horizontal trajectories form a graph \mathcal{G} embedded in $X \setminus \{z_1, \dots, z_n\}$ and whose faces F_i are centered around the z_i 's. Moreover the length of the faces F_i are the p_i .

This allows one to transform a geometric problem into a combinatorial one. In fact using a JS HQD η , one can describe any Riemann surface, and one can describe η by the mean of graphs embedded in a 2-manifold, so to say a ribbon graph. Moreover we add that we can restrict to ribbon graphs with 3-valent vertices as in fact a small local deformation of η can transform a zero of order 2 into a pair of zero of order 1. From these considerations one constructs the *combinatorial* moduli space $\mathcal{M}_{g,n}^{\text{comb}}$.

Definition 7. $\mathcal{M}_{g,n}^{\text{comb}}$ denotes the set of equivalence classes of ribbon graphs \mathcal{G} of genus g and n faces with the following additional features. The edges of \mathcal{G} are labelled by positive

2.4. INTERSECTION THEORY ON THE MODULI SPACES OF CURVES

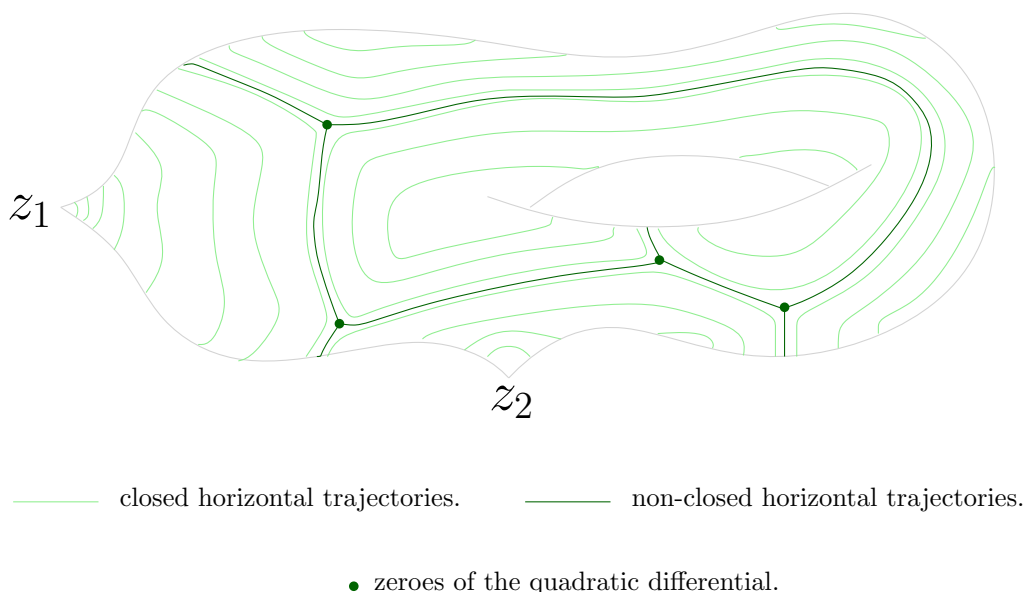


Figure 2.2: Example of the trajectories of a JS HQD on the torus with two punctures z_1 , z_2 . The underlying graph is pictured with a darker green.

real numbers turning it into a metric graph. The vertices are all of degree $d_v \geq 3$. We call $s : \mathcal{M}_{g,n} \times \mathbb{R}_+^n \rightarrow \mathcal{M}_{g,n}^{comb}$ the map that sends the Riemann surface X with numbers $\{p_1, \dots, p_n\}$ to the graph of its canonical JS HQD.

In fact the map s is one-to-one. The equivalence classes of graphs are defined with respect to the automorphisms of *labelled* graphs. The equivalence under the finite groups of automorphism of graphs translates the orbifold structure of the $\mathcal{M}_{g,n}$ at the level of combinatorics.

These combinatorial techniques can be used to gain insight into the structure of moduli spaces. In fact, one can consider the intersection theory of these spaces. Avoiding technicalities as much as possible, one can consider intersection theory as the theory counting the intersection of subsets in a larger set. For example one can count the number of intersection points in the plane. Generically, two lines intersect in one point. More generally, if one considers a subset A of codimension d and a subset B of codimension d' , then, generically, the two subsets intersect in a set of codimension $d + d'$. Considering the case in which we have n subset of codimensions d_i in a space of dimension D , such that $\sum_i d_i = D$, their generic intersection is a set of points. The number of such points is called an intersection number [EH13].

One can define intersection theory in moduli spaces. Natural objects of codimension 2

2.4. INTERSECTION THEORY ON THE MODULI SPACES OF CURVES

in $\mathcal{M}_{g,n}$ are the *psi-classes*. They are heuristically defined as the area generated in $\mathcal{M}_{g,n}$ when one moves a point z_k of the Riemann surface X . These area elements are represented by two-forms $\psi_k \in H_2(\mathcal{M}_{g,n}, \mathbb{Q})$. The intersection numbers of moduli spaces are defined as:

$$\langle \tau_{d_1} \cdots \tau_{d_n} \rangle := \int_{\mathcal{M}_{g,n}} \psi_1^{d_1} \cdots \psi_n^{d_n}. \quad (2.41)$$

One can construct a representant of each ψ_i class in the following way. Consider a Riemann surface X with its n marked points z_1, \dots, z_n . Consider the family of cotangent spaces $T_{z_i}^* X$ at z_i . We define a family of line bundles on $\mathcal{M}_{g,n}$ denoted \mathcal{L}_i as the bundles whose fibers are the cotangent spaces $T_{z_i}^* X$. Of course one has to give the transition maps between these fibers. This is done by considering the first Chern class $c_1(\mathcal{L}_i)$. A representant of the first Chern class is given by the curvature form of any given connection on \mathcal{L}_i . Such a curvature form can be built directly on the ribbon graphs of the JS HQD. The face F_i encircling the point z_i has perimeter p_i and the edges being adjacent to F_i have independently length l_e , *i.e.* $p_i = \sum_{e \in F_i} l_e$. Choosing coordinates on the perimeter φ_j , $j \in \llbracket 1, |\{e \in F_i\}| \rrbracket$, we consider the locally defined 1-form:

$$\alpha_i = \sum_{e \in F_i} \frac{l_e}{p_i} d \frac{\varphi_e}{p_i}. \quad (2.42)$$

This 1-form can be extended globally and its curvature is the first Chern class of \mathcal{L}_i . Then we have a representative of the ψ_i on the ribbon graph. This can be used to compute the intersection number. Denoting $\omega_i = d\alpha_i$ we have:

$$\omega_i = \sum_{e, e' \in F_i} \frac{d\varphi_e}{p_i} \wedge \frac{d\varphi_{e'}}{p_i}. \quad (2.43)$$

The intersection numbers can be represented from this two form as

$$\langle \tau_{d_1} \cdots \tau_{d_n} \rangle = \int \bigwedge_{i=1}^n \omega_i^{d_i}, \quad (2.44)$$

where here $\omega_i^{d_i}$ really means $\underbrace{\omega_i \wedge \cdots \wedge \omega_i}_{d_i \text{ times}}$. Consider the volume form $\Omega = \sum_i p_i^2 \omega_i$ over

$\mathcal{M}_{g,n}^{\text{comb}}$. Setting $pr_2 : \mathcal{M}_{g,n}^{\text{comb}} \rightarrow \mathbb{R}_+$, the projection on the second factor given by the perimeter of the faces, we can compute the volume of the fibers and obtain:

$$\text{vol}(p_1, \dots, p_n) = \sum_{d_i} \prod_i \frac{p_i^{2d_i}}{d_i!} \langle \tau_{d_1} \cdots \tau_{d_n} \rangle. \quad (2.45)$$

2.4. INTERSECTION THEORY ON THE MODULI SPACES OF CURVES

The Laplace transform with respect to the p_i is given by:

$$\text{vol}^*(\lambda_1, \dots, \lambda_n) = \sum_{d_i} \langle \tau_{d_1} \cdots \tau_{d_n} \rangle \prod_i \frac{(2d_i)!}{d_i!} \frac{1}{\lambda^{2d_i+1}}. \quad (2.46)$$

By summing over open strata it is possible to evaluate the volume integral $I_{g,n}(\{\lambda_i\})$ over $\mathcal{M}_{g,n}^{\text{comb}}$. Each stratum being indexed by a ribbon graph, passing to edge variables $\lambda(e)$ we have

$$I_{g,n}(\{\lambda(e)\}) = \sum_{d_i} \langle \tau_{d_1} \cdots \tau_{d_n} \rangle \prod_i \frac{(2d_i)!}{d_i!} \frac{1}{\lambda^{2d_i+1}} = \sum_{\mathcal{G} \in \Gamma_{g,n}} \frac{1}{|\text{Aut}(\mathcal{G})|} \prod_{e \in E(\mathcal{G})} \frac{1}{\lambda(e)}. \quad (2.47)$$

A generating function of the $I_{g,n}$ can be constructed from a matrix model. This matrix model is of the form:

$$Z_K[\Lambda] = \int_{\text{formal}} dM \exp\left(-\frac{1}{2} \text{Tr}(M \Lambda M) + \frac{i}{3} \text{Tr}(M^3)\right). \quad (2.48)$$

In this very short presentation we have left aside a lot of “technical details”. We especially discarded the problem of compactification of the moduli spaces. It is related to what happen when one of the edges label goes to zero. We just gave heuristic arguments. The proof can be found in the original paper of Maxim Kontsevitch [Kon92] (see also [Zvo02]). Using this matrix model it is possible to show that it satisfies KdV equations, thus proving a conjecture of Edward Witten [Wit91]. One ends with the following theorem:

Theorem 3 (Kontsevitch). *$F[t_0(\Lambda), t_1(\Lambda), \dots] = \log(Z_K[\lambda])$ is a generating series of the intersection numbers of moduli spaces of Riemann surfaces. The counting variables $t_i(\Lambda)$ are defined as $t_i(\Lambda) := -(2i-1)!! \text{Tr}(\Lambda^{-(2i+1)})$. Moreover Z_K is a τ function for the KdV equation, in particular it satisfies the Korteweg de Vries equation, setting $u = \frac{\partial^2 F}{\partial^2 t_1}$:*

$$\frac{\partial u}{\partial t_3} = u \frac{\partial u}{\partial t_1} + \frac{1}{12} \frac{\partial^3 u}{\partial^3 t_1}. \quad (2.49)$$

This kind of problem can be generalized. Instead of considering Riemann surfaces, one considers the moduli spaces of embedding of a Riemann surface into a target space \mathcal{C} . This is of course related to problems of string theory, in which one considers the dynamic of a string in space-time. One wants to understand the intersection theory of the moduli spaces $\mathcal{M}_{g,n}(\mathcal{C})$. This problem can be extremely difficult, depending on the geometry of the space \mathcal{C} , however for some classes of spaces it is possible to define properly the classes, and the resulting numbers that one computes are called *Gromov-Witten invariants* [Eyn15b, Eyn09, EKPM14]. In some cases, the geometry of \mathcal{C} allows one to compute explicitly these numbers as in fact the integration over $\mathcal{M}_{g,n}(\mathcal{C})$ can be ‘localized’. In these cases one can use matrix models and/or combinatorial techniques to provide generating series of these numbers [Eyn09, EKPM14]. We should point out that we gave only a heuristic description of the problem, and that we forgot a lot of technicalities which we do not feel competent to review here.

2.4. INTERSECTION THEORY ON THE MODULI SPACES OF CURVES

2.5 Inspiration from matrix models.

These considerations about matrix models are of importance. In fact they provide a simpler context in which some of the features of tensor models already appear. Moreover matrix models showed their incredible richness. They have been able to shed light on numerous problems ranging from mathematics, physics and combinatorics. So one is tempted to approach similar problems about higher dimensional geometry and 'combinatorics' using tensor models. Some great questions appearing from these considerations are the following:

- Is it possible to use tensor models to get new combinatorial results about higher dimensional combinatorial maps?
- Does the framework of tensor models provide a new approach to the quantization of the Riemann-Hilbert action? Are the usual methods of higher geometry quantization recovered in the tensor models framework?
- Can one extend the success of matrix models to compute geometrical quantities, and for instance extend Kontsevitch's work to the context of higher dimensional geometry (e.g. three-dimensional geometry) using tensor models?
- Finally, what is the relationship of tensor models to matrix models?

In this thesis we have been mainly working on the first and last questions. However, it seems there are doors opening in the direction of the two others questions. Moreover tensor models have provided tools to another formalism related to the quantization of gravity, namely *group field theories*, allowing in particular their renormalization [BGR13b]. We now turn to the description of this formalism in the next Chapter.

Chapter 3

Group Field Theories

In this chapter I introduce very crudely another motivation for the study of random tensor models. This motivation comes from a set of theories related to the problem of quantizing gravity. These theories are called *Group Field Theory* (GFT) and were introduced to solve in relation to the framework of *Loop Quantum Gravity* (LQG). Tensor models techniques (especially combinatorial ones) have been extended and used a lot to gain understanding about GFT (and up to some extent LQG). For this reason I give a brief introduction to the ideas leading to GFT. As a warning I tell that this chapter may not be easily readable by combinatorists. However it is at the source of the combinatorial problems that can be tackled by tensor models. A set of references for this chapter is provided by [BM94], [Rov07], [Ori06], [Fre05].

3.1 Quantum gravity ideas

We introduce roughly the ideas that lead to the spinfoam formalism, and its appearance when considering the problem of quantizing gravity. The starting point is almost the same as what we have described in the context of random matrix models. Contrary to the approach of string theory (which is much more ambitious), LQG is a very conservative approach to quantum gravity. In fact, in this approach one only starts with the content of general relativity as formulated by Einstein. Then one tries to extend the quantization techniques of usual quantum mechanics to the setting of general relativity (GR) [Thi07]. This is, when done rigorously, a very difficult task, as already the topic of quantization is very non trivial in the framework of regular quantum mechanics¹. In this approach GR is first re-expressed in term of parallel transport on the manifold M instead of the metric on M . In this setting the theory resembles more to a gauge theory, thus we can use this

¹In fact, a not that well known fact about quantum mechanics, is that the usual physicist quantization of the free particle does not exist mathematically speaking. One already has to deploy new mathematics to achieve the quantization of the free particle. See [Sch11]

similarity as a source of inspiration to describe a correct quantization of GR. Practically, this is done by using the vielbein variables. In this context one understands that the states of the theory represent states of space. References for this section are [Bae96, BM94, Bae00]

3.1.1 Connection variables for general relativity.

As we explained in the previous chapter, the Einstein-Hilbert action on a (pseudo-) Riemannian manifold (M, g) writes [BM94]:

$$S_{EH}[M, g] = \int_M R[g] \, vol. \quad (3.1)$$

Actually, one can write the same action with respect to the vielbein variables². The vielbein formalism is well introduced in for instance [BM94].

Some remarks have first to be made. The metric g is in fact a bilinear form defined on the fibers of the tangent bundle TM of the manifold M . Moreover, it should vary smoothly from fibers to fibers. Then one obtains $g : \Gamma(TM) \times \Gamma(TM) \rightarrow C^\infty(M)$ as a section of a cotangent bundle of (symmetric) bilinear forms on M . As long as one is interested in describing the tangent bundle locally, one can use a local trivialization. That is exactly what are the vielbein variables of the Palatini formalism. Moreover, they have the additional feature that they reconstruct the metric on a flat trivialization (so to say it is an orthonormal trivialization). Consider a $SO(p, q)$ bundle $B \simeq_{\text{locally}} M \times \mathbb{R}^n$ over M . We can define an invariant flat metric over it, metric that we call η (typically the Minkowski metric, in a physics context). The vielbein variables are³ a local trivialization of TM .

$$\begin{array}{ccc} & e & \\ TM & \xleftarrow{\quad} & B \\ & e^{-1} & \\ & \xrightarrow{\quad} & \\ \downarrow & & \downarrow \\ M & \xrightarrow{id} & M \end{array}$$

The vielbein variables satisfy

$$g(e(x), e(y)) = \eta(x, y) \, \forall x, y \in \Gamma(B), \quad (3.2)$$

or, in local coordinates,

$$g_{\mu\nu}(x) e_i^\mu(x) e_j^\nu(x) = \eta_{ij}. \quad (3.3)$$

²I avoid here the names triad, tetrad, drei- end vier-bein as they refer to the dimensionality of M .

³is or are? In fact the vielbein variables as used by physicists are a local representation of a bundle isomorphism, then it is described by a set of coordinates, but it is only one object mathematically...

3.1. QUANTUM GRAVITY IDEAS

Using the inverse vielbein, this writes:

$$g(v, w) = \eta(e^{-1}(v), e^{-1}(w)) \quad \forall v, w \in \Gamma(TM). \quad (3.4)$$

In the LQG framework, e^{-1} is called the gravitational field. It can be described as a set of 1-forms $\{(e^{-1})^i = (e^{-1})^i_\mu dx^\mu\}$ in local coordinates. Moreover, B is a $SO(p, q)$ bundle and thus comes with an associated connection often called *spin connection* ω . We have

$$(De^{-1})^i = d(e^{-1})^i + \omega^i_j(e^{-1})^j, \quad (3.5)$$

in local coordinates. One can rewrite the Einstein-Hilbert equations in this formalism ; for instance in four dimensions, one has:

$$S_{EH}[e^{-1}, \omega] = \frac{1}{\kappa} \text{Tr} \int_M (\star e^{-1} \wedge e^{-1} + \frac{1}{\gamma} e^{-1} \wedge e^{-1}) \wedge F[\omega]. \quad (3.6)$$

In three dimensions, the action takes the simpler form $\text{Tr} \int_M e^{-1} \wedge F[\omega]$. This implies some simplifications when one considers the quantization of the three dimensional case (see next subsection). In fact, this form of the action contains more than the Einstein field equations. There is a first set of equations equivalent to a torsion free condition for ω . It is possible to write an action in terms of $\omega[e]$ being a torsion free connection (by solving the first set of equations). This is called the second order formalism.

The two formalisms are not equivalent in the presence of matter fields as the physical predictions differ. The first order formalism is the starting point for LQG. In fact gravity, at least at classical level, is described for the Lorentzian signature $p = 3$ and $q = 1$. The $SO(3, 1)$ bundles structure translates the fact that physics is invariant under local Lorentz transformation. The gravitational field e transforms as an element of the fundamental representation of $SO(3, 1)$ when, of course, ω transforms in the adjoint representation. Moreover, one has to implement the invariance through diffeomorphisms. The action of a diffeomorphism $\phi : M \rightarrow M$ is given by the pullback of the gravitational field and of the spin connection (and of matter fields when coupled to matter). Implementing the diffeomorphism invariance is one of the most (if not the most) challenging part of quantizing gravity in the LQG setting.

A simpler case is when the space-time M is three dimensional. This is also the one we will be interested in since it leads more directly to the problem we want to expose. The 4 dimensional case comes with some additional complications as we have to implement the simplicity constraint, and this is not fully understood yet. In this situation the Lorentzian signature corresponds to $p = 2$ and $q = 1$. To further simplify the problem the literature often considers $SO(3)$ as the gauge group. Indeed one needs to deal with the representations of the gauge group, and the ones of a compact group are simpler than the ones of a non-compact group. This corresponds to the problem of quantizing *Euclidean* gravity. We can formulate this problem through the so-called *topological BF* theory.

3.1. QUANTUM GRAVITY IDEAS

3.1.2 Topological BF theory

The setting of BF theory in n dimensions is as follows. Consider a semi-simple⁴ Lie group G , its Lie algebra is endowed with a canonical non-degenerate bilinear form $(a, b) \mapsto \text{Tr}(ab)$. BF theory is built out of a connection A on a G -bundle, and a $(n-2)$ -form B taking value in $\text{ad}(G)$ bundle. The action for this theory is given by:

$$S_{BF} = \int_M \text{Tr}(B \wedge F), \quad (3.7)$$

where F is the curvature associated with A . The classical equations for this theory are:

$$F = 0, \quad (3.8)$$

$$D_A B = 0. \quad (3.9)$$

The action S_{BF} is invariant under gauge transformation $B \mapsto B + d_A g$ as long as there are no boundary terms in \int_M .

One then notices the following fact. In *dimension* $d = 3$, B is an $\text{ad}(G)$ valued 1-form, so it can be used to define a map $B : TM \rightarrow \text{ad}(G)$. Assuming B is one-to-one we obtain a bundle isomorphism and can define a metric on M by setting:

$$g(v, w) = \text{Tr}(B(v)B(w)), \quad \forall v, w \in TM. \quad (3.10)$$

The classical equations on B and F imply that g is a flat metric on M . Finally, this theory has only global degrees of freedom, which means that it is a *topological* field theory. A quantum (statistical) version of this theory should heuristically be of the form of the functional

$$Z_{\text{gravity 3d}} = \int \mathcal{D}B \mathcal{D}A \exp(-S_{BF}). \quad (3.11)$$

In principle, one should be very careful when integrating on B , as in fact this construction really leads to gravity as long as B is *one-to-one*. So one should enforce this constraint. However, the philosophy of the quantum gravity researchers usually has been to accept B fields that do not lead to bundle isomorphisms and consider that quantum gravity can contain degenerate metrics. Admitting this, one could understand B as a Lagrange multiplier for $F(A)$, and thus understand that a rigorous definition of this integral should compute the volume of the set of zero curvature connections on M . In fact this is not possible yet since one has to define a measure on this space in order to give a meaning to its volume. However one is tempted to reproduce the heuristic ideas of matrix models described in Chapter 2. We want to discretize M . When a suitable discretization has been chosen, consider the space of flat connections on the dual 2-skeleton of the chosen discretization instead of the space of flat connections. The dual 2-skeleton in a triangulation \mathcal{T}_M of M can be thought as follows:

⁴This is not really necessary, but is helpful as it avoids some technicalities. Moreover it corresponds to the situation we are interested in.

3.1. QUANTUM GRAVITY IDEAS

- each n -simplex has one vertex at its center,
- each $(n - 1)$ -simplex is intersected by an edge of the 2-skeleton,
- each $(n - 2)$ -simplex intersects a face of the 2-skeleton.

A *connection on a 2-skeleton* is a map a from $G \times \mathbb{Z}_2$ to the set of edges of the 2-skeleton [BS12a]. Each edge e is assigned a group element $g_e \in G$ plus an orientation $o_e \in \mathbb{Z}_2$. There is a natural involution on each edge i_e that sends (g_e, o_e) to (g_e^{-1}, o_e^{-1}) . A connection is really defined up to the action of these involutions. Holonomies h of the connection are the ordered product of group elements along a face: $h_f = \prod_{e \in f} g_e$. Flat connections correspond to connections whose holonomies around dual faces are the identity, *i.e.* $h_f = 1 \forall f$. We can then try to define the volume of the moduli space of flat G connections on M by:

$$z([\mathcal{T}_M]) = \int \prod_{e \in E_{\mathcal{T}_M}} dg_e \prod_{f \in F_{\mathcal{T}_M}} \delta\left(\prod_{e' \in f} g'_{e'}\right). \quad (3.12)$$

Unfortunately this expression is not well defined yet as it involves products of δ distributions. Moreover, we labelled this number by \mathcal{T}_M and not M as in fact there is no proof that it is independent of the chosen triangulation⁵. The problem is actually even worse. In fact consider two manifold M, N . It is, *a priori* possible that these two manifolds admit two triangulations \mathcal{T}_M and \mathcal{T}_N such that their 2-skeletons are the same. This explains the notation $[\mathcal{T}_M]$. Indeed the volume z here is not really a function of the triangulations but only of the 2-skeletons of triangulations, so they can be written as function of classes of triangulation $[\mathcal{T}_M]$ admitting the same 2-skeleton. We can use the Peter-Weyl expansion of the delta distribution on G ,

$$\delta(g) = \sum_{\rho \in \text{Irred}(G)} \dim(\rho) \text{Tr}(\rho(g)), \quad (3.13)$$

thus obtaining,

$$z([\mathcal{T}_M]) = \sum_{\rho: \{h_f\} \rightarrow G} \int \prod_{e \in E_{\mathcal{T}_M}} dg_e \prod_{f \in F_{\mathcal{T}_M}} \dim(\rho_f) \text{Tr}(\rho_f(h_f)). \quad (3.14)$$

As a reminder of the fact that the first expression was not well defined, this sum does not converge in general. Ignoring the convergence issue, the integral is defined by summing over decorations of the dual 2-skeleton of \mathcal{T}_M . These decorations are given by attaching an irreducible representation of G to each edge of the dual as well as a group element of G . With these issues in mind we keep $z([\mathcal{T}_M])$ as a tentative definition of quantum gravity for 3-dimensional manifolds M .

⁵It is possible to prove this independence in the 2-dimensional case. In this case, $z([\mathcal{T}_M]) = z(M)$ for any M of genus $g \geq 2$.

3.1. QUANTUM GRAVITY IDEAS

We can then develop some diagrammatic calculus for this problem. This is described in [Bae00]. However, in order to construct *group field theories* (GFT) we further follow the line of thought of matrix models. We consider the generating function of the quantities $z([\mathcal{T}_M])$ for all M and \mathcal{T}_M .

3.2 Group field theory as generating function for spinfoams

GFT are defined in the following way. Consider a Lie group $G^{\times D}$. Consider a complex valued field on it:

$$\phi : G^{\times D} \rightarrow \mathbb{C}. \quad (3.15)$$

The theory is described by a generating functional of the form,

$$Z[\lambda] = \int \mathcal{D}\mu(\phi) \mathcal{D}\mu(\bar{\phi}) \exp(+S_{int}[\phi] + \overline{S_{int}[\phi]}), \quad (3.16)$$

where

$$\mathcal{D}\mu(\phi) \mathcal{D}\mu(\bar{\phi}) = \mathcal{D}\bar{\phi} \mathcal{D}\phi \exp\left(-\frac{1}{2} \int \prod_{i=1}^d \bar{\phi}(g_1, \dots, g_d) \phi(g_1, \dots, g_d)\right). \quad (3.17)$$

This is not a well defined expression for several reasons. The main problem is to construct a Lebesgue measure on the set of functions on G . However we can use the usual Feynman graphs approach to get a working definition of this integration. For simplicity, we restrict ourselves to $d = 3$. Set, for instance,

$$S_{int}[\phi] = \frac{\lambda}{4} \int \prod_{i=1}^6 dg_i \phi(g_1, g_2, g_3) \phi(g_1, g_4, g_5) \phi(g_5, g_2, g_6) \phi(g_6, g_4, g_3). \quad (3.18)$$

This sum can then be written in term of 2-cellular complexes:

$$Z[\lambda] = \sum_{\text{2-cell complexes } \gamma} \frac{1}{|Aut(\gamma)|} \lambda^{V(\gamma)} z(\gamma). \quad (3.19)$$

One of the problem when considering these integrals in the quantum gravity context is that this does not provides much information on the manifold that underlies these 2-cell complexes. As pointed out above, the 2-cell structure is not sufficient to understand fully the geometry at quantum level. There is, of course, an argument against this idea. If one follows the usual interpretation of discretized gravity, then one knows that the curvature concentrates on the $(n - 2)$ -simplices of the discretization of the manifold. So the total d dimensional structure of the manifold can be seen as partly irrelevant. This may be understood as a manifestation of a form of *dimensional reduction* [tH93]. This phenomenon

3.2. GROUP FIELD THEORY AS GENERATING FUNCTION FOR SPINFOAMS

is not a real problem as long as one considers only the quantities $z([\mathcal{T}_M])$. Indeed in this situation one knows about M before choosing a triangulation and extracting a 2-skeleton out of it. This is the usual situation in LQG. But if one generates all 2-cell complexes without referring first to a manifold, then one is left with ambiguities. One has to make arbitrary choices to recover a full d dimensional homology out of the 2-cell complexes. These choices may or may not be physically relevant. Moreover the sum is weighted by the cardinal of the group of automorphism of the 2-cell complex. This would be natural if the γ represented well defined manifolds M . If this was the case the automorphism group would be the combinatorial setting for the diffeomorphism group of M . This is a hint that this direction of research should be pursued further. Some possible, at least, partial solutions to these problems are described in the next chapter.

3.2.1 Implementing gauge symmetry

As we have seen already, BF theory is invariant under gauge transformations of the connection A . So in fact the discrete analog a should be invariant under discrete analog of gauge transformations. A gauge transformation of a is defined as [BS12b, BS12a]:

Definition 8. *Set γ a 2-cell complex. A discrete connexion a associates a group element $a(e) = g_e$ to each edge e of γ . Set h a map that associate a group element to all the vertices of γ . A gauge transformation h of a is a new map a_h such that $a_h(e) = h(p(e))a(e)h(f(e))^{-1}$. Since each edge is oriented, $p(e)$ is the point of the arrow orienting the edge and $f(e)$ its feather.*

In principle one is interested in integrating over connections A up to gauge transformations, as the presence of gauge symmetry is the proof of existence of non-physically relevant degrees of freedom in the model. In the context of GFT this can be done in two ways. Either one integrates on functions ϕ that are invariant under gauge transformations

$$\phi(h \cdot g_1, h \cdot g_2, \dots, h \cdot g_D) = \phi(g_1, g_2, \dots, g_D) \quad \forall h, \{g_1, \dots, g_D\} \in G, \quad (3.20)$$

or one changes the covariance of $\mathcal{D}\mu(\phi)$ in such a way that only the part that is gauge invariant has a non trivial covariance. So to say, setting $\phi = \phi_{\text{invariant}} + \phi_{\text{non-invariant}}$,

$$\langle \phi(\{g_i\}) \phi(\{\tilde{g}_i\}) \rangle_{\mathcal{D}\mu(\phi)} = \langle \phi_{\text{invariant}}(\{g_i\}) \phi_{\text{invariant}}(\{\tilde{g}_i\}) \rangle_{\mathcal{D}\mu(\phi)}. \quad (3.21)$$

Such a measure can not be written in the form of (3.17).

3.3 Concluding remarks

As we have seen in this chapter, when quantizing gravity in more than two dimensions many new problems appear. These problems are of very different nature but have to be solved if one wants to gain understanding of the introduced models. In order to quantize

3.3. CONCLUDING REMARKS

gravity, one is very much tempted to consider the case in which the underlying manifold is not fixed. It is very natural in the line of thought of background independence that is at the heart of the LQG approach. However a naive treatment of the problem lead to generating series of 2-cell complexes that cannot be interpreted as d dimensional spaces. The list of problems to tackle includes at least:

- to provide generating series for d dimensional triangulations \mathcal{T} or d -cell complexes \mathcal{C} ,
- to provide techniques that allow one to describe the behaviour of these generating series in physically interesting regimes,
- to extend these techniques to generating series for $z(\mathcal{T})$ or $z(\mathcal{C})$.

3.3. CONCLUDING REMARKS

Chapter 4

Tensor Models and Colored Triangulations

In this chapter we will explore the geometrical ambiguities arising from the analog of dimensional reduction that undergo in GFT. We will propose a solution of this problem in three dimensions. But unfortunately this solution is very involved when one wants to generalize the idea to the d dimensional context. Moreover it is difficult to write generating series for the objects that combinatorially describe 3-cell complexes. Finally this solution is not well explored at the level of geometry. There remains plenty of work to do in order to classify the possible geometrical singularities.

In a second section we describe a different solution. In this case one introduces combinatorial restrictions on the graphs supporting the dual 1-skeleton of the simplicial complex in order to ensure the existence of a full d dimensional structure in any d . This solution is known since the 1980's and has been first explored in an attempt to provide a proof of the Poincaré-Perelman theorem. Of course one can argue that there is no physical reason to restrict the set of possible simplicial decomposition of the manifolds M to this kind of triangulation. However this provides a possible solution and thus deserves to be investigated.

4.1 Solving geometrical ambiguities: the 3-dimensional case

The problem when considering the dual 2-skeleton of a triangulation of a manifold M is that, if one forgets about the original triangulation of M , one forgets all the structure contained in the higher (≥ 2) dimensional cells of the dual complex of the triangulation. There is no, *a priori*, canonical procedure to reconstruct the lost information [Sme11, Gur10, Gur11d]. So one relies only on ad-hoc procedure (as the one introduced in [BS12b] for instance). To be more precise, let us consider the following problem. Set two tetrahedra labelled t, \bar{t} . Give labels to each of their four vertices. The vertices of t are

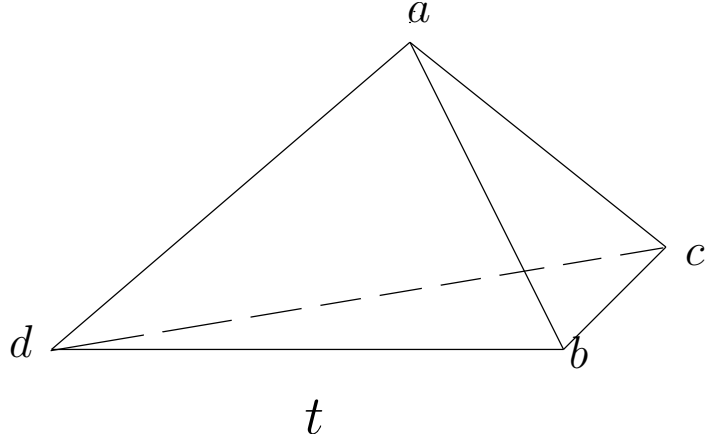


Figure 4.1: A geometric tetrahedron t with labelled vertices. For the sake of precision one can picture \bar{t} as the mirror image of t .

$v(t) = \{t_a, t_b, t_c, t_d\}$ and the ones of \bar{t} are $v(\bar{t}) = \{\bar{t}_a, \bar{t}_b, \bar{t}_c, \bar{t}_d\}$. A tetrahedron t is pictured in Fig.4.1. Each of its faces is labelled by a triplet $f(t) = \{t_{abc}, t_{bcd}, t_{cda}, t_{dab}\}$ and similarly for \bar{t} . Each edge is labelled by a pair $e(t) = \{t_{ab}, t_{ac}, t_{bc}, t_{bd}, t_{da}, t_{cd}\}$ (and respectively the same for \bar{t}). Consider the triangulation of Fig.4.2. In this case two triangles are glued along one face. One then obtains a simplicial decomposition of the ball \mathbb{B}^3 . We call \mathfrak{D} the dual 2-skeleton of the triangulation. It can be seen as a 2-cell complex. Now let us forget that this is the dual skeleton of the pictured triangulation of the 3-ball. All that is left, is the information that there are two tetrahedra - two vertices in \mathfrak{D} - glued along one face - one shared edge \mathfrak{D} between the two vertices - and that the edges of this face are glued by the identification $t_{ab} = \bar{t}_{ab}$, $t_{ac} = \bar{t}_{ac}$ and $t_{bc} = \bar{t}_{bc}$. This is the information contained in the adjacency relations of the blue curves. Unfortunately, we do not know how the vertices of these edges are glued one to another. So one cannot recover the triangulated manifold out of the dual 2-skeleton. In fact one could imagine that there is one twist before gluing the edges, for instance one could decide to identify $t_a = \bar{t}_b$ and $t_b = \bar{t}_a$. This would not lead to a triangulation of the 3-ball but to another manifold while keeping \mathfrak{D} fixed. The problem of GFTs is that the graph they generate have the combinatorial structure of 2-cell complexes, thus they cannot define a precise manifold in dimension more than two without requiring *ad hoc* conditions. One example of such *ad hoc* conditions is to ask that all closed 2-chains are boundary of 3-cells, see for instance [BS12b].

To fix this problem, one has to generate the full structure of a 3-cell complex and so to encode the gluing relations of the vertices. A possible solution is to thicken the blue lines in order to keep track of how the vertices of their dual edges project to the lines. This thickening is shown in Fig. 4.3.

4.1. SOLVING GEOMETRICAL AMBIGUITIES: THE 3-DIMENSIONAL CASE

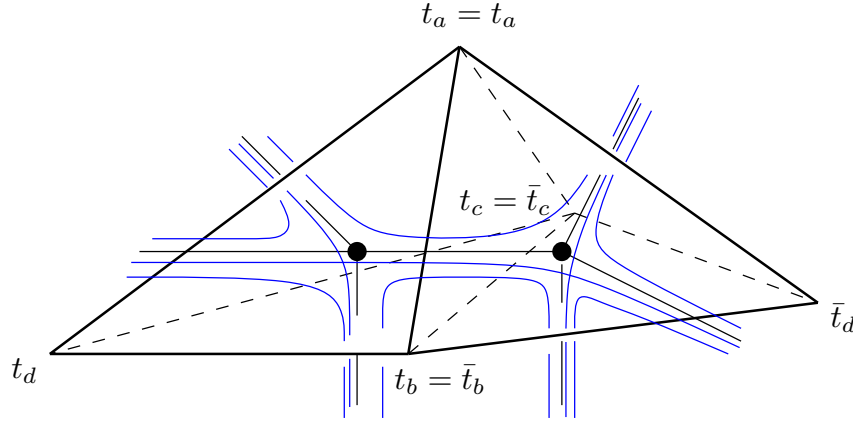


Figure 4.2: Two tetrahedra glued along one face. The identification goes as follow: $t_{abc} = \bar{t}_{abc}$; $t_{ab} = \bar{t}_{ab}$, $t_{ac} = \bar{t}_{ac}$, $t_{bc} = \bar{t}_{bc}$; $t_a = \bar{t}_a$, $t_b = \bar{t}_b$, $t_c = \bar{t}_c$. This defines without ambiguities the gluing of the two tetrahedra along their two faces. The black dots picture the dual 0-skeleton of this triangulation. The light black lines represent the edges of the dual 1-skeleton. The blue curves correspond to the 2 cells of the dual 2-skeleton. In this representation one recovers the dual 2-skeleton by gluing discs along their boundary to the blue curves.

4.1.1 Generating function of dual 2-skeleton.

Being aware of the difference between the representation of a triangulation and the one of its dual 2-skeleton, let us write a generating function for the dual 2-skeleton of triangulations. In doing so we follow the ideas of matrix models. In matrix models the lines of ribbon graphs are obtained from the indices of the matrix. Therefore it is tempting to reproduce the lines of the 2-skeletons of triangulation by choosing a set of variables with more indices. Let us call these variables $\Theta_{ijk} \in \mathbb{R}$, where i, j , and k range from 1 to N . We define the following formal integral:

$$\mathfrak{Z}[q] := \int_{\mathbb{R}^{3N}, \text{ formal}} d\Theta \exp\left(-\frac{1}{2} \sum_{ijk} \Theta_{ijk} \Theta_{ijk}\right) \exp\left(+q \sum_{ijk} \Theta_{ijk} \Theta_{kj'k'} \Theta_{k'ji'} \Theta_{i'ji}\right). \quad (4.1)$$

We consider $\mathfrak{Z}[q] \in \mathbb{C}[[q]]$ so we do not have to worry about the sign of q . We have $d\Theta = \frac{1}{3[0]} \prod_{ijk} d\Theta_{ijk}$. By definition $\mathfrak{Z}[q]$ is a formal series in q whose coefficients are Gaussian integrals of the variables Θ_{ijk} . In particular, one defines:

$$[q^n] \mathfrak{Z}[q] := \frac{1}{4^q} \int_{\text{formal}} d\Theta \left(\sum_{ijk i' j' k'} \Theta_{ijk} \Theta_{kj'k'} \Theta_{k'ji'} \Theta_{i'ji} \right)^n \exp\left(-\frac{1}{2} \sum_{ijk} \Theta_{ijk} \Theta_{ijk}\right). \quad (4.2)$$

4.1. SOLVING GEOMETRICAL AMBIGUITIES: THE 3-DIMENSIONAL CASE

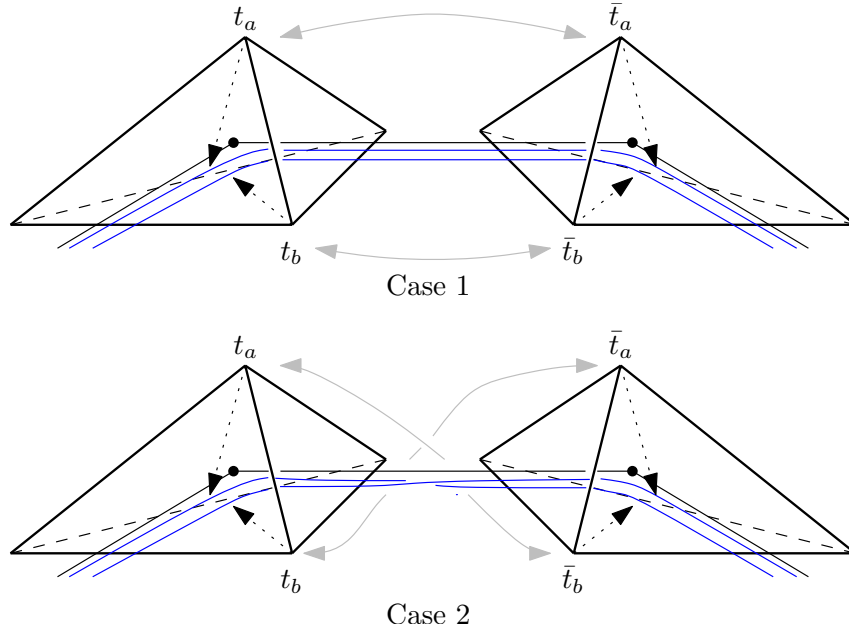


Figure 4.3: Two possible cases for gluing the edges. In the representation of Fig. 4.2, these two possibilities collapse to the same 2-skeleton. Here the edges are represented by a pair of blue lines instead of one unique blue line. This encodes the gluing of vertices. The light gray arrows picture the identification of vertices while the dashed arrows represent the projection of each vertex of the edge on the blue line.

4.1. SOLVING GEOMETRICAL AMBIGUITIES: THE 3-DIMENSIONAL CASE

One relies on Wick theorem to compute these integrals. In fact one only needs to compute the covariance *i.e.*

$$\int_{\text{formal}} d\Theta \Theta_{ijk} \Theta_{i'j'k'} \exp\left(-\frac{1}{2} \sum_{ijk} \Theta_{ijk} \Theta_{ijk}\right) = \delta_{ii'} \delta_{jj'} \delta_{kk'}. \quad (4.3)$$

In this way one obtains an expansion over graphs. Each graph is made of edges with three strands, and each vertex is a model of the vertices of a dual 2-skeleton of a triangulation (see Fig 4.2). However, one has to assume symmetry of the tensor variables to generate graphs like the one made of blue lines in Fig. 4.2. In fact if one does not consider any symmetry under permutations of the first and third indices of the Θ variable, one needs to introduce twists of the strands in order to represent all possible matches of the strands going out of the vertices. This problem could also be avoided by introducing two sets of complex variables $\Theta_{ijk}, \bar{\Theta}_{ijk}$ instead of one. This is how the problem was introduced in the 1990's by Ambjorn and al. [ADJ91]. They considered the case of symmetric tensors. But as we have seen already this kind of techniques is bound to fail at the geometrical level because of the lack of information needed to reconstruct the full manifold triangulation.

One could also try to generate the graphs with thickened blue lines. This could be in principle done by introducing sets of variables $\Theta_{\vec{i}\vec{j}\vec{k}}$, where $\vec{i}, \vec{j}, \vec{k}$ belong to $\mathbb{Z} \times \mathbb{Z}$. But the precise matching of these indices is not clear, and remains to be studied. As we will point out later, there may be some guiding principles to write such generating series. However, this is not the solution chosen in this work. Instead we use decorations on the graphs called *colors*.

4.2 Graph Encoded Manifold

In this section we define the combinatorial setting that solves in a simple way the problem of generating proper manifold triangulations from formal integration.

In fact it is possible to represent some restricted types of triangulations in any dimension by graphs that can be generated by formal integrals. These triangulations are *colored* triangulations. They are defined as follows. Each d dimensional tetrahedron is equipped with further informations

- each of its $(d-1)$ -faces is labelled by a number $c \in \llbracket 0, d \rrbracket$, called the *color*
- each of its $(d-2)$ -faces is labelled by a pair $(c, c') \in \llbracket 0, d \rrbracket^2$ of different colors
- each of its $(d-3)$ -faces is labelled by a triplet $(c, c', c'') \in \llbracket 0, d \rrbracket^3$ of different colors.
- More generally its $(d-k)$ -faces is labelled by a k -uplet of different colors.

4.2. GRAPH ENCODED MANIFOLD

The triangulation of a (pseudo)-manifold is built in such a way that if t and \bar{t} are two d -dimensional tetrahedra with colors, their $(d-k)$ -faces are glued with respect to the k -uplets labelling them [FG82, LM85]. Only $(d-k)$ -faces with the same k -uplets can be identified one to another. If one takes interest in the dual skeleton of such a triangulation, then one is led to notice the following facts:

- each tetrahedron is dual to a vertex,
- each $(d-1)$ -face is dual to an edge, thus the edge carries a color index c ,
- each $(d-2)$ -face is dual to a face of the dual skeleton and thus is labelled by a pair of color (c, c') . In fact each face of color (c, c') in the dual skeleton are recovered as the connected components of color c, c' of the 1-skeleton graph of the triangulation.
- each $(d-k)$ -face is dual to a k -cell of the dual skeleton. More precisely the $(d-k)$ -face labelled by a k -uplet of colors (c_1, \dots, c_k) are exactly the connected components of colors c_1, \dots, c_k .

This motivates the following definitions:

Definition 9. We call the pair (\mathcal{G}, γ) a $(d+1)$ colored graph if $\mathcal{G} = (V, E)$ is a graph of degree at most $(d+1)$, and $\gamma : E \rightarrow \mathcal{C}$ is a map such that for e, e' two edges adjacent to a vertex v $\gamma(e) \neq \gamma(e')$. γ is called an edge coloration of \mathcal{G} . A boundary vertex v is a vertex whose degree is strictly smaller than $(d+1)$. A regular or vacuum colored graph is a colored graph whose all vertices are of constant degree $(d+1)$.

This colored graph is also a GEM. We define the *bubbles* or *residues*¹ of a colored graphs

Definition 10. We call a n -bubble (or n -residue) with colors $\{i_1, \dots, i_n\}$ of a $(d+1)$ colored graph \mathcal{G} a connected component $\mathcal{B}^{i_1, \dots, i_n}$ of \mathcal{G} made of edges of colors $\{i_1, \dots, i_n\}$.

For each $(d+1)$ colored graph we can construct a (pseudo)-manifold of dimension d by gluing d -simplices along their faces respecting their color. In fact no faces of a simplex can be glued to another face of itself. We show examples of colored graphs in Fig. 4.4, 4.5. The reason for the appearance of pseudo-manifolds is that given any colored graphs it is possible that the neighbourhood of a vertex can be something more complicated than a ball. This can be understood in this way. From the duality relations enumerated above one has that a $(d+1-k)$ -bubble is dual to a k -simplex in a colored triangulation. In fact one realizes that a d -bubble graph is a colored graph representation of the boundary of the neighbourhood of a vertex in the triangulation. This can be seen on Fig 4.6. It is easy to construct a pseudo-manifold in 3 dimensions. Consider *e.g.* Fig. 4.5. It is a triangulation of the cone over the torus. Then if one joins the remaining magenta lines

¹*Bubbles* is the established term in the context of random tensor models literature while *residues* is the one used in the context of Graph Encoded Manifolds and Crystallization literature.

4.2. GRAPH ENCODED MANIFOLD

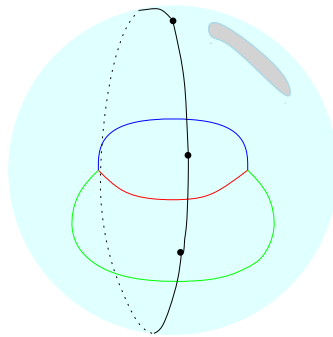


Figure 4.4: Triangulation of the 2-sphere with two triangles. This is a colored triangulation and the corresponding colored graph is drawn with colors on the edges.

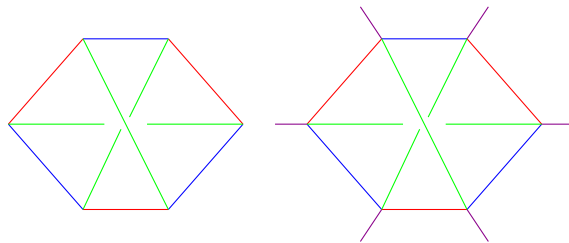


Figure 4.5: Left: colored graph representing a triangulation Δ of the 2-dimensional torus. Right: Triangulation of the cone over it $C\Delta = (\Delta \times [0, 1]) / (\Delta \times \{0\})$. The magenta lines (say half-edges) represent the boundary faces of this triangulation.

4.2. GRAPH ENCODED MANIFOLD

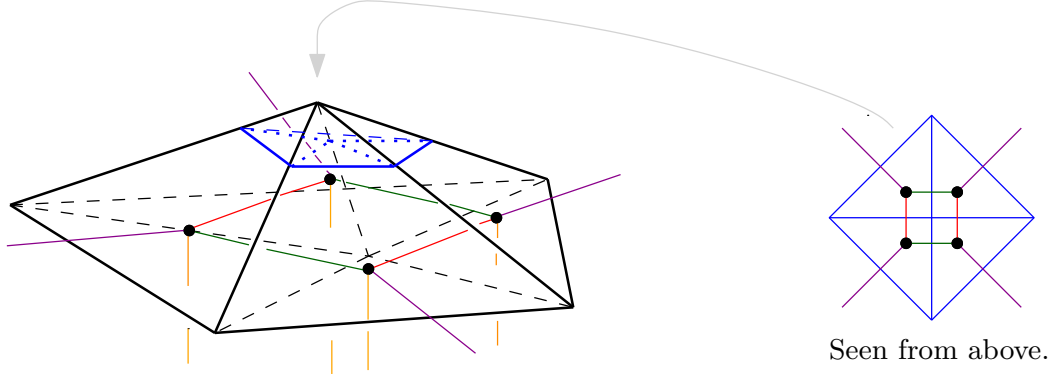


Figure 4.6: This is the representation for gluing four tetrahedra along four of their face. The dual colored graph is represented with edges of different colors. Moreover the triangulation of the boundary of the upper vertex is shown in blue. One sees that the connected component of the graph of color $\{\text{red, green, magenta}\}$ is dual to this blue triangulation.

one gets a triangulation of a pseudo-manifold since one has, at least, one bubble graph which is the triangulation of the torus. Then at least one vertex has a neighbourhood which is not homeomorphic to the ball (it is instead homeomorphic to CT^2), and thus is a pseudo-manifold. So in the three dimensional case it is rather simple to distinguish pseudo-manifolds from manifolds through the colored representations. Given a 4-colored graph \mathcal{G} one can compute the genera $g_{\mathcal{B}}$ of all its 3-bubbles. The condition for this colored graph to represent a manifold is $g_{\mathcal{B}} = 0 \forall \mathcal{B} \subset \mathcal{G}$. Hence, we have shown the following proposition:

Proposition 1. *A 4-colored graph \mathcal{G} represents a manifold if and only if*

$$g_{\mathcal{B}} = 0, \forall \mathcal{B} \subset \mathcal{G}, \quad (4.4)$$

where \mathcal{B} runs over the 3-bubbles of \mathcal{G} and $g_{\mathcal{B}}$ is the genus of the surface represented by \mathcal{B} .

To each colored graphs we can associate a collection of $d!/2$ ribbon graphs.

Definition 11. *Set \mathcal{G} a $(d+1)$ colored graph. A jacket \mathcal{J}_{τ} of \mathcal{G} is a ribbon graph whose 1-skeleton is \mathcal{G} and such that the set of faces is given by cycles of colors $(\tau^q(0), \tau^{q+1}(0))$ for a given permutation of $(d+1)$ elements modulo orientation $(\tau \sim \tau^{-1})$.*

The choice of a permutation τ amounts to the choice of an ordering of the colored edge at each vertex of the graph. These jackets are important for several reasons. When \mathcal{G} represents a 3-manifold M , then each \mathcal{J} is dual to a quadrangulation of a normal Heegaard surface of M . In fact the choice of a cyclic ordering of the colors at any vertex leads to

4.2. GRAPH ENCODED MANIFOLD

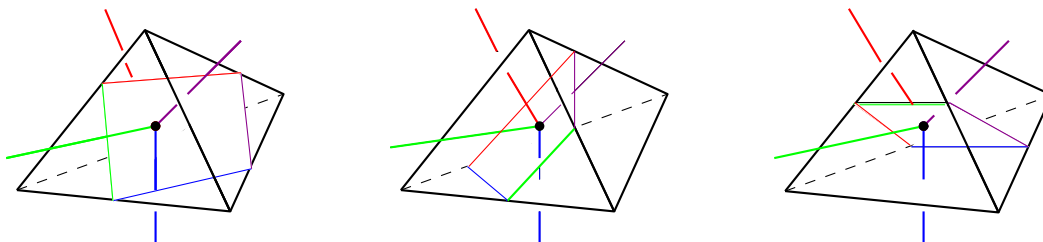


Figure 4.7: The three quads of a tetrahedron. On each of these quads there is a unique projection of the colored edges of the dual 1-skeleton such that the edges of the quad are dual to the projection of the colored edges of the 1-skeleton. Each of these projections correspond to a choice of cyclic ordering (up to orientation) of the colored edges around the vertex of the dual 1-skeleton.

a choice of a quad in the tetrahedron dual to the vertex (see Fig. 4.7). These quads are by definition² normal surfaces in the tetrahedron. When gluing tetrahedra one gets a gluing of these quads along their edges (with respect to their colors) and they form a normal surface in the 3-manifold obtained by the gluing. These normal surfaces are actually Heegaard surfaces S_τ of the manifold as they bound two handlebodies H_τ, H'_τ of genera the genera of the surfaces glued along S_τ [FG82]. This can be used to construct a generalization of the genus for 3-dimensional manifolds M . This extension is called the regular genus of the manifold and it can be shown to coincide with the Heegaard genus (which is the minimal genus of a stable Heegaard splitting of M). For instance \mathbb{S}^3 has regular genus 0 [Fer82]. Being more specific a Heegaard splitting can be represented by a Heegaard diagram. A Heegaard diagram consists of a surface F of genus g which is the boundary of the handlebodies, with a system of non-intersecting curves $\mathbf{x} = (x_1, \dots, x_g)$ and $\mathbf{y} = (y_1, \dots, y_g)$ on it. The manifold M is recovered by gluing the two handlebodies along their two sets of curves *i.e.* x_1 is glued along y_1 , x_2 along y_2 and so on... One can show that fixing the gluing along the set of curves fixes the gluing of the whole surface. The choice of a cyclic ordering of the colors of a GEM \mathcal{G} induces a quadrangulation of a surface F . Consequently \mathcal{G} regularly embeds in F . This embedding induces a Heegaard diagram. In fact the 2-bubbles of the graph can be used to define a system of curves of F , as in Fig 4.8. One can define a set of moves on the GEM preserving the homeomorphism class of the considered triangulation. These moves are called *k-dipole moves*

Definition 12. A *k-dipole* of a GEM \mathcal{G} is a sub-graph made of 2 vertices ν and μ joined by k edges of colors i_1, \dots, i_k with the additional condition that the 2 vertices belong to two different $(d+1-k)$ -bubbles of colors $\mathcal{C}/\{i_1, \dots, i_k\}$.

²For the not geometrically skilled reader a normal surface in M is defined as a surface which meets each tetrahedron of a triangulation of M in a collection of triangles or quadrilaterals.

4.2. GRAPH ENCODED MANIFOLD

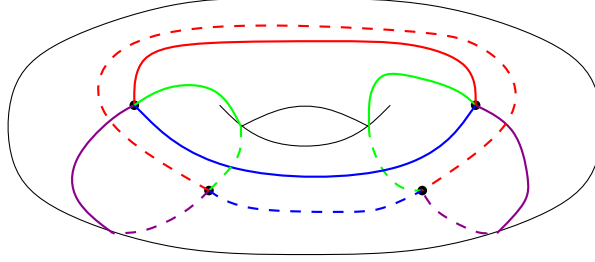


Figure 4.8: A canonical embedding of a GEM in the torus. This GEM is a representation of \mathbb{S}^3 . It has one canonical embedding of genus 1 (the two others being of genus 0). The system of curves is given by choosing one of the {magenta, green} 2-gon as $\mathbf{x} = x_1$ and one of the {blue, red} 2-gon as $\mathbf{y} = y_1$. This example has been chosen for its simplicity. In fact this colored graph is a GEM but has some additional properties turning it into a *crystallization*. It is easier to produce an example of an induced system of curves on a crystallization than on a general GEM. However it is possible to obtain a crystallization from any GEM by 1-dipoles moves⁴.

Definition 13. A k -dipole contraction is the deletion of the k edges and the deletion of ν and μ followed by a reconnection of the edges of the remaining colors, respecting their coloration.

One can of course perform the inverse operation by choosing a set of $(d + 1 - k)$ edges that when cut do not belong to the same $(d + 1 - k)$ -bubbles. Reconnect these cut edges to two different vertices and connect these vertices by k edges of the missing colors. This is called a k -dipole creation. The set of k -dipoles creations and contractions on a GEM are called *dipole moves*. They generate discrete homeomorphisms of the represented manifold. One can also introduce the *stranded representation* of a GEM. It is obtained by choosing one of the canonical embedding of the colored graph (generally the one associated to the trivial permutation $(1, \dots, d)$ of the colors). Then one draws the set of 2-bubbles of the GEM as curves passing through the edges and vertices they are adjacent to. This stranded representation reminds us about combinatorial maps of dimension d . In fact the GEM can be seen as specific types of combinatorial maps with some more structures coming from the colors.

This GEM representation is believed to be useful for the study of quantum gravity since as we will see later that these graphs can be generated from formal integrals as the coloring condition can be implemented locally. Even more importantly because of a very important theorem of Pezzana [FG82] (which is necessary - though not sufficient - for this representation to be interesting in the quantum gravity context).

⁴A crystallization is a GEM without 1-dipoles.

4.2. GRAPH ENCODED MANIFOLD

Theorem 4. *Every closed connected PL d -manifold admits a crystallization.*

Actually this means that any manifold admits a GEM representation as it is possible to obtain all GEM representations of manifolds from crystallizations and *vice versa*. We are now ready for the definition of colored tensor models, but let us pause briefly for a remark about *knot complements*.

4.2.1 Knot complements.

This subsection contains an unpublished remark I made after discussing the subject with Roland Van der Veen. I include it here as it may be useful later, for the readers interested in the geometric meaning of random tensor models.

We describe an algorithm that allows one to map the diagram of a knot K to a colored triangulation of its complement $|K| = \mathbb{S}^3 \setminus K$ with ideal boundaries. Unfortunately this triangulation is not minimal. It means that, of course it is not minimal among triangulations, as it is colored, but it is not even minimal as a colored triangulation. This is a typical problem for all this kind of algorithms. One can end with very complicated triangulations of very simple manifolds. However, the complicated triangulations obtained can always be reduced by a sequence of dipole moves to simpler ones.

Consider a knot K in \mathbb{S}^3 . Its complement is obtained by taking a tubular neighborhood \mathcal{T}_K of K in \mathbb{S}^3 . \mathcal{T}_K is a torus embedded in \mathbb{S}^3 . The complement $|K|$ of K is defined as $|K| = \mathbb{S}^3 - \text{interior}(\mathcal{T}_K)$. Intuitively, one can picture it as what one would obtain by thickening the knot in \mathbb{S}^3 and then digging in the knotted tube thus obtained. The complement $|K|$ of a knot is thus a 3-manifold with boundary, $\partial|K|$ having the topology of a torus.

Let us make precise what we mean by triangulations with ideal boundaries. A regular triangulation of a (pseudo)-manifold with boundary is a triangulation such that all the faces of the simplices may not match. Restricting our attention to colored triangulations and using their dual graph language this would mean that the boundaries correspond to the edges adjacent to only one vertex of the graph.

Definition 14. *We define a triangulation with ideal boundary, as a triangulation whose boundary $(n-1)$ -simplices have been coned. The resulting additional vertex are called ideal vertices.*

Making ideal the boundaries of a triangulation adds one vertex by for each component of the boundary. The links of the additional vertices have the topologies of the corresponding boundary components. The initial triangulation can be recovered by cutting out the new vertices produced by the cone procedure (see Fig. 4.9). If one restricts to colored triangulations and their GEM counterpart, then one understands that colored triangulations with ideal boundary correspond to GEM such that the boundary components are

4.2. GRAPH ENCODED MANIFOLD

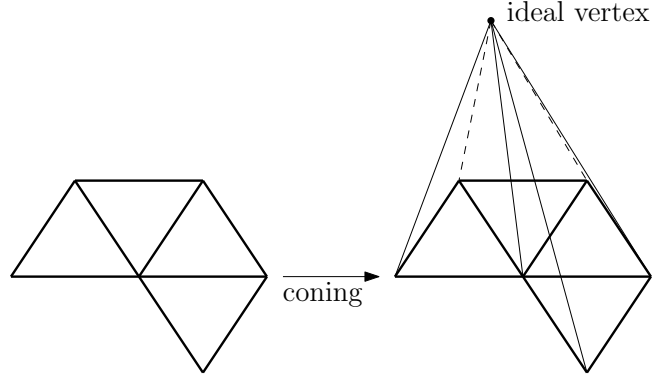


Figure 4.9: On the left is schematically pictured a piece of a boundary of a $3d$ triangulation, triangulated by boundary triangles of the tetrahedra. On the right we show the coning of this boundary, producing an ideal vertex.

represented by a subset of bubbles of the colored graph. We now want to describe a way to produce a triangulation with ideal boundaries of a knot complement from a knot diagram. The triangulation obtained by this algorithm depends on the diagram. The algorithm is as follows:

- We start with a knot diagram of K . We call the set of its crossings $\text{Cr}(K)$.
- For each $C \in \text{Cr}(K)$, we distinguish between the under-strand C_- and the upper-strand C_+ . For each under-strand C_- we draw a rectangular band made of edges of colors 1 and 2. The edges of the same color are parallel. The edges of color 2 are parallel to the under-strand while the lines of colors 1 are perpendicular to the under-strand.
- For each upper-strand C_+ we draw a rectangular band made of edges of colors 1 and 2. The edges of color 1 are parallel to the upper-strand and the edges of color 2 are perpendicular to it. Locally around a crossing C it looks like Fig. 4.10.
- Then around each corner (they will become the vertices of the corresponding GEM) of the rectangular bands surrounding the strands one adds half-edges of color 0 and 3. The half edges of color 3 are matched in such a way that they form rectangular bands around the part of the strands that do not cross in the knot diagram. Doing so, the edges of color 3 must be parallel to the strand. The bands thus formed must have edges of colors 1, 2, 3.
- The diagram of K is an immersed plane curve together with additional data allowing to distinguish under- and upper- crossings. Thus at the crossings there is an ordering

4.2. GRAPH ENCODED MANIFOLD

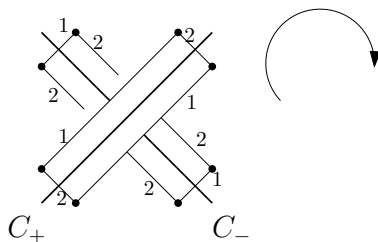


Figure 4.10: This shows what would one obtain after performing the two first items of the algorithm around a crossing. The black dots represent the corners of the rectangles, and are the future vertices of the GEM. The number designates the color of the edges. The chosen orientation of the plane is figured at the top right corner of the figure. The heavier black lines represent the knot diagram strands at a crossing.

of the strands induced by the orientation of the plane. This induces an ordering of the rectangular bands. One branches the half edges of color 0 by respecting this rule. The orientation of the plane gives an orientation of the edges of color 1 or 2 that are perpendicular to strands of the knot diagram. One draws little arrows on these edges to picture this orientation. Starting from the vertex of one of these edges that is at the end of the arrow one connects this vertex to its neighbour with respect to the orientation of the plane with an edge of color 0. The two connected vertices belong to two different rectangular bands. One continues this process by connecting all the vertices that are at the end of an arrowed edge of color 1 or 2 with their respecting neighbours, see Fig. 4.11. One consequently obtains a color graph that is a GEM of the complement of K with ideal boundary the bubbles of color 0.

We notice that for the unknot, one has to start with a complicated enough diagram of it to apply this algorithm. Indeed one needs at least one crossing to apply it. This algorithm produces a lot of extra balls, and so the number of tetrahedra of the obtained triangulations is, *a priori*, far from minimal. We show examples of what one obtains by applying this algorithm in the case of the trefoil knot and the figure eight knot, see Fig. 4.17, 4.18.

Theorem 5. *Applying the algorithm described above to a knot diagram \mathcal{D}_K of a knot K results in a colored graph \mathcal{G} that is a GEM representation of a triangulation of $|K|$ with ideal boundary. $\partial|K| = \mathcal{B}_{\mathcal{G}}^0$, where $\mathcal{B}_{\mathcal{G}}^0$ is the bubble of color 0 of \mathcal{G} and has only one connected component.*

This algorithm and theorem extend straightforwardly to links.

Proof. Let us now explain why this algorithm leads to a complement of K . This requires a lot of figures and I hope it does not affect too much the readability. The idea is to look first

4.2. GRAPH ENCODED MANIFOLD

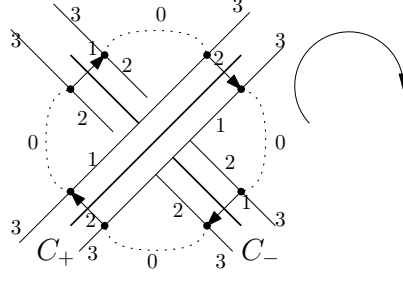


Figure 4.11: This picture shows what one obtains locally around a crossing of the knot after applying the last item of the algorithm. The edges of color 3 are branched to other patterns like this one. The edges of color 0 are pictured as dotted lines, as is now traditional in the tensor models literature.

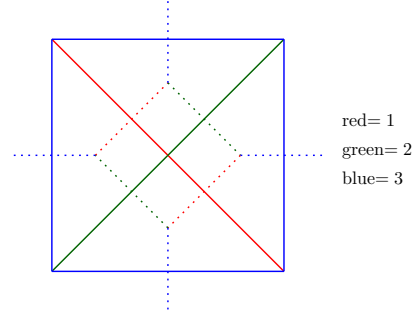


Figure 4.12: This figure shows the triangulation of the disc corresponding to the rectangular bands used in the algorithm.

at the embedding of a crossing. Of course the notion of crossing depends on an immersion of the knot in \mathbb{R}^2 and is not an intrinsic property of the knot.

So we consider a tubular neighborhood \mathcal{T}_C of a crossing C and find a colored triangulation of its boundary with colors 1, 2, 3. In fact one starts with two colored triangulations of the disc. A good one is shown in Fig. 4.12. This corresponds to the rectangular bands described in the algorithm before adding edges of color 0. By coning the triangulation of Fig. 4.12, we obtain a triangulation of the neighborhood of the two strands that cross, see Fig 4.13. At the level of GEM graphs, it corresponds to adding the half-edges of color 0 as it is done in the algorithm. To materialize the crossing in \mathbb{S}^3 one has to glue the triangular faces of color 0 as shown on Fig. 4.13 by using balls \mathbb{B}^3 . One can do it at the GEM level by using a 3-dipole of color 0 as it corresponds to a triangulated ball with two boundary triangles of color 0. But a 3-dipole can be reduced to a line, so one only needs to connect the added lines of color 0 as explained before.

4.2. GRAPH ENCODED MANIFOLD

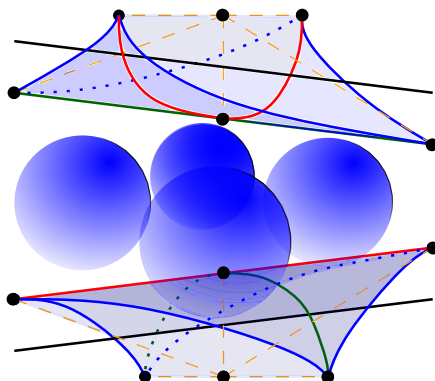


Figure 4.13: This shows a triangulation of the tubular neighborhood of the strands at a crossing. The black lines represents the strand of the knot. In order to glue these triangulation one has to glue the triangular faces of color 0 (*i.e.* the ones that are bounded by edges of color 1 = red, 2 = green, 3 = blue) by using the balls \mathbb{B}^3 situated between them. The upper triangular faces have to be glued to the north hemisphere of the balls just under them. The under triangular faces have to be glued to the south hemisphere of the balls just above them.

Finally one has to connect these crossings with balls along the strands of the knot. This can be done using balls. Again since one wants a colored triangulation, with the knot localized at the bubbles of color 0, one chooses a colored triangulation of \mathbb{B}^3 with four boundary faces of color 3 such that suppressing the edges of color 0 does not disconnect the GEM. It is provided for example by the one depicted on Fig. 4.14. In fact it is possible to replace it by double lines of color 3, as can be checked by first performing a 1-dipole move on the line of color j , then canceling the obtained 3-dipole of color 3.

□

This algorithm provides a simple way to generate a GEM representation of a knot complement in \mathbb{S}^3 with ideal boundary. There exist algorithms that provide triangulations of knot complements with ideal boundary (one could refer for example to the algorithm of Jeffrey Weeks used in SnapPea [Wee03]), but they do not lead to colored triangulations and thus are not well suited to random tensor models combinatorics. One could argue that we could perform a barycentric subdivision in order to obtain a colorable triangulation and then translate it in the GEM language. However this would lead to colored triangulations with at least 48 tetrahedra for the simplest non-trivial knot (the figure eight) while with this algorithm the figure eight is triangulated with 32 tetrahedra and can easily be simplified by performing a sequence of dipole moves. In fact the triangulation is far from being minimal,

4.2. GRAPH ENCODED MANIFOLD

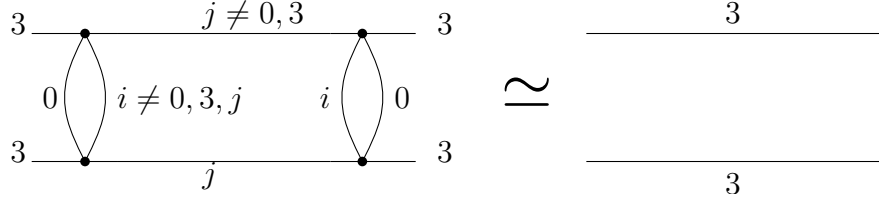


Figure 4.14: This is a GEM representation of the triangulation of the tubular neighborhood of one strand of the knot. This is used to connect the crossing pattern.

since a ball of color 3 has been added at each crossing. Still this algorithm provides a starting point that can be easily enhanced on a case by case basis, as one only has to be a bit more careful on how one glues the ball of Fig. 4.13. This is shown on the example of Fig. ??.

This algorithm allows us to understand the topology of the Feynman graphs contributing to genus 1 observables of three dimensional invariant random tensor models. To gain a more complete understanding one should find a technique to obtain a GEM representation of a complement of a knot in any three dimensional manifold or pseudo-manifold M . Also it would be interesting to extend this algorithm to knotted graphs in order to combinatorially understand the topology of Feynman graphs contributing to higher genus observables.

4.3 Random tensor models and colored GFT.

4.3.1 Random multi-tensor models.

The problem is to write formal integrals that generate GEM as Gaussian expectation values. This can be done as follows. Set ϕ_{i_1, \dots, i_d}^k a set of N^d complex random variables with i_α ranging from 1 to N for $k \in \llbracket 0, d \rrbracket$. Consider the following

$$S_{\text{quad}} = - \sum_k \sum_{\mathbf{n}_k} \bar{\phi}_{\mathbf{n}_k}^k \phi_{\mathbf{n}_k}^k \quad (4.5)$$

$$S_{\text{int}}[\lambda, \bar{\lambda}] = \frac{\lambda}{N^{D(D-1)}} \sum_{\mathbf{n}} \prod_k \phi_{\mathbf{n}_k}^k + \frac{\bar{\lambda}}{N^{D(D-1)}} \sum_{\mathbf{n}} \prod_k \bar{\phi}_{\mathbf{n}_k}^k \quad (4.6)$$

$$S[\lambda, \bar{\lambda}] = S_{\text{quad}} + S_{\text{int}}[\lambda, \bar{\lambda}], \quad (4.7)$$

where $\sum_{\mathbf{n}}$ means sum over all indices $\mathbf{n}_{k,j}$ setting $\mathbf{n}_{k,j} = \mathbf{n}_{j,k}$. Then set up the following formal integral in λ and $\bar{\lambda}$:

$$Z[\lambda, \bar{\lambda}] = \int \prod_k d\phi^k d\bar{\phi}^k \exp(S_{\text{quad}} + S_{\text{int}}[\lambda, \bar{\lambda}]). \quad (4.8)$$

4.3. RANDOM TENSOR MODELS AND COLORED GFT.

$d\phi^k d\bar{\phi}^k$ really means the product measure of independent variables $\prod_{\mathbf{n}_k} \frac{1}{2\pi} d\phi_{\mathbf{n}_k}^k \phi_{\mathbf{n}_k}^-$. In fact the graphs generated by the formal integral are remainder for the computation of Gaussian integrals of the form

$$\int \prod_k d\phi^k d\bar{\phi}^k \left(\frac{\lambda}{N^{D(D-1)}} \sum_{\mathbf{n}} \prod_k \phi_{\mathbf{n}_k}^k + \frac{\bar{\lambda}}{N^{D(D-1)}} \sum_{\mathbf{n}} \prod_k \phi_{\mathbf{n}_k}^{\bar{k}} \right)^q e^{S[\lambda, \bar{\lambda}]}, \quad (4.9)$$

for some q . The Feynman graphs are stranded graphs with d strands described as follows.

- They have two type of vertex: black and white, which represent the tensor variable and its complex conjugate.
- Each vertex of a graph has degree 4.
- To each of the vertices is adjacent one edge with a color label $1, \dots, d$. Each color is adjacent only once to each vertex. The resulting graph is therefore d -regular edge-colored, it thus has a GEM structure.
- The graphs are bipartite: black vertices are only linked to white vertices. This comes from the form of S_{quad} .
- The strands of the graphs are in correspondence with the 2-bubbles of the GEM corresponding to the colored graph. This is due to the specific form of $S_{\text{int}}[\lambda, \bar{\lambda}]$ in which every variable of color k contracts to every variable of the other colors.

Similarly to the matrix model case, we associate a variable λ to every black vertex, a $\bar{\lambda}$ to every white vertex. To every closed strand one associates a N factor. Then this formal integral leads to a generating series of GEM counted with respect to their number of vertices and 2-bubbles. This is physically motivated by the fact that one wants to make the correspondence between the volume of the triangulated manifold and its number of d -simplexes and the curvature and the dihedral angles around $(d-2)$ -simplexes of the triangulation.

However let us point out that this description still does not hold the promise of the title, namely to be the expansion of a random tensor model. For now we only see a set of random variables organized with the help of color indices.

4.3.2 Invariant random tensor model.

Another way to approach tensor models is to follow even more closely the way random matrix models are defined [BGR12]. This leads to another definition of tensor models and we will show later how these two approach are related. Matrix models are usually defined by the formal integration of *invariant* Boltzmann weights, the invariance being the invariance under a unitary change of basis. There is in fact for some models an additional invariance required, but this is not the one that generically restricts the form of the potential. This

4.3. RANDOM TENSOR MODELS AND COLORED GFT.

is rather an invariance which restricts the domain of integration. For instance in the case of unitary ensemble (not necessarily Gaussian), the potential is generically invariant under $GL(N, \mathbb{C})$, but the set of matrices one integrates on is invariant under the action of a smaller $U(N) \subset GL(N, \mathbb{C})$ group⁵. The generic invariance of the potential of matrix model is a $GL(N, \mathbb{C})$ ⁶. We will follow this idea to define random tensor models.

Consider a family $\{(V_i, h_i)\}_{i=1\dots d}$ of Hermitian spaces of dimension N_i (the real case is very similar and we forget about it). We write their duals as $\{V_i^*\}$. We set $\mathfrak{T} = \bigotimes_{i=1}^d V_i$ the tensor product of these vector spaces. There is a natural action of $GL(V_1) \times \dots \times GL(V_d)$ on it. An element $T \in \mathfrak{T}$ can be seen as a multi-linear form

$$T : V_1^* \times \dots \times V_d^* \rightarrow \mathbb{C}. \quad (4.10)$$

It can be written in a basis as:

$$T = \sum_{\{i_k\}_{k=1\dots d}} T_{i_1\dots i_d} \bar{u}_{i_1}^1 \otimes \dots \otimes \bar{u}_{i_d}^d, \quad (4.11)$$

where $\{\bar{u}_{i_k}^k\}_{i_k=1\dots N_k}$ is a basis of V_k . Its dual is denoted $\bar{T} \in \mathfrak{T}^*$:

$$\bar{T} = \sum_{\{i_k\}_{k=1\dots d}} \bar{T}_{i_1\dots i_d} u_{i_1}^1 \otimes \dots \otimes u_{i_d}^d, \quad (4.12)$$

with $\bar{u}_{i_k}^k = h_i(u_{i_k}^k, \cdot)$.

By an *invariant* of the tensor we actually mean a quantity (typically, polynomial in the coefficients) which is invariant under any change of basis of the V_i the dual change in V_i^* 's. If we change the basis by an element $g_i^{-1} \in GL(N_i, \mathbb{C})$ the coordinates of a vector $v_i \in V_i$ are changed by the matrix $U_i(g_i)$ of g_i and the coordinates of the dual vector are changed by $U_i(g_i^{-1}) = U_i^{-1}(g_i)$. This induces the change of basis in the tensor product space, and thus on tensors:

$$T'_{i_1\dots i_d} = \sum_{j_1\dots j_d} U_1(g_1^{-1})_{i_1 j_1} U_2(g_2^{-1})_{i_2 j_2} \dots U_d(g_d^{-1})_{i_d j_d} T_{j_1\dots j_d} \quad (4.13)$$

$$\bar{T}'_{i_1\dots i_d} = \sum_{j_1\dots j_d} U_1(g_1)_{i_1 j_1} U_2(g_2)_{i_2 j_2} \dots U_d(g_d)_{i_d j_d} \bar{T}_{j_1\dots j_d} \quad (4.14)$$

This observation allows us to describe the possible tensor invariants. The invariants of order $2p$ are p -linear in both T and \bar{T} . Using the transformation rule given above, one notices that the only requirement for the quantity to be invariant is that the indices of

⁵*i.e.* a Hermitian matrix is mapped to another hermitian matrix under a $U(N)$ transformation, this is no longer necessarily true for a $GL(N, \mathbb{C})$ transformation).

⁶That is why they deserve the name 'matrix models', otherwise they should be just 'array of numbers'.

4.3. RANDOM TENSOR MODELS AND COLORED GFT.

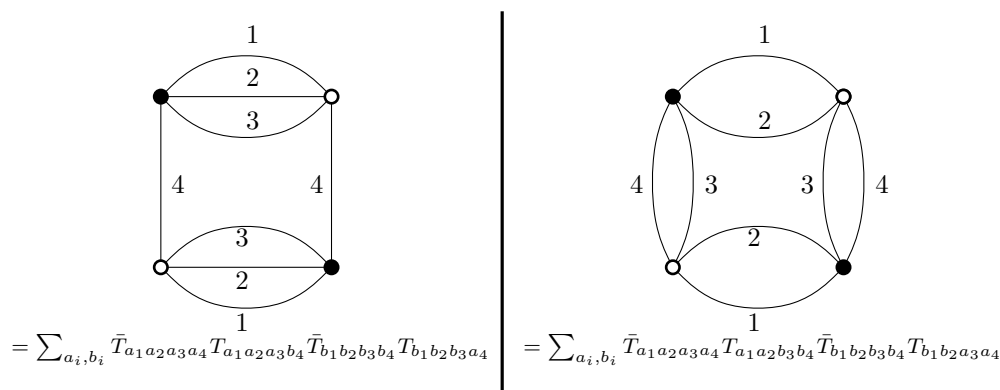


Figure 4.15: Examples of colored graphs indexing invariants of a rank 4 tensor.

a T should contract to the indices of a \bar{T} *respecting their position*, the first index of a T contracting with the first index of a \bar{T} and so on. Thus to describe an invariant of order $2p$ one only has to describe the contraction pattern of the p T 's with the p \bar{T} 's. This can be represented by bipartite graphs with colored edges. We adopt the convention that the T 's are represented by white vertices with D half-edges indexed from 1 to d representing the position of the indices of T and the \bar{T} 's by black vertices with D half-edges also indexed from 1 to d representing the position for the \bar{T} . The contraction of the j^{th} index of a T with the j^{th} of a \bar{T} is then represented by contracting the respecting half-edges in the graph. Thus the set of invariants of order $2p$ are represented by all bipartite regular graphs of valence d with a proper d -coloration of the edges.

We now define the degree of a colored graph.

Definition 15. The degree $\omega : \{d\text{-colored graphs}\} \rightarrow \mathbb{N}$ associates a positive integer to a d -colored graph \mathcal{G} by:

$$\omega(\mathcal{G}) = \sum_{\mathcal{J}(\mathcal{G})} g_{\mathcal{J}}, \quad (4.15)$$

i.e. it is the sum of the genera of all the jackets \mathcal{J} of \mathcal{G} .

This attaches an integer to any d -colored graph and consequently to any colored triangulation. A simple corollary of Theorem 5 comes with this definition.

Corollary 1. Let K be a knot in \mathbb{S}^3 which admits a diagram representation D_K with n crossings. Then there exists a colored triangulation T_K of $|K|$ satisfying $\omega(T_K) \leq 3(n+1)$.

Proof. The proof is a combination of Theorem 5 and Lemma 1 of [GR11]. In fact the algorithm produces a GEM with $8n$ vertices. Moreover there is a unique connected bubble

4.3. RANDOM TENSOR MODELS AND COLORED GFT.

of genus 1, all the others bubbles are of genus 0. Finally one can count the bubbles of color 3, and there are n of them. So we obtain

$$\omega(T_K) \leq \frac{1}{2}(8n - 2n) + 3 = 3n + 3 \quad (4.16)$$

□

These kinds of results will be interesting in some deeper study of the property of the degree. See the comments in subsection 4.3.3.

This is sufficient to define the generic 1-tensor model.

Definition 16. *The generic tensor model of dimension $d + 1$ is defined by the formal integral*

$$Z[N, \{t_{\mathcal{B}}\}] = \int dT d\bar{T} \exp\left(-N^{d-1} \sum_{\mathcal{B}} \frac{N^{-\frac{2}{(d-2)!}\omega(\mathcal{B})}}{|Aut(\mathcal{B})|} t_{\mathcal{B}} \mathcal{B}(T, \bar{T})\right), \quad (4.17)$$

where \mathcal{B} runs over the regular d -colored graphs indexing the invariants. The $t_{\mathcal{B}}$ are the coupling constants, the one corresponding to the only invariant of order 2 being generically fixed to one-half. $\mathcal{B}(\cdot, \cdot)$ being the invariant of T and \bar{T} indexed by the graph \mathcal{B} . $\omega(\mathcal{B})$ is the degree of \mathcal{B} .

Of course $Z[N, \{t_{\mathcal{B}}\}]$ has to be understood as a formal series in the counting variables $t_{\mathcal{B}}$, i.e. $Z[N, \{t_{\mathcal{B}}\}] \in \mathbb{C}[[V(\mathcal{B}) = \infty]]$, where we defined $\mathbb{C}[[V(\mathcal{B}) = \infty]]$ in a similar way than $\mathbb{C}[[\infty]]$. It is the inductive limit of the $\mathbb{C}[[\{t_{\mathcal{B}}\}_p]]$ such that the number of vertices $V(\mathcal{B})$ of type \mathcal{B} is smaller or equal to p . Indeed the number of vertices provides a filtrating order allowing us to take the inductive limit: $\mathbb{C}[[V(\mathcal{B}) = \infty]] = \varinjlim \mathbb{C}[[\{t_{\mathcal{B}}\}_p]]$. Finally let us note that we can consider the case in which the sum over the $t_{\mathcal{B}}$ is finite. Again this generating series has coefficients that are Gaussian integrals of the form $[\prod_{\mathcal{B}'} t_{\mathcal{B}'}^{q_{\mathcal{B}'}}] Z[N, \{t_{\mathcal{B}}\}]$:

$$\int dT d\bar{T} \prod_{\mathcal{B}'} \mathcal{B}'(\bar{T}, T)^{q_{\mathcal{B}'}} \exp\left(-\frac{N^{d-1}}{2} \sum_{i_1 \dots i_d} \bar{T}_{i_1 \dots i_d} T_{i_1 \dots i_d}\right). \quad (4.18)$$

We consider a simple example of one of these Gaussian integrals where \mathcal{B}' is an invariant of degree 4 in order to reveal the combinatorics of these integrals. First we compute the value of the only invariant of order 2.

$$\int dT d\bar{T} \bar{T}_{i_1 \dots i_d} T_{j_1 \dots j_d} \exp\left(-\frac{N^{d-1}}{2} \sum_{i_1 \dots i_d} \bar{T}_{i_1 \dots i_d} T_{i_1 \dots i_d}\right) = N^{1-d} \delta_{i_1 j_1} \dots \delta_{i_d j_d}. \quad (4.19)$$

We can now compute the invariant pictured at the left of Fig. 4.15.

$$\int dT d\bar{T} \sum_{\text{all indices}} \bar{T}_{i_1 i_2 \dots i_d} T_{j_1 i_2 \dots i_d} \bar{T}_{j_1 j_2 \dots j_d} T_{i_1 j_2 \dots j_d} \exp\left(-\frac{N^{d-1}}{2} \sum_{i_1 \dots i_d} \bar{T}_{i_1 \dots i_d} T_{i_1 \dots i_d}\right). \quad (4.20)$$

4.3. RANDOM TENSOR MODELS AND COLORED GFT.

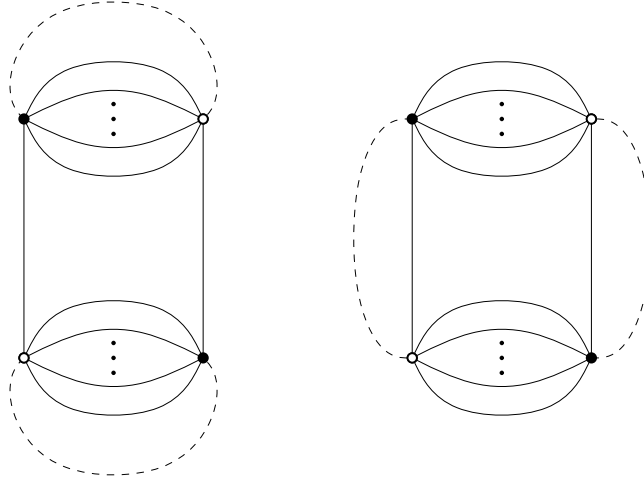


Figure 4.16: These graphs are examples of Wick contractions made out of a simple invariant. The dashed lines represent the extra line of color 0.

Applying Wick theorem:

$$\begin{aligned}
 & N^{2(1-d)} \sum_{\text{all indices.}} \langle \bar{T}_{i_1 i_2 \dots i_d} T_{j_1 i_2 \dots i_d} \rangle \langle \bar{T}_{j_1 j_2 \dots j_d} T_{i_1 j_2 \dots j_d} \rangle \\
 & + \langle \bar{T}_{i_1 i_2 \dots i_d} T_{i_1 j_2 \dots j_d} \rangle \langle \bar{T}_{j_1 j_2 \dots j_d} T_{j_1 i_2 \dots i_d} \rangle
 \end{aligned} \tag{4.21}$$

First term of the sum gives $N^{2(1-d)} N^{1+2(d-1)} = N$. The second term leads to $N^{2(1-d)} N^{2+(d-1)} = N^{3-d}$. So one gets $N + 1$. A moment of reflection reveals that these two terms can be represented by Feynman graphs. They are obtained by considering the graphs representing tensor invariants as vertices and by making Wick contractions between black and white vertices with extra lines of color zero. The weight associated to these graphs are as follows:

- each edge of color 0 comes with a factor $\frac{1}{N^{d-1}}$.
- each face of color 0 i for $i \in \llbracket 1, d \rrbracket$ comes with a factor of N .
- each vertex \mathcal{B} (*i.e.* connected component of color different from zero) comes with a factor $N^{-\frac{2}{(d-2)!} \omega(\mathcal{B})}$.

Applying these rules one can recover the result of the example. The first term is represented as the leftmost graph of Fig. 4.16 while the second is represented as the rightmost graph of Fig. 4.16. Actually one can also compute formal expectation values of invariants as

$$\langle B(\bar{T}, T) \rangle = \int dT d\bar{T} B(\bar{T}, T) \exp \left(-N^{d-1} \sum_{\mathcal{B}} \frac{N^{-\frac{2}{(d-2)!} \omega(\mathcal{B})}}{|Aut(\mathcal{B})|} t_{\mathcal{B}} \mathcal{B}(T, \bar{T}) \right). \tag{4.22}$$

4.3. RANDOM TENSOR MODELS AND COLORED GFT.

These expectation values generate family of graphs with a marked sub-graph B and can be computed as derivatives of $Z[\{t_B\}]$. These graphs can be interpreted as dual graphs of ideal colored triangulations of a (pseudo-)manifold with boundary the surface triangulated by B (where boundary means *ideal* boundary). We can represent the corresponding vertices in the triangulation as hollow vertices of truncated tetrahedra.

4.3.3 Comments.

After this presentation some questions emerge.

- After exploring the problems of rigorously associating triangulations to manifolds, we have seen that one can provide a much better graphical solution when restricting to colored triangulations. This graphical description is well suited to the language of field theory, and allows one to write an integral representation for generating series of such colored triangulations. The weight of such triangulation mimics in a very close way the weight in the case of 2 dimensional triangulations. So one could ask whether or not it is sufficient to understand properly a theory of emergent/random geometry in more than two dimensions. In fact the three dimensional geometry, though simpler than the higher dimensional case, is already much richer than the two dimensional case. So it may be an over-simplification to try to probe this richness of three-dimensional geometry with so simple weights.
- Indeed there exists several ways of providing generating series of colored triangulations. The first one we described is by the use of several fields. It can be related to the second one by integrating out all of them but one. Nevertheless it is only possible in this way to explore a small part of the parameter space of the theory. In fact, the invariant theory will then have equal couplings for invariant that differ only through color permutations: $t_B = (\bar{\lambda}\lambda)^{p(B)}$. A natural question then arises. Is there a way to reconcile entirely these two formulations? There exists something similar in the context of Hermitian matrix models. One can in fact formulate the generic Hermitian one matrix model in the limit of a big size matrix as a matrix model with a $\text{Tr } M^4$ interaction and a non-trivial covariance (similar to the Kontsevitch model). We still consider the case of large matrices. The non trivial covariance is what allows one to probe the parameter space.
- The construction of invariant random tensor models may seem very similar to the construction of matrix models, as it is guided by the principle that the action shall be invariant with respect to change of basis. Yet, it differs in some noticeable way. In fact when considering the matrix models, we distinguish between several "ensembles", that are invariant with respect to the *adjoint* actions of, for instance, $O(N), U(N), Sp(2N)$. The action of these models is always invariant with respect to the group of linear transformation. But, the set of integration is not, and in fact

4.3. RANDOM TENSOR MODELS AND COLORED GFT.

one integrates on the Lie algebra of the respective invariance groups (as the model is invariant with respect to the *adjoint* action of the orthogonal, unitary or symplectic group). There is no such structure in the case of tensor models. Indeed one integrates on $(\mathbb{C}^N)^{\otimes d}$, and this set is invariant under the action of the tensor products of fundamental representations of $GL(N, \mathbb{C})$. Consequently it resembles to a vector model at this level and as we will see later this may be a clue of what we obtain in the $N \rightarrow \infty$ limit in the next chapter. Moreover, generalizing the invariance under the adjoint action in a proper way may answer to the combinatorial questions of representing generating series of generic triangulations, not just colored.

- To end this series of remarks let us notice that the meaning of the parameter controlling the $1/N$ expansion (the degree) is not clear *a priori*, even though it collapses to the genus in the two dimensional case. However, its definition can be generalized so that it can be attached to any (pseudo-)triangulations of any pseudo-manifolds in any dimension. In the particular three dimensional case it is possible to attach a half-integer to any manifold, this number being formed from the degrees of its triangulations. This provides a filtration of the space of three dimensional manifolds in a way that is very similar to filtrations obtained thanks to quantities such as the Matveev complexity, the Gromov norm or the Heegaard genus. The properties of this filtration are under investigation, but I conjecture it can be thought as a new measure of complexity, with the conjectural property of finiteness. This finiteness property is what turns the Matveev complexity into an interesting quantity when it comes to classification of 3-manifolds⁷.

4.4 More figures.

We show here examples of knot complements GEM representations with ideal boundary.

⁷In fact the Heegaard genus and the Gromov norm do not possess this finiteness property. There are for example, infinitely many 3-manifolds of Heegaard genus $g_H = 2$.

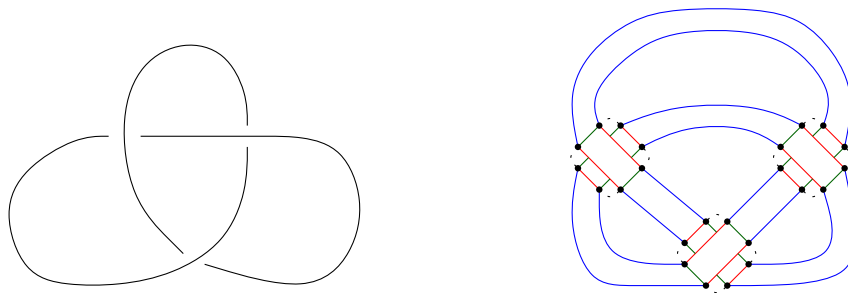


Figure 4.17: A trefoil knot diagram and a GEM representation of the triangulation of its complement in S^3 with ideal boundary are shown. One can read the GEM representation directly from the diagram. The convention is that color 0 = dotted lines, 1 = red, 2 = green, 3 = blue. The black dots are the vertices of the GEM graphs.

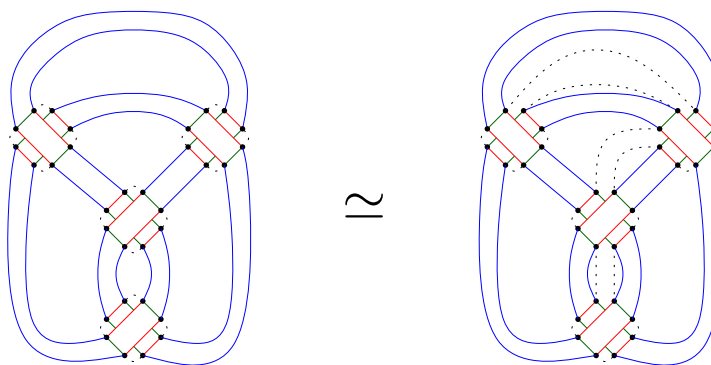


Figure 4.18: On the left a GEM of the Figure eight knot complement obtained by application of the algorithm. On the right another GEM of the same knot complement obtained by enhancing a bit the algorithm on the basis of this specific case. We connect the half-lines of color 0 in a different way that still produces a Figure eight complement but with less bubbles of color three and thus with a smaller degree. Moreover on the rightmost GEM one easily notices several two dipoles that can be reduced lowering the degree by one at each reduction.

4.4. MORE FIGURES.

Chapter 5

Single Scaling Limit of Tensor Models

After introducing the colored random tensor models we will express the problem of the $1/N$ expansion for tensor models. This is done by discussing this expansion in several settings for colored models, and also for a model generating the so-called *multi-orientable* 2-cell complexes. The leading behaviour of these models is recalled and further results about the sub-leading terms of these developments established. We end this chapter with a few comments on the physics and combinatorics.

5.1 $1/N$ expansion of multi-tensor models

5.1.1 Setting the $1/N$ expansion

In this section we recall the results obtained in [Gur11c, Gur11b, Gur12a] concerning the expansion of multi-tensor models. We recall here the definition of this multi-tensor model. Set ϕ_{i_1, \dots, i_d}^k a set of N^d complex random variables with i_α ranging from 1 to N for $k \in \llbracket 0, d \rrbracket$. Consider the following

$$S_{\text{quad}} = - \sum_k \sum_{\mathbf{n}_k} \bar{\phi}_{\mathbf{n}_k}^k \phi_{\mathbf{n}_k}^k \quad (5.1)$$

$$S_{\text{int}}[\lambda, \bar{\lambda}] = \frac{\lambda}{N^{D(D-1)}} \sum_{\mathbf{n}} \prod_k \phi_{\mathbf{n}_k}^k + \frac{\bar{\lambda}}{N^{D(D-1)}} \sum_{\mathbf{n}} \prod_k \bar{\phi}_{\mathbf{n}_k}^k \quad (5.2)$$

$$S[\lambda, \bar{\lambda}] = S_{\text{quad}} + S_{\text{int}}[\lambda, \bar{\lambda}]. \quad (5.3)$$

The model is then defined by the generating series:

$$Z[\lambda, \bar{\lambda}] = \int \prod_k d\phi^k d\bar{\phi}^k \exp(S_{\text{quad}} + S_{\text{int}}[\lambda, \bar{\lambda}]). \quad (5.4)$$

The quantity of interest is $F[\lambda, \bar{\lambda}] = -\log(Z[\lambda, \bar{\lambda}])$ generating connected graphs. What has been shown in [Gur11b, Gur12a] is that F can also be expanded in $1/N$, N being the size of the corresponding array of numbers. In fact these models also produce formal series in $1/N$ as the coefficients in front of each power of $1/N$ ranging from $-d$ to $+\infty$ are finite for a certain range of values of $\lambda, \bar{\lambda}$. In particular, F can be represented as a formal series of the form

$$F[\lambda, \bar{\lambda}] = \sum_{\omega \in \mathbb{N}} N^{d - \frac{2}{(d-1)!}} C^{[\omega]}(\lambda, \bar{\lambda}), \quad (5.5)$$

where $C^{[\omega]}(\lambda, \bar{\lambda})$ is given by:

$$C^{[\omega]}(\lambda, \bar{\lambda}) = \sum_{\mathcal{G} | \omega(\mathcal{G}) = \omega} (\lambda \bar{\lambda})^{p(\mathcal{G})}. \quad (5.6)$$

These coefficients can be seen as being finite in a certain domain for $z = \lambda \bar{\lambda}$ (and thus the $1/N$ expansion exists). Indeed for each value of ω one can choose a jacket \mathcal{J} such that $g_{\mathcal{J}} \leq \omega$ for any \mathcal{J} . The number of graphs $n_{G_{\mathcal{J}}}$ with a jacket of genus $g_{\mathcal{J}}$ is exponentially bounded in $g_{\mathcal{J}}$, $n_{G_{\mathcal{J}}} \leq K(g_{\mathcal{J}})^p$, thus the number of graphs m_{ω} with degree ω is exponentially bounded in ω , $m_{\omega} \leq K'(\omega)^p$. Consequently the $C^{[\omega]}$ exist as functions of $\lambda \bar{\lambda}$. F is then a formal series in $N, 1/N$.

The first term of this expansion can be computed. In fact the leading graphs are the so-called (colored) melonic graphs [BGRR11]. The proof is similar (but with further simplifications) to the one described in Section 5.2.

Definition 17. *We call the colored graphs \mathcal{G} such that $\omega(\mathcal{G}) = 0$ the (colored) melonic graphs.*

At the geometric level the melonic graphs are GEM representations of the sphere \mathbb{S}^d . This is easy to prove, as they can be reduced to the only GEM with two vertices, which represents a sphere, by d -dipole moves¹.

The melonic graphs can be built recursively by inserting d -dipoles on the edges of the unique colored graphs with two vertices [BGRR11, GS13].

Melonic graphs with a marked edge can be put in bijection with d -ary trees [BGRR11]. This is done as follows. Consider the smallest colored graph \mathcal{G} with a marked edge. This is a melonic graph. Set, without loss of generality, that this marked edge has color 0. It is adjacent to two vertices v, \bar{v} . There is a natural orientation on this graph $v \rightarrow \bar{v}$. Consider this melon with its marked edges, represent it as a marked vertex V with $d+1$ leaves colored 0 up to d , then

- when inserting a d -dipoles of color i on this smallest melon, change the univalent vertex of the leaf with color i into a vertex with $d+2$ adjacent edges, $d+1$ being new leaves colored from 0 to d .

¹Also they, since their degree is 0 they are triangulations of regular genus 0 d -manifolds, and so they are spheres in any dimension d [Fer82].

5.1. $1/N$ EXPANSION OF MULTI-TENSOR MODELS

- each times one inserts a d -dipole on an edge of this new graph, one changes the corresponding univalent vertex into a $d+2$ valent vertex with $d+1$ leaves. The order of insertion of d -dipoles along edges of the original 2 vertices graph should respect the initial orientation of the edges of the graph, *i.e.* from v to \bar{v} .
- when inserting d -dipoles on the marked edge of color 0, the new marked edge is chosen (arbitrarily) to be the edge attached to v .

It is easy to check that this is really a bijection. One can write a functional relation for the generating series $G(z = \lambda\bar{\lambda})$ of these graphs from this algorithm. Then the coefficient of the first order in z of this generating series is 1. Moreover, we have seen that melons can be obtained by insertions of d -dipoles on the edges of this unique melonic graph. But a d -dipole is nothing but a 2-vertices melonic graph with a marked edge. Moreover a d -dipole has two vertices weighted respectively by λ and $\bar{\lambda}$. Lastly, one has $d+1$ choices to insert a d -dipole on the edges of the 2-vertices melonic graph. Then one deduces the following functional relation

$$G(z) = 1 + zG(z)^{d+1}. \quad (5.7)$$

One can find the critical points of this equation:

$$dz = -d \frac{dG}{G^{d+1}} + (d+1) \frac{dG}{G^{d+2}}. \quad (5.8)$$

At criticality, $dz = 0$, thus one has

$$G_c = \frac{d+1}{d}. \quad (5.9)$$

One thus finds

$$\frac{d+1}{d} = 1 + z_c \left(\frac{d+1}{d} \right)^{d+1}, \quad (5.10)$$

i.e. $z_c = \frac{d^d}{(d+1)^{d+1}}$. The combinatorial solution of this equation is unique², regular at $z = 0$ and writes $G_{\text{comb}}(z) = \sum_{p=0} a_p z^p$

$$\begin{cases} a_0 = 1, \\ a_p = \sum_{\{q_i\}_{i=1 \dots d+1} | \sum q_i = p} a_{q_1} \cdots a_{q_{d+1}}, \text{ for } p > 0. \end{cases} \quad (5.11)$$

This recursion is solved by Fuss-Catalan numbers $a_p = \frac{1}{dp+1} \binom{(d+1)p}{p}$. This can be showed by setting $\varsigma = G_{\text{comb}}(z)$

$$\frac{\varsigma - 1}{\varsigma^{d+1}} = z, \quad (5.12)$$

²Uniqueness follows from the unicity of the power series expansion.

5.1. $1/N$ EXPANSION OF MULTI-TENSOR MODELS

then

$$a_p = \frac{1}{2i\pi} \int_{C_0} \frac{G_{\text{comb}}(z)}{z^{p+1}} dz = \int_{C_1} \left((-d) \frac{\varsigma^{p(d+1)+1}}{(\varsigma-1)^{p+1}} + (d+1) \frac{\varsigma^{p(d+1)}}{(\varsigma-1)^{p+1}} \right) d\varsigma, \quad (5.13)$$

where C_0 is a small contour of radius $r < |z_c|$ surrounding 0 and C_1 a small contour surrounding 1. Noticing

$$\begin{aligned} \varsigma^{p(d+1)+1} &= \sum_{k=0}^{p(d+1)+1} \binom{p(d+1)+1}{k} (\varsigma-1)^k \\ \varsigma^{p(d+1)} &= \sum_{k=0}^{p(d+1)} \binom{p(d+1)}{k} (\varsigma-1)^k, \end{aligned}$$

we get

$$\begin{aligned} a_p &= -d \binom{p(d+1)+1}{p} + (d+1) \binom{p(d+1)}{p} \\ &= \frac{1}{pd+1} \binom{p(d+1)}{p}. \end{aligned} \quad (5.14)$$

From this result we can compute the critical exponent of $G_{\text{comb}}(z) \sim_{\text{critical}} (z - z_c)^{1/2}$.

5.1.2 Next-to-leading order

Finding the leading term amounts to find the cardinality of the set of graphs with a marked edge, n vertices and degree $\omega = \frac{(d-1)!}{2}(d-2)$ [KOR14b]. We denote this set of graph $\mathbf{T}_{p,NLO}$, where NLO stands for Next-to-Leading Order. We sketch below the ideas used to compute this contribution.

As stated in Chapter 4, all colored graphs can be constructed from crystallizations by inserting 1-dipoles. This is of great use for us. In fact, we can easily construct a list of NLO crystallizations. All these crystallizations are obtained by considering the fundamental melon graph and performing a 2-dipole insertion in this graph. There are $\binom{d+1}{2}$ possibilities for such an insertion. Therefore there are $\binom{d+1}{2}$ crystallizations of degree $\frac{(d-1)!}{2}(d-2)$ in dimension d . See Figure 5.1.

We first consider the $1PI$ graphs, or in a combinatorial language the *bridgeless* graphs. The generating series of bridgeless colored graphs with a marked edge is denoted $\Sigma(z, N)$. We have the following well known relation:

$$G(z, N) = (1 - \Sigma(z, N))^{-1}. \quad (5.15)$$

5.1. $1/N$ EXPANSION OF MULTI-TENSOR MODELS

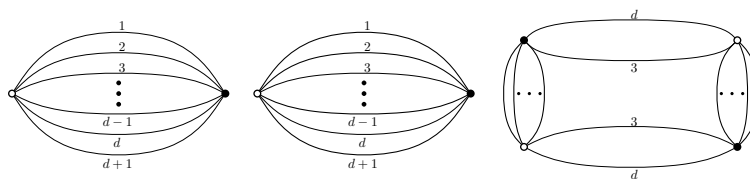


Figure 5.1: On the left the fundamental melon. The middle graph shows a possible choice of edges for a 2-dipole creation. The chosen edges are the light lines. On the right the graph after the creation of the 2-dipole associated to this choice of edges.

By expanding the relation, and matching the $1/N$ term, one finds:

$$\begin{aligned} G_0(z) &= \frac{1}{1 - \Sigma_0(z)}, \\ G_1(z) &= G_0(z) \Sigma_1 G_0(z). \end{aligned} \quad (5.16)$$

We now consider the different possibilities for constructing these graphs. First we fix our choice of marked edge. It is chosen to be a line of color 0. There are basically three cases contributing to Σ_1 :

- either we have the fundamental melon with a marked edge of color 0, and we insert a *NLO* graph with a marked edge of color $i \neq 0$ onto an edge of color i of the marked fundamental melon,
- or we consider an *NLO* crystallization of species $\{0i\}$ with a marked edge of color zero and we insert a melonic graph with 2 marked edges of color i by breaking the 2 edges of color i of the crystallization,
- or lastly, we start from a crystallization of species $\{ij\}$ with $i, j \neq 0$. We choose to insert a melonic graph with 2 marked edges of a color chosen among i and j breaking the corresponding chosen edges of the crystallization.

After some algebra this can be translated as a closed equation at the level of generating series of graphs with marked edges:

$$G_1(z) = \frac{\frac{d(d+1)}{2} z^2 G_0(z)^{2d+2}}{(G_0(z) - 2)(1 - dz G_0(z))}. \quad (5.17)$$

In the next section we describe another model. It generates Feynman graphs that are 2-cell complexes. They are also called Euler combinatorial maps by combinatorists, since they have the structure of a three dimensional combinatorial map with Euler type conditions for the gluing of their vertices [FT14]. At the level of combinatorics they can be seen as richer, since as we will see, they contain all the 3-dimensional colored graphs.

5.1. $1/N$ EXPANSION OF MULTI-TENSOR MODELS

5.2 Expansion of multi-orientable model

We study the extension of $1/N$ expansion for multi-orientable models. This is mainly based on the paper [DRT14].

5.2.1 Definition of the model

We introduce the i.i.d., m.o. model and we study its symmetries. We consider a complex field ϕ taking values in a tensor product of three vector spaces $W = E_1 \otimes E_2 \otimes E_3$. Suppose we have a Hermitian or real scalar product in each E_i , $i = 1, 2, 3$. In analogy with complex matrices, we would like to introduce a Hermitian conjugation for the field ϕ . Since in any orthonormal basis, the field has three indices, there is no canonical notion of transposition. Nevertheless, giving a special role to the indices 1 and 3, which we call *outer* indices, we can define a tensor field $\hat{\phi}$ *via* the relation $\hat{\phi}_{kji} = \bar{\phi}_{ijk}$. In the limit of zero dimension for E_2 we recover the usual matrix model conjugation.

A natural action for such a tensor model is:

$$S[\phi] = S_0[\phi] + S_{int}[\phi],$$

$$S_0[\phi] = \frac{1}{2} \sum_{i,j,k} \hat{\phi}_{kji} \phi_{ijk}, \quad S_{int}[\phi] = \frac{\lambda}{4} \sum_{i,j,k,i',j',k'} \phi_{ijk} \hat{\phi}_{ij'k'} \phi_{k'ji'} \hat{\phi}_{i'j'k}. \quad (5.18)$$

Let us emphasize that the quadratic part of the action thus defined is positive. A second remark is that the transposition of the outer indices in the definition of $\hat{\phi}$ implies that $\hat{\phi} \in E_3 \otimes E_2 \otimes E_1$ ³. The index contractions impose no additional constraints on the space W .

Let us now suppose that each vector space E_i carries a representation of a Lie group G_i . The tensor product W then carries a natural representation of the group $G_1 \times G_2 \times G_3$ namely the tensor product representation. More explicitly, in a given basis the field transforms as

$$\phi'_{ijk} = \rho_1(g_1)_{ii'} \rho_2(g_2)_{jj'} \rho_3(g_3)_{kk'} \phi_{i'j'k'}, \quad (5.19)$$

$$\overline{\phi'_{ijk}} = \overline{\rho_1(g_1)_{ii'}} \overline{\rho_2(g_2)_{jj'}} \overline{\rho_3(g_3)_{kk'}} \overline{\phi_{i'j'k'}}, \quad (5.20)$$

where ρ are the matrices of the group representations. The corresponding transformation on $\hat{\phi}$ is:

$$\hat{\phi}'_{ijk} = \overline{\rho_3(g_3)_{ii'}} \overline{\rho_2(g_2)_{jj'}} \overline{\rho_1(g_1)_{kk'}} \hat{\phi}_{i'j'k'}. \quad (5.21)$$

The natural invariance of the quadratic part in (5.18) is under the unitary groups $G_i = U(N_i)$. However the interaction term restrains this invariance. The contraction of the second index of a ϕ (resp. $\hat{\phi}$) with the second index of a ϕ (resp. $\hat{\phi}$) field imposes G_2

³We can remark here that $\hat{\phi}$ could be interpreted as an object living in the dual of W , but the Hermitian product provides a canonical isomorphism between W and its dual.

5.2. EXPANSION OF MULTI-ORIENTABLE MODEL

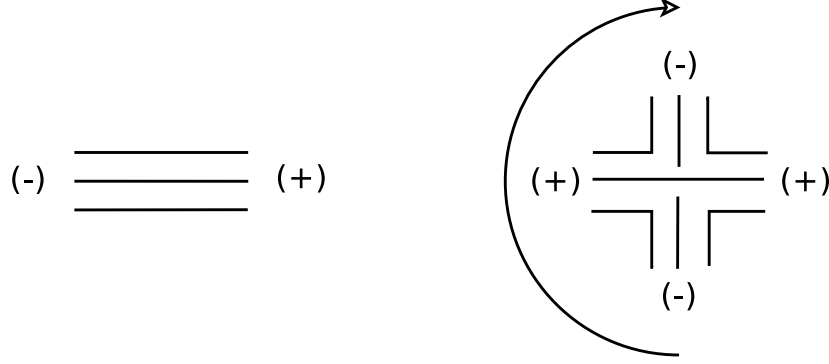


Figure 5.2: Propagator and vertex of the m.o. model.

to be an orthogonal group $O(N_2)$. The action of the m.o. model is thus invariant under $U(N_1) \times O(N_2) \times U(N_3)$, and natural m.o. models have a real rather than Hermitian scalar product on a real inner space E_2 . The spaces E_1 and E_3 could be either complex or real, in which case the invariance is $O(N_1) \times O(N_2) \times O(N_3)$.

In the limit of vanishing dimension for E_2 one recovers the matrix model action

$$S[M] = \frac{1}{2} \text{Tr}[M^\dagger M] + \frac{\lambda}{4} \text{Tr}[(M^\dagger M)^2]. \quad (5.22)$$

This provides a natural interpolation between random tensors and random matrix models. In fact this is also true for a colored model in which one of the vector space's dimension vanishes. We obtain a Hermitian matrix model with a quartic interaction. For other vanishing dimensions one does not get a matrix model but a model which is not invariant under the adjoint action of a (matrix) Lie group.

The Feynman graphs associated to the action (5.18) are built from the propagator and the vertex of Figure 5.2. These Feynman graphs are stranded graphs but contrary to the colored graphs they don't have the full homology turning them into representation of 3-manifolds. The strands represent the indices of the tensor field (analogous to ribbon boundaries in the case of the ribbon graphs of matrix models). The (+) and (-) signs appearing at the vertex represent (respectively) the ϕ and $\hat{\phi}$ fields occurring in the interaction term of the action. The propagator has no twist on the strands (as a consequence of the form of the quadratic part of the action). The order of the strands (representing indices) at the vertex is induced by the choice of a cyclic orientation around the vertex. As in [Tan12], we call these Feynman graphs m.o. graphs. They are stranded graphs for which there exists a labeling with (+) and (-) at the vertices such that an edge always connects a (+) sign with a (-) sign, hence edges are *oriented*.

Finally we equate the dimensions of the three spaces $N_1 = N_2 = N_3 = N$ in order to

5.2. EXPANSION OF MULTI-ORIENTABLE MODEL

perform a $1/N$ expansion⁴. The GFT case corresponds to these three spaces being finite dimensional truncations of $L_2(G)$ where G is a compact Lie group. Indeed, a compact Lie group has a unique Haar measure and a unique corresponding infinite dimensional space of square integrable function $L_2(G)$. A finite dimensional truncation $E_i = L_2^\Lambda(G)$ of this space can be obtained by retaining Fourier modes (or characters in the Peter-Weyl expansion) up to some cutoff Λ . This space is finite dimensional and is Hilbertian (since it inherits the Hermitian product of $L_2(G)$). For instance, in the simplest case of the group $U(1)$, the truncation which retains modes $n \in \mathbb{Z}$ with $|n| \leq \Lambda$ correspond to a space $L_2^\Lambda(U(1))$ of dimension $N = 2\Lambda + 1$.

5.2.2 Classification of Feynman graphs

In order to understand the $1/N$ expansion of this model we have to make some classification of the generated Feynman graphs with respect to different combinatorial characteristics. The partition function of the m.o. model is given by:

$$Z(\lambda) = \int \mathcal{D}\phi e^{-S[\phi]} = e^{-F(\lambda)}. \quad (5.23)$$

As usual the quantity of interest is its logarithm (up to some normalization),

$$F(\lambda) = -\ln[Z(\lambda)] = \sum_{\mathcal{G}} \frac{1}{s(\mathcal{G})} A(\mathcal{G}), \quad (5.24)$$

where the sum runs over connected vacuum m.o. Feynman graphs \mathcal{G} . From now on we consider only vacuum connected graphs.

Since we do not allow twists on the edges of these models, there is a one-to-one correspondence between these CW-complexes and graphs. We can thus apply to these objects several results known from graph theory. We call *four-edge colorable* a graph for which the edge chromatic number is equal to four.

Proposition 2. *The set of Feynman graphs generated by the 3-dimensional colored action of Section 5.1 is a strict subset of the set of Feynman graphs generated by the m.o. action (5.18).*

Proof. As already mentioned above, the action (5.1) generates Feynman graphs with exactly two colors on each face. The m.o. action (5.18) generates graphs which are four-edge colorable, but with faces having more than two colors in any coloring choice. An example of such a graph is given in Figure 5.5 right. Hence, the m.o. graphs form a strictly larger class than the colored graphs. \square

Since the generated graphs have maximal incidence number equal to four, we have:

⁴In GFT a stronger restriction $E_1 = E_2 = E_3$ is required, because models such as the Boulatov model [Bou92] include a projector which averages over a common action on these spaces.

5.2. EXPANSION OF MULTI-ORIENTABLE MODEL

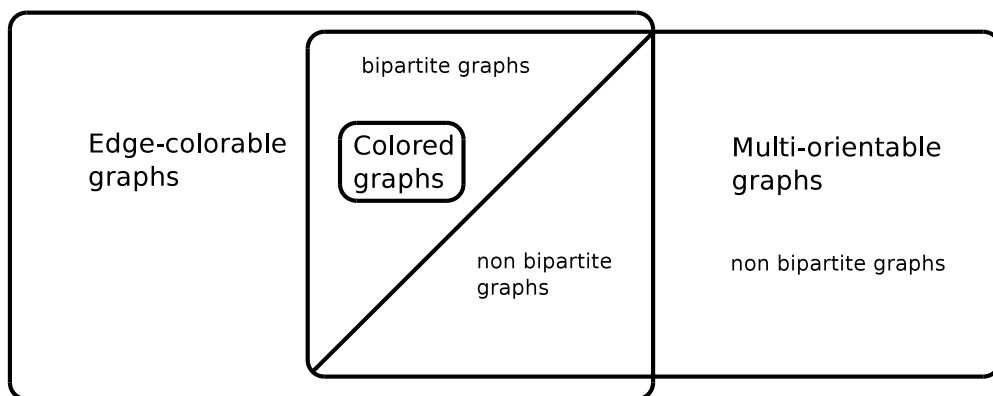


Figure 5.3: Tensor graphs classification.

Proposition 3. *A bipartite graph is four-edge colorable.*

Proof. The proof is a direct consequence of Theorem 2 of Chapter 12 of [Ber73], which states that the chromatic number of a bipartite graph⁵ is equal to the maximum degree of its vertices. In our case all vertices have constant degree equal to four. Then all bipartite graphs appearing in the multi-orientable model are four-edge colorable. \square

We then get the classification of Figure 5.3. Let us also give some examples of different graphs appearing in each subset of this classification, see Figures 5.4, 5.5, 5.6 and 5.7. An important example is the one of Figure 5.7 - a graph without tadface (a tadface being a face “going” several times through the same edge) which is not m.o. . Let us recall that the condition of multi-orientability discards tadfaces (see Theorem 3.1 of [Tan12]). Figure 5.5 left gives an example of a m.o. graph which is non bipartite (and non colorable). Figure 5.5 right gives an example of a graph which is 4-edge colorable and multi-orientable but not colorable in the sense of action (5.1). In fact one can check that it has two faces with four colors, hence this graph cannot be generated by the action of the colored tensor model.

One last example is the graph of Figure 5.7. It can be drawn on the torus (the side of the box having the same types of arrows being identified). This graph has no tadface and yet is not multi-orientable. As checked later it has no well-defined jackets.

5.2.3 Combinatorial and topological tools

As we have seen, in the colored case the $1/N$ expansion [Gur11b] relies on the notion of jackets. In the multi-orientable case we want to implement a similar $1/N$ expansion, hence we need to generalize the notion of jackets. We remark that six strands meet at any vertex v . In the most general case of all CW-complexes there is no way to split them

⁵The theorem is stated for bipartite multigraphs.

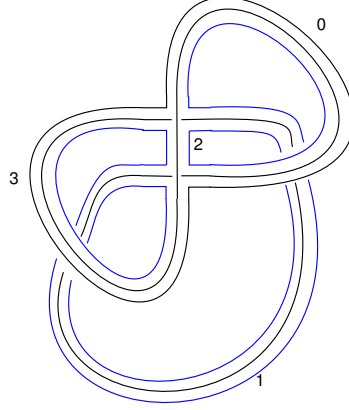


Figure 5.4: Example of a graph with a tadface which is edge-colorable. The tadface line is shown in blue. The numbers 0, 1, 2, 3 are the color labels of the edges.

into three pairs a_v, b_v, c_v in a coherent way throughout the graph, namely in such a way that any face is made out only of strands of the *same type*, a , b or c (see Figure 5.7 for an example of a stranded graph where such a splitting is impossible). In the m.o. case, such a coherent splitting is possible. Indeed at each vertex the inner pair of strands (those acting on the E_2 space) is unique and well-defined. Let us say that this pair has type c . This pair is coherent, that is throughout the graph any face containing an inner strand is made of inner strands only. But we can also split at each vertex the four outer strands, or “corner strands”, into two coherent pairs, of *opposite strands*. Consider indeed a vertex and turn clockwise around it starting at the inner strand of a $\hat{\phi}$ field, as shown on Figure 5.8. We call the first and third corner strands we meet corners of type a , and the second and fourth corner strands of type b . Thus the opposite strands at any vertex all have the same label (see Figure 5.9). Since in a multi-orientable graph all vertices have canonical orientation, any a (respectively b type) type corner of a vertex always connects to an a (resp. b) type corner of another vertex, hence faces made out of outer strands are made either entirely of a strands or entirely of b strands. This can be understood also because the a strand correspond to the space E_3 in W and the b strands to the space E_1 . The theory is consistent even for $E_1 \neq E_3$, hence cannot branch together strands of type a with strands of type b . Remark also that each edge contains three strands of the three different types, a , b and c .

Strand type allows one to define the three *jackets* \bar{a} , \bar{b} and \bar{c} of an m.o. tensor graph:

Definition 18. A *jacket* of an m.o. graph is the graph made by excluding one type of strands throughout the graph. The outer jacket \bar{c} is made of all outer strands, or equivalently excludes the inner strands; jacket \bar{a} excludes all strands of type a and jacket \bar{b} excludes all strands of type b .

5.2. EXPANSION OF MULTI-ORIENTABLE MODEL

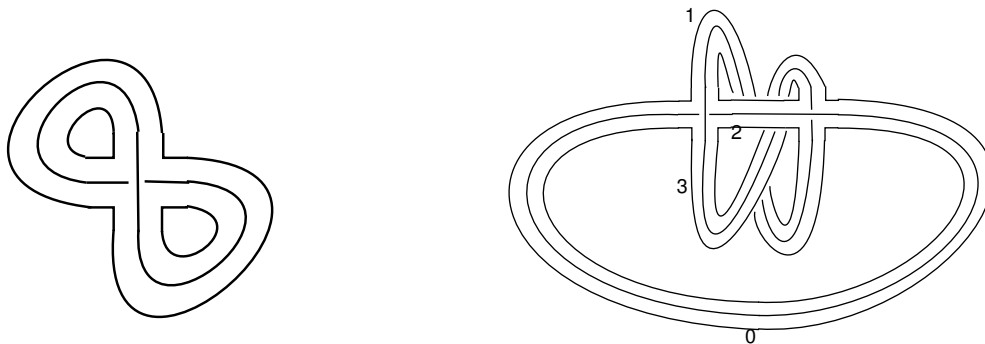


Figure 5.5: On the left one can see the planar double tadpole as an example of a m.o. graph which is not colorable. On the right is pictured the "twisted sunshine" as an example of a m.o. graph which is 4-edge colorable but does not occur in colorable models.

This definition together with the preceding paragraph leads to Proposition 4.

Figure 5.10 gives an example of a m.o. graph with its three jackets. The rest of this section is devoted to the following Proposition 4:

Proposition 4. *Any jacket of a m.o. graph is a (connected vacuum) ribbon graph (with uniform degree 4 at each vertex).*

Let us emphasize that Proposition 4 does not hold for general non-m.o. graphs, for example in the case of a graph with a tadface (see Figure 5.11).

Let us now give more explanations on this issue. *A priori* a 2-stranded graph may not be a ribbon graph because vertices may be *twisted*. Remark that this cannot happen for the outer jacket but may happen for the two others, see Figure 5.10. In that case we just have to untwist the vertices coherently throughout the whole graph (*i.e.* keeping the same set of faces and the same adjacency relations), as shown in Figure 5.12. This untwisting procedure can be performed by labelling the strands, then cutting the edges around the twisted vertex, untwisting the vertex and then reconnecting the strands respecting the labeling of the strands. This last step may twist the new edges, but since these twists are introduced locally around the vertex the procedure can be continued coherently on all the vertices of the graph, resulting in as much twists as necessary along the edges.

Recall that ribbon graphs can represent either orientable or non-orientable surfaces. Since the adjacency relation are invariant under the untwisting procedure, we can compute their Euler characteristic directly on the jacket independently of whether their vertices are twisted or not. Recall again that the Euler characteristic is related to the non-orientable genus k through $\chi(\mathcal{J}) = v - e + f = 2 - k$, where k is the non-orientable genus, v is the number of vertices, e the number of edges and f the number of faces. When the surface

5.2. EXPANSION OF MULTI-ORIENTABLE MODEL

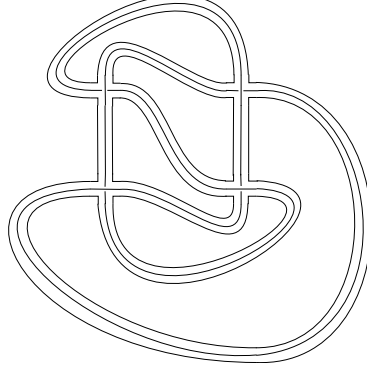


Figure 5.6: A 4-edge colorable m.o. graph which is not bipartite.

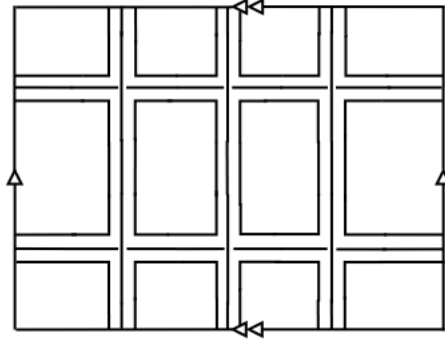


Figure 5.7: A graph without tadface which is not m.o. Edges of the box are identified so that the graph is drawn on the torus.

is orientable, k is even and equal to twice the usual orientable genus g (so that we recover the usual relation $\chi(\mathcal{J}) = 2 - 2g$).

We give a slightly more general definition of the degree suited to m.o. graphs. The *degree* of a m.o. graph \mathcal{G} is given by:

Definition 19. *Given a multi-orientable graph \mathcal{G} , its degree $\varpi(\mathcal{G})$ is defined by*

$$\varpi(\mathcal{G}) = \sum_{\mathcal{J}} \frac{k_{\mathcal{J}}}{2},$$

the sum over \mathcal{J} running over the three jackets of \mathcal{G} .

In the colored case, all jackets are orientable and this formula gives back the colored degree. We also notice that the degree is a positive integer or half-integer.

5.2. EXPANSION OF MULTI-ORIENTABLE MODEL

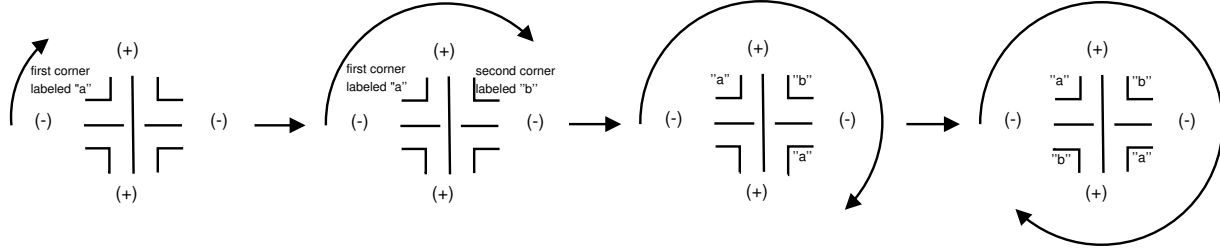


Figure 5.8: Labeling procedure of a m.o. vertex.

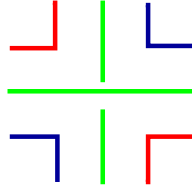


Figure 5.9: This figure shows the three pairs of opposite corner strands at a vertex.

5.2.4 $1/N$ expansion of m.o. i.i.d. model

Let us now organize the series (5.24) according to powers of N , N being the size of the tensor. Since each face corresponds to a closed cycle of Kronecker δ functions, each face contributes with a factor N , where N is the dimension of E_1, E_2 and E_3 .

$$A(\mathcal{G}) = \lambda^{v_{\mathcal{G}}} (k_N)^{-v_{\mathcal{G}}} N^{f_{\mathcal{G}}}, \quad (5.25)$$

where $v_{\mathcal{G}}$ is the number of vertices of \mathcal{G} , $f_{\mathcal{G}}$ is the number of faces of \mathcal{G} and k_N is a rescaling constant. We choose this rescaling k_N to get the same divergence degree for the leading graphs at any order. We first count the faces of a general graph \mathcal{G} using the jackets \mathcal{J} of \mathcal{G} . From Euler characteristic formula, one has:

$$f_{\mathcal{J}} = e_{\mathcal{J}} - v_{\mathcal{J}} - k_{\mathcal{J}} + 2. \quad (5.26)$$

Since each jacket of \mathcal{G} is a connected vacuum ribbon graph, one has: $e_{\mathcal{J}} = 2v_{\mathcal{J}}$. Let us recall here that the numbers of vertices (resp. edges) of a jacket \mathcal{J} of \mathcal{G} are the same than the numbers of vertices (resp. edges) of \mathcal{G} . Since each graph has three jackets and each face of a graph occurs in two jackets, summing (5.26) over all the jackets of \mathcal{G} leads to:

$$f_{\mathcal{G}} = \frac{3}{2}v_{\mathcal{G}} + 3 - \sum_{\mathcal{J} \subset \mathcal{G}} \frac{k_{\mathcal{J}}}{2} = \frac{3}{2}v_{\mathcal{G}} + 3 - \varpi(\mathcal{G}). \quad (5.27)$$

5.2. EXPANSION OF MULTI-ORIENTABLE MODEL

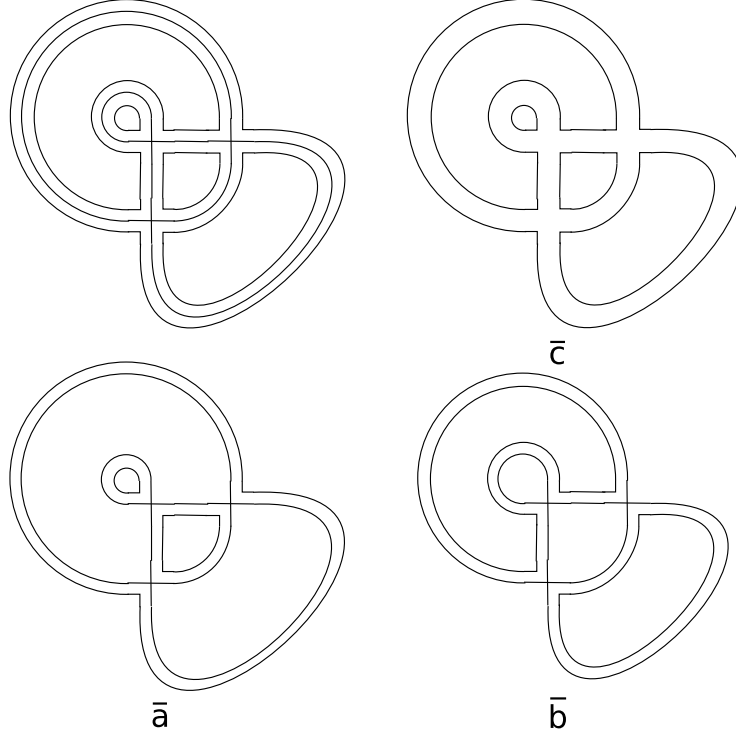


Figure 5.10: A m.o. graph with its three jackets \bar{a} , \bar{b} , \bar{c} .

The amplitude rewrites as:

$$A(\mathcal{G}) = \lambda^{v_{\mathcal{G}}} (k_N)^{-v_{\mathcal{G}}} N^{\frac{3}{2}v_{\mathcal{G}} + 3 - \varpi(\mathcal{G})}. \quad (5.28)$$

To get the same divergence degree for the leading graphs at any order, we choose the scaling constant k_N as being equal to $N^{\frac{3}{2}}$. The amplitude finally writes as:

$$A(\mathcal{G}) = \lambda^{v_{\mathcal{G}}} N^{3 - \varpi(\mathcal{G})}. \quad (5.29)$$

Thus using the expression (5.29) for the amplitude we can rewrite the free energy as a formal series in $1/N$:

$$F(\lambda, N) = \sum_{\varpi \in \mathbb{N}/2} C^{[\varpi]}(\lambda) N^{3 - \varpi}, \quad (5.30)$$

$$C^{[\varpi]}(\lambda) = \sum_{\mathcal{G}, \varpi(\mathcal{G}) = \varpi} \frac{1}{s(\mathcal{G})} \lambda^{v_{\mathcal{G}}}. \quad (5.31)$$

5.2. EXPANSION OF MULTI-ORIENTABLE MODEL

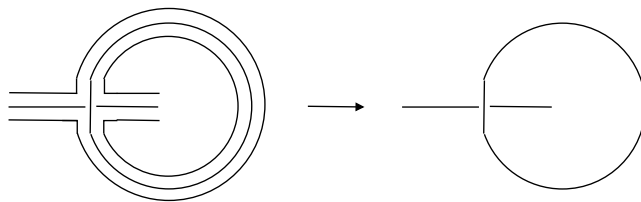


Figure 5.11: Deleting a pair of opposite corner strands in this tadpole (which has tadfaces), does not lead to a 2-stranded graph.

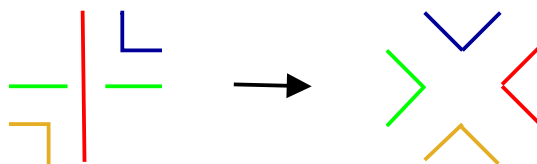


Figure 5.12: Untwisting a vertex. The strands are colored in order to clearly make the correspondence between the strands before and after the untwisting of the vertex.

5.2.5 Leading graphs

As seen on equation (5.30), the graphs which lead the $1/N$ expansion are those satisfying the relation $\varpi = 0$. Let us now identify them from a combinatorial point of view. In the colored case the leading graphs, those of degree 0, called melonic graphs [BGRR11], are obtained by recursive insertions of the fundamental melonic two-point function on any line, starting from the fundamental elementary vacuum melon (see Figure 5.13). This fundamental vacuum melon has two vertices and four internal lines and the fundamental melonic two-point function has two vertices and three internal lines and two external legs of a fixed color. Melon graphs can be mapped to 3-ary trees, and counted exactly (by Catalan numbers).

As a first step let us compute the degree of three different m.o. graphs, the “double tadpole”, the “twisted sunshine”, and the elementary melon.

Consider the jackets of the double tadpole of Figure 5.5 left. Its outer jacket is planar hence has genus $k_1 = 2g_1 = 0$. The second jacket is the one obtained by the elimination of the two faces of length one. This gives a ribbon graph representation of the real projective plane $\mathbb{R}P^2$ with non-orientable genus $k_2 = 1$. It can be seen in two ways that the associated surface is non orientable. The first one is to directly glue a disc D^2 on the external face of the two stranded graph, to get a Möbius band. Then gluing a disc on the remaining face we get $\mathbb{R}P^2$. Otherwise we can untwist the vertex, obtaining a ribbon graph with one twist on each edge. This means that we can find a path on the ribbon graph such that the local orientation is reversed after one turn. Finally the third jacket is equivalent to the first one

5.2. EXPANSION OF MULTI-ORIENTABLE MODEL

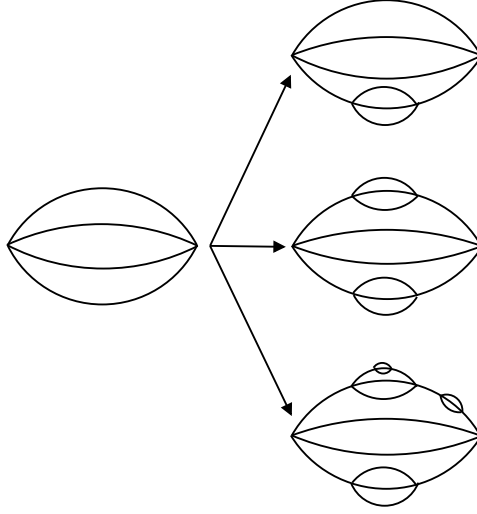


Figure 5.13: Some members of the melonic family.

and represents the sphere. Thus the generalized degree of the double tadpole is $\varpi = \frac{1}{2}$.

The twisted sunshine is a bipartite 4-edge colorable graph. Its outer jacket is orientable (as is always the case for the outer jacket), and it has genus $g_1 = 1$. The two remaining jackets are isomorphic and represent the real projective plane. They have a non-orientable genus $k_2 = k_3 = 1$. Thus the degree of the twisted sunshine is $\varpi = 2$.

The elementary melon [BGRR11] is even simpler. Its first jacket, the outer one, is planar. The two others also have genus zero (as follows directly from their Euler characteristic). Hence the generalized degree of this graph is $\varpi = 0$. This is the first example of a graph leading the $1/N$ expansion of the m.o. model.

Let us now determine the class of graphs which are leading in the $1/N$ expansion.

Theorem 6. *Non bipartite m.o. graphs contain at least one non-orientable jacket and thus are of degree $\varpi \geq \frac{1}{2}$.*

Proof. Let \mathcal{G} be a non bipartite multi-orientable graph. Then there is at least one odd cycle in \mathcal{G} (see, for example, [Ber73]) with n vertices, n being an odd integer.

Firstly we cut all the edges adjacent to any vertex of the cycle, but which do not belong to the cycle, and replace them by pairs of half-edges. We distinguish two types of vertices:

1. The first, type *I*, corresponds to vertices with opposite half-edges
2. The second, type *II*, corresponds to vertices with adjacent half-edges (i.e. carrying different labels $(+)$ and $(-)$ at the vertex).

5.2. EXPANSION OF MULTI-ORIENTABLE MODEL

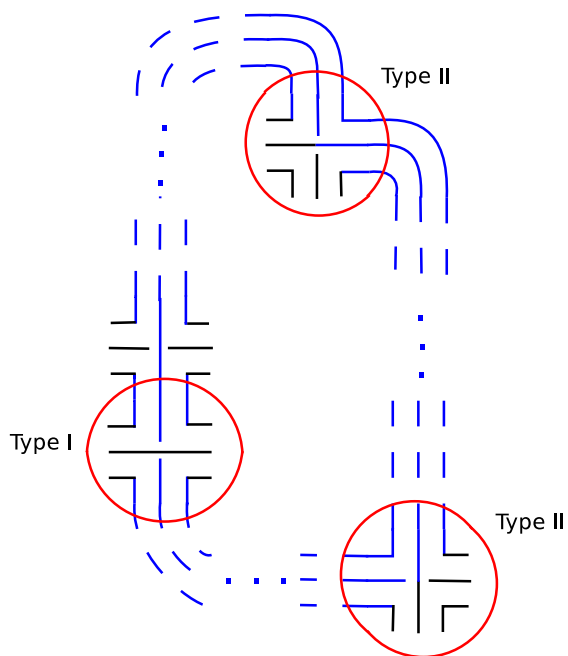


Figure 5.14: An odd cycle of a non bipartite graph (after cutting out all edges not in the cycle).

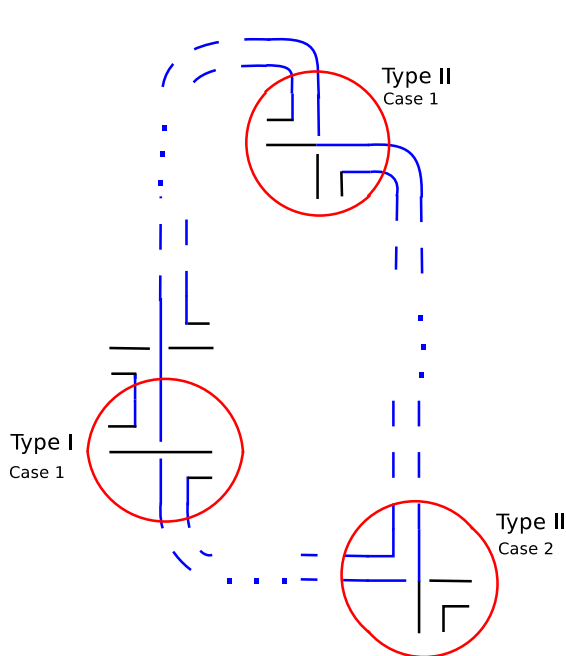


Figure 5.15: Different possibilities that can arise in the type II vertices when one chooses a jacket with the central strand.

We first notice that the number of type I vertices must be even. This is a direct consequence of the multi-orientability of the graph. We obtain a cycle of the form of the Figure 5.14. We know that the outer jacket is orientable hence we search for a non orientable jacket of type either \bar{a} or \bar{b} . In such jackets every vertex is twisted. Suppose the jacket is of type \bar{a} . It contains two corner strands of type b . Either each such corner strand contains one half-edge (case 1) or one of them contains two half-edges and the other none (case 2). Figure 5.15 shows all these possibilities. Notice that a type I vertex is always in the case 1. Moreover it can be checked that if a type II vertex is case 1 for \bar{a} then it is case 2 for \bar{b} .

Each type I vertex, when untwisted, introduces one twist on one of its adjacent edges. A vertex of type II , when untwisted, introduces on its adjacent edges one twist in case 1 and none in case 2. An odd total number of twists along the cycle implies that the jacket is non orientable. Since the number of type I vertices is even, the number of type II vertices is odd. Hence either jacket \bar{a} or jacket \bar{b} must have an odd number of type I case 1 vertices (as case 1 and 2 are exchanged when \bar{a} and \bar{b} are exchanged). Then that jacket is non orientable. As long as one non orientable jacket has been found (as can be done in following the steps described above), the degree of the graph must be at least $\frac{1}{2}$. \square

Let us now state the following:

5.2. EXPANSION OF MULTI-ORIENTABLE MODEL

Proposition 5. *If \mathcal{G} is a bipartite vacuum graph of degree zero, then \mathcal{G} has a face with two vertices.*

Proof. Let's call \mathcal{F}_p the number of faces of length p , l_ρ the length of the ρ^{th} face. We have the following identities:

$$\sum_{p \geq 1} \mathcal{F}_p = \mathcal{F}_{\mathcal{G}} = \frac{3}{2} \mathcal{V}_{\mathcal{G}} + 3, \quad (5.2.1)$$

$$\sum_{\rho} l_{\rho} = \sum_{p \geq 1} p \mathcal{F}_p = 6 \mathcal{V}_{\mathcal{G}}. \quad (5.2.2)$$

Let us recall here that for bipartite graphs there cannot be faces of length one. We now write equation (5.2.1) as:

$$4\mathcal{F}_2 + 4 \sum_{p \geq 3} \mathcal{F}_p = 6\mathcal{V}_{\mathcal{G}} + 12, \quad (5.2.3)$$

$$2\mathcal{F}_2 + \sum_{p \geq 3} p \mathcal{F}_p = 6\mathcal{V}_{\mathcal{G}}. \quad (5.2.4)$$

We then get by subtracting the second line from the first one:

$$2\mathcal{F}_2 = 12 + \sum_{p \geq 3} (p - 4) \mathcal{F}_p. \quad (5.2.5)$$

Since $\mathcal{F}_3 = 0$, this implies that $\mathcal{F}_2 > 0$. \square .

We notice that this lemma remains true for non bipartite graphs but with odd cycles of minimum length 5.

Proposition 6. *If \mathcal{G} is null degree bipartite vacuum graph, then it contains a three-edge colored subgraph with exactly two vertices.*

Proof. From the previous proposition we know that \mathcal{G} has a face with two vertices, which we denote by f_1 . Since \mathcal{G} is bipartite, we can choose a four-coloration of its edges. Once we have chosen a coloration, f_1 has two colors, denoted by i and j . We then consider the jacket \mathcal{J} not containing the face f_1 . Since $\varpi(\mathcal{G}) = 0$, this jacket \mathcal{J} is planar and of the form of Figure 5.16. We delete the two lines of color k and we get a new ribbon graph \mathcal{J}' . Since the number of vertices and faces does not change, and the number of edges decreases by two, we have

$$\chi(\mathcal{J}') = \chi(\mathcal{J}) + 2 = 4 \quad (5.2.6)$$

and thus \mathcal{J}' has two planar components. This implies that \mathcal{G} is two particle reducible for any couple of colored lines touching i, j . The graph \mathcal{G} is thus of the form of Figure 5.17.

If the subgraph \mathcal{G}^q is empty then the lines of color different of k form a subgraph with three colors. Otherwise, we cut the external lines of \mathcal{G}^q and reconnect the two external

5.2. EXPANSION OF MULTI-ORIENTABLE MODEL

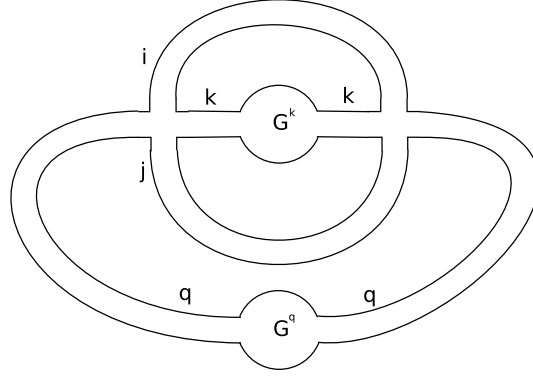
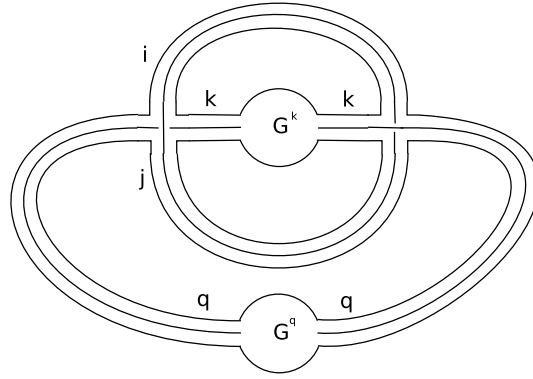


Figure 5.16: Form of the jacket not containing the face with two vertices

Figure 5.17: Form of the graph \mathcal{G} .

half lines into a new line of color q ; we call the resulting new graph $\tilde{\mathcal{G}}^q$. One remarks that the bipartite character is conserved through this procedure. Moreover $\tilde{\mathcal{G}}^q$ is of null degree, thus from the previous proposition it has a face of length two. We can thus apply the same reasoning, recursively, to this graph. Finally, the graph \mathcal{G} is of the form of Figure 5.18. \square

We have thus proved in these last two sections the main result of this chapter:

Theorem 7. *The i.i.d., m.o. model (5.24) admits a $1/N$ expansion whose leading graphs are the melonic ones.*

5.2. EXPANSION OF MULTI-ORIENTABLE MODEL

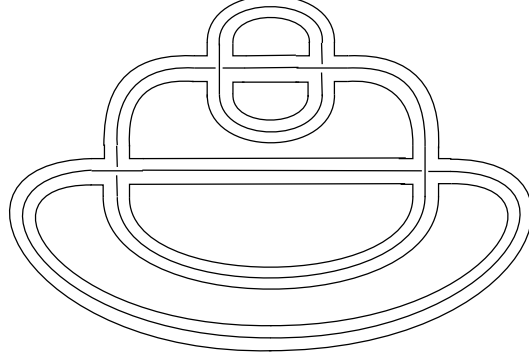


Figure 5.18: Form of the graph \mathcal{G} . It is made of successive insertion of three-edge colored subgraphs with two vertices on the edges of a "bigger" graph.

5.2.6 Next-to-leading order multi-orientable graphs.

It is possible to identify the graphs that contribute to the next-to-leading order (*NLO*) of the m.o. model. This has been done in [RT15]. As we have seen, the m.o. model contains graphs with a possibly non-orientable jacket. This implies that the NLO term is computed from the set of graphs with $\varpi = 1/2$. It is a non empty set as the planar double tadpole of Figure 5.5 is of (generalized) degree $\varpi = 1/2$.

In fact one can construct all the NLO graphs of the m.o. model from it, the idea being roughly the same as the one leading to construction of the NLO graphs for multi-tensor model. One defines a generalization of crystallization called core graphs.

Definition 20. *A NLO core graph is a connected graph \mathcal{G} , which is multi-orientable, and with no melonic sub-graphs.*

To be more precise let us explain what we mean by sub-graphs here. A sub-graph here in this case is a graph that is obtained by choosing two edges and cutting them in half such that it leads to two disconnected components. Then one has to glue half-edges belonging to the same connected components together and check whether or not the resulting graphs are melonic.

One then can show that the only NLO core graph is the planar double tadpole of Figure 5.5:

Proposition 7. *The only NLO core graph of the m.o. model is the planar double tadpole.*

The idea goes as follows. Since $\varpi = 1/2$, the outer jacket is planar. This leads to a first constraint on the number of vertices of the graph

$$F_{\text{outer}} = v_{\mathcal{G}} + 2. \quad (5.2.7)$$

5.2. EXPANSION OF MULTI-ORIENTABLE MODEL

Moreover we have from 5.27,

$$1/2 = 3 + \frac{3}{2}v_{\mathcal{G}} - (F_{\text{outer}} + F_{\text{inner}}) = 3 + \frac{1}{2}v_{\mathcal{G}} + F_{\text{inner}}. \quad (5.2.8)$$

Notice that the inner faces have to cross each other at vertices of the graphs. For a NLO core graphs one shows that if $F_{\text{inner}} \geq 2$ then all inner faces have to cross another inner face at least twice. In fact it is easy to convince oneself that otherwise a NLO core graph would be disconnected and thus we would have a contradiction.

However one can show that if two inner faces cross each other (twice) in a NLO core graph then it has a 2-bridge (*i.e.* the graph can be disconnected by cutting two edges). Nevertheless one has the following lemma [RT15],

Lemma 1. *A NLO core graph of the m.o. model has no 2-bridge.*

Thus one obtains that the inner faces have to cross at least four times. But in this case a simple calculation shows that $\varpi \geq 1 \Rightarrow F_{\text{inner}} = 1$ and so $V = 1$. By simple inspection one gets that the only NLO graph is the one of Figure 5.5. After that, one essentially shows that all NLO m.o. graphs are obtained by inserting melonic m.o. graphs with a marked edge on the edges of the planar double tadpole.

The 2-point function is computed by realizing that one has to

- either mark an edge on the planar double tadpole and insert melonic m.o. graphs with a marked edge on the non marked edge
- or start from the 2-vertex melonic m.o. graph with a marked edge and to insert one NLO graph with a marked edge on one non marked edge of the melonic m.o. graph and inserting melonic graphs on the other edges to obtain the NLO bridgeless m.o. graphs.

Through the usual relations (5.16), we can translate this to the generating series of NLO m.o. graphs with a marked edge. This allows us to compute

$$G_{1/2}^{\text{m.o.}} = \frac{\lambda(G_0^{\text{m.o.}}(\lambda))^3}{1 - 3\lambda^2(G_0^{\text{m.o.}}(\lambda))^4}. \quad (5.2.9)$$

From this equation we deduce the critical behaviour of $G_{1/2}^{\text{m.o.}}$.

$$G_{1/2}^{\text{m.o.}} \propto (\lambda^2 - \lambda_c)^{-1/2}. \quad (5.2.10)$$

Thus the corresponding critical exponent (the “string susceptibility”) at leading order is $\gamma_{1/2} = 3/2$, the same than in [KOR14b].

5.3 Generic 1-tensor model.

The $N \rightarrow \infty$ limit can also be rephrased in the context of a generic 1-tensor model. The 2-point function is given as the mean value of $\bar{T} \cdot T$.

5.3. GENERIC 1-TENSOR MODEL.

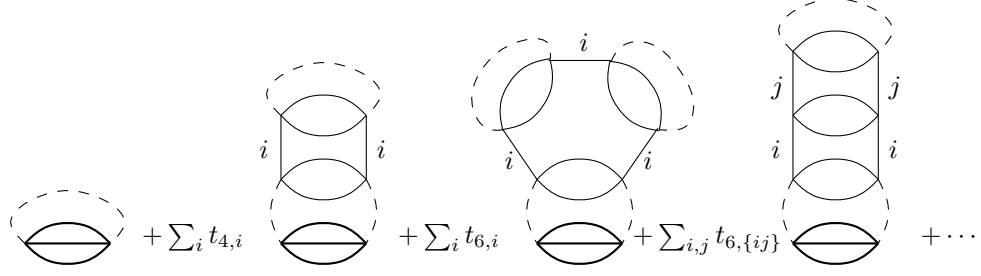


Figure 5.19: The heavier black invariant corresponds to a marked invariant of order two. It can be seen as a triangulation of the spherical boundary. The other invariants are connected to this marked invariant through lines of color zero. They come from the expansion of the exponential in the integral.

The two point function of the generic tensor model is computed at leading order as:

$$G_0(\{t_B\}, N) = [N^0] \frac{1}{N^{d-1}} \langle \bar{T} \cdot T \rangle. \quad (5.3.11)$$

Graphically, $\langle \bar{T} \cdot T \rangle$ is represented by the only colored graph with two vertices. As we have seen in Chapter 4, the amplitude of this invariant is obtained by contracting edges of color zero between vertices of invariants. For the generic tensor model one has, at leading order, that only melonic invariant contributes. Moreover the edges of color zero have to be contracted in a melonic way. Some typical graphs contributing to the leading order evaluation of the 2-point function are shown in Figure 5.19. From this analysis follows that the graphs contributing to the two point function at leading order are melonic graphs with one marked bubble with two vertices. The number of these graphs is exactly the same than the number computed in the first section. Indeed it suffices to erase the marked bubble and reconnect the two resulting half-edges of color 0 to obtains melonic graphs with a marked edge counted before.

5.4 Conclusion

In this chapter we have described the $1/N$ expansion of tensor models. We explored first the multi-tensor model, then the multi-orientable model. They show essentially the same behaviour, however the multi-tensor model is able to produce well defined triangulations of pseudo-manifolds in any dimension. The multi-orientable model, in contrast, is defined only in dimension 3. It generates 2-cell complexes from which there is, *a priori*, no canonical way to retrieve a manifold or pseudo-manifold structure. However its combinatorics is richer, hence it is definitely an interesting model. A challenging open question would be to extend it to dimensions larger than 3. The study of different scaling limits may be the

5.4. CONCLUSION

source of new critical behaviours.

The generic 1-tensor model can be related to the multi-tensor model. In fact if one integrates out all tensor fields but one, one obtains the generic 1-tensor model for a specific choice of the coupling constant $t_{\mathcal{B}} = (\lambda\bar{\lambda})^{p(\mathcal{B})}$.

From this exposition, one sees that the degree plays a central role in the tensor framework as this combinatorial quantity drives the $1/N$ expansion, classifying triangulations with respect to some combinatorial quantity that relates to embedded surfaces in the pseudo-manifold.

5.4. CONCLUSION

Chapter 6

Double Scaling Limit of Tensor Models

This chapter is concerned with the *double scaling limit* of random tensor. This concept already appears in matrix models and is of importance as it has been thought to give a non-perturbative definition of String Theory. Moreover this limit is related to some integrable structures present in matrix models. The generalization of this concept is motivated by the need to explore new geometrical phases in tensor models. The phase corresponding to a double scaling limit should be a continuum limit for the triangulated space, but in such a way that not only melonic triangulations contribute to the obtained phase. One can hope that these new triangulations bring enough new geometrical features to change the branched polymers (Aldous random tree) behavior of the melonic phase [GR14]. The results presented here are mostly extracted from [DGR13].

6.1 Double scaling of matrix models.

In this section, we introduce the double scaling limit in the context of matrix models. This is well known in the literature (see for instance [DFGZJ95]). For explanatory purpose, let us consider the following model

$$Z[N, t] = \int_{H_N} dM \exp(-N(\frac{1}{2} \text{Tr}(M^2) + \frac{t}{4} \text{Tr}(M^4))). \quad (6.1.1)$$

The double scaling limit is defined as the asymptotic of the correlation functions in x when both $N \rightarrow \infty$ and $t \rightarrow t_c$ in a correlated way, such that $x = N(t - t_c)^\alpha$ is kept constant for some well chosen value of α . In fact, the formal model is a natural formal series in N, N^{-1} . Their coefficients are functions of t with a common singular point at t_c negative.

Consequently it writes as,

$$F = \log(Z) = \sum_{g \geq 0} N^{2-2g} F_g(t), \quad (6.1.2)$$

where $F_g(t)$ is the generating series of the genus g ribbon graphs. All F_g are holomorphic in a given domain and meet a singularity at $t = t_c$. The behaviour of F_g at t_c is of the form

$$F_g \simeq K_g (t_c - t)^{\frac{1}{2}(2-\gamma)\chi(g)}, \quad (6.1.3)$$

with¹ $\gamma = -\frac{1}{m}$ for some $m \geq 2$, K_g some constant and $\chi(g) = 2 - 2g$. Setting $x = N^{-1}(t - t_c)^{\frac{\gamma-2}{2}}$, we obtain an asymptotic expansion of F

$$F = \sum_{g \geq 0} x^{2g-2} K_g. \quad (6.1.4)$$

This asymptotic expansion is not summable in general. This is due to the behaviour of the coefficients K_g that are all positive. Moreover the K_g behave as $(2g)!$ as in fact combinatorially the resulting series sums all Feynman graphs. However, when treating the problem with convergent matrix integrals instead of formal ones, in some cases it is possible to derive a well defined double scaling limit using techniques that are not presented in this manuscript. See for example [BI02]. The next section generalizes the idea presented here for tensor models.

6.2 Double Scaling of melonic T^4 tensor model.

In this section we deal with a specific tensor model. The melonic T^4 model. The results of this section are extracted from [DGR13]. The quartically perturbed Gaussian tensor measure with which we will deal in this chapter (see [Gur14]) is the simplest interacting tensor model, with measure

$$d\mu = \frac{1}{Z(\lambda, N)} \left(\prod_{\vec{n}} N^{d-1} \frac{dT_{\vec{n}} d\bar{T}_{\vec{n}}}{2\pi i} \right) e^{-N^{d-1} S^{(4)}(T, \bar{T})}, \quad (6.2.5)$$

$$S^{(4)}(T, \bar{T}) = \sum_{\vec{n}} T_{\vec{n}} \delta_{\vec{n}\vec{n}} \bar{T}_{\vec{n}} + \lambda \sum_{i=1}^d \sum_{n\bar{n}} T_{\vec{n}} \bar{T}_{\vec{m}} T_{\vec{m}} \bar{T}_{\vec{n}} \delta_{n^i \bar{m}^i} \delta_{m^i \bar{n}^i} \prod_{j \neq i} \delta_{n^j \bar{n}^j} \delta_{m^j \bar{m}^j},$$

with $Z(\lambda, N)$ some normalization constant.

Some explanations here are in order. The d different quartic interactions correspond to those of Fig. 6.1, namely to the leading quartic melonic stable interactions at tensor rank (i.e. dimension) d . We deal with this problem by using the intermediate field representation of this model. It has been first introduced in [Gur14] in order to give a constructive (convergent) meaning to the integral of tensors.

¹ $\gamma = -\frac{1}{2}$ in the specific model introduced above.

6.2. DOUBLE SCALING OF MELONIC T^4 TENSOR MODEL.

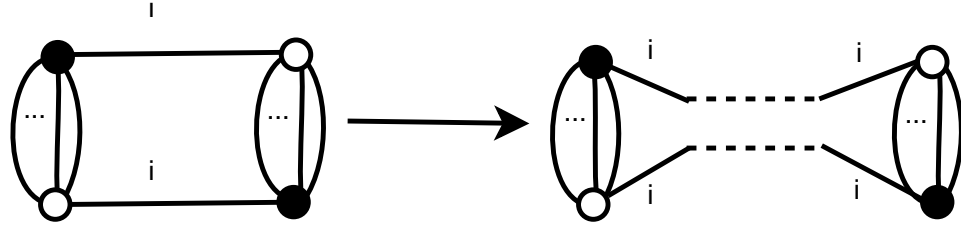


Figure 6.1: The model is obtained by perturbing the Gaussian measure by the invariants shown on the figure for $i \in \llbracket 1, d \rrbracket$.

The melonic interactions turn out to be the easiest ones to decompose according to intermediate fields. Higher order stable melonic (or even submelonic) interactions can in principle be treated as well by the same method but require more intermediate fields [RW10]. In principle, each of the d interactions can have its own different coupling constant λ_i , but in this work we treat only the symmetric case in which all λ_i are equal to λ .

The idea of the double scaling is the following. When sending λ to λ_c , the melons become critical. One can then restrict to graphs \bar{G} with no melonic subgraphs and sum, for every such graph, the family of graphs obtained by arbitrary insertions of melons. This will lead to an expansion of the two point function

$$\begin{aligned} \mathcal{G}_2 &= \mathcal{G}_{2,\text{melon}} + \sum_{\bar{G}} \frac{1}{N^{h(\bar{G})}} \frac{1}{(\lambda - \lambda_c)^{e(\bar{G})}} \\ &= \mathcal{G}_{2,\text{melon}} + \sum_{e \geq 1} \sum_{\bar{G}, e(\bar{G})=e} \left(\frac{1}{N^{h(\bar{G})/e(\bar{G})}(\lambda - \lambda_c)} \right)^e \end{aligned} \quad (6.2.6)$$

where $h(\bar{G})$ is the scaling with N of \bar{G} , $e(\bar{G})$ counts the number of places where we can insert melons in \bar{G} . We now select the family of graphs for which $h(\bar{G})/e(\bar{G})$ is minimal. Denoting this minimal value α , the two point function becomes

$$\begin{aligned} \mathcal{G}_2 &= \mathcal{G}_{2,\text{melon}} + \sum_{e \geq 1} \left[\sum_{\bar{G}, e(\bar{G})=e, \alpha(\bar{G})=\alpha} \left(\frac{1}{N^\alpha(\lambda - \lambda_c)} \right)^e \right. \\ &\quad \left. + \sum_{\bar{G}, e(\bar{G})=e, h(\bar{G})/e(\bar{G}) > \alpha} \left(\frac{1}{N^{h(\bar{G})/e(\bar{G})-\alpha} N^\alpha(\lambda - \lambda_c)} \right)^e \right]. \end{aligned} \quad (6.2.7)$$

When tuning λ to λ_c while keeping $N^\alpha(\lambda - \lambda_c)$ fixed the last sum cancels and all the terms in the first sum admit a well defined limit. The expansion obtained in this limit is an expansion in a new double scaled parameter $x = N^\alpha(\lambda - \lambda_c)$. The rest of this chapter is dedicated to establishing (6.2.7). From now on we denote $z = -2\lambda$.

We use the intermediate field representation introduced in [Gur14] as it leads to a very convenient organization of the set of graph with respect to their weight in N . In fact in

6.2. DOUBLE SCALING OF MELONIC T^4 TENSOR MODEL.

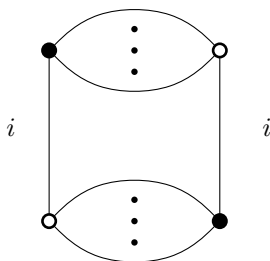


Figure 6.2: Interaction terms of the quartically perturbed gaussian measure of T^4 melonic tensor model. There is one such invariant for each color i . The graphs generated by this tensor model are made of this building blocks linked by additional lines of color 0.

this representation the melonic graphs introduced before are exactly trees. This allows one to track more easily the factor of N . The rough idea is that the graph of a melonic T^4 tensor model are made with building pieces of the form Fig. 6.2 that are linked by lines of color 0 (see Fig. 6.3). As seen on Fig. 6.3 the cycles made of lines of color 0 and d -dipoles are oriented. We can use this property to transform these cycles into ribbon vertices (*i.e.* vertex with a cyclic orientation of the lines adjacent to it). The fat edges ending to these ribbon vertices then being the double lines of a given color leaving the d -dipoles. This is shown on Fig. 6.4. The intermediate field representation amount to a change of integral representation of the generating function of the melonic tensor model. This new representation is better expressed in term of the new ribbon graphs. This is useful in particular for constructive theory [Gur14].

6.2.1 Graphs classification: Pruning and Grafting.

We now work with the formal series, *i.e.* with the perturbative expansion of the theory. The form of the obtained graphs is presented for instance on Fig. 6.4. The associated Feynman rules are described in [Gur14]. It is a bit lengthy, thus it is not reproduced here.

From now on we denote $V(G) = n$ the number of vertices, $E(G) = n - 1 + L$ the number of edges and $F(G)$ the number of faces of the map G . The ciliated vertex in G corresponds to the external faces of the two point function \mathcal{G}_2 .

To every map G we will associate a map \tilde{G} which captures all its essential characteristics. The map \tilde{G} is obtained through the operations of *pruning* and *reduction* defined below. There exists an infinity of maps G which correspond to the same \tilde{G} . All such G sum together and yield a contribution associated to \tilde{G} . The perturbative series can then be re-indexed in terms of \tilde{G} and the double scaling limit is analyzed in terms of \tilde{G} .

We now remove iteratively all non-ciliated vertices of coordination one of G . This is called *pruning*. For simplicity, in the sequel we shall refer to maps as graphs.

6.2. DOUBLE SCALING OF MELONIC T^4 TENSOR MODEL.

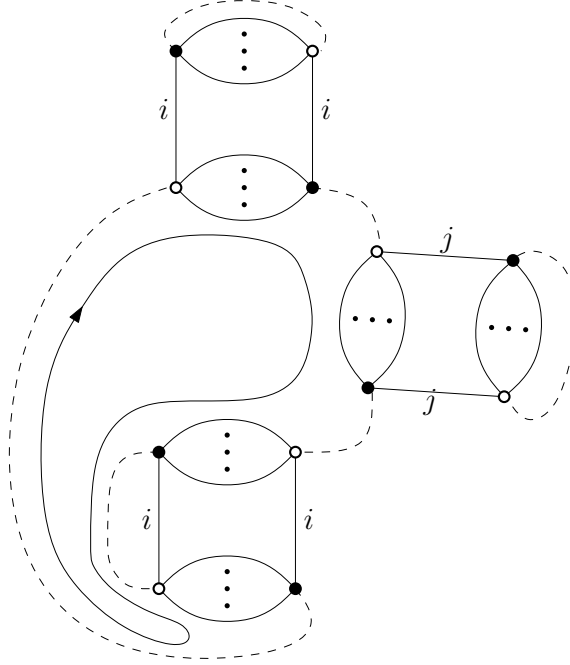


Figure 6.3: An orientation of the lines of color 0 (shown using dashed lines here), conventionally chosen to be from black to white vertices, induces an orientation of the cycles made of lines of color 0 and d -dipoles. This can be exploited to make up a bijection between the set of tensor model graphs and a set of 2-dimensional combinatorial maps that are generated by a matrix model.

6.2. DOUBLE SCALING OF MELONIC T^4 TENSOR MODEL.

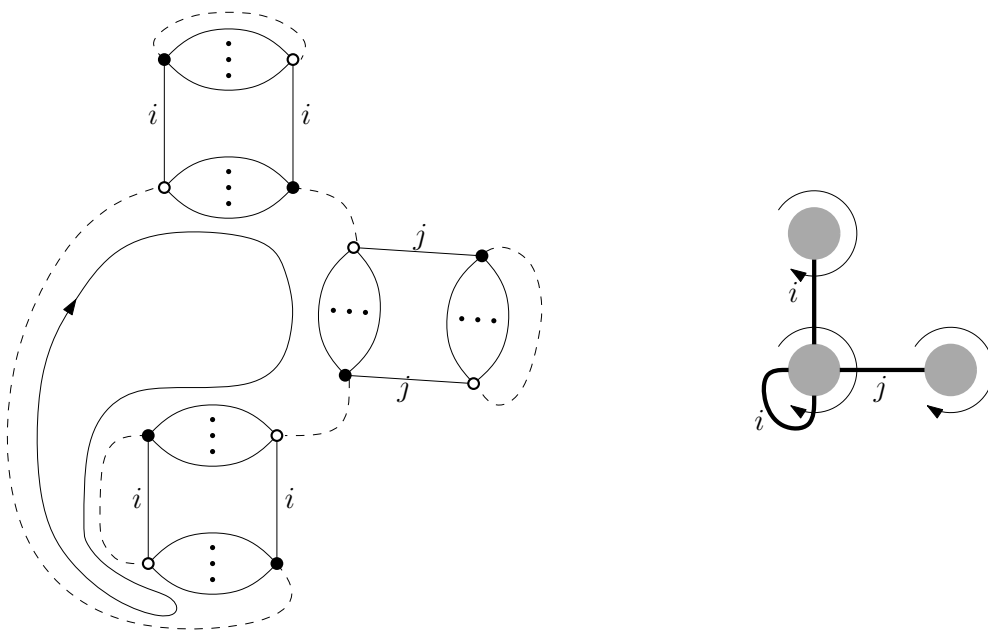


Figure 6.4: The cycles made of lines of color 0 and d -dipoles of the graph of the left are mapped to the grey vertices of the graph on the right. The orientation of the grey vertices induced from the orientation of the cycles is shown. The double lines of colors i and j are mapped to edges of a ribbon graph with color respectively i and j .

6.2. DOUBLE SCALING OF MELONIC T^4 TENSOR MODEL.

Definition 21. A reducible leaf of G is a vertex of G of coordination 1 which is not the ciliated vertex. The pruned graph \tilde{G} associated to G is obtained by removing inductively all reducible leaves and their unique attaching edge.

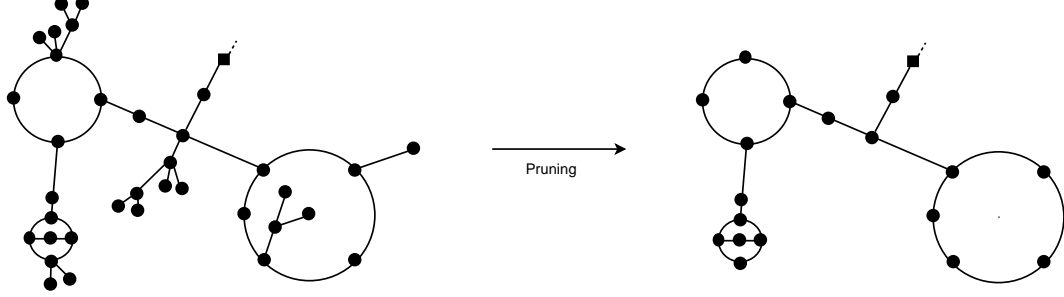


Figure 6.5: Pruning

The pruned graph is therefore obtained by removing from G all rooted tree subgraphs with only reducible leaves, see Fig. 6.5. Again the map $\pi_1 : G \rightarrow \pi_1(G) = \tilde{G}$ is onto but not one to one. Remark that the pruned graph \tilde{G} is never empty, as it contains at least the ciliated vertex. It also contains L independent cycles, like G . Remark also that pruning is compatible with the coloring: the initial graph G is colored, and the corresponding pruned graph \tilde{G} , which is a subgraph of G , is also colored.

The “inverse” operation of pruning is grafting: the initial graph G is obtained by grafting some (possibly empty) rooted plane tree on each *corner* of the pruned graph \tilde{G} (see Fig. 6.6). Considering all the possible graftings on \tilde{G} reconstructs the entire family of graphs G which reduces to \tilde{G} by pruning.

Remark that the pruned graph \tilde{G} has fewer vertices and fewer edges than G . However, at every step in the pruning process the number of edges and vertices of the graph decreases by 1, hence \tilde{G} and G have the same number of cycles

$$L(\tilde{G}) = E(\tilde{G}) - V(\tilde{G}) + 1 = E(G) - V(G) + 1 = L(G) . \quad (6.2.8)$$

Furthermore, all the graphs G corresponding to the same pruned graph \tilde{G} have the same scaling in N . Indeed, when deleting an univalent vertex (and the edge connecting it to the rest of the graph, say of color c) the number of faces of the graph decreases by $d - 1$, as all the faces of color $c \neq c'$ containing the vertex are deleted, but the face of color c is not. Hence

$$-1 - (E(G) + 1)(d - 1) + F(G) = -1 - (E(\tilde{G}) + 1)(d - 1) + F(\tilde{G}). \quad (6.2.9)$$

Definition 22. A one particle irreducible component \tilde{G}_k (1PI) of a pruned graph \tilde{G} is a maximal (non empty) connected set of edges, together with their attached vertices, which

6.2. DOUBLE SCALING OF MELONIC T^4 TENSOR MODEL.

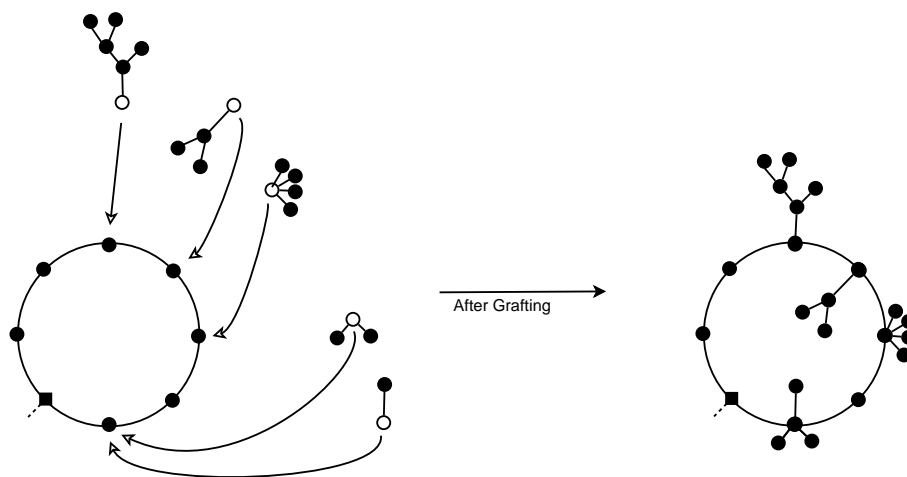


Figure 6.6: Grafting

cannot be separated into two connected components by deleting one of its edges. The ciliated vertex can either be part of a one particle irreducible component, or not, in which case it is called *bare*. An irreducible component of a pruned graph \tilde{G} is either a one particle irreducible component \tilde{G}_k , or the ciliated vertex if it is bare.

Remark that since each one particle irreducible component must include at least one loop edge (i.e. it must have at least a cycle), the number $p(\tilde{G})$ of irreducible components in a pruned graph \tilde{G} with L loops is at least 1 and at most $L + 1$, and if $p(\tilde{G}) = L + 1$, the ciliated vertex must be *bare*.

6.2.2 Reduction.

We now remove all non-ciliated vertices of coordination 2. This is called *reduction*.

Definition 23. A vertex of a pruned graph is called *essential* if it is of degree strictly greater than 2 or if it is the ciliated vertex. A *bar* of a pruned graph is a maximal chain of edges with internal vertices all of degree 2. The number of essential vertices and of bars of a pruned graph \tilde{G} will be noted $V^e(\tilde{G})$ and $B(\tilde{G})$.

If we picture each bar of a pruned graph \tilde{G} as a (fat) edge, we obtain a new graph \bar{G} associated to \tilde{G} , which is made of $V(\bar{G}) = V^e(\tilde{G})$ vertices plus $E(\bar{G}) = B(\tilde{G})$ (fat) edges between them (see Fig. 6.7). It has still the same number $L(\bar{G}) = L(\tilde{G}) = L(G) \equiv L$ of independent cycles as \tilde{G} and G , and every tree of \bar{G} has $E(\bar{G}) - L$ edges.

Lemma 2. We have $E(\bar{G}) \leq 3L - 1$, and $V(\bar{G}) \leq 2L$. Moreover $E(\bar{G}) = 3L - 1$ implies that every vertex of \bar{G} is of degree 3, except the ciliated vertex v_c which is of degree 1.

6.2. DOUBLE SCALING OF MELONIC T^4 TENSOR MODEL.

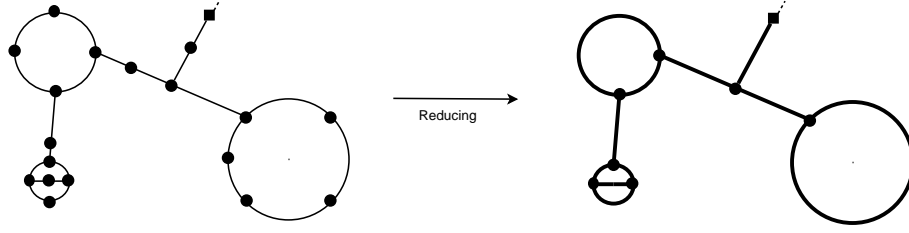


Figure 6.7: Reduction of a pruned graph

Proof. Let d_v be the degree of vertex $v \in \bar{G}$. We have $d_v \geq 3$ for any v except maybe for the ciliated vertex, with degree d_c . Furthermore $V(\bar{G}) - 1 + L = E(\bar{G})$, as \bar{G} can always be decomposed into a tree of $V(\bar{G}) - 1$ edges plus a set of L loop edges. We have

$$2E(\bar{G}) = \sum_v d_v \geq 3(V(\bar{G}) - 1) + d_c = 3(E(\bar{G}) - L) + d_c \quad (6.2.10)$$

which proves that $E(\bar{G}) \leq 3L - d_c \leq 3L - 1$. Equality can happen only if $d_v = 3$ for $v \neq v_c$ and $d_c = 1$. Finally since \bar{G} is connected $E(\bar{G}) = V(\bar{G}) - 1 + L$, hence $E(\bar{G}) \leq 3L - 1$ implies $V(\bar{G}) \leq 2L$. \square

If a chain of edges of \tilde{G} which we reduce is made of edges all with the same color c , we color the new fat edge in \bar{G} with c . If on the contrary the chain of edges contained at least two edges of two different colors, we will call the fat edge multicolored, and we will associate to it an index m .

Definition 24. A reduced graph \bar{G} is a regular graph with one ciliated vertex, such that all other vertices have coordination at least 3, plus the choice of a color c or a label m on any of its edges. Forgetting the labels, one gets an associated unlabeled reduced graph.

The reduction operation π_2 is now well-defined from the category of (colored) pruned graphs to the category of reduced graphs. The map $\pi_2 : \tilde{G} \rightarrow \pi_2(\tilde{G}) = \bar{G}$ is onto but not one to one. The reverse of the reduction map, called *expansion*, expands any edge into an arbitrarily long chain with degree 2 intermediate vertices, and sums over colorings compatible with the colors or the label m .

We denote $E^m(\bar{G})$ the number of multicolored edges of the reduced graph \bar{G} . We define the (possibly disconnected) graph \bar{G}_c as the subgraph of \bar{G} made of all the vertices of \bar{G} and all the edges of color c . As \bar{G}_c is a map, it has a certain number of faces, $F(\bar{G}_c)$, and a total genus $g(\bar{G}_c)$ (i.e. the sum of the genera of the connected components of \bar{G}_c). We denote the number of cycles of \bar{G}_c by $L(\bar{G}_c)$.

6.2. DOUBLE SCALING OF MELONIC T^4 TENSOR MODEL.

Lemma 3. *The scaling with N of all the pruned graphs associated to the reduced graph \bar{G} is*

$$-dL(\bar{G}) + 2 \sum_c L(\bar{G}_c) - 2 \sum_c g(\bar{G}_c) . \quad (6.2.11)$$

Proof. The scaling with N of a pruned graph \tilde{G} is

$$-1 - (E(\tilde{G}) + 1)(d-1) + F(\tilde{G}) . \quad (6.2.12)$$

When deleting a bivalent vertex on an unicolored edge of color c the number of edges of the graph decreases by 1 and the number of faces by $d-1$ (one for each $c' \neq c$). On the contrary, when deleting all the bivalent vertices on a multicolored edge with p intermediate vertices, the number of edges decreases by p , and the number of faces by $d-2 + (d-1)(p-1)$, hence the scaling with N writes in terms of the data of the reduced graph as

$$-1 - (E(\bar{G}) + 1)(d-1) - E^m(\bar{G}) + \sum_c F(G_c) . \quad (6.2.13)$$

The graphs G_c have $C(G_c)$ connected components, $V(G_c)$ vertices, $E(G_c)$ edges and total genus $g(G_c)$, hence the scaling with N writes

$$\begin{aligned} & -1 - (E(\bar{G}) + 1)(d-1) - E^m(\bar{G}) \\ & + \sum_c (-V(G_c) + E(G_c) + 2C(G_c) - 2g(G_c)) . \end{aligned} \quad (6.2.14)$$

The number of connected components of G_c can be computed in terms of the number of cycles, $E(G_c) = V(G_c) - C(G_c) + L(G_c)$, and we get

$$\begin{aligned} & -1 - (E(\bar{G}) + 1)(d-1) - E^m(\bar{G}) \\ & + \sum_c [-V(G_c) + E(G_c) + 2(V(G_c) - E(G_c) + L(G_c)) - 2g(G_c)] \\ & = -1 - (E(\bar{G}) + 1)(d-1) - E^m(\bar{G}) \\ & + \sum_c (V(G_c) - E(G_c) + 2L(G_c) - 2g(G_c)) . \end{aligned} \quad (6.2.15)$$

As $V(G_c) = V(\bar{G})$ and $E(\bar{G}) = E^m(\bar{G}) + \sum_c E(G_c)$ we rewrite this as

$$-1 - (E(\bar{G}) + 1)(d-1) - E(\bar{G}) + dV(\bar{G}) + \sum_c (2L(G_c) - 2g(G_c)) , \quad (6.2.16)$$

and using $E(\bar{G}) = V(\bar{G}) - 1 + L(\bar{G})$ the lemma follows. \square

Summing the family of graphs which, through pruning and reduction, lead to the same reduced graph \bar{G} we obtain the *amplitude* of \bar{G} .

6.2. DOUBLE SCALING OF MELONIC T^4 TENSOR MODEL.

Theorem 8. *The amplitude of a reduced graph \bar{G} is*

$$\begin{aligned} \mathcal{A}(\bar{G}) &= N^{-dL(\bar{G})+2\sum_c L(\bar{G}_c)-2\sum_c g(\bar{G}_c)} T(dz)^{1+2E(\bar{G})} \\ &\quad \left(\frac{z}{1-zT^2(dz)} \right)^{\sum_c E(\bar{G}_c)} \left(\frac{d(d-1)z^2T^2(dz)}{[1-dzT^2(dz)][1-zT^2(dz)]} \right)^{E^m(\bar{G})}. \end{aligned} \quad (6.2.17)$$

The proof of this theorem is presented in subsection 6.2.4.

A further simplification comes from the fact that the 1PR bars of \bar{G} do not in fact need any label c or m . This comes from the fact that such graphs have the same scaling in N , but the graphs with colored 1PR edges are suppressed in the double scaling limit: one can chose to group together or not the graphs which differ only by the label of their 1PR bars without changing the double scaling limit. Indeed, if one combines together all the reduced graphs differing only by the labels of the 1PR edges (which in this case we call free) one gets a contribution

$$\begin{aligned} &N^{-dL(\bar{G})+2\sum_c L(\bar{G}_c)-2\sum_c g(\bar{G}_c)} T(dz)^{1+2E(\bar{G})} \\ &\quad \left(\frac{z}{1-zT^2(dz)} \right)^{\sum_c E(\bar{G}_c)} \left(\frac{d(d-1)z^2T^2(dz)}{[1-dzT^2(dz)][1-zT^2(dz)]} \right)^{E^m(\bar{G})} \\ &\quad \left(\frac{dz}{[1-dzT^2(dz)]} \right)^{E^{\text{free}}(\bar{G})}, \end{aligned} \quad (6.2.18)$$

having the same critical behavior as (6.2.17), where $E^{\text{free}}(\bar{G})$ denotes the number of free edges of \bar{G} and $E^m(\bar{G})$ the number of multicolored edges in \bar{G} .

6.2.3 Cherry Trees

Definition 25. *A reduced graph with $L(\bar{G})$ loops and one cilium is called a cherry tree (or, in short a cherry) if $E(\bar{G}) = 3L(\bar{G}) - 1$, $L(\bar{G}) = \sum_c L(\bar{G}_c)$, and $V(G_c) = C(G_c)$.*

Remark that such a graph is a rooted binary tree made of multicolored edges, with $L(\bar{G}) + 1$ univalent vertices (the leaves and the root) and $L(\bar{G}) - 1$ trivalent vertices decorated by one self loop of color $c = 1, \dots, d$ on each of its leaves. Indeed, $E(\bar{G}) = 3L(\bar{G}) - 1$ implies that the root vertex is univalent and all other vertices are trivalent, $V(G_c) = C(G_c)$ implies that all the connected components of G_c have exactly one vertex, $L(\bar{G}) = \sum_c L(\bar{G}_c)$ and the fact that all vertices except the root are trivalent implies on one hand that $L(\bar{G})$ vertices are decorated by self loops of a fixed color, and on the other that the graph obtained by erasing these self loops has no more cycles and is connected, hence is a tree (see Fig. 6.8).

The mixed pruned expansion for the two-point function then splits into two parts, the sum over cherry trees and the rest, which is the sum over all other graphs:

$$\mathcal{G}_2^L(z, N) = \mathcal{G}_{2,\text{cherry}}^L(z, N) + \mathcal{G}_{2,\text{rest}}^L(z, N). \quad (6.2.19)$$

6.2. DOUBLE SCALING OF MELONIC T^4 TENSOR MODEL.

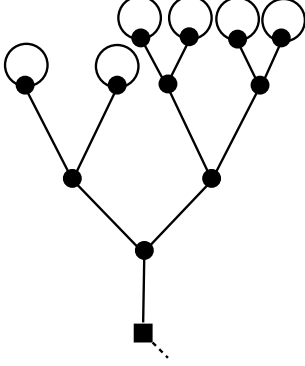


Figure 6.8: An example of cherry tree

The next step is to change z to the *rescaled variable* $x = N^{d-2}(z_c - z)$ with $z_c = (4d)^{-1}$,

$$\mathcal{G}_{2,\text{cherry}}^L(z, N) = \mathcal{G}_{2,\text{cherry}}^{L,x}(N); \quad \mathcal{G}_{2,\text{rest}}^L(z, N) = \mathcal{G}_{2,\text{rest}}^{L,x}(N) \quad (6.2.20)$$

and to consider now at *fixed* L and x the asymptotic expansion of these quantities when $N \rightarrow \infty$.

Our main result is that in this regime the cherry trees contribution $\mathcal{G}_{2,\text{cherry}}^{L,x}(N)$ has a leading term proportional to $N^{1-d/2}$ with a coefficient which can be computed *exactly*, and that for $3 \leq d \leq 5$ this leading term dominates all the rest by at least one additional $N^{-1/2}$ factor:

Theorem 9 (Main Bound). *For $3 \leq d \leq 5$, $L \geq 1$ fixed and for x in some neighborhood of $x_c = \frac{1}{4(d-1)}$, we have*

$$\mathcal{G}_{2,\text{cherry}}^{L,x}(N) = N^{1-d/2} \frac{8\sqrt{d}C_{L-1}}{[16(d-1)]^L} x^{-L+1/2} + O(N^{1/2-d/2}), \quad (6.2.21)$$

where $C_{L-1} = \frac{1}{2L-1} \binom{2L-1}{L-1}$ is the Catalan number of order $L-1$. Moreover there exists a constant K_L such that

$$|\mathcal{G}_{2,\text{rest}}^{L,x}(N)| \leq N^{1/2-d/2} K_L x^{-\frac{3}{2}L+\frac{1}{2}}. \quad (6.2.22)$$

Thus for $d < 6$ the cherry trees yield the leading contribution in the double scaling limit $N \rightarrow \infty$, $z \rightarrow z_c$, $x = N^{d-2}(z_c - z)$ fixed. However remark that there is a *certain degree of arbitrariness* in the separation between cherry trees and the rest. The cherry trees are just the simplest convenient sub series displaying the leading double scaling behavior. The rest term is less singular, which means that adding part of it to the cherry trees would typically not change the nature of the singularity. However adding *all* graphs at once would certainly at some point meet the problem of divergence of perturbation theory².

²Hence analytic continuation of the Borel sum might be the ultimate justification of (multiple) scalings.

6.2. DOUBLE SCALING OF MELONIC T^4 TENSOR MODEL.

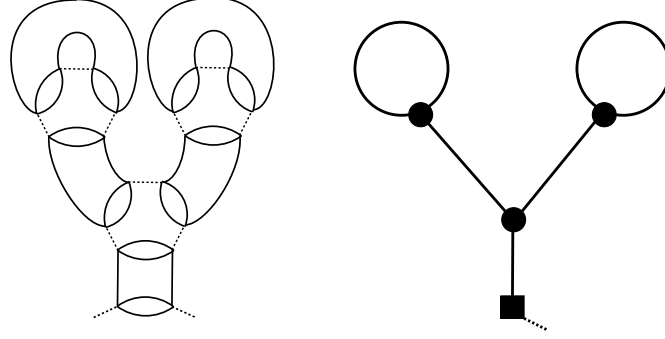


Figure 6.9: A cherry tree in the direct representation and in the LVE representation.

6.2.4 Reduced graphs amplitudes

We prove in this section Theorem 8.

The family of pruned graphs associated to \bar{G} is obtained by arbitrary insertions of bivalent vertices on any of its edges. The grafting operation adds arbitrary trees with colored edges independently on each of the corners of the pruned graphs. From (??) each edge of a graph has a weight z .

We denote $T(z)$ the generating function of plane trees with weight z per edge

$$T(z) = \sum_{n \geq 0} \frac{1}{2n+1} \binom{2n+1}{n} z^n, \quad T(z) = 1 + zT^2(z), \quad T(z) = \frac{1 - \sqrt{1-4z}}{2z}. \quad (6.2.23)$$

As the edges of the LVE trees have a color $1, \dots, d$ on each edge, their generating function is $T(dz)$. We have

$$T(dz) = 1 + dzT^2(dz) \Rightarrow 1 - dzT^2(dz) = 2 - T(dz) = T(dz)\sqrt{1-4dz}. \quad (6.2.24)$$

Every corner of a pruned graphs represents a place where a tree can be inserted, hence has a weight $T(dz)$. Exactly $1 + 2E(\bar{G})$ of the corners of the pruned graph \tilde{G} appear in the reduced graph \bar{G} , hence the corners of \bar{G} bring in total a factor

$$T(dz)^{1+2E(\bar{G})}. \quad (6.2.25)$$

The weight of the edges of the reduced graph are obtained by summing over the number of intermediate bivalent vertices in the associated pruned graphs from 0 to infinity. Every intermediate vertex brings two new corners and a new edge, hence a factor $zT(dz)^2$. As a function of the label c or m of the edge in \bar{G} we distinguish several cases:

6.2. DOUBLE SCALING OF MELONIC T^4 TENSOR MODEL.

- The edge in \bar{G} has a color c . Then all the intermediate edges in \tilde{G} have the same color, and we get a total weight

$$\sum_{k=0}^{\infty} z^{k+1} T^{2k}(dz) = \frac{z}{1 - zT^2(dz)} \quad (6.2.26)$$

- The edge in \bar{G} has an index m . Then there must be at least two edges of different colors in \tilde{G} which are replaced by the edge m , hence the weight is

$$\begin{aligned} & \sum_{k=0}^{\infty} d^{k+1} z^{k+1} T^{2k}(dz) - d \sum_{k=0}^{\infty} z^{k+1} T^{2k}(dz) \\ &= \frac{dz}{1 - dzT^2(dz)} - \frac{dz}{1 - zT^2(dz)} \\ &= \frac{d(d-1)z^2 T^2(dz)}{[1 - dzT^2(dz)][1 - zT^2(dz)]} . \end{aligned} \quad (6.2.27)$$

Note that if we were to consider the 1PR edges free, there weight becomes

$$\frac{dz}{1 - dzT^2(dz)} . \quad (6.2.28)$$

Putting together the scaling in Lemma 3 with the contributions of (6.2.25), (6.2.26) and (6.2.27) proves Theorem 8. We present here some low order examples of reduced graphs and their amplitudes.

Zero Loop. At the leading order in $1/N$ only the trees with zero loops contribute. By pruning they reduce to the single ciliated vertex, which we call the graph \bar{G}_0 ³. The series of graphs G corresponding to this trivial pruned graph is obtained by grafting a plane tree with colored edges on the single corner of the ciliated vertex, hence

$$\mathcal{A}(\bar{G}_0) = T(dz) . \quad (6.2.29)$$

reproducing the result of [Gur14] and rederived in Chap. 5.

One Loop. The first $1/N$ corrections arise from graphs having one loop edge. There are two reduced graphs, see Fig. 6.10 showing two of the pruned graphs corresponding to each of the two reduced graphs.

Consider the leftmost graph. If the loop edge in \bar{G} has a color c we get an amplitude

$$\frac{1}{N^{d-2}} T(dz)^3 \frac{z}{1 - zT^2(dz)} , \quad (6.2.30)$$

³The reduction is trivial in this case as there are no two valent vertices in the pruned graph.

6.2. DOUBLE SCALING OF MELONIC T^4 TENSOR MODEL.

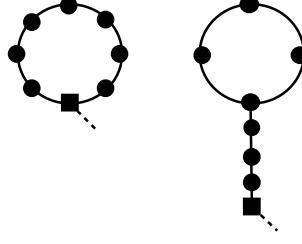


Figure 6.10: Two pruned graphs in the 1 loop case

while if the loop edge is multicolored we get an amplitude

$$\frac{1}{N^d} T(dz)^3 \frac{d(d-1)z^2 T^2(dz)}{[1 - dzT^2(dz)][1 - zT^2(dz)]} \quad (6.2.31)$$

For the graph on the right hand side the loop edge and the 1PR edge can be either unicolored or multicolored. Denoting l the self loop and t the vertical edge we get in each case the amplitude

$$\begin{aligned} l = c; t = c & \quad \frac{1}{N^{d-2}} T(dz)^5 \left(\frac{z}{1 - zT^2(dz)} \right)^2 \\ l = c; t = c' \neq c & \quad \frac{1}{N^{d-2}} T(dz)^5 \left(\frac{z}{1 - zT^2(dz)} \right)^2 \\ l = c; t = m & \quad \frac{1}{N^{d-2}} T(dz)^5 \left(\frac{z}{1 - zT^2(dz)} \right) \left(\frac{d(d-1)z^2 T^2(dz)}{[1 - dzT^2(dz)][1 - zT^2(dz)]} \right) \\ l = m; t = m & \quad \frac{1}{N^d} T(dz)^5 \left(\frac{d(d-1)z^2 T^2(dz)}{[1 - dzT^2(dz)][1 - zT^2(dz)]} \right)^2. \end{aligned} \quad (6.2.32)$$

The contribution of these graphs is obtained by summing over the choices of colors c and c'

$$\begin{aligned} & \frac{d}{N^{d-2}} T(dz)^5 \left(\frac{z}{1 - zT^2(dz)} \right)^2 + \frac{d(d-1)}{N^{d-2}} T(dz)^5 \left(\frac{z}{1 - zT^2(dz)} \right)^2 \\ & + \frac{d}{N^{d-2}} T(dz)^5 \left(\frac{z}{1 - zT^2(dz)} \right) \left(\frac{d(d-1)z^2 T^2(dz)}{[1 - dzT^2(dz)][1 - zT^2(dz)]} \right) \\ & + \frac{1}{N^d} T(dz)^5 \left(\frac{d(d-1)z^2 T^2(dz)}{[1 - dzT^2(dz)][1 - zT^2(dz)]} \right)^2. \end{aligned} \quad (6.2.33)$$

Taking into account that

$$1 - dzT^2(dz) = T(dz)\sqrt{1 - 4dz}, \quad T(dz) \xrightarrow{z \rightarrow (4d)^{-1}} 2, \quad (6.2.34)$$

and summing up all contributions, the one loop correction to the two point function exhibits the critical behavior

$$\mathcal{G}_2^1(z) \sim \frac{1}{N^{d-2}} \frac{d}{(d-1)\sqrt{1 - 4dz}} + \frac{1}{N^d} \frac{1}{2(1 - 4dz)}. \quad (6.2.35)$$

6.2. DOUBLE SCALING OF MELONIC T^4 TENSOR MODEL.

The first term reproduces the results found in [KOR14a]: the non analytic behaviour of the first correction in $1/N$ has a susceptibility exponent $\mathcal{G}_2^1(z) \sim (z_c - z)^{1-\gamma}$, $\gamma = +3/2$. This can be rewritten as

$$\mathcal{G}_2^1(z) \sim \frac{1}{N^{\frac{d-2}{2}}} \left(\frac{\sqrt{d}}{2(d-1)\sqrt{N^{d-2}[(4d)^{-1} - z]}} + \frac{N^{\frac{d-6}{2}}}{8dN^{d-2}[(4d)^{-1} - z]} \right), \quad (6.2.36)$$

hence the second term is washed out for $d < 6$ in the double scaling limit $N \rightarrow \infty$, $z \rightarrow (4d)^{-1}$, $N^{d-2}[(4d)^{-1} - z]$ fixed.

Two Loops. There are several graphs contributing at two loops whose edges can furthermore be unicolored or multicolored. We will analyze here only some relevant examples.

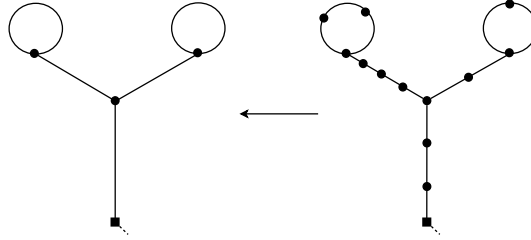


Figure 6.11: A pruned graph corresponding to the reduced graph \bar{G}_1

Consider the reduced graph \bar{G}_1 presented in Fig. 6.11 on the left with both loops having some color c and c' , and the 1PR edges multicolored. It is a cherry tree. The corresponding $1/N$ contribution is given by summing on the family of pruned graphs presented in Fig. 6.11 on the right and it is

$$\begin{aligned} \mathcal{A}(G_1) &= \frac{1}{N^{2(d-2)}} T^{11}(dz) \left(\frac{z}{(1 - zT^2(dz))} \right)^2 \left(\frac{d(d-1)z^2 T^2(dz)}{[1 - dzT^2(dz)][1 - zT^2(dz)]} \right)^3 \\ &= \frac{1}{N^{2(d-2)}} \frac{d^3(d-1)^3 z^8 T^{14}(dz)}{(1 - zT^2(dz))^5 (1 - 4dz)^{\frac{3}{2}}} \sim \frac{1}{N^{2(d-2)} (1 - 4dz)^{\frac{3}{2}}}. \end{aligned} \quad (6.2.37)$$

If one of the two loops is multicolored, the graph \bar{G}'_1 has an extra N^{-2} suppression in N and an extra $\frac{1}{\sqrt{1-4dz}}$ enhancement factor. Thus its amplitude is

$$\mathcal{A}(\bar{G}'_1) \sim \frac{1}{N^2 \sqrt{1-4dz}} \mathcal{A}(\bar{G}_1) \sim \frac{N^{\frac{d-6}{2}}}{\sqrt{N^{d-2}(1-4dz)}} \mathcal{A}(\bar{G}_1), \quad (6.2.38)$$

hence such reduced graphs are strictly suppressed with respect to \bar{G}_1 in the double scaling limit $N \rightarrow \infty$, $z \rightarrow (4d)^{-1}$, $N^{d-2}[(4d)^{-1} - z]$ fixed. Furthermore, the reduced graphs having

6.2. DOUBLE SCALING OF MELONIC T^4 TENSOR MODEL.

the same structure but without the vertical $1PR$ edge have less singular factors $\frac{1}{\sqrt{1-4dz}}$, hence are suppressed.

A second example is the reduced graph \bar{G}_2 of Fig. 6.12. If its 1PI bars are unicolored, its scaling with N is at best $N^{-2(d-2)}$ (if the two unicolored edges in the middle have the same color)⁴ the rest of its amplitude is



Figure 6.12: The reduced graph \bar{G}_2 and one pruned graph which projects onto it.

$$\begin{aligned} T^{11}(dz) \left(\frac{z}{(1 - zT^2(dz))} \right)^3 \left(\frac{d(d-1)z^2T^2(dz)}{[1 - dzT^2(dz)][1 - zT^2(dz)]} \right)^2 \\ = \frac{z^7 d^2 (d-1)^2 T^{13}(dz)}{(1 - zT^2(dz))^3 (1 - 4dz)}, \end{aligned} \quad (6.2.39)$$

and, as this graph has fewer factors $\frac{1}{\sqrt{1-4dz}}$, it is strictly suppressed in the double scaling regime with respect to \bar{G}_1 .

We now consider the case when some of the 1PI edges are multicolored. Note that if the tadpole edge is multicolored one always gets a suppressing factor $\frac{1}{N^2\sqrt{1-4dz}}$ with respect to the same reduced graph where the tadpole edge is unicolored (the scaling with N decreases by N^{-2} , while only one edge becomes critical). The most singular case is to have both 1PI edges in the middle multicolored. Such graphs scale like

$$\frac{1}{N^{2d-2}} \frac{1}{(1-4dz)^2} \sim \frac{1}{N^{2(d-2)}(1-4dz)^{\frac{3}{2}}} \frac{1}{N^2\sqrt{1-4dz}}, \quad (6.2.40)$$

and again are suppressed with respect to \bar{G}_1 .

Finally our last example is the graph \bar{G}_3 shown in Fig. 6.13. As it has one fewer $1PR$ edge than \bar{G}_2 , its amplitude is less singular.

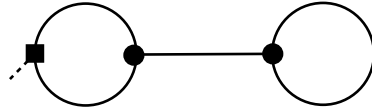


Figure 6.13: The reduced graph G_3 .

⁴The suppression is enhanced to $N^{-2(d-1)}$ if the two edges in the middle have different colors).

6.2. DOUBLE SCALING OF MELONIC T^4 TENSOR MODEL.

6.2.5 Proof of Theorem 9: Bounds.

This subsection is devoted to the proof of identity (6.2.21) in Theorem 9. Recall that, as a consequence of Theorem 8, the amplitude of any reduced graph is

$$\begin{aligned} \mathcal{A}(\bar{G}) &= N^{-dL(\bar{G})+2\sum_c L(\bar{G}_c)-2\sum_c g(\bar{G}_c)} T(dz)^{1+2E(\bar{G})} \\ &\quad \left(\frac{z}{1-zT^2(dz)} \right)^{\sum_c E(\bar{G}_c)} \left(\frac{d(d-1)z^2T^2(dz)}{[1-dzT^2(dz)][1-zT^2(dz)]} \right)^{E^{\text{m}}(\bar{G})}. \end{aligned} \quad (6.2.41)$$

Hence, for z close enough to z_c , it admits a bound

$$|\mathcal{A}(\bar{G})| \leq K_L N^{-dL(\bar{G})+2\sum_c L(\bar{G}_c)-2\sum_c g(\bar{G}_c)} (z_c - z)^{-\frac{E^{\text{m}}(\bar{G})}{2}}. \quad (6.2.42)$$

Passing to the rescaled variable $x = N^{d-2}(z_c - z)$ this bound writes

$$|\mathcal{A}(\bar{G})| \leq K_L N^{-dL(\bar{G})+2\sum_c L(\bar{G}_c)-2\sum_c g(\bar{G}_c)+\frac{d-2}{2}E^{\text{m}}(\bar{G})} x^{-\frac{E^{\text{m}}(\bar{G})}{2}}. \quad (6.2.43)$$

Using $E(\bar{G}) \leq 3L(\bar{G}) - 1$ and $E(\bar{G}_c) = V(\bar{G}_c) - C(\bar{G}_c) + L(\bar{G}_c)$ we have

$$E^{\text{m}}(\bar{G}) = E(\bar{G}) - \sum_c E(\bar{G}_c) \leq 3L(\bar{G}) - 1 - \sum_c L(\bar{G}_c) \quad (6.2.44)$$

choosing $x < 1$ (which includes a neighborhood of $x_c = \frac{1}{4(d-1)}$),

$$x^{-\frac{E^{\text{m}}(\bar{G})}{2}} \leq x^{-\frac{3}{2}L+\frac{1}{2}}. \quad (6.2.45)$$

Furthermore, the scaling with N can be bounded as

$$\begin{aligned} &-dL(\bar{G}) + 2\sum_c L(\bar{G}_c) - 2\sum_c g(\bar{G}_c) + \frac{d-2}{2}E(\bar{G}) - \frac{d-2}{2}\sum_c E(\bar{G}_c) \\ &\leq -\frac{d-2}{2} + \left(-d + \frac{d-2}{2}3\right)L(\bar{G}) + \left(2 - \frac{d-2}{2}\right)\sum_c L(\bar{G}_c) \\ &= -\frac{d-2}{2} - \frac{6-d}{2}L(\bar{G}) + \frac{6-d}{2}\sum_c L(\bar{G}_c), \end{aligned} \quad (6.2.46)$$

and the bound is saturated only if $E(\bar{G}) = 3L(\bar{G}) - 1$ and $V(\bar{G}_c) = C(\bar{G}_c)$ and $g(\bar{G}_c) = 0$. If the bound is not saturated then one gets at least a suppressing factor $N^{-\frac{1}{2}}$. As $d < 6$, using the fact that $\sum_c L(\bar{G}_c) \leq L(\bar{G})$, we obtain that the amplitude of any reduced graph is bounded by

$$A(\bar{G}) \leq K_L N^{\frac{2-d}{2}} x^{-\frac{3}{2}L+\frac{1}{2}} \quad (6.2.47)$$

and the scaling in N is saturated only if $E(\bar{G}) = 3L(\bar{G}) - 1$, $V(\bar{G}_c) = C(\bar{G}_c)$ and $\sum_c L(\bar{G}_c) = L(\bar{G})$, that is \bar{G} is a cherry tree. For all other graphs one gets at least an extra $N^{-\frac{1}{2}}$ suppressing factor, which establishes (6.2.22).

6.2. DOUBLE SCALING OF MELONIC T^4 TENSOR MODEL.

6.2.6 Computation of Cherry Trees

It remains to prove (6.2.21) by a direct computation. A full rooted binary tree is a plane tree in which every vertex has either two children or no children. The number of full binary trees with L leaves is the Catalan number C_{L-1} . This is also the number of cherry trees with L leaves since a cherry tree is just a full binary tree plus a single edge from the full binary tree to the ciliated vertex, plus addition of a tadpole with label c on each leaf. Hence the map from full binary trees to cherry trees is one to one.

In the special case $L = 0$, the reduced graph is just the bare ciliated vertex. It corresponds to melons, which we can consider as special degenerate cases of cherry trees. Hence

$$\mathcal{G}_{2,\text{cherry}}^0 = T(dz). \quad (6.2.48)$$

For $L \geq 1$ we get from definition 25 and Theorem 8, taking into account all the possible colorings of the tadpole edges,

$$\begin{aligned} \mathcal{G}_{2,\text{cherry}}^L(z, N) &= N^{-(d-2)L} C_{L-1} d^L \frac{z^{5L-2} d^{2L-1} (d-1)^{2L-1} T^{10L-3}}{(1-zT^2)^{3L-1} (1-zdT^2)^{2L-1}} \\ &= N^{-(d-2)L} C_{L-1} \frac{z^{5L-2} d^{3L-1} (d-1)^{2L-1} T^{8L-2}}{(1-zT^2)^{3L-1} (1-4dz)^{L-\frac{1}{2}}}. \end{aligned} \quad (6.2.49)$$

In the critical regime $z \rightarrow (4d)^{-1}$ we have $T \rightarrow 2$, $1 - zT^2 \rightarrow \frac{d-1}{d}$, $N^{d-2}(1-4dz) = 4dx$, hence collecting all the factors we get

$$\mathcal{G}_{2,\text{cherry}}^{L,x}(N) = N^{1-\frac{d}{2}} \frac{8\sqrt{d}C_{L-1}}{[16(d-1)]^L} x^{-L+\frac{1}{2}} + O(N^{\frac{1}{2}-\frac{d}{2}}). \quad (6.2.50)$$

We recover again the susceptibility of [KOR14a] by looking at equation (6.2.49) at $L = 1$ which give a correction in $N(\lambda - \lambda_c)^{-1}$ to the melonic term hence changes γ_0 from $1/2$ to $3/2$.

6.2.7 The Double Scaling Limit

Having completed the proof of Theorem 9 we can leave aside, for $d < 6$, all non cherry tree contributions. We can also forget the $O(N^{1/2-d/2})$ corrections in the cherry trees themselves (since they are of same order as the other discarded terms), keeping their main asymptotic behavior in (6.2.50) which is

$$\bar{\mathcal{G}}_{2,\text{cherry}}^{L,x}(N) = \frac{8\sqrt{d}C_{L-1}}{[16(d-1)]^L} x^{-L+1/2} N^{1-d/2}. \quad (6.2.51)$$

Double scaling then consists in summing these contributions over L to find out the leading singularity of the sum at the critical point $x = x_c = \frac{1}{4(d-1)}$.

6.2. DOUBLE SCALING OF MELONIC T^4 TENSOR MODEL.

The $L = 0$ contribution is the melonic contribution $T_{melo} = T(dz)$. Adding the sum over cherries gives the melonic + cherry approximation:

$$\bar{\mathcal{G}}_{2,cherry}^x(N) = T_{melo} + 8\sqrt{dx}N^{(1-d/2)} \sum_{L \geq 1} \frac{C_{L-1}}{[16x(d-1)]^L} \quad (6.2.52)$$

$$= T_{melo} + 8\sqrt{dx}N^{(1-d/2)} A \sum_{L \geq 1} A^{L-1} C_{L-1}, \quad (6.2.53)$$

with $A = [16x(d-1)]^{-1}$. Hence

$$\bar{\mathcal{G}}_{2,cherry}^x(N) = T_{melo} + 8\sqrt{dx}N^{(1-d/2)} AT(A) \quad (6.2.54)$$

$$= T_{melo} + 4\sqrt{dx}N^{(1-d/2)}(1 - \sqrt{1-4A}). \quad (6.2.55)$$

Since $\sqrt{1-4A} = x^{-1/2}\sqrt{x-x_c}$

$$\bar{\mathcal{G}}_{2,cherry}^x(N) = T_{melo} + 4\sqrt{d}N^{(1-d/2)}(\sqrt{x} - \sqrt{x-x_c}) \quad (6.2.56)$$

Substituting further $z = z_c - xN^{-d+2} = \frac{1}{4d} - xN^{-d+2}$ into T_{melo} we can reexpress

$$\bar{T}_{melo} = \frac{2}{1-4dxN^{-d+2}}[1 - 2\sqrt{dxN^{-d+2}}] \quad (6.2.57)$$

and we have obtained

Theorem 10. *The critical point in x is at $x_c = 1/4(d-1)$ and the double scaling limit of the quartic tensor model two point function is*

$$\bar{\mathcal{G}}_{2,cherry}^x(N) = \frac{2}{1-4dxN^{-d+2}}[1 - 2\sqrt{dxN^{-d+2}}] + 4\sqrt{d}N^{(1-d/2)}[\sqrt{x} - \sqrt{x-x_c}]. \quad (6.2.58)$$

If we rewrite everything in terms of z instead of x , we would obtain instead

$$\begin{aligned} \bar{\mathcal{G}}_{2,cherry}^x(N) &= \frac{2}{1-4d(z_c-z)}[1 - 2\sqrt{d(z_c-z)}] \\ &+ 4\sqrt{d}\left(\sqrt{(z_c-z)} - \sqrt{(z_c-z) - \frac{N^{2-d}}{4(d-1)}}\right) \\ &= \frac{2}{1-4d(z_c-z)}[1 - 8d^{3/2}(z_c-z)^{3/2}] - 4\sqrt{d}\sqrt{(z_c-z) - \frac{N^{2-d}}{4(d-1)}}. \end{aligned} \quad (6.2.59)$$

where we used $x = N^{d-2}(z_c - z)$.

The interpretation of these formulas requires further study. Theorem 10 shows a square root singularity in $x - x_c$ of same critical exponent than the melonic singularity. Equation

6.2. DOUBLE SCALING OF MELONIC T^4 TENSOR MODEL.

(6.2.59) seems to confirm that the melonic singularity has moved rather than changed structure. However the correct physical interpretation may be that the system undergoes two successive phase transitions.

Triple scaling would consist in writing $(x - x_c)N^\alpha = y$ and finding a new correcting expansion in powers of y .

6.3 Further results.

In this section we have described the double scaling of the quartic melonic tensor model in dimensions $2 < d < 6$. In fact we have not been able to extend our results above dimensions five as there is a problem of divergence of the generating series of the leading graphs. Typically in six dimensions all graphs are on the same footage thus the generating series is not summable anymore.

This problem can be attacked by purely combinatorial means by describing cleverly the set of d -colored graphs. This is done in [GS13], and allows a more general description of the double scaling of tensor models (where by “more general” we mean that the results concern the generic tensor model). In this description dimension six also appear to be a singular case. The fundamental reason have not been elucidated yet. This question deserves further investigation.

The same kind of techniques can be applied to explore the multi-orientable case. These studies have been explored by Eric Fusy and Adrian Tanasa in a purely combinatorial way [FT14]. Their results have been translated in physics language in [GT15]. However the critical behaviour is the same whatever one explores only colored graphs or the multi-orientable ones (in dimensions three).

These sets of further results are then a severe motivation for the exploration of new scaling. One could reach new phases by defining triple scaling as shown above, or by using the results of saddle points equations described in chap. 7 (see the remarks section therein).

6.3. FURTHER RESULTS.

Chapter 7

Matrix Model Representation of Tensor Models

In this chapter we pursue further the idea of decomposing the T^4 melonic tensor models into matrix variables using the technique of intermediate fields presented before. In this part of the thesis we shall focus on the results that can be obtained by using techniques coming from the study of formal matrix integrals. A set of references for this chapter is [NDE15, Dar14, DGR13].

7.1 Saddle point technique

In this section we use the saddle point technique for matrix models in order to rederive the results concerning the T^4 (i.e. quartic) melonic tensor model.

7.1.1 T^4 melonic tensor models and intermediate field representation.

The partition function of the model at rank d is given by:

$$Z = \int_{(\mathbb{C}^N)^{\otimes d}} dT d\bar{T} \exp \left(-N^{d-1} \left(\frac{1}{2} (\bar{T} \cdot T) + \frac{\lambda}{4} \sum_c (\bar{T} \cdot_{\hat{c}} T) \cdot_c (\bar{T} \cdot_{\hat{c}} T) \right) \right). \quad (7.1.1)$$

We again introduce an intermediate matrix field $M^{(c)}$ used to split the interaction terms $(\bar{T} \cdot_{\hat{c}} T) \cdot_c (\bar{T} \cdot_{\hat{c}} T)$. We recall briefly how it works. Doing this allows one to build a matrix model that is equivalent to the tensor model under consideration. We write the interaction term as:

$$\exp \left(-N^{D-1} \frac{\lambda}{4} (\bar{T} \cdot_{\hat{c}} T) \cdot_c (\bar{T} \cdot_{\hat{c}} T) \right) = \int dM^{(c)} \exp \left(-\frac{N^{d-1}}{2} \text{Tr}((M^{(c)})^2) - i\sqrt{\lambda/2} N^{d-1} \text{Tr}((\bar{T} \cdot_{\hat{c}} T) M^{(c)}) \right). \quad (7.1.2)$$

This choice of scaling for the matrix model allows us to suppress the factor N in the logarithmic potential that is obtained after integrating out the tensor degrees of freedom. Indeed rewriting the tensor model using this representation of the interaction term we get:

$$Z = \int_{(\mathbb{C}^N)^{\otimes d}} dT d\bar{T} \int_{H_N^d} \prod_c dM^{(c)} \exp\left(-\frac{N^{d-1}}{2} \bar{T} \left(\mathbb{1}^{\otimes d} + i\sqrt{\lambda/2} \sum_{k=1}^d \mathcal{M}_k\right) T\right) \exp\left(-\frac{1}{2} \sum_m \text{Tr}(\mathcal{M}_m^2)\right),$$

where we introduced the notation $\mathcal{M}_m = \mathbb{1}^{\otimes(m-1)} \otimes M^{(m)} \otimes \mathbb{1}^{\otimes(d-m)}$ for any $m \in \llbracket 1, d \rrbracket$. Integrating out the T 's we obtain

$$Z = \int_{(H_N)^d} \prod_c dM^{(c)} \det^{-1} \left(\mathbb{1}^{\otimes d} + i\sqrt{\lambda/2} \sum_{k=1}^d \mathcal{M}_k \right) \exp\left(-\frac{1}{2} \sum_m \text{Tr}(\mathcal{M}_m^2)\right).$$

This is the intermediate field representation of the T^4 melonic tensor model.

There are simple relations between the observables of this matrix model and some of the observables of the related tensor model.

Proposition 8. *We have:*

$$\langle \text{Tr}(\Theta_c^p) \rangle = \left(\frac{2i\sqrt{2}}{\sqrt{\lambda}} \right)^p \langle \text{Tr} H_p(M^{(c)}) \rangle, \quad (7.1.3)$$

and

$$\langle \text{Tr}(M^{(c)p}) \rangle = \langle \text{Tr} H_p \left(\frac{\sqrt{\lambda}}{2i\sqrt{2}} \Theta_c \right) \rangle, \quad (7.1.4)$$

where $\Theta_c = (\bar{T} \cdot_{\hat{c}} T)$ is a matrix, and H_p is the Hermite polynomial of order p .

Proof. Consider the mixed matrix-tensor representation of (7.1.3). One can write $\langle \text{Tr}(\Theta_c^p) \rangle$ as:

$$\begin{aligned} \left(\frac{N^{d-1}\sqrt{\lambda/2}}{2i} \right)^p \langle \text{Tr}(\Theta_c^p) \rangle &= \frac{1}{Z} \int_{(\mathbb{C}^N)^{\otimes d}} dT d\bar{T} \int_{(H_N)^d} \prod_c dM^{(c)} \\ &\left(\frac{\partial^p}{\partial M_{a_1 a_2}^{(c)} \partial M_{a_2 a_3}^{(c)} \cdots \partial M_{a_p a_1}^{(c)}} \exp\left(-\frac{N^{d-1}}{2} \bar{T} \left(\mathbb{1}^{\otimes d} + i\sqrt{\lambda/2} \sum_{k=1}^d \mathcal{M}_k\right) T\right) \right) \\ &\exp\left(-\frac{1}{2} \sum_m \text{Tr}(\mathcal{M}_m^2)\right), \end{aligned} \quad (7.1.5)$$

7.1. SADDLE POINT TECHNIQUE

with the convention that repeated indices are summed ¹. Up to integration by parts:

$$\begin{aligned} \left(\frac{-iN^{d-1}\sqrt{\lambda/2}}{2}\right)^p \langle \text{Tr}(\Theta_c^p) \rangle &= (-1)^p \int_{(\mathbb{C}^N)^{\otimes d}} dT d\bar{T} \int_{(H_N)^d} \prod_c dM^{(c)} \\ &\quad \exp\left(-\frac{N^{d-1}}{2} \bar{T} \left(\mathbb{1}^{\otimes d} + i\sqrt{\lambda/2} \sum_{k=1}^d \mathcal{M}_k\right) T\right) \\ &\quad \left(\frac{\partial^p}{\partial M_{a_1 a_2}^{(c)} \partial M_{a_2 a_3}^{(c)} \cdots \partial M_{a_p a_1}^{(c)}} \exp\left(-\frac{1}{2} \sum_m \text{Tr}(\mathcal{M}_m^2)\right)\right). \end{aligned} \quad (7.1.6)$$

Recall the definition of Hermite polynomials $H_p(x) = (-1)^p \exp(\frac{x^2}{2}) \frac{d^p}{dx^p} \exp(-\frac{x^2}{2})$. This leads to:

$$\left(\frac{-iN^{d-1}\sqrt{\lambda/2}}{2}\right)^p \langle \text{Tr}(\Theta_c^p) \rangle = N^{p(d-1)} \langle H_p(M^{(c)}) \rangle. \quad (7.1.7)$$

For the second equation it suffices to use the Weierstrass transform. It is defined as the linear operator sending a monomial of degree n to the corresponding Hermite polynomial H_n . Explicitly we have:

$$H_n(x) = e^{-\frac{1}{4} \frac{d^2}{dx^2} x^n}, \forall x \in \mathbb{R}. \quad (7.1.8)$$

Inverting the operator and using the property of Hermite polynomials $\frac{d}{dx} H_n(x) = n H_{n-1}(x)$ we get:

$$x^n = \sum_{k=0}^{[n/2]} \frac{1}{4^k} \frac{n!}{(n-2k)!k!} H_{n-2k}(x). \quad (7.1.9)$$

This can be further used to obtain:

$$\langle \text{Tr}(M^{(c)n}) \rangle = \sum_{k=0}^{[n/2]} \frac{1}{4^k} \frac{n!}{(n-2k)!k!} \left(\frac{\sqrt{\lambda}}{2i\sqrt{2}}\right)^{n-2k} \langle \text{Tr}(\Theta_c^{n-2k}) \rangle. \quad (7.1.10)$$

Hence $\langle \text{Tr}(M^{(c)n}) \rangle = \langle \text{Tr}(H_n(\frac{\sqrt{\lambda}}{2i\sqrt{2}} \Theta_c)) \rangle$. □

7.1.2 Leading Order $1/N$ Computation.

First we write the matrix model in eigenvalues variables:

$$\begin{aligned} Z &= \int \prod_{c=1}^d \prod_{j=1}^N d\lambda_j^{(c)} \exp\left(-\frac{N^{d-1}}{2} \sum_{c,j} \lambda_j^{(c)2}\right) \\ &\quad \prod_{\{j_c=1\}_{c=1\dots d}}^N \frac{1}{1 + i\sqrt{\lambda/2} \sum_{c=1}^d \lambda_{j_c}^{(c)}} \prod_{c=1}^d \Delta(\{\lambda_j^{(c)}\}_{j=1\dots N})^2, \end{aligned} \quad (7.1.11)$$

¹The factor $1/Z$ is generally omitted in the following computations since it is irrelevant.

Δ being the Vandermonde determinant. This can be rewritten as:

$$Z = \int \prod_{c=1}^d \prod_{j=1}^N d\lambda_j^{(c)} \exp(-N^d S(\{\lambda_j^{(c)}\}_{j=1 \dots d}^N)), \quad (7.1.12)$$

S being:

$$\begin{aligned} S(\{\lambda_j^{(c)}\}_{j=1 \dots d}^N) = & -\frac{1}{2N} \sum_{c,j} \lambda_j^{(c)2} + \frac{1}{N^d} \log \left[\prod_{c=1}^d \Delta(\{\lambda_j^{(c)}\}_{j=1 \dots N})^2 \right] \\ & + \frac{1}{N^d} \log \left[\prod_{\{j_c=1\}_{c=1 \dots d}}^N \frac{1}{1 + i\sqrt{\lambda/2} \sum_{c=1}^d \lambda_{j_c}^{(c)}} \right]. \end{aligned} \quad (7.1.13)$$

The saddle point equations are given by $\frac{\partial S}{\partial \lambda_k^{(c)}} = 0$ for all $(k, c) \in \llbracket 1, N \rrbracket \times \llbracket 1, d \rrbracket$. Thus we obtain the following equations:

$$\begin{aligned} 0 = & \frac{\partial S}{\partial \lambda_k^{(c)}} \\ = & -\frac{\lambda_k^{(c)}}{N} + \frac{1}{N^d} \sum_{l \neq k} \frac{1}{\lambda_k^{(c)} - \lambda_l^{(c)}} - \frac{i\sqrt{\lambda/2}}{N^d} \sum_{\{j_b\}_{b \neq c}} \frac{1}{1 + i\sqrt{\lambda/2}(\lambda_k^{(c)} + \sum_{b \neq c} \lambda_{j_b}^{(b)})}. \end{aligned} \quad (7.1.14)$$

As usual we retrieve the Coulomb potential between eigenvalues of the same color coming from the Vandermonde determinant. Also the tensor product interaction between the different matrices leads to an interaction term that tends to push all the eigenvalues towards $i\sqrt{\frac{2}{\lambda}}$. Finally, the usual Gaussian term tends to attract all the eigenvalues to zero. But this has to be analyzed with care. In fact the scaling in N coming from the tensor model scaling is very different from the one of usual matrix models. Since we do not know how to solve these equations exactly we have to make some assumptions. First we see that the equations are symmetric under the permutations of the color index c . This indicates that the saddle point might obey $\lambda_k^{(c)} = \lambda_k^{(b)}$ for any $b, c = 1 \dots d$. So we postulate this property. With this in mind the equations rewrite:

$$0 = \frac{\lambda_k^{(c)}}{N} - \frac{2}{N^d} \sum_{l \neq k} \frac{1}{\lambda_k^{(c)} - \lambda_l^{(c)}} + \frac{i\sqrt{\lambda/2}}{N^d} \sum_{\{j_r\}_{r=1 \dots d-1}} \frac{1}{1 + i\sqrt{\lambda/2}(\lambda_k^{(c)} + \sum_{r=1}^{d-1} \lambda_{j_r}^{(c)})} \quad (7.1.15)$$

Now taking care of the N factors, we see that if we make the hypothesis that $\lambda_k^{(c)} = O(1)$, the first and third terms are leading whereas the second term is a sub-leading $O(\frac{1}{N^{d-2}})$ term, by simple counting arguments. This motivates an Ansatz (that is checked later) for the expansion of $\lambda_k^{(c)}$ in $1/N$, $\lambda_k^{(c)} = \lambda_{k,0}^{(c)} + \frac{\lambda_{k,1}^{(c)}}{\sqrt{N^{(d-2)}}} + \frac{\lambda_{k,2}^{(c)}}{N^{(d-2)}} + \dots$. We compute $\lambda_{k,0}^{(c)} = \alpha$.

7.1. SADDLE POINT TECHNIQUE

In fact the formulation of the matrix model in terms of eigenvalues is totally symmetric with respect to the exchange of these eigenvalues. Thus it should not depend on either k or c . We can neglect the second term and we obtain:

$$\alpha_{\pm} = \frac{-1 \pm \sqrt{1 + 2d\lambda}}{2id\sqrt{\lambda/2}}. \quad (7.1.16)$$

We choose the $' + '$ root in order to avoid singularities in the contour of integration. Hereafter this root is simply denoted α . One has:

Proposition 9. *The partition function Z at the saddle point is given by $\exp(-N^d S_{\text{saddle}})$:*

$$Z = (1 + 2d\lambda)^{N^d/2} \exp\left(-\frac{N^d}{4d\lambda}(1 + 2d\lambda - 2\sqrt{1 + 2d\lambda})\right), \quad (7.1.17)$$

moreover, the free energy $F = -\log Z$, is given by

$$N^d \left(\frac{1}{4d\lambda}(1 + 2d\lambda - 2\sqrt{1 + 2d\lambda} + 1) - \frac{1}{2} \log(1 + 2d\lambda) \right) \quad (7.1.18)$$

Proof: Straightforward.

We also get the 2-point function of the tensor model.

Proposition 10. *The 2-point function $G_2(\lambda) = \frac{1}{N} < \bar{T} \cdot T >$ is given in the $N \rightarrow \infty$ limit by:*

$$\lim_{N \rightarrow \infty} G_2(\lambda) = \frac{1}{N} < \bar{T} \cdot T > = \frac{1}{N} < \text{Tr} \Theta_c > = \frac{2i\sqrt{2}}{\sqrt{\lambda}} \alpha = \frac{2}{d\lambda} (-1 + \sqrt{1 + 2d\lambda}). \quad (7.1.19)$$

Proof: Recall the relation of Proposition 8 $< \text{Tr}(\Theta_c^p) > = \left(\frac{2i\sqrt{2}}{\sqrt{\lambda}} \right)^p < \text{Tr}(H_p(M^{(c)})) >$.

In the $N \rightarrow \infty$ limit we can compute $< \text{Tr}(M^{(c)}) >$ at the saddle point approximation as $\sum_j \lambda_j^c = Na$. Thus within this approximation we get $< \text{Tr}(\Theta_c^1) > = \frac{2i\sqrt{2}}{\sqrt{\lambda}} N\alpha$. $< \bar{T} \cdot T > = < \text{Tr}(\Theta_c) >$ for an arbitrary $c \in \llbracket 1, d \rrbracket$. Moreover $H_1(x) = x$, from which we deduce the result. Note that it is easy to compute all the $\text{Tr}(\Theta_c^p)$'s in this approximation. \square

7.2 Schwinger-Dyson Equations

The Schwinger-Dyson equations are a set of equations that follows from the invariance of the functional integral under change of variables. In the realm of matrix models and combinatorics, they are the matrix integral formulation of Tutte's equations for combinatorial maps (at least if one assumes nice properties for the matrix integrals under consideration).

As suggested by the above study, we will consider the loop equations in terms of new variables $\tilde{M}^{(c)}$ defined by $M^{(c)} = \alpha \mathbb{1} + \frac{\tilde{M}^{(c)}}{\sqrt{N^{d-2}}}$. In fact the previous study showed that in the

7.2. SCHWINGER-DYSON EQUATIONS

$N \rightarrow \infty$ all the eigenvalues collapse to a point α and the NLO term follows a distribution which is more regular for a matrix model. Coming back to the expression of Z we have:

$$\begin{aligned} Z &= \int_{(H_N)^d} \prod_c dM^{(c)} \det^{-1} \left(\mathbb{1}^{\otimes d} + i\sqrt{\lambda/2} \sum_{k=1}^d \mathcal{M}_k \right) \exp \left(-\frac{1}{2} \sum_m \text{Tr}(\mathcal{M}_m^2) \right) \\ &= \int_{(H_N)^d} \prod_c dM^{(c)} \exp \left(-\frac{1}{2} \sum_m \text{Tr}(\mathcal{M}_m^2) - \text{Tr} \log \left(\mathbb{1}^{\otimes d} + i\sqrt{\lambda/2} \sum_{k=1}^d \mathcal{M}_k \right) \right). \end{aligned} \quad (7.2.20)$$

After the change of variables we obtain:

$$\begin{aligned} Z &= \frac{\exp(-\frac{N^d}{2}\alpha^2)}{N^{d-2}} \int_{(H_N)^d} \prod_c d\tilde{M}^{(c)} \exp \left(-\frac{N}{2} \sum_c \text{Tr} \tilde{M}_c^2 - \alpha N^{\frac{d}{2}} \sum_c \text{Tr} \tilde{M}_c \right. \\ &\quad \left. - \text{Tr} \log \left((1 + i\sqrt{\lambda/2}\alpha) \mathbb{1}^{\otimes d} + i\sqrt{\frac{\lambda}{2N^{d-2}}} \sum_c \tilde{\mathcal{M}}_c \right) \right), \end{aligned} \quad (7.2.21)$$

with the obvious extension of the previous notation: $\tilde{\mathcal{M}}_c = \mathbb{1}^{\otimes(c-1)} \otimes \tilde{M}_c \otimes \mathbb{1}^{\otimes(d-c)}$. We are now ready to compute the Schwinger-Dyson equations of this model in term of the \tilde{M} 's matrices,

$$\begin{aligned} 0 &= \frac{\exp(-\frac{N^d}{2}\alpha^2)}{N^{2(d-1)}(1 + i\sqrt{\lambda/2}\alpha)} \sum_{ij} \int \prod_c d\tilde{M}^{(c)} \frac{\partial}{\partial \tilde{M}_{ij}^{(c)}} \left((\tilde{M}^{(c)})_{ij}^k \exp \left(-\frac{N}{2} \sum_c \text{Tr} \tilde{M}_c^2 \right. \right. \\ &\quad \left. \left. - \alpha N^{\frac{d}{2}} \sum_c \text{Tr} \tilde{M}_c - \text{Tr} \log \left(\mathbb{1}^{\otimes d} - \frac{\alpha}{N^{(d-2)/2}} \sum_c \tilde{\mathcal{M}}_c \right) \right) \right), \end{aligned} \quad (7.2.22)$$

from which we obtain:

$$\begin{aligned} 0 &= \left\langle \sum_{n=0}^{k-1} \text{Tr}(\tilde{M}^{(c)n}) \text{Tr}(\tilde{M}^{(c)k-1-n}) \right\rangle - N \langle \text{Tr}(\tilde{M}^{(c)k+1}) \rangle \\ &\quad - \left\langle N^{\frac{d}{2}} \alpha \text{Tr}(\tilde{M}^{(c)k}) \right\rangle + \left\langle \sum_{p \geq 0} \left(\frac{\alpha}{N^{(d-2)/2}} \right)^{p+1} \right. \\ &\quad \left. \sum_{\{q_i\}_{i=1 \dots d} | \sum_i q_i = p} \binom{p}{q_1, \dots, q_d} \left(\prod_{i \neq c} \text{Tr}(\tilde{M}^{(i)q_i}) \right) \text{Tr}(\tilde{M}^{(c)q_c+k}) \right\rangle, \end{aligned} \quad (7.2.23)$$

the third term cancelling with the $p = 0$ term of the last sum:

$$\begin{aligned} 0 &= \left\langle \sum_{n=0}^{k-1} \text{Tr}(\tilde{M}^{(c)n}) \text{Tr}(\tilde{M}^{(c)k-1-n}) \right\rangle - N \langle \text{Tr}(\tilde{M}^{(c)k+1}) \rangle \\ &\quad + \left\langle \sum_{p \geq 1} \left(\frac{\alpha}{N^{(d-2)/2}} \right)^{p+1} \right. \\ &\quad \left. \sum_{\{q_i\}_{i=1 \dots d} | \sum_i q_i = p} \binom{p}{q_1, \dots, q_d} \left(\prod_{i \neq c} \text{Tr}(\tilde{M}^{(i)q_i}) \right) \text{Tr}(\tilde{M}^{(c)q_c+k}) \right\rangle. \end{aligned} \quad (7.2.24)$$

7.2. SCHWINGER-DYSON EQUATIONS

In the last sum of this equation the only leading term at $N \rightarrow \infty$ limit is the $p = 1$ term. In this regime the relevant equation writes:

$$\begin{aligned} 0 = & \left\langle \sum_{n=0}^{k-1} \text{Tr}(\tilde{M}^{(c)n}) \text{Tr}(\tilde{M}^{(c)k-1-n}) \right\rangle - N \langle \text{Tr}(\tilde{M}^{(c)k+1}) \rangle \\ & + \langle \alpha^2 N \text{Tr}(\tilde{M}^{(c)k+1}) \rangle + \langle \alpha^2 \text{Tr}(\tilde{M}^{(c)k}) \sum_{j \neq c} \text{Tr}(\tilde{M}^{(j)}) \rangle. \end{aligned} \quad (7.2.25)$$

At the $N \rightarrow \infty$ limit the mean values factorize. In fact, looking at the Feynman rules for the model of eq. (7.2.21) we obtain the following prescription:

- edges $\rightarrow \frac{1}{N}$
- faces $\rightarrow N$.

The contribution of the vertices of the graph is more involved. Expanding the potential we notice that the linear term of the expansion vanishes with the term $\alpha N^{\frac{d}{2}} \sum_c \text{Tr} \tilde{M}_c$. The remaining term of the expansion can be represented as vertices of Feynman graphs that are themselves made of k fat vertices of different colors $c \in \mathcal{S} \subset \llbracket 1, d \rrbracket$, $|\mathcal{S}| = k$ for $1 \leq k \leq d$. Each fat vertex of color c is of valence $p_c \geq 2$ and comes with a factor $N^{\frac{2-d}{2} \sum p_c + (d-k)}$ (where $d \geq 3$). Since we are interested in the $N \rightarrow \infty$ limit we focus on graphs that are made out of “leading vertices”. These are the ones for which $k = 1$ and $p := p_c = 2$ for a given c . The factor coming with these vertices is N , which is the usual scaling for matrix models.

One can extend the argument for $p \geq 2$ and find the scaling for such graphs G with E edges, F faces and V vertices. It is $N^{F-E+\sum_{v \in G} [(2-d)+(p_v-2)\frac{2-d}{2}+(d-1)]} = N^{\chi(G)-(d-2)(E-V)}$, with $\chi(G)$ the Euler characteristic of G . The leading graphs are thus the ones for which $(E-V)$ vanishes and χ is maximum. Finally this scaling favors at leading order disconnected contributions maximizing $\chi(G)$. Thus the observables factorize:

$$\langle \text{Tr}(\tilde{M}^{(l)s}) \text{Tr}(\tilde{M}^{(m)t}) \rangle = \langle \text{Tr}(\tilde{M}^{(l)s}) \rangle \langle \text{Tr}(\tilde{M}^{(m)t}) \rangle + O(N^{-(d-2)}). \quad (7.2.26)$$

Because of the symmetry we assume $\langle \text{Tr}(\tilde{M}^{(c)}) \rangle = 0$. This leads to:

$$0 = \left\langle \sum_{n=0}^{k-1} \text{Tr}(\tilde{M}^{(c)n}) \text{Tr}(\tilde{M}^{(c)k-1-n}) \right\rangle - N(1 - \alpha^2) \langle \text{Tr}(\tilde{M}^{(c)k+1}) \rangle. \quad (7.2.27)$$

Introducing the bi-resolvent $W_c(z_1, z_2) = \langle \text{Tr}(\frac{1}{z_1 - \tilde{M}^{(c)}}) \text{Tr}(\frac{1}{z_2 - \tilde{M}^{(c)}}) \rangle_{\text{cumulant}}$ and the resolvent $W_c(z) = \frac{1}{N} \langle \text{Tr}(\frac{1}{z - \tilde{M}^{(c)}}) \rangle$ and summing eq. (7.2.27) over k weighted with a counting variable z at the leading order in $1/N$, we get

$$W_c(z)^2 = (1 - \alpha^2)zW_c(z) - (1 - \alpha^2). \quad (7.2.28)$$

7.2. SCHWINGER-DYSON EQUATIONS

7.3 Double Scaling revisited.

In this section we describe a trick that sheds a new light on the shifted matrix model and its relation to the double scaling limit. This has been noticed by Razvan Gurau, and I thank him for explaining me this idea [Gursh].

Let us first make a few mathematical comments. We will consider the shifted model as a model for the random variables $\mathbf{M} \in \mathbf{H}_N = \bigoplus_{c=1}^d H_N^c$,

$$\mathbf{M} = \begin{pmatrix} M_1 \\ \vdots \\ M_d \end{pmatrix}. \quad (7.3.29)$$

The algebra structure on \mathbf{H}_N is the natural algebra structure inherited from the product law on H_N . As remarked by Razvan Gurau [Gursh], it is the source of some subtleties as the potential term is rather a function defined on $\bigotimes_{c=1}^d H_N^c$. Then one has to be precise by what we mean by covariance here. We will write the quadratic part of the action in term of the natural scalar product $(\cdot, \cdot) = \bigoplus_c (\cdot, \cdot)_c$ induced by the usual scalar product $(\cdot, \cdot)_c : H_N^c \times H_N^c \rightarrow \mathbb{R}$ given by the trace of the product on each summand, and operators in $\text{End}(\mathbf{H}_N)$. This will lead to new Feynman rules. This expression of the covariance will split into different parts that one can match with the different types of edges of the reduced graphs. Thus in this setting, the reduced graphs appear not only as a combinatorial trick to deal with the counting of Feynman graphs of the intermediate field theory in the double scaling regime, but more naturally as the Feynman graphs of the shifted theory. The physical interpretation is the same in both approaches. The melonic sector is resummed and the field acquires a non-zero expectation value. One then makes a translation of the field variables in order to write the theory in term of fluctuations around the new vacuum.

First, consider the model after the shift of variables. Expanding the term $-\text{Tr} \log(\mathbb{1}^{\otimes d} - \frac{\alpha}{N^{(d-2)/2}} \sum_c \mathcal{M}_c) = \sum_{p \geq 1} \frac{\alpha^p}{p N^{p(d-2)/2}} \text{Tr} \left(\sum_c \mathcal{M}_c \right)^p$, we have seen that the first term at $p = 1$ cancels with the term coming from the change of variables of the Gaussian part. However we can pursue further and notice that we can reabsorb the term at $p = 2$ as a covariance term for the random variables introduced above,

$$\mathbf{M} = \begin{pmatrix} M_1 \\ \vdots \\ M_d \end{pmatrix}. \quad (7.3.30)$$

7.3. DOUBLE SCALING REVISITED.

Indeed we have the measure:

$$\begin{aligned} & \prod_c dM_c \exp\left(-\frac{N}{2} \sum_c \text{Tr}(M_c^2) + \sum_{p \geq 2} \frac{\alpha^p}{N^{p(d-2)/2}} \text{Tr}\left(\sum_c \mathcal{M}_c\right)^p\right) \\ &= \prod_c dM_c \exp\left(-\frac{1}{2}(\mathbf{M}, \mathbf{V} \mathbf{M}) + \sum_{p \geq 3} \frac{\alpha^p}{N^{p(d-2)/2}} \text{Tr}\left(\sum_c \mathcal{M}_c\right)^p\right). \end{aligned} \quad (7.3.31)$$

Restricting our attention to the quadratic part of the action we have

$$\begin{aligned} & -\frac{N}{2}(1 - \alpha^2) \sum_c \text{Tr} M_c^2 + \alpha^2 \sum_{\substack{c, c' \\ c \neq c'}} \text{Tr} M_c \text{Tr} M_{c'} \\ &= \frac{1}{2} \left(-N(1 - \alpha^2) \sum_c \text{Tr} M_c^2 - \alpha^2 \sum_c (\text{Tr} M_c)^2 + \alpha^2 \left(\sum_c \text{Tr} M_c \right)^2 \right). \end{aligned} \quad (7.3.32)$$

This can be written in term of (\cdot, \cdot) and an operator \mathbf{V} on \mathbf{H}_N . We first consider the identity operator $\mathbb{I} : \mathbf{H}_N \rightarrow \mathbf{H}_N$. We also introduce the partial identity matrices $I_c \in \mathbf{H}_N$ by setting $I_c = \underbrace{0 \oplus \cdots \oplus 0}_{(c-1)\text{times}} \oplus 1 \oplus \cdots \oplus 0$.

From this we construct the projector $P_c : \mathbf{H}_N \rightarrow \mathbf{H}_N$ on $\text{Span}\{I_c\}$ as the tensor product of the linear form $\mathfrak{e}_c = \frac{(I_c, \cdot)}{\|I_c\|^2}$ on \mathbf{H}_N with I_c . Hence

$$P_c = I_c \otimes \mathfrak{e}_c. \quad (7.3.33)$$

We have

$$\begin{cases} P_c \mathbf{M} = \frac{I_c}{\|I_c\|^2} \text{Tr} M_c \\ P_c^2 = (I_c \otimes \mathfrak{e}_c(I_c)) \otimes \mathfrak{e}_c = P_c. \end{cases} \quad (7.3.34)$$

Then,

$$(\mathbf{M}, P_c \mathbf{M}) = \frac{\text{Tr} M_c}{\|I_c\|^2} (\mathbf{M}, I_c) = \frac{(\text{Tr} M_c)^2}{N}. \quad (7.3.35)$$

Also we use the projector on $\text{Span}\{I = \sum_c I_c\}$. We denote it P and

$$P = I \otimes \mathfrak{e}, \quad (7.3.36)$$

where \mathfrak{e} is the normalized form dual to I . It is a projector as one can check

$$\begin{cases} P^2 = P, \\ P \mathbf{M} = \frac{\sum_{c=1}^d \text{Tr}(M_c)}{dN} I. \end{cases} \quad (7.3.37)$$

Thus,

$$(M, P M) = \frac{(\sum_c \text{Tr} M_c)^2}{dN}. \quad (7.3.38)$$

7.3. DOUBLE SCALING REVISITED.

One can decompose \mathbf{V} on the operators \mathbb{I} , P_c and P . From (7.3.32),

$$\mathbf{V} = N(1 - \alpha^2)\mathbb{I} + N\alpha^2 \sum_{c=1}^d (P_c - P). \quad (7.3.39)$$

One has to inverse this operator \mathbf{V} . This can be done easily by writing \mathbf{V} in terms of orthogonal operators. First notice that

$$\begin{cases} P_c P_{c'} = \delta_{cc'}, \\ P_c P = \frac{I_c}{\|\mathbb{I}\|^2} \otimes \mathbf{e}. \end{cases} \quad (7.3.40)$$

One thus writes:

$$\mathbf{V} = N(1 - \alpha^2)(\mathbb{I} - \sum_c P_c) + N(\sum_c P_c - P) + N(1 - d\alpha^2)P. \quad (7.3.41)$$

One checks that this diagonalizes \mathbf{V} as in fact as $\text{Im}(P) \subset \ker((\mathbb{I} - \sum_c P_c)$, $\text{Im}(\sum_c P_c - P) \subset \ker(\mathbb{I} - \sum_c P_c)$ and $\text{Im}(P) \subset \ker(\sum_c P_c)$. Therefore

$$\begin{cases} (\mathbb{I} - \sum_c P_c)P = P - (\sum_c P_c)P = P - \frac{\sum_c I_c}{\|\mathbb{I}\|^2} \otimes \mathbf{e} = 0, \\ (\mathbb{I} - \sum_c P_c)(\sum_c P_c - P) = 0, (\sum_c P_c - P)P = 0. \end{cases} \quad (7.3.42)$$

$(\mathbb{I} - \sum_c P_c)$, P and $(\sum_c P_c - P)$ are projectors on mutually orthogonal subspaces. Moreover, $\text{Im}(\sum_c P_c - P) \oplus \text{Im}(P) \oplus \text{Im}(\mathbb{I} - \sum_c P_c) = \mathbf{H}_N$. One then deduces the inverse of \mathbf{V}

$$\mathbf{V}^{-1} = \frac{1}{N(1 - \alpha^2)}(\mathbb{I} - \sum_c P_c) + \frac{1}{N}(\sum_c P_c - P) + \frac{1}{N(1 - d\alpha^2)}P. \quad (7.3.43)$$

One further rewrites this operator,

$$\mathbf{V}^{-1} = \frac{1}{N(1 - \alpha^2)}\mathbb{I} - \frac{\alpha^2}{N(1 - \alpha^2)} \sum_c P_c + \frac{d\alpha^2}{N(1 - d\alpha^2)}P. \quad (7.3.44)$$

One has obtained the following proposition

Proposition 11. *The covariance operator for the Gaussianly distributed random variables \mathbf{M} and its inverse are given by*

$$\begin{cases} \mathbf{V} = N(1 - \alpha^2)\mathbb{I} + N\alpha^2 \sum_{c=1}^d (P_c - P), \\ \mathbf{V}^{-1} = \frac{1}{N(1 - \alpha^2)}\mathbb{I} - \frac{\alpha^2}{N(1 - \alpha^2)} \sum_c P_c + \frac{d\alpha^2}{N(1 - d\alpha^2)}P. \end{cases} \quad (7.3.45)$$

Note that \mathbf{V} and \mathbf{V}^{-1} are symmetric operators.

7.3. DOUBLE SCALING REVISITED.

We want to construct the formal partition function of the T^4 tensor model as a formal sum of polynomial moments of the Gaussian distribution of the random variables \mathbf{M} . To this aim we use a rather funny trick. We now show the following,

Lemma 4. *Polynomial moments of a non-degenerate Gaussian distribution of random vectors in E a finite dimensional \mathbb{R} Euclidean space, with covariance operator O can be written in differential form as*

$$\langle P(x_1, \dots, x_n) \rangle = \left[e^{\frac{1}{2}(\nabla, O^{-1}\nabla)} P(x_1, \dots, x_n) \right]_{x_i=0}, \quad (7.3.46)$$

where P is a polynomial of all variables. ∇ denotes the gradient operator on the affine space associated to E .

Proof. Consider the Gaussian distribution

$$\frac{dx}{\sqrt{\det(2\pi O)}} e^{-\frac{1}{2}(x, Ox)}. \quad (7.3.47)$$

For a smooth function f of the x_i 's, one associates the transform

$$W_O[f](x) = f * \left(\frac{e^{-\frac{1}{2}(x, Ox)}}{\sqrt{\det(2\pi O)}} \right) = \int \frac{dx}{\sqrt{2\pi \det(O)}} f(x-y) e^{-\frac{1}{2}(y, Oy)}. \quad (7.3.48)$$

Then write

$$f(x-y) = e^{-(y, \nabla_x)} f(x). \quad (7.3.49)$$

One thus has

$$W_O[f](x) = \int \frac{dy}{\sqrt{\det(2\pi O)}} e^{-\frac{1}{2}(y, Oy)} e^{-(y, \nabla_x)} f(x). \quad (7.3.50)$$

Moreover, since O is symmetric,

$$(y, Oy) = (y + O^{-1}\nabla_x, O(y + O^{-1}\nabla_x)) - 2(y, \nabla_x) - (\nabla_x, O^{-1}\nabla_x). \quad (7.3.51)$$

Thus, after translating the variable y ,

$$W_O[f](x) = \int \frac{dy}{\sqrt{\det(2\pi O)}} e^{-\frac{1}{2}(y, Oy)} e^{\frac{1}{2}(\nabla_x, O^{-1}\nabla_x)} f(x) = e^{\frac{1}{2}(\nabla_x, O^{-1}\nabla_x)} f(x). \quad (7.3.52)$$

Thus expression is well defined as long as $f = P$ is a polynomial in the x_i 's since the number of non-zero term in the sum is finite. Finally, the corresponding Gaussian moments are $W_O[f](0)$ and thus one has the expected result

$$\langle P(x) \rangle = \left[e^{\frac{1}{2}(\nabla_x, O^{-1}\nabla_x)} P(x) \right]_{x=0}. \quad (7.3.53)$$

7.3. DOUBLE SCALING REVISITED.

□

Applying this formula in our case, the operator O is our V and the vector random variable x is \mathbf{M} . Moreover the scalar product $(,)$ is the one defined at the beginning of the section. More explicitly we have

$$\begin{aligned} (\nabla_{\mathbf{M}}, \mathbf{V}^{-1} \nabla_{\mathbf{M}}) &= \frac{1}{N(1-\alpha^2)} \sum_c \text{Tr} \left(\frac{\partial}{\partial M_c} \frac{\partial}{\partial M_c} \right) - \frac{\alpha^2}{N^2(1-\alpha^2)} \sum_c \text{Tr} \left(\frac{\partial}{\partial M_c} \right) \text{Tr} \left(\frac{\partial}{\partial M_c} \right) \\ &+ \frac{\alpha^2}{N^2(1-d\alpha^2)} \sum_{c,c'} \text{Tr} \left(\frac{\partial}{\partial M_c} \right) \text{Tr} \left(\frac{\partial}{\partial M_{c'}} \right). \end{aligned} \quad (7.3.54)$$

In order to compute the partition function we have to compute the action of $\exp(\frac{1}{2}(\nabla_{\mathbf{M}}, \mathbf{V}^{-1} \nabla_{\mathbf{M}}))$ on the potential of our model, understood as a formal series in α and N . Thus one is left with understanding the action of $\exp(\frac{1}{2}(\nabla_{\mathbf{M}}, \mathbf{V}^{-1} \nabla_{\mathbf{M}}))$ on polynomials of the form $(\sum_c \mathcal{M}_c)^n$. For a given $n \geq 1$, the action of $\text{Tr} \left(\frac{\partial}{\partial M_c} \right)$ does not depend on c . This leads to the following theorem

Theorem 11. *The partition function of the T^4 tensor model can be rewritten as*

$$\begin{aligned} Z[\lambda, N] &= \frac{\exp(-\frac{N^d}{2} d\alpha^2)}{N^{2(d-1)}(1+i\sqrt{\lambda/2}\alpha)} \int d\mathbf{M} \exp \left(-\frac{N}{2} \sum_c \text{Tr} M_c^2 - \frac{d-1}{dN} \alpha^2 \sum_{c,c'} \text{Tr}(M_c) \text{Tr}(M_{c'}) \right) \\ &\exp \left(-\text{Tr} \sum_{p \geq 3} \frac{1}{p} \text{Tr} \left(\frac{\alpha}{N^{(d-2)/2}} \sum_c \tilde{\mathcal{M}}_c \right)^p \right). \end{aligned} \quad (7.3.55)$$

Proof. As noticed above,

$$\text{Tr} \left(\frac{\partial}{\partial M_c} \right) (\sum_c \mathcal{M}_c)^n = n (\sum_c \mathcal{M}_c)^{n-1} \quad (7.3.56)$$

which does not depend on the color c . Thus the action of $\exp(\frac{1}{2}(\nabla_{\mathbf{M}}, \mathbf{V}^{-1} \nabla_{\mathbf{M}}))$ on polynomials of $\sum_c \mathcal{M}_c$ reduces to the action of a simpler operator built out of $\tilde{\mathbf{V}}^{-1}$

$$\tilde{\mathbf{V}}^{-1} = \frac{1}{N(1-\alpha^2)} \mathbb{I} + \frac{(d-1)\alpha^2}{N(1-\alpha^2)(1-d\alpha^2)} P, \quad (7.3.57)$$

whose expression is obtained by just changing $\sum_c P_c \rightarrow \frac{1}{d}P$, as allowed by the above remark.

This inverse covariance $\tilde{\mathbf{V}}^{-1}$ corresponds to a well defined covariance $\tilde{\mathbf{V}}$:

$$\tilde{\mathbf{V}} = N(1-\alpha^2) \mathbb{I} - N(d-1)\alpha^2 P. \quad (7.3.58)$$

7.3. DOUBLE SCALING REVISITED.

Thus, from Lemma 4, up to proportionality factors, $Z[\lambda, N]$

$$Z[\lambda, N] \propto e^{\frac{1}{2}(\nabla_{\mathbf{M}}, \tilde{\mathbf{V}} \nabla_{\mathbf{M}})} \exp \left(\sum_{p \geq 3} \frac{1}{p} \text{Tr} \left(\frac{\alpha}{N^{(d-2)/2}} \sum_c \mathcal{M}_c \right)^p \right). \quad (7.3.59)$$

This expression can be translated in terms of Gaussian integrals,

$$\begin{aligned} Z[\lambda, N] \propto & \int \prod_c dM_c \exp \left(-\frac{N}{2} \left((1 - \alpha^2) \sum_c \text{Tr}(M_c^2) - \frac{d-1}{dN} \alpha^2 \sum_{cc'} \text{Tr}(M_c) \text{Tr}(M_{c'}) \right) \right) \\ & \exp \left(\sum_{p \geq 3} \frac{1}{p} \text{Tr} \left(\frac{\alpha}{N^{(d-2)/2}} \sum_c \mathcal{M}_c \right)^p \right). \end{aligned} \quad (7.3.60)$$

□

One can recognize on $\tilde{\mathbf{V}}$ two types of terms, the one proportional to \mathbb{I} and the one proportional to P . This is the translation of the phenomenon we encountered in Chapter 6. In fact in this chapter we computed the double scaling limit in term of reduced graphs. These graphs had two types of edges, either uni-colored edges, or multi-colored ones. This can be read at the level of the covariance $\tilde{\mathbf{V}}$ as the unicolored edges correspond to the \mathbb{I} term and the multi-colored ones to the P term. When reaching the critical point λ_c the P term is enhanced while the \mathbb{I} term is killed thus the covariance becomes singular. This technique can be further used to re-derive the full double scaling limit of the quartic melonic tensor model.

7.4 Bilinear identities

This Hubbard-Stratanovitch representation can be of further use. In fact one knows that the 1-matrix model satisfies bilinear identities called *Hirota's equations*. These equations are in a sense a generalization of the orthogonality relations for orthogonal polynomials of random matrices.

In this section I will be very pedestrian, even more than in [Dar14], giving motivations (but not always proofs as they can be a bit lengthy) for the different equalities I am going to use as they are not much known in the tensor framework². But one must be aware that they are well known in the matrix model and integrable system context.

7.4.1 Orthogonality Relations

We consider the generic one matrix model. In this case we are looking for sets of orthogonal polynomials with respect to the measure $d\mu = d\lambda e^{-\frac{N}{2}\lambda_i^2 + N \sum_p t_p \lambda^p}$. Such orthogonal

²This has been reflected by the questions I received on the subject.

polynomials are provided by *Heine's formula* [Eyn15a] as $P_{N,\{t_p\}}(x) = \langle \det(x - M) \rangle$. Here N is the size of the matrix M . In fact using eigenvalues variables one has:

$$P_{N,\{t_p\}}(x) = \frac{1}{Z_N} \int \prod_{i=1}^N d\mu(x_i) (x - x_i) \prod_{i < j} (x_i - x_j)^2. \quad (7.4.61)$$

One has

$$(N+1)Z_N \int d\mu(x) P_{N,\{t_p\}}(x) P_{M,\{t_p\}} = Z_{N+1} \delta_{M,N}. \quad (7.4.62)$$

This can be useful to compute iteratively the values for Z_N as long as one can compute $P_{N,\{t_p\}}(x)$. Typically one finds something of the form $Z_N = \prod_i K_i / K_i^{(0)}$. There exists techniques to compute the $K_i = \frac{Z_{i+1}}{(i+1)Z_i}$'s. Some of them are described in [Eyn15a, DFGZJ95, Di04]. The lower the degree of the potential is, the more efficient and explicit they are. However, as we said, this orthogonality identity is the glimpse of a more general identity. Consider $Z_{1MM}[\{t_p\}]$. The respective orthogonal polynomial at matrix size N is given by the mean value of the characteristic polynomial

$$\begin{aligned} P_{N,\{t_p\}}(x) &= \langle \det(x - M) \rangle = \langle \exp(\text{Tr} \log(x - M)) \rangle \\ &= \exp(N \log x) \sum_{k \geq 0} \frac{1}{k!} \left\langle \left(\sum_{n \geq 1} \frac{1}{n} \frac{\text{Tr}(M^n)}{x^n} \right)^k \right\rangle. \end{aligned} \quad (7.4.63)$$

One has another representation of the orthogonality relations [AK96]:

$$\frac{1}{2i\pi} \oint_{\mathcal{C}} dz \langle \det(z - M) \rangle_{N,\{t_p\}} \langle \det(z - M)^{-1} \rangle_{n+1,\{t_p\}} = \pm \delta_{N,n}. \quad (7.4.64)$$

The contour \mathcal{C} surrounds 0 as well as the integration domain in $\gamma \in \mathbb{C}^{N^2}$ of eigenvalues. In general it is built out of a real segment such as $[\lambda_{min}, \lambda_{max}]^{N^2}$, however the segment can be deformed in the complex plane as long as one avoids singularities. Being careful to avoid such singularities one can *prove* this equality (as well as the general Hirota equations) for *convergent* matrix integrals. In our case we will give the idea for formal matrix models, thus we will be able to deform the integration domain without much care and take the limit λ_{min} (λ_{max}) going to $-\infty$ (resp. $+\infty$). The above expression rewrites

$$\begin{aligned} & \frac{1}{2i\pi Z_{n+1}} \oint_{\mathcal{C}} dz P_{N,\{t_p\}}(z) \int \prod_{i=1}^{n+1} d\mu(\lambda_i) \prod_{i < j} (\lambda_i - \lambda_j)^2 \prod_k (z - \lambda_k)^{-1} \\ &= \frac{1}{2i\pi Z_{n+1}} \sum_k \int \prod_{i=1}^{n+1} d\mu(\lambda_i) P_{N,\{t_p\}}(\lambda_k) \prod_{i < j} (\lambda_i - \lambda_j)^2 \prod_{i \neq k} (\lambda_k - \lambda_i)^{-1}, \end{aligned} \quad (7.4.65)$$

7.4. BILINEAR IDENTITIES

where we just noticed that the poles in the integrand in z are when $z \rightarrow \lambda_k$ since $P_{N,\{t_p\}}(z)$ is a polynomial and has no poles on the complex plane. Moreover we remark that poles of order strictly greater than one corresponds to cases in which several eigenvalues coincide. These cases correspond to subspaces of zero measure and thus do not contribute. We can go along and write that the above expression is equal to

$$\frac{1}{Z_{n+1}} \sum_k \int \prod_j d\mu(\lambda_j) P_{N,\{t_p\}}(\lambda_k) \prod_{\substack{i < j \\ i, j \neq k}} (\lambda_i - \lambda_j)^2 \prod_{i \neq k} (\lambda_i - \lambda_k). \quad (7.4.66)$$

From this expression after the change of variables $\{\lambda_1, \dots, \hat{\lambda}_k, \dots, \lambda_{n+1}\} \rightarrow \{\lambda_1, \dots, \lambda_n\}$ and $\lambda_k \rightarrow \lambda$, one recognizes

$$\frac{Z_n}{Z_{n+1}} \sum_{k=1}^{n+1} \int d\mu(\lambda) P_{N,\{t_p\}}(\lambda) P_{n,\{t_p\}}(\lambda). \quad (7.4.67)$$

One thus obtains the identity (7.4.64). In fact one can use the fact that the $P_{N,\{t_p\}}(x)$ are orthogonal to any polynomial of degree less than N to demonstrate in a very similar fashion that

$$\frac{1}{2i\pi} \oint dz e^{\sum_{p \geq 0} t_p - t'_p} \langle \det(z - M) \rangle_{N,\{t_p\}} \langle \det(z - M)^{-1} \rangle_{N',\{t'_p\}} = 0, \quad \forall N \geq N'. \quad (7.4.68)$$

Now notice that

$$\frac{1}{N} \frac{\partial}{\partial t_p} Z_{1MM}[\{t_p\}] = Z_{1MM}[\{t_p\}] \langle \text{Tr}(M^p) \rangle. \quad (7.4.69)$$

This can be used to write $P_{N,\{t_p\}}(x)$ as the action of a differential operator on $Z_{1MM}[\{t_p\}]$. By using the exponential formula for the determinant, we have up to a normalization factor, $P_{N,\{t_p\}}(x)$

$$P_{N,\{t_p\}}(x) \propto \exp(N \log x) \exp\left(\frac{1}{N} \sum_{n \geq 1} \frac{1}{n} x^{-n} \frac{\partial}{\partial t_n}\right) Z_{1MM}[\{t_p\}]. \quad (7.4.70)$$

This writing has to be understood in its more general form as a formal integral. Thus we define the *vertex operators*

Definition 26. *The vertex operators $V_{\pm}(z)$ are formal differential operators on $\mathbb{C}[[\infty]]$ defined by*

$$V_{\pm}(z) = \exp(\log(z^{\pm 1}) \frac{\partial}{\partial t_o}) \exp(\pm \frac{1}{N} \sum_{n \geq 1} \frac{1}{n} x^{-n} \frac{\partial}{\partial t_n}) \quad (7.4.71)$$

where this identity has to be understood as a formal series in the $\frac{\partial}{\partial t_p}$'s.

7.4. BILINEAR IDENTITIES

See [JM85] for more precisions on the meaning of these operators³. This can be used to write the orthogonality relations (7.4.64) in a operatorial form, so to say,

$$\frac{1}{2i\pi} \oint_C (V_+(z)Z_{1MM}[N, \{t_p\}]) (V_-(z)Z_{1MM}[N', \{t'_p\}]) = 0, \quad \forall N \geq N'. \quad (7.4.72)$$

This is actually a form of the Hirota equations as stated by Jimbo and Miwa [JM85]. It is an equation that is bilinear in its entries $Z_{1MM}[N, \{t_p\}]$ and $Z_{1MM}[N', \{t'_p\}]$. This is one, among others, manifestation of integrability properties in matrix models. Indeed one has the following theorem

Theorem 12. $\tau[\{t_p\}] \in \mathbb{C}[[\infty]]$ is a tau function if it satisfies

$$\oint e^{\sum_p (t_p - t'_p) z^p} \tau[\{t_p\} + [z^{-1}]] \tau[\{t_p\} - [z^{-1}]] = 0, \quad (7.4.73)$$

where $\{t_p\} \pm [z^{-1}]$ means that the set of formal variables $\{t_p\}$ is replaced by the set of formal variables $\{t_p \pm z^{-p}\}$ where z is considered as a new formal variable in the resulting formal series.

Actually, this theorem is valid in the finite number of formal variables case and when τ is a function. Moreover in our case the formal series in z is a polynomial and a meromorphic function so that z belongs to $\mathbb{C} - \{\text{points}\}$. More can be said once one has seen the concept of (classical) spectral curve for a matrix model, z being a point of the spectral curve. However this is not really necessary here.

7.4.2 Decomposition of matrix models.

The preceding remark is important. In fact this operatorial form of the Hirota equations, allows us to obtain (at least at the formal level) a series of bilinear identities on a family of different models. This is done by the aim of *Givental* decomposition. We describe here a few ideas of this decomposition. Typically, one is able to decompose some matrix models with partition function \mathcal{Z} as

$$\mathcal{Z} = e^{\mathcal{U}} \prod_{k=1}^M Z_{1MM}[\{t_p^k\}] = e^{\hat{\mathcal{U}}} \prod_{k=1}^M Z_K[\Lambda_k], \quad (7.4.74)$$

where \mathcal{U} is a quadratic formal differential operator in the t_p^k 's. It is called *intertwining* operator, as it mixes the different models together. Its counterpart $\hat{\mathcal{U}}$ is a differential operator in the $\text{Tr}(\Lambda_k^p)$ that mixes different Kontsevitch τ functions in order to reconstruct the model \mathcal{Z} . This is interesting as one knows the geometric meaning of the quantities computed by

³They are related to the interpretation of τ function in terms of representation of $gl(\infty)$ Lie algebra. If it is a very interesting topics, which would deserve a thesis on its own.

7.4. BILINEAR IDENTITIES

the Kontsevitch matrix model. More explanation can be found in [EO08, NDE15]. So it relates numerous matrix models correlation functions to intersection numbers of moduli spaces of Riemann surfaces. One may ask whether or not this can be understood in a combinatorial way, using bijective techniques? The author is not aware of such works but this would be a very interesting question to investigate.

From this decomposition one may form bilinear identities for the corresponding models \mathcal{Z} by dressing the vertex operators $V_{\pm}^k(z_k)$ acting on each $Z_{1MM}[\{t_p^k\}]$ [AK96], so that the dressed operators are

$$V_{\pm, \text{dressed}}^k(z_k) = e^{\mathcal{U}} V_{\pm}^k(z_k) e^{-\mathcal{U}} \quad (7.4.75)$$

for each $k \in \llbracket 1, M \rrbracket$. This type of strategies apply directly to the $O(n)$ matrix model for example. This is a model of self-avoiding loops on random surfaces⁴. It is built out of a $(n+1)$ matrix model defined by the partition function [Eyn15a]

$$\begin{aligned} \mathcal{Z}_{O(n)} = & \int_{H_N^{n+1}, \text{formal}} dM \prod_i^n dA_i \exp\left(-\frac{N}{2}(\text{Tr}(M^2) + \sum_i^n \text{Tr}(A_i^2))\right) \\ & \exp\left(N \sum_p t_p \text{Tr}(M^p) + N \sum_i \text{Tr}(MA_i^2)\right). \end{aligned} \quad (7.4.76)$$

In fact the combinatorics of this matrix integral has the specific feature that there are n vertices of the form 7.1. The half-edges of color i represent the A_i^2 in the $\text{Tr}(MA_i^2)$ of the

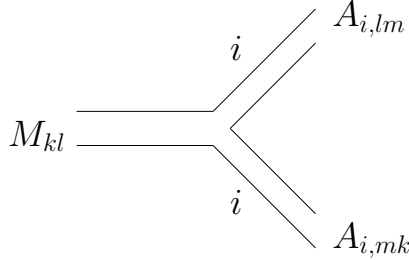


Figure 7.1: The vertices of the $O(n)$ loop model. Two of the adjacent half-edges are colored i , for each $i \in \llbracket 1, n \rrbracket$.

defining integral. Moreover the action is only quadratic in the A_i so that the edges of color i can only form loops. Furthermore, since the action is only quadratic in the A_i one can integrate them

$$\mathcal{Z}_{O(n)} = \int_{\text{formal}} dM e^{-\frac{N}{2} \text{Tr}(M^2) + N \sum_p t_p \text{Tr}(M^p)} \det(\mathbb{1}^{\otimes 2} - \mathbb{1} \otimes M - M \otimes \mathbb{1})^{-n}. \quad (7.4.77)$$

⁴This model has been much studied in statistical physics as when one make an analytical continuation on its parameter n one is able to describe Kosterlitz-Thouless transition. Moreover it can be thought of a model for $2+1$ gravity and generalizations appear in the context of string theory.

7.4. BILINEAR IDENTITIES

Indeed this decomposes on a Hermitian one matrix model as

$$\mathcal{Z}_{O(n)} = e^{-\frac{n}{N^2} \sum_{p \geq 1} \frac{(-1)^p}{p} \sum_{0 \leq k \leq p} \binom{p}{k} \frac{\partial}{\partial t_k} \frac{\partial}{\partial t_{p-k}}} Z_{1MM}[\{t_p\}] \Big|_{\{t_0=0, t_1=0, t_2=0\}}. \quad (7.4.78)$$

The operator \mathcal{U} in this case is the differential operator in the exponential.

7.4.3 Decomposition of tensor models.

Following the preceding line of thought one can obtain this type of result for our T^4 melonic tensor models. However there are a few drawbacks that we point out already. First the intertwining operator will contain $1/N$ factors mixing in a non-trivial way the expansion of the several Hermitian matrix models and the factors coming from the \mathcal{U} operator. Moreover the operator \mathcal{U} will be, *a priori*, d -linear in the formal variables in d dimensions. Although one can of course consider classes of models that contains only two T^4 melonic interactions, that seems unnatural at first sight. The main problem is that the integrability properties of the models that decomposes in a Givental form depend crucially on this property. However one feature that does not depend on this property is the fact that the quantity generated by the model can be written in term of moduli spaces integrals. This has been shown in a recent⁵ work [BS15] of Gaetan Borot and Sergey Shadrin in the case of multi-trace Hermitian one matrix models. We have good reasons to think that it also applies at least to some subsets of melonic T^4 tensor models.

One has the following theorem [Dar14]

Theorem 13. *The partition function of the d -dimensional melonic T^4 model can be rewritten as:*

$$Z[\lambda, N] = e^{\hat{X}} e^{\hat{Y}} \prod_{i=1}^d Z_{1MM}[\{t_p^i\}_{p \in \mathbb{N}}] = e^{\hat{O}} \prod_{i=1}^d Z_{1MM}^i[\{t_p^i\}_{p \in \mathbb{N}}] \quad (7.4.79)$$

where $Z_{1MM}[\{t_p^i\}_{p \in \mathbb{N}}]$ is a Hermitian 1-matrix model partition function and $\hat{X}, \hat{Y}, \hat{O}$ are differential operators acting on the times t_p^i (or coupling constants) of the 1-matrix model:

$$\hat{X} = - \sum_{i,p} t_p^i \frac{\partial}{\partial t_p^i} \quad (7.4.80)$$

$$\hat{Y} = \frac{(-1)^d}{N^d} \sum_{(q_1, \dots, q_d) \in (\mathbb{N}^d)^*} \frac{(-i)^{\sum q_i}}{\sum q_i} \sqrt{\frac{\lambda}{2N^{d-2}}}^{q_1 + \dots + q_d} \binom{q_1 + \dots + q_d}{q_1, \dots, q_d} \frac{\partial^d}{\partial t_{q_1}^1 \dots \partial t_{q_d}^d} \quad (7.4.81)$$

⁵In fact during the time this thesis was written.

7.4. BILINEAR IDENTITIES

and

$$\hat{\mathcal{O}} = \ln(e^{\hat{X}} e^{\hat{Y}}) = \hat{X} + \frac{d \exp(d/2)}{2 \sinh(d/2)} \hat{Y}, \quad (7.4.82)$$

Proof. The proof is detailed [Dar14]. The sketch goes as follows. The tensor model can be written, using intermediate field decomposition as

$$\begin{aligned} Z[\lambda, N] &= \int_{\text{formal}} \prod_c dM_c \exp\left(-\frac{N}{2} \sum_c \text{Tr}(M_c^2) - \text{Tr} \log(\mathbb{1}^{\otimes d} - i\sqrt{\lambda/2} \sum_c \mathcal{M}_c)\right) \\ &= \sum_{k \geq 0} \frac{1}{k!} \int_{\text{formal}} \prod_c dM_c \exp\left(-\frac{N}{2} \sum_c \text{Tr}(M_c^2)\right) \\ &\quad \cdot \left(\sum_{p \geq 1} \frac{(-i\sqrt{\lambda/2})^p}{p} \sum_{\substack{(q_i \geq 0)_{i \in \llbracket 1, d \rrbracket} \\ \sum_i q_i = p}} \binom{p}{\vec{q}} \prod_c \text{Tr}(M_c^{q_c}) \right)^k. \end{aligned} \quad (7.4.83)$$

The T^4 melonic model is thus formally a linear combination of Gaussian correlation of products of traces of the M_i . This can be obtained from products of Hermitian matrix models as

$$\prod_c \frac{1}{N} \frac{\partial}{\partial t_{q_c}^c} \prod_k Z_{1MM}[\{t_p^k\}] = \langle \prod_c \text{Tr}(M_c^{q_c}) \rangle \prod_k Z_{1MM}[\{t_p^k\}]. \quad (7.4.84)$$

The role of the \hat{Y} operator is, when exponentiated, to reconstruct the correct combination of correlation functions in such a way that one obtains the T^4 model. However the correlation thus obtained are not Gaussian. This can be solved by acting with a dilaton operator that cancels the non-trivial part of the potential. That is the role of \hat{X} . These two operators obviously do not commute. However since one can check that $[\hat{X}, \hat{Y}] = d\hat{Y}$, it is possible to compute the corresponding operator $\hat{\mathcal{O}}$, by just using the Baker-Hausdorff-Campbell formula. \square

This is a Givental-like decomposition. However one can consider the case of T^4 melonic tensor model with only two interactions, say one of color i and one of color $j \neq i$. In this case one finds a proper Givental decomposition. On the other hand there is a difference that may be of importance. The N scaling is not a strict topological scaling, thus the interpretation in term of an integral over moduli space may not be as natural.

Also we point out the study [Bor13, BS15] in which Hermitian one matrix models, with arbitrary multi-trace interactions and topological scaling is treated. It is given a beautiful interpretation in term of integrals over moduli spaces of curves and in terms of solution set of the Topological Recursion that is briefly exposed in the next chapter.

7.4. BILINEAR IDENTITIES

7.4.4 Deformation of Hirota equations.

As roughly explained in the previous sections, when a decomposition of the form 13 is available, one is able to derive bilinear identities on the partition function of the model. That is what we now discuss and it corresponds to a generalization of ideas presented in [AK96] for ADE matrix models.

In this section we consider the deformed random tensor model obtained by the action of $\exp(\hat{Y})$ on the product of d matrix models, *i.e.*

$$Z_{\text{def}} := Z[\lambda, \{t_p^k\}_{p=0 \dots \infty, k=1 \dots d}, N] = \exp(\hat{Y}) \prod_{c=1}^d Z_{1MM}[\{t_p^c\}]. \quad (7.4.85)$$

We introduce the family of deformed vertex operators,

$$V_{\pm}^c(\lambda, z) = \exp(\hat{Y}) V_{\pm}^c(z) \exp(-\hat{Y}), \quad (7.4.86)$$

where $V_{\pm}^c(z)$ is the vertex operator associated to the Hermitian matrix model $Z_{1MM}[\{t_p^c\}]$ of color c . For each value of c we have the following,

$$\begin{aligned} & \oint dz \left(V_+^c(z, \lambda) \exp(\hat{Y}) \prod_{c'=1}^D Z_{1MM}[\{t_i^{c'}\}] \right) \left(V_-^c(z, \lambda) \exp(\hat{Y}) \prod_{c'=1}^D Z_{1MM}[\{\tilde{t}_i^{c'}\}] \right) = 0 \\ \Leftrightarrow & \oint dz \left(V_+^c(\lambda, z) Z[\lambda, \{t_p^k\}, N] \right) \left(V_-^c(\lambda, z) Z[\lambda, \{t_p^k\}, N] \right) = 0. \end{aligned} \quad (7.4.87)$$

This identity holds as the action of $V_{\pm}^c(\lambda, z)$ on $Z[\lambda, \{t_p^k\}, N]$ first cancels the $\exp(\hat{Y})$ of

$$\exp(\hat{Y}) \prod_{c'=1}^D Z_{1MM}[\{t_i^{c'}\}]. \quad (7.4.88)$$

Then one recovers a factor

$$\oint dz e^{\sum_{p \geq 0} t_p^c - \tilde{t}_p^c} \langle \det(z - M_c) \rangle_{N, \{t_p^c\}} \langle \det(z - M_c)^{-1} \rangle_{N', \{\tilde{t}_p^c\}} \quad (7.4.89)$$

thus leading to a vanishing result.

One can make explicit the form of the deformed operators:

Proposition 12. *The explicit form of the operators $V_{\pm}^c(z, \lambda)$ for $c \in \llbracket 1, D \rrbracket$ is given by:*

$$\begin{aligned} V_{\pm}^c(z, \lambda) = & e^{\pm \sum_{p=0}^{\infty} t_p^c z^p} e^{\mp \log(\frac{1}{z}) \frac{\partial}{\partial t_0^c} \mp \sum_{n=0}^{\infty} \frac{z^{-n}}{n} \frac{\partial}{\partial t_n^c}} \\ & \pm \frac{(-1)^D}{N^D} \sum_{(q_1, \dots, q_D) \in (\mathbb{N}^D)^*} \frac{(-i)^{\sum q_i}}{\sum q_i} \sqrt{\frac{\lambda}{2N^{D-2}}}^{q_1 + \dots + q_D} \binom{q_1 + \dots + q_D}{q_1, \dots, q_D} z^{q_c} \frac{\partial^{D-1}}{\partial t_{q_1}^1 \dots \partial t_{q_c}^c \dots \partial t_{q_D}^D}. \end{aligned} \quad (7.4.90)$$

7.4. BILINEAR IDENTITIES

The proof goes as follows

Proof. First set $\hat{A}^c = \sum_{p \geq 0} z^p t_p^c$ and $\hat{B}^c = \log(\frac{1}{z}) \frac{\partial}{\partial t_0^c} + \sum_{n=1}^{\infty} \frac{z^{-n}}{n} \frac{\partial}{\partial t_n^c}$, so that, for $c \in \llbracket 1, D \rrbracket$:

$$\begin{aligned} [\hat{B}^c, \hat{Y}] &= 0 \\ [\hat{A}^c, \hat{Y}] &= -\frac{(-1)^D}{N^D} \sum_{(q_1, \dots, q_D) \in (\mathbb{N}^D)^*} \frac{(-i)^{\sum q_i}}{\sum q_i} \sqrt{\frac{\lambda}{2N^{D-2}}}^{q_1 + \dots + q_D} \binom{q_1 + \dots + q_D}{q_1, \dots, q_D} z^{q_c} \frac{\partial^{D-1}}{\partial t_{q_1}^1 \dots \partial t_{q_c}^c \dots \partial t_{q_D}^D}. \end{aligned}$$

and $ad_{\hat{A}^c}^n(Y) = 0$ for $n \geq 2$. Consequently,

$$\begin{aligned} V_{\pm}^c(z, \lambda) &= \exp(\pm \hat{A}^c) \exp(\mp \hat{A}^c) \exp(\hat{Y}) \exp(\pm \hat{A}^c) \exp(\mp \hat{B}^c) \exp(-\hat{Y}) \\ &= \exp(\pm \hat{A}^c) \exp(e^{\mp ad_{\hat{A}^c}} \hat{Y}) \exp(\mp \hat{B}^c) \exp(-\hat{Y}). \end{aligned} \quad (7.4.91)$$

This rewrites,

$$\begin{aligned} V_{\pm}^c(z, \lambda) &= \exp(\pm \hat{A}^c) \exp(\hat{Y} \mp [\hat{A}^c, \hat{Y}]) \exp(\mp \hat{B}^c) \exp(-\hat{Y}) \\ &= \exp(\pm \hat{A}^c) \exp(\mp [\hat{A}^c, \hat{Y}]) \exp(\mp \hat{B}^c). \end{aligned} \quad (7.4.92)$$

□

This can be translated in a determinantal form,

$$\begin{aligned} 0 &= \oint dz e^{\sum_n z^n (t_n - \bar{t}_n)} \\ &\left\langle \frac{\det(z - M_c)}{\det\left(\mathbb{1}^{\otimes D} (1 + z \sqrt{\frac{\lambda}{2N^{D-2}}}) + \sqrt{\frac{\lambda}{2N^{D-2}}} \sum_{i \neq c} \mathbb{1}^{\otimes (D-c)} \otimes M_c \otimes \mathbb{1}^{\otimes (c-1)}\right)} \right\rangle_{N, t} \\ &\left\langle \frac{\det\left(\mathbb{1}^{\otimes D} (1 + z \sqrt{\frac{\lambda}{2N^{D-2}}}) + \sqrt{\frac{\lambda}{2N^{D-2}}} \sum_{i \neq c} \mathbb{1}^{\otimes (D-c)} \otimes M_c \otimes \mathbb{1}^{\otimes (c-1)}\right)}{\det(z - M_c)} \right\rangle_{N', \bar{t}} \end{aligned} \quad (7.4.93)$$

7.5 Remarks.

In this chapter we have considered the matrix formulation of the T^4 melonic tensor model. From this formulation one can use the well known techniques and properties of matrix models and extend them to this peculiar tensor model. This proves a useful approach to investigate numerous aspects of tensor models as it allows us to derive precise properties using analytic techniques. For instance one obtains the $N \rightarrow \infty$ limit and the next-to-leading order. It gives a new interpretation of the combinatorics of the double scaling limit

7.5. REMARKS.

and can actually be used to derive entirely this limit. Moreover it leads to completely new properties such as the bilinear equations on tensor models.

However one should go more thoroughly into this study. There are several tracks one may follow, and the choice is difficult to make. However one can list some of them without being exhaustive at all.

- As we have seen, one can resum the melonic sector by performing a shift of the matrix variables. Is there a way to translate this idea at the level of tensor variables?
- There are two solutions of the saddle point equations. We chose the '+' root as in fact it corresponds to the Feynman graphs expansion of the model (*i.e.* it is the combinatorial solution). However from a physical viewpoint there is no reason *a priori* for this solution not to be an interesting one. In fact it looks like an instanton solution and one knows from field theory that non trivial physics can be hidden in such solutions. One should investigate the possibility of performing a shift around this solution, or more generally that the eigenvalues of the intermediate field model collapse, with a fraction ϵ_1 to α_+ while a fraction ϵ_2 localizes to the α_- solution. This should be doable by transforming the initial matrix field as $\alpha_+ E_1 + \alpha_- E_2 +$ fluctuation fields, where $E_{1,2}$ are matrices with 1 on the first n_1 diagonal elements (resp. the $n_2 = N - n_1$ remaining) and zeroes elsewhere such that $\epsilon_i = n_i/N$.
- The obtained bilinear identities are unable to tell us what are the possible integrable structures that arise in the tensor model framework. However it is an interesting project to discover how they are deformed or even suppressed in the transition between matrices and tensors. So one should deepen this kind of study, treating several known sets of equations and structures arising in the case of the Hermitian matrix model and study the transition to tensor models, at least in the specific case of the T^4 melonic model.
- One could also wonder if it is possible to deepen the connection to Givental decompositions (and their generalization)? One may ask whether or not it is possible to write the action of a given Givental-like operator on product of matrix integrals as a tensor integral. If it is possible in some cases, what are the specificities of these cases which allow such decompositions?
- This also leads to the question of changing the scaling of tensor models. In fact when transforming the tensor integral using the Hubbard-Stratanovitch transformation one obtains a matrix model which does not have a topological expansion. But it is certainly possible to build the corresponding topological matrix model and to rephrase it in terms of tensor integrals. What would be the combinatorics of such a tensor model? One could try to investigate the leading order of such a model and compare it to the usual tensor model.

7.5. REMARKS.

- Finally, one can raise the question of the triple scaling limit. We saw in the current chapter and the preceding one that the double scaling limit can be well treated using the matrix representation of the T^4 melonic tensor model. In this chapter we have seen that it as a natural interpretation in terms of the shift on matrix variables which corresponds to a change of vacuum after a symmetry has been broken. Can this kind of interpretation be extended in order to define properly the concept of triple scaling? One could expect that the new vacuum also undergoes a breaking of symmetry creating a third vacuum and explore fluctuations around it.

In the next chapter we present the Eynard-Orantin Topological recursion in the context of matrix models. Then we will give some clues on how to adapt this technique to the T^4 melonic tensor model, hoping that some of the beautiful properties and mathematical structures carried by the Topological Recursion are reminiscent in this specific model. However this is a work which is currently undergoing, and everything is not understood yet. In fact I was not able to provide the necessary results before the end of the writing period of this manuscript. But I hope this can give to the reader a glimpse of the possibilities offered by such matrix formulations for tensor models.

Chapter 8

Loop Equations for Tensor Models

In this chapter we explore relations between observables of tensor models in several different settings and forms. First we derive the Schwinger-Dyson equations of generic tensor models and derive an algebra of constraints for this model [Gur12b]. One shows that this algebra form a Lie algebra. Then we recall the Schwinger-Dyson equations of matrix models and show how it leads to a very rich technique, called *Topological Recursion* for solving these models [EO08]. Finally we present how this technique can be partly adapted in the case of the T^4 tensor model.

8.1 Schwinger-Dyson equations of generic tensor model.

Generic tensor models obey Schwinger-Dyson equations that reflect their (formal) functional integral nature.

Consider a tensor invariant B with a marked (say white) vertex v . Call $B_{\cdot v}(\bar{T}, T)_{i_1 \dots i_d}$ the linear form represented by the graph without the vertex v . This can take a tensor $Q \in V^{\otimes d}$ as a variable. We have the following identity:

$$\int dT d\bar{T} \sum_{i_1, \dots, i_d} \frac{\partial}{\partial \bar{T}_{i_1 \dots i_d}} \left(B_{\cdot v}(\bar{T}, T)_{i_1 \dots i_d} \exp(N^{d-1} V(\{t_B\}, \bar{T}, T)) \right) = 0. \quad (8.1.1)$$

There are several contributions to the left hand side. The first one corresponds to the derivative term acting on the T 's of $B_{\cdot v}(\bar{T}, T)_{i_1 \dots i_d}$. This writes as a sum over white vertices v' of $B_{\cdot v}(\bar{T}, T)_{i_1 \dots i_d}$ of the form:

$$\sum_{v'} \sum_{i_1 \dots i_d} B_{\cdot v, \cdot v'}(\bar{T}, T)_{i_1 \dots i_d}. \quad (8.1.2)$$

$B_{\cdot v, \cdot v'}(\bar{T}, T)_{i_1 \dots i_d}$ is the graph with two vertices v (white) and v' (black) taken out. It represents a bilinear form on $V^{\otimes d} \times V^{\otimes d*}$. This contribution can be pictured as follows.

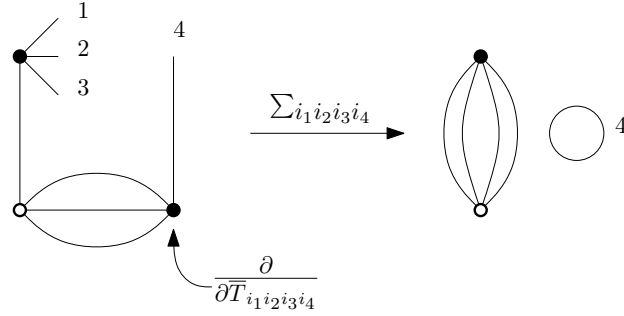


Figure 8.1: The effect of the action of a derivative operator on a marked invariant. In this case one obtains two connected components, a unique circle line corresponding to a factor of N and the fundamental melon.

Consider the graph B with a marked vertex v . Each term of the sum is represented by a graph obtained from B by drawing a line of color 0 from v to the black vertex v' and making a contraction of this new line. However we warn the reader that this is not a regular 1-dipole contraction. This contraction may disconnect the graph. When disconnected the resulting graph may be formed of several component B_ρ . Some of these components may be composed of a single line. To any such single isolated line corresponds an N^d factor. See for instance Fig. 8.1. This operation is called *bubble contraction*. The resulting (maybe not connected) bubble (isolated lines included) is denoted $B/(v, v')$. The second term comes

from the quadratic part of $V(\{t_B\}, \bar{T}, T)$. It contracts $B_v(\bar{T}, T)_{i_1 \dots i_d}$ with a T at v , so one obtains the bubble $B(\bar{T}, T)$ as a result. The last term is obtained by acting with $\frac{\partial}{\partial T_{i_1 \dots i_d}}$ on each $t_B \mathcal{B}(\bar{T}, T)$ of the potential. For each of these terms one obtains a sum over the black vertices $v' \in \mathcal{B}$ of the form

$$\sum_{v'} \sum_{i_1 \dots i_d} B_v(\bar{T}, T)_{i_1 \dots i_d} \mathcal{B}_{v'}(\bar{T}, T)_{i_1 \dots i_d}. \quad (8.1.3)$$

Again each term can be pictured by a graph B with v as a marked vertex and \mathcal{B} with a black vertex v' . One draws a line of color 0 between these two vertices and performs a 1-dipole contraction of this new line. In this case this is a proper 1-dipole contraction (as in fact the vertices v and v' are in two different bubbles).

Definition 27. Consider a bubble B with a white marked vertex v and a bubble \mathcal{B} , such that v' is a black vertex belonging to \mathcal{B} . We define the operation $*_{v'}$,

$$\mathcal{B} *_{v'} B = \sum_{i_1 \dots i_d} B_v(\bar{T}, T)_{i_1 \dots i_d} \mathcal{B}_{v'}(\bar{T}, T)_{i_1 \dots i_d}. \quad (8.1.4)$$

8.1. SCHWINGER-DYSON EQUATIONS OF GENERIC TENSOR MODEL.

We obtain the following Schwinger-Dyson equations:

$$\langle -N^{d-1}B(\bar{T}, T) + \sum_{v'} \sum_{i_1 \dots i_d} B_{\cdot v, \cdot v'}(\bar{T}, T)_{i_1 \dots i_d} + N^{d-1} \sum_{v'} t_{\mathcal{B}} \frac{N^{-\frac{2}{(d-1)!}\omega(\mathcal{B})}}{|Aut(\mathcal{B})|} (\mathcal{B} *_{v'} B)(\bar{T}, T) \rangle = 0. \quad (8.1.5)$$

We can rewrite these equations as actions of differential operators on the generating partition function of the generic one tensor model:

$$L_B Z[\{t_{\mathcal{B}}\}] = 0 \quad (8.1.6)$$

$$\begin{aligned} L_B &= |Aut(B)| N^{\frac{2}{(d-1)!}\omega(B)} \frac{\partial}{\partial t_B} \\ &+ \sum_{v'} N^{\frac{2}{(d-1)!}\omega(B/(v, v'))} |Aut(B/(v, v'))| \frac{\partial}{\partial t_{B/(v, v')}} \\ &+ \sum_{v'} N^{\frac{2}{(d-1)!}\omega(B)} \frac{|Aut(\mathcal{B} *_{v'} B)|}{|Aut(\mathcal{B})|} \frac{\partial}{\partial t_{\mathcal{B} *_{v'} B}}. \end{aligned} \quad (8.1.7)$$

We denoted

$$\frac{\partial}{\partial t_{B/(v, v')}} = \prod_{\rho} \frac{\partial}{\partial t_{B_{\rho}}}, \quad (8.1.8)$$

where B_{ρ} are the connected components and $\frac{\partial}{\partial t_{B_{\rho}}}$ reduces by convention to a factor of N when B_{ρ} is made of a unique line. One has the following Lie algebra defined in any dimension, generated by the differential operators with brackets

$$[L_{B_1}, L_{B_2}] = \sum_{v'} L_{B_1 *_{v'} B_2} - \sum_{v'} L_{B_2 *_{v'} B_1}. \quad (8.1.9)$$

This Lie algebra contains an infinite number of ideals turning the study of its representation into a very hard problem. Trying to extend these algebras in a way that would suppress these ideals has been unsuccessful until now. But there is no *no-go* theorem that states that it is impossible.

8.2 Loop equations for Hermitian matrix model and topological recursion.

The invariants of a Hermitian matrix are its traces. They play the same role as the \mathcal{B} 's for the tensor case. The same techniques leads to the same kind of equations, *i.e*

$$\int dM \frac{\partial}{\partial M_{ab}} \left((M^k)_{ab} \exp\left(-\frac{N}{2} \text{Tr}(M^2) + N \sum_{p \geq 1} \frac{t_p}{p} \text{Tr}(M^p)\right) \right) = 0. \quad (8.2.10)$$

8.2. LOOP EQUATIONS FOR HERMITIAN MATRIX MODEL AND TOPOLOGICAL RECURSION.

We write $\sum_{p \geq 1} \frac{t_p}{p} \text{Tr}(M^p) = \text{Tr} V(M)$.

$$\left\langle \sum_{n=0}^{k-1} \text{Tr}(M^n) \text{Tr}(M^{k-n-1}) - N \text{Tr}(M^{k+1}) + N \text{Tr}(M^k V'(M)) \right\rangle = 0 \quad (8.2.11)$$

This can also be pictured graphically by representing $\text{Tr}(M^p)$ by a cycle of length p . One can define the same kind of operation \ast_v and construct the same type of algebra as before. This leads to the positive part of the Witt algebra.

Define the following generating functions:

$$W_1(x) = \sum_{p \geq 0} \frac{\langle \text{Tr}(M^p) \rangle}{x^{p+1}} \quad (8.2.12)$$

$$\overline{W}_2(x_1, x_2) = \sum_{p, q \geq 0} \frac{\langle \text{Tr}(M^p) \text{Tr}(M^q) \rangle}{x_1^{p+1} x_2^{q+1}}, \quad (8.2.13)$$

where we have introduced the counting variable $x \in \mathbb{C}$. This allows us to rewrite (8.2.11) as [Eyn15b, Eyn04]:

$$\overline{W}_2(x, x) - N \langle \text{Tr} \frac{M}{x-M} \rangle + N \langle \text{Tr} \frac{V'(M)}{x-M} \rangle = 0. \quad (8.2.14)$$

We then consider the connected function $W_2(x_1, x_2) = \overline{W}_2(x_1, x_2) - W_1(x_1)W_1(x_2)$. Moreover we use the following trick $\text{Tr} \frac{M}{x-M} = \text{Tr} \frac{x+M-x}{x-M}$ and $\text{Tr} \frac{V'(M)}{x-M} = \text{Tr} \frac{V'(x)+V'(M)-V(x)}{x-M}$. We call $N \langle \text{Tr} \left(\frac{x-M+V'(M)-V(x)}{x-M} \right) \rangle = P_1(x)$. Thus,

$$W_2(x, x) + W_1(x)^2 - xW_1(x) + NV'(x)W_1(x) + P_1(x) = 0. \quad (8.2.15)$$

Using the fact that $\langle \text{Tr}(M^p) \rangle$ expands as $\langle \text{Tr}(M^p) \rangle = \sum_{g \geq 0} N^{1-2g} \langle \text{Tr}(M^p) \rangle_g$ we obtain a topological expansion for $W_1(x) = \sum_{g \geq 0} N^{1-2g} W_1^g(x)$. In fact, it can be generalized to $W_2(x_1, x_2) = \sum_{g \geq 0} N^{-2g} W_2^g(x_1, x_2)$. For every value of g we then get an equation on $W_1^g(x)$ and $W_2^g(x, x)$. For instance

$$\begin{cases} W_1^0(x)^2 - xW_1^0(x) + V'(x)W_1^0(x) + P_1^0(x) = 0, & g = 0 \\ W_2^0(x, x) + 2W_1^0(x)W_1^1(x) - xW_1^1(x) + V'(x)W_1^1(x) + P_1^1(x) = 0, & g = 1 \end{cases} \quad (8.2.16)$$

The first equation is non linear, while the second is linear. Indeed it can be checked that all equations for $g \geq 1$ are linear [Eyn04]. For potentials $V(x)$ that are polynomial in x (*i.e.* all t_p vanishes for p greater than a certain d^1), $P_1(x)$ is a polynomial. In fact, without doing any assumption on the form of the solution for the moment we arrived at a set of

¹This can be extended to $V(x)$ such that $V'(x)$ is rational.

8.2. LOOP EQUATIONS FOR HERMITIAN MATRIX MODEL AND TOPOLOGICAL RECURSION.

recurrent equations. They can be written in full generality by defining the multi-point generating functions

$$W_n(x_1, \dots, x_n) = \sum_{p_i \geq 1} \frac{\langle \text{Tr}(M^{p_1}) \text{Tr}(M^{p_2}) \dots \text{Tr}(M^{p_n}) \rangle_c}{x_1^{p_1+1} \dots x_n^{p_n+1}}, \quad (8.2.17)$$

where $\langle \dots \rangle_c$ means connected.

$$W_n(x_1, \dots, x_n) = \sum_g N^{2-2g-n} W_n^g(x_1, \dots, x_n). \quad (8.2.18)$$

The equations over W_n are obtained by acting on the equation (8.2.15) with the loop insertion operator $\delta_{x_i} = \frac{1}{N} \sum_{m \geq 0} \frac{1}{m x_i^{m+1}} \frac{\partial}{\partial t_m}$

$$\begin{aligned} W_{n+2}(x, x, I) &+ \sum_{J \subset I} W_{1+|J|}(x, J) W_{1+|I-J|}(x, I-J) + \sum_{i=1}^n \frac{\partial}{\partial x_i} \frac{W_n(x, I-x_i) - W_n(I)}{x-x_i} \\ &- NV'(x) W_{n+1}(x, I) - NP_{n+1}(x, I) = 0, \quad I = \{x_1, \dots, x_n\}. \end{aligned} \quad (8.2.19)$$

By Brown's lemma [Eyn15b, Eyn06] we are interested, for combinatorics, in the so-called 1-cut solution. This is a restriction on the accepted form for the solution of (8.2.16) for $g = 0$. It states that the solution is of the form

$$W_1^0(x) = \frac{1}{2}(x - V'(x) + M(x)\sqrt{(x-a)(x-b)}) = \frac{1}{2}(x - V'(x) + y(x)) \quad (8.2.20)$$

$M(x)$ being a polynomial. Inserting this expression in (8.2.16) we get:

$$(x - V'(x))y(x) + y(x)^2 + 2P_1^0(x) = 0. \quad (8.2.21)$$

The chosen form of $y(x)$ completely constrains $P_1^0(x)$. For $V(x)$ polynomial of degree d , this can be seen (up to homogenization) as an algebraic curve in \mathbb{CP}^2 $(x - V'(x))y + y^2 + 2P_1^0(x) = 0$. The choice of the 1-cut solution corresponds to choice of P_1^0 turning this curve into a plane curve of genus $g = 0$. W_1^0 is called a parametrization of this curve, however it is better to use another parametrization, called Zhukhovky variables². For $z \in \mathbb{C}$, we set

$$x(z) = \frac{a+b}{2} + \frac{a-b}{4} \left(z + \frac{1}{z} \right). \quad (8.2.22)$$

In particular, $\{a, b\} \rightarrow \{+1, -1\}$. Doing so, y (or W_1^0) and x (or rather their pullback under the Zhukovsky map) are functions of the Riemann sphere to \mathbb{C} . In these variables we have that

$$W_1^0(x(z)) = \sum_{k=1}^{d-1} v_k z^{-k} \quad (8.2.23)$$

²These are the transformation of the complex plane that allows one to map a wing profile to a circle. Since the fluid equations are easier to derive around a disc this has been used a lot in $2d$ fluid mechanics studies.

8.2. LOOP EQUATIONS FOR HERMITIAN MATRIX MODEL AND TOPOLOGICAL RECURSION.

is a rational function of z . By studying the singularities of the W_n^g it is possible to provide an expression for them that only involves computations of residues at $z = \pm 1$ of $W_n^{g'}$ such that $2g' + n' - 2 < 2g + n - 2$. It is then a recursion on g and n , the initial conditions being provided by W_1^0 and W_2^0 that have to be computed separately. As residues on a Riemann surface Σ are well defined for forms [Sch07] on it we use Schwarz representation theorem to switch from functions to the forms

$$w_n^g(z_1, \dots, z_n) = W_n^g(x(z_1), \dots, x(z_n)) dx_1 \otimes \dots \otimes dx_n \in H^0(\Sigma^n, K_\Sigma(- * \{\pm 1\})^{\boxtimes n})^{\mathfrak{S}_n}. \quad (8.2.24)$$

This is called the *topological recursion*.

8.3 Loop equations for the T^4 model

We can play the same kind of game for the matrix model introduced in chapter 7. This matrix model is shifted, this shift corresponding to the double scaling of chapter 6. Its form is

$$Z = \frac{\exp\left(-\frac{N^D}{2}\alpha^2\right)}{N^{D-2}} \int_{(H_N)^D} \prod_c dM_c \exp\left(-\frac{N}{2} \sum_c \text{Tr} M_c^2 - \alpha N^{\frac{D}{2}} \sum_c \text{Tr} M_c - \text{Tr} \log\left((1 + i\sqrt{\lambda/2}\alpha)\mathbb{1}^{\otimes D} + i\sqrt{\frac{\lambda}{2N^{D-2}}} \sum_c \mathcal{M}_c\right)\right). \quad (8.3.25)$$

Let us recall some facts. One can still consider the generating function of loop observables $\langle \text{Tr}(M_c^p) \rangle$. But this model is a multi-matrix model and thus one should also consider the generating function for observable of different colors such that $\langle \text{Tr}(M_1^q) \text{Tr}(M_2^p) \rangle$. Moreover the $1/N$ expansion is not topological as the potential contains terms that do not scale topologically. This is inherited from the specific scaling of tensor models. The computation of the leading order $W_1^0(x)$ is shown in Chapter 7. The information contained in the Schwinger-Dyson equations used to construct the following loop equations is certainly contained in the set of constraints derived in section 8.1. However it is easier to treat this information in the form presented below.

8.3.1 Exact 'disc' and 'cylinder' equations.

We write here the exact disc equation. First let us introduce some notations. The generating series of loop observables are defined in a way analogous to section 8.2, but there are some differences because we have several matrices.

Definition 28. Consider a d -uplet $\mathbf{k} \in \mathbb{N}^d$, $k = (k_1, k_2, \dots, k_d)$. Consider the following

8.3. LOOP EQUATIONS FOR THE T^4 MODEL

associated quantity

$$\langle \overbrace{\text{Tr}(M_1^{p_1^{(1)}}) \cdots \text{Tr}(M_1^{p_{k_1}^{(1)}})}^{k_1 \text{ times}} \underbrace{\text{Tr}(M_2^{p_1^{(2)}}) \cdots \text{Tr}(M_2^{p_{k_2}^{(2)}})}_{k_2 \text{ times}} \cdots \overbrace{\text{Tr}(M_d^{p_1^{(d)}}) \cdots \text{Tr}(M_d^{p_{k_d}^{(d)}})}^{k_d \text{ times}} \rangle. \quad (8.3.26)$$

The associated generating function is

$$\begin{aligned} & \overline{W}_{\mathbf{k}}(\underbrace{x_1^{(1)}, \dots, x_{k_1}^{(1)}}_{k_1 \text{ times}}, \dots, x_1^{(d)}, \dots, x_{k_d}^{(d)}) \\ &= \sum_{\text{all } p_j^{(i)} \geq 0} \frac{\langle \text{Tr}(M_1^{p_1^{(1)}}) \cdots \text{Tr}(M_1^{p_{k_1}^{(1)}}) \text{Tr}(M_2^{p_1^{(2)}}) \cdots \text{Tr}(M_2^{p_{k_2}^{(2)}}) \cdots \text{Tr}(M_d^{p_1^{(d)}}) \cdots \text{Tr}(M_d^{p_{k_d}^{(d)}}) \rangle}{x_1^{(1)p_{k_1}^{(1)}+1} \cdots x_1^{(d)p_{k_1}^{(d)}+1} \cdots x_1^{(d)p_{k_d}^{(d)}+1}}. \end{aligned} \quad (8.3.27)$$

We also denote

$$\overline{W}_{\mathbf{1}}(x_1^{(1)}, x_1^{(2)}, \dots, x_1^{(d)}) = \overline{W}_{\mathbf{k}=(1, \dots, 1)}(x_1^{(1)}, x_1^{(2)}, \dots, x_1^{(d)}). \quad (8.3.28)$$

This set of notations also applies for the connected generating functions W such that

$$\overline{W}_{\mathbf{k}} = \sum_{J \vdash C^{\mathbf{k}}} \prod_{J_i} W_{J_i}. \quad (8.3.29)$$

We assume that we have a symmetry among colors. This means that if $\sigma \in \mathfrak{S}_d$ acts on $\mathbf{k} = (k_1, \dots, k_d)$ by permuting its elements $\sigma\mathbf{k} = (\sigma(k_1), \dots, \sigma(k_d))$ then

$$\overline{W}_{\mathbf{k}}(x_{\mathbf{k}}) = \overline{W}_{\sigma\mathbf{k}}(x_{\sigma\mathbf{k}}) \quad (8.3.30)$$

$$W_{\mathbf{k}}(x_{\mathbf{k}}) = W_{\sigma\mathbf{k}}(x_{\sigma\mathbf{k}}). \quad (8.3.31)$$

We also use a short notation when the correlation function involves only the matrix of a single color i

$$W_{n,i}(x_1^{(i)}, \dots, x_n^{(i)}). \quad (8.3.32)$$

Exact disc equation

We consider the equation for 'disc' generating function of color 1

$$\begin{aligned} & W_{1,1}(x)^2 + W_{2,1}(x, x) - N \oint \frac{d\zeta_1}{2i\pi} \zeta_1 W_{1,1}(\zeta_1) \\ & + \sum_{p \geq 2} \frac{\alpha^p}{p} N^{-p \frac{(d-2)}{2}} \sum_{\vec{q} \in F_p} \binom{p}{\vec{q}} \oint \left(\prod_{i=1}^d \frac{d\zeta_j}{2i\pi} \right) \left(\prod_{j \neq 1} \zeta_j^{q_j} \right) \frac{\zeta_1^{q_1-1}}{x - \zeta_1} \overline{W}_{\mathbf{1}}(\zeta_1, \zeta_2, \dots, \zeta_d) = 0, \end{aligned} \quad (8.3.33)$$

8.3. LOOP EQUATIONS FOR THE T^4 MODEL

where $F_p = \{(q_1, \dots, q_d) \in \mathbb{N} | q_1 \geq 1; \quad q_{i \neq 1} \geq 0, \quad \sum_i q_i = p \geq 2\}$. Unless stated otherwise \oint means a contour integral along a closed path $\gamma \subset U_{[a,b]}$ surrounding the cut $[a, b]$. Using only connected correlation functions

$$W_{1,1}(x)^2 + W_{2,1}(x, x) - N \oint \frac{d\zeta_1}{2i\pi} \zeta_1 W_{1,1}(\zeta_1) + \sum_{J \vdash \mathcal{C}} \sum_{p \geq 2} \frac{\alpha^p}{p} N^{-p \frac{(d-2)}{2}} \sum_{\vec{q} \in F_p} \binom{p}{\vec{q}} \oint \left(\prod_{i=1}^d \frac{d\zeta_j}{2i\pi} \right) \left(\prod_{j \neq 1} \zeta_j^{q_j} \right) \frac{\zeta_1^{q_1-1}}{x - \zeta_1} \prod_{J_i} W_{J_i}(\zeta_{J_i}) = 0, \quad (8.3.34)$$

The leading order equations gives the result of chapter 7. We consider the equation on $W_{2,1}(x_1, x_2)$

Exact 'cylinder' equation:

$$2W_{1,1}(x_1)W_{2,1}(x_1, x_2) + W_{3,1}(x_1, x_1, x_2) + \frac{\partial}{\partial x_2} \frac{W_{1,1}(x_1) - W_{1,1}(x_2)}{x_1 - x_2} - N \oint \frac{d\zeta_1}{2i\pi} \zeta_1 W_{2,1}(\zeta_1, x_2) + \sum_{J \vdash \mathcal{C}} \sum_{p \geq 2} \bigcup_{i=1}^{[J]} h_i = \{x_2\} \frac{\alpha^p}{p} N^{-p \frac{(d-2)}{2}} \sum_{\vec{q} \in F_p} \binom{p}{\vec{q}} \oint \left(\prod_{i=1}^d \frac{d\zeta_j}{2i\pi} \right) \left(\prod_{j \neq 1} \zeta_j^{q_j} \right) \frac{\zeta_1^{q_1+1}}{x - \zeta_1} \prod_{J_i} W_{J_i}(\zeta_{J_i}, h_i) = 0. \quad (8.3.35)$$

Bicolored 'cylinder function':

We consider the bicolored cylinder function of color (12), so $\mathbf{k} = (1, 1, \vec{0}_{d-2})$ the resulting exact equation is

$$2W_{1,1}(x_1)W_{(1,1,\vec{0}_{d-2})}(x_1, x_2) + W_{(2,1,\vec{0}_{d-2})}(x_1, x_1, x_2) - N \oint \frac{d\zeta_1}{2i\pi} W_{(1,1,\vec{0}_{d-2})}(\zeta_1, x_2) + \sum_{\substack{K \vdash \mathcal{C} \\ \bigcup_{i=1}^{[K]} J_i = \{x_2\}}} \sum_{p \geq 2} \frac{\alpha^p}{p} N^{\frac{2-d}{2}p} \sum_{F_p} \oint \binom{p}{\vec{q}} \left(\prod_{i=1} \zeta_i^{q_i} \right) \frac{\zeta_1^{q_1-1}}{x_1 - \zeta_1} \prod_{i=1}^{[K]} W_{|K_i|+|J_i|}(\zeta_{K_i}, x_{J_i}) = 0. \quad (8.3.36)$$

One notices the absence of derivative terms in this equation.

8.3. LOOP EQUATIONS FOR THE T^4 MODEL

8.3.2 First term of $1/N$ expansion.

The generating function $W_{2,1}$ expands in powers of $1/N$, and we compute the first term of this expansion. This can be done in any dimension. In fact we obtain

$$\begin{aligned}
& 2W_{1,1}^0(x_1)W_{2,1}^0(x_1, x_2) + \partial_{x_2} \left(\frac{W_{1,1}^0(x_1) - W_{1,1}(x_2)}{x_1 - x_2} \right) \\
& + \alpha^2 \left(2 \oint \frac{d\zeta_1}{2i\pi} \zeta_1 \frac{W_{2,1}^0(\zeta_1, x_2)}{x_1 - \zeta_1} + 2(d-1) \oint \left(\prod_{j=1}^d \frac{d\zeta_j}{2i\pi} \right) \frac{W_{2,1}^0(\zeta_1, x_2)}{x_1 - \zeta_1} \zeta_2 \left(\prod_{j \geq 2}^d W_{1,1}^0(\zeta_j) \right) \right. \\
& \left. + 2(d-1) \oint \left(\prod_{j=1}^d \frac{d\zeta_j}{2i\pi} \right) \frac{W_{1,1}^0(\zeta_1)}{x_1 - \zeta_1} \zeta_2 W_{(1,1, \vec{0}_{d-2})}^0(\zeta_2, x_2) \left(\prod_{j \geq 3}^d W_{1,1}^0(\zeta_j) \right) \right), \tag{8.3.37}
\end{aligned}$$

where we used assumption (8.3.30). Moreover, one has $W_{1,1}^0(x) = \frac{1-\alpha^2}{2}(x - \sqrt{x^2 - \frac{4}{1-\alpha^2}})$.

$$2 \oint \frac{d\zeta_1}{2i\pi} \zeta_1 \frac{W_{2,1}^0(\zeta_1, x_2)}{x_1 - \zeta_1} = 2 \oint \frac{d\zeta_1}{2i\pi} (\zeta_1 - x_1 + x_1) \frac{W_{2,1}^0(\zeta_1, x_2)}{x_1 - \zeta_1} \tag{8.3.38}$$

and so eq. (8.3.37) rewrites

$$\begin{aligned}
& 2W_{1,1}^0(x_1)W_{2,1}^0(x_1, x_2) + \partial_{x_2} \left(\frac{W_{1,1}^0(x_1) - W_{1,1}(x_2)}{x_1 - x_2} \right) - \oint \frac{d\zeta_1}{2i\pi} \zeta_1 \frac{W_{2,1}^0(\zeta_1, x_2)}{x_1 - \zeta_1} \\
& + \frac{\alpha^2}{2} \left(2x_1 W_{2,1}^0(x_1, x_2) + 2(d-1) W_{2,1}^0(x_1, x_2) \frac{1}{N} \langle \text{Tr}(M_1) \rangle^0 \right. \\
& \left. + 2(d-1) W_{1,1}^0(x_1) \frac{1}{N^2} \langle \text{Tr}(M_1)(x_2 - M_2)^{-1} \rangle_c^0 \right) = 0, \tag{8.3.39}
\end{aligned}$$

or equivalently,

$$\begin{aligned}
& -(1-\alpha^2) \sqrt{x_1^2 - \frac{4}{1-\alpha^2}} W_{2,1}^0(x_1, x_2) + \partial_{x_2} \left(\frac{W_{1,1}^0(x_1) - W_{1,1}(x_2)}{x_1 - x_2} \right) \\
& + (d-1) W_{1,1}^0(x_1) \frac{1}{N^2} \langle \text{Tr}(M_1)(x_2 - M_2)^{-1} \rangle_c^0 = 0. \tag{8.3.40}
\end{aligned}$$

Considering the limit $x_1 \rightarrow \infty$ one obtains the following relation

$$\begin{aligned}
& \frac{1-\alpha^2}{N^2} \langle \text{Tr}(M_1) \text{Tr}(x_2 - M_1)^{-1} \rangle_c^0 + \partial_{x_2} W_{1,1}^0(x_2) \\
& = \frac{(d-1)}{N^2} \langle \text{Tr}(M_1)(x_2 - M_2)^{-1} \rangle_c^0. \tag{8.3.41}
\end{aligned}$$

8.3. LOOP EQUATIONS FOR THE T^4 MODEL

We now simply refer to the bicolored cylinder equation (8.3.36) and extract the leading $1/N$ term

$$\begin{aligned}
& - (1 - \alpha^2) \sqrt{x_1^2 - \frac{4}{1 - \alpha^2}} W_{(1,1,\vec{0}_{d-2})}(x_1, x_2) \\
& + \frac{\alpha^2}{2} W_{1,1}^0(x_1) \left(2 \oint \left(\prod_{j>1} \frac{d\zeta_j}{2i\pi} \right) \zeta_2 W_{2,1}^0(\zeta_2, x_2) \prod_{j>2} W_{1,1}^0(\zeta_j) \right. \\
& \left. + 2(d-2) \oint \left(\prod_{j>1} \frac{d\zeta_j}{2i\pi} \right) \zeta_2 W_{(1,1,\vec{0}_{d-2})}^0(\zeta_2, x_2) \prod_{j>2} W_{1,1}^0(\zeta_j) \right) = 0. \quad (8.3.42)
\end{aligned}$$

It rewrites

$$\begin{aligned}
& - (1 - \alpha^2) \sqrt{x_1^2 - \frac{4}{1 - \alpha^2}} W_{(1,1,\vec{0}_{d-2})}(x_1, x_2) + \alpha^2 W_{1,1}(x_1) \\
& \cdot \left(\frac{1}{N^2} \langle \text{Tr}(M_2) \text{Tr}(x_2 - M_2)^{-1} \rangle + \frac{(d-2)}{N^2} \langle \text{Tr}(M_1) \text{Tr}(x_2 - M_2) \rangle \right) = 0 \quad (8.3.43)
\end{aligned}$$

where we also used (8.3.30) several times. Again extracting the coefficient of $1/x_1$ of this equation leads to

$$\frac{[1 - \alpha^2(d-1)]}{\alpha^2} \langle \text{Tr}(M_1) \text{Tr}(x_2 - M_2)^{-1} \rangle = \langle \text{Tr}(M_2) \text{Tr}(x_2 - M_2)^{-1} \rangle. \quad (8.3.44)$$

One thus has:

$$\frac{d(2\alpha^2 - \alpha^4) + \alpha^4 - \alpha^2 - 1}{\alpha^2 N^2} \langle \text{Tr}(M_1) \text{Tr}(x_2 - M_2)^{-1} \rangle_c^0 = \partial_{x_2} W_{1,1}^0(x_2). \quad (8.3.45)$$

This leads to:

$$\begin{aligned}
& -(1 - \alpha^2) \sqrt{x_1^2 - \frac{4}{1 - \alpha^2}} W_{2,1}^0(x_1, x_2) + \partial_{x_2} \left(\frac{W_{1,1}^0(x_1) - W_{1,1}^0(x_2)}{x_1 - x_2} \right) \\
& + \frac{\alpha^2(d-1)}{d(2\alpha^2 - \alpha^4) + \alpha^4 - \alpha^2 - 1} W_{1,1}^0(x_1) \partial_{x_2} W_{1,1}^0(x_2) = 0. \quad (8.3.46)
\end{aligned}$$

One thus has:

$$\begin{aligned}
(1 - \alpha^2) W_{2,1}^0(x_1, x_2) &= \frac{1}{\sqrt{x_1^2 - \frac{4}{1 - \alpha^2}}} \left(\partial_{x_2} \left(\frac{W_{1,1}^0(x_1) - W_{1,1}^0(x_2)}{x_1 - x_2} \right) \right. \\
&\quad \left. + \frac{\alpha^2(d-1)}{d(2\alpha^2 - \alpha^4) + \alpha^4 - \alpha^2 - 1} W_{1,1}^0(x_1) \partial_{x_2} W_{1,1}^0(x_2) \right). \quad (8.3.47)
\end{aligned}$$

This determines entirely $W_{2,1}^0(x_1, x_2)$. It can be written more compactly using the z variable introduced earlier. Let us set the dictionary for this specific case.

8.3. LOOP EQUATIONS FOR THE T^4 MODEL

Dictionary $z \leftrightarrow x$ variables.
$x(z) = \frac{a+b}{2} + \frac{a-b}{4}(z + 1/z), z(x) = \frac{2}{a-b}(x - \frac{a+b}{2} + \sqrt{(x-a)(x-b)}).$
$W_{1,i}^0(x) = \frac{1-\alpha^2}{2}(x - \sqrt{x^2 - \frac{4}{1-\alpha^2}}), a = \frac{2}{\sqrt{1-\alpha^2}}, b = -\frac{2}{\sqrt{1-\alpha^2}}.$
$\sqrt{\sigma_x} := \sqrt{(x-a)(x-b)} = \frac{a-b}{4}(z - \frac{1}{z}), \frac{dx}{\sqrt{\sigma_x}} = \frac{dz}{z}.$
$W_{1,i}^0(z) = \sqrt{1-\alpha^2} \frac{1}{z}, \partial_x W_{1,i}^0(x) dx = -\sqrt{1-\alpha^2} \frac{dz}{z^2}.$

Using this dictionary we compute the 2-form $\omega_{2,1}^0 = W_{2,1}^0(x_1, x_2) dx_1 \otimes dx_2$. Notices that the second term of the r.h.s. of (8.3.47) writes

$$\begin{aligned} & \frac{\alpha^2(d-1)}{d(2\alpha^2 - \alpha^4) + \alpha^4 - \alpha^2 - 1} \frac{W_{1,1}^0(x_1)}{\sqrt{\sigma_{x_1}}} \partial_{x_2} W_{1,1}^0(x_2) dx_1 \otimes dx_2 \\ &= -(1-\alpha^2) \frac{\alpha^2(d-1)}{d(2\alpha^2 - \alpha^4) + \alpha^4 - \alpha^2 - 1} \frac{dz_1 \otimes dz_2}{z_1^2 z_2^2}. \end{aligned} \quad (8.3.48)$$

This has poles at $z_i \rightarrow 0$. The first term of the r.h.s. of (8.3.47) is given by

$$\begin{aligned} & (1-\alpha^2) \left[\frac{(z_2 - 1/z_2)}{(z_1 - z_2)^2 (1 - \frac{1}{z_1 z_2})^2} \frac{dz_1 \otimes dz_2}{z_1^2 z_2^2} + \frac{1}{(z_1 - z_2)(1 - \frac{1}{z_1 z_2})} \frac{dz_1 \otimes dz_2}{z_1 z_2^2} \right. \\ & \left. - \frac{(z_2 - 1/z_2)}{(z_1 - z_2)^2 (1 - \frac{1}{z_1 z_2})^2} \frac{dz_1 \otimes dz_2}{z_1 z_2^2} \right] = \frac{(1-\alpha^2)}{(z_1 z_2 - 1)^2} dz_1 \otimes dz_2. \end{aligned} \quad (8.3.49)$$

Finally,

$$\tilde{\omega}_{2,1}^0 = \frac{dz_1 \otimes dz_2}{(z_1 z_2 - 1)^2} - \frac{\alpha^2(d-1)}{d(2\alpha^2 - \alpha^4) + \alpha^4 - \alpha^2 - 1} \frac{dz_1 \otimes dz_2}{z_1^2 z_2^2}. \quad (8.3.50)$$

Proposition 13. *The degree zero 1 point and 2 points resolvents of color i are given by*

$$\omega_{1,i}^0 = \sqrt{1-\alpha^2} \frac{dz}{z} \quad (8.3.51)$$

$$\tilde{\omega}_{2,i}^0 = \frac{dz_1 \otimes dz_2}{(z_1 z_2 - 1)^2} - \frac{\alpha^2(d-1)}{d(2\alpha^2 - \alpha^4) + \alpha^4 - \alpha^2 - 1} \frac{dz_1 \otimes dz_2}{z_1^2 z_2^2}. \quad (8.3.52)$$

Proof. The proof is straightforward once given the above results and the symmetry property (8.3.30). \square

Let us remark the following fact. First call

$$h_{2,1}^0(z_1, z_2) = -\frac{\alpha^2(d-1)}{d(2\alpha^2 - \alpha^4) + \alpha^4 - \alpha^2 - 1} \frac{dz_1 \otimes dz_2}{z_1^2 z_2^2}. \quad (8.3.53)$$

8.3. LOOP EQUATIONS FOR THE T^4 MODEL

We recall the definition of the Bergman kernel of \mathbb{CP}^1 as the following two form

$$B(z_1, z_2) = \frac{dz_1 \otimes dz_2}{(z_1 - z_2)^2}. \quad (8.3.54)$$

It is the self-reproducing kernel on the Riemann sphere. We now remark the following equality

$$\tilde{\omega}_2^0 = -B_{\iota^* z_2}(z_1, z_2) + h_{2,1}^0(z_1, z_2) = \frac{dz_1 \otimes dz_2}{(z_1 z_2 - 1)^2} + h_{2,1}^0(z_1, z_2) \quad (8.3.55)$$

where ι is the involution that sends $z \rightarrow \frac{1}{z}$. ι acts by pullback on the second variable of B . Indeed

$$B_{\iota^* z_2}(z_1, z_2) = \frac{dz_1 \otimes d\iota(z_2)}{(z_1 - \iota(z_2))^2} = -\frac{dz_1 \otimes dz_2}{(z_1 z_2 - 1)^2}. \quad (8.3.56)$$

Compared to the usual topological recursion, the 2-point resolvent is translated by a non-universal term $h_{2,1}^0(z_1, z_2)$.

8.3.3 Three-dimensional higher degree term

In this subsection we compute explicitly the higher degree 1-point resolvent. There is already in this case a difference with the usual matrix model computations: no 2-point resolvent arises in this equation, whereas in the usual topological recursion the 2-point resolvent arises already for the next to leading term.

$$\begin{aligned} & 2W_{1,1}^0(x)W_{1,1}^{1/2}(x) - \oint \frac{d\zeta_1}{2i\pi}(\zeta_1 - x + x) \frac{W_{1,1}^{1/2}(\zeta_1)}{x - \zeta_1} \\ & + \frac{\alpha^2}{2} \sum_{\substack{s_1, s_2, s_3 \\ s_1 + s_2 + s_3 = 1/2}} 2 \oint \left(\prod_{i=1}^3 W_{1,1}^{s_i}(\zeta_i) \frac{d\zeta_i}{2i\pi} \right) \frac{(\zeta_1 - x + x) + \zeta_2 + \zeta_3}{x - \zeta_1} \\ & + \alpha^3 \oint \left(\prod_{i=1}^3 W_{1,1}^0(\zeta_i) \frac{d\zeta_i}{2i\pi} \right) \frac{\zeta_1^2 + \zeta_2^2 + \zeta_3^2}{x - \zeta_1} = 0 \end{aligned} \quad (8.3.57)$$

After some algebra, this reduces to

$$\begin{aligned} (1 - \alpha^2) \sqrt{(x-a)(x-b)} W_{1,1}^{1/2}(x) &= 4\alpha^2 \left\langle \frac{\text{Tr}(M_1)}{N} \right\rangle^{(1/2)} W_{1,1}^0(x) + \alpha^3 x^2 W_{1,1}^0(x) \\ &\quad - \alpha^3 x + 2\alpha^3 W_{1,1}^0(x) \left\langle \frac{\text{Tr}(M_1^2)}{N} \right\rangle^{(0)}. \end{aligned} \quad (8.3.58)$$

First we have,

$$\left\langle \frac{\text{Tr}(M_1^2)}{N} \right\rangle^0 = \oint dz z^2 W_{1,1}^0(z) = \frac{1}{1 - \alpha^2}. \quad (8.3.59)$$

8.3. LOOP EQUATIONS FOR THE T^4 MODEL

Plugging this expression into (8.3.58) and computing the action of $\oint dz z \cdot$ on (8.3.58) one gets

$$\left\langle \frac{\text{Tr}(M_1)}{N} \right\rangle^{(1/2)} = \frac{3\alpha^3}{(1-\alpha^2)(1-5\alpha^2)}. \quad (8.3.60)$$

One ends up with

$$W_{1,1}^{1/2}(x) = \frac{1}{(1-\alpha^2)\sqrt{(x-a)(x-b)}} \left[\left(\frac{12\alpha^5}{(1-\alpha^2)(1-5\alpha^5)} + \alpha^3 x^2 + \frac{2\alpha^3}{1-\alpha^2} \right) W_{1,1}^0(x) - \alpha^3 x \right]. \quad (8.3.61)$$

As a consistency check, one can compute the series expansion near $x = \infty$ and confirm that $W_{1,1}^{1/2}(x) \sim_{x=\infty} \frac{3\alpha^3}{(1-\alpha^2)(1-5\alpha^5)} \cdot \frac{1}{x^2}$. One rewrites it in the z variables as

$$\omega_{1,1}^{1/2} = W_{1,1}^{1/2}(x)dx = \frac{\alpha^2}{1-\alpha^2} \left(\frac{3(4+\alpha-5\alpha^3)}{1-5\alpha^2} + \frac{\alpha^3}{z^2} \right) \frac{dz}{z^2}. \quad (8.3.62)$$

Notice that this expression has neither poles at $+1$ nor at -1 . This is different from the Hermitian matrix model case and comes from the absence of $W_{2,1}^0$ in the computation. This is due to the fact that tensor models have a different scaling which, in some way, “lifts the degeneracy” of the genus. This effect translates on the singularities of the loop equation solutions. In fact $\omega_{1,1}^{1/2}$ has a pole at $z = 0$ but no poles on the branching points. One expects to find poles at order corresponding to a topological order.

We obtain from these results that the next-to-next-to leading order 2-point function of the melonic T^4 tensor model in $d = 3$ dimensions is

Proposition 14. *The next-to-next-to leading order two points function of random tensor models is*

$$G_{2,NNLO}(\lambda) = -\frac{9(\sqrt{6\lambda+1}-1)^3}{(-18\lambda+\sqrt{6\lambda+1}-1)(-24\lambda+5\sqrt{6\lambda+1}-5)}. \quad (8.3.63)$$

Proof. Use the coefficient of x^{-2} given in (8.3.60). Recall the relation (in chap. 7), which is linear in the case of the 2-point function and the value of α in term of λ . This has a Taylor series expansion with positive coefficients in $-\lambda = 0$. \square

The combinatorial interpretation is that this result provides (up to some factors) a generating series for a specific class of degree $\omega = 2$ four colored graphs with one marked sphere made out of two triangles. The conclusion of this subsection is that, very much like the loop equations of the Hermitian matrix model, the loop equations of the shifted quartic melonic tensor models can be used to derive systematically the higher orders (in N) of the n -point function.

8.3. LOOP EQUATIONS FOR THE T^4 MODEL

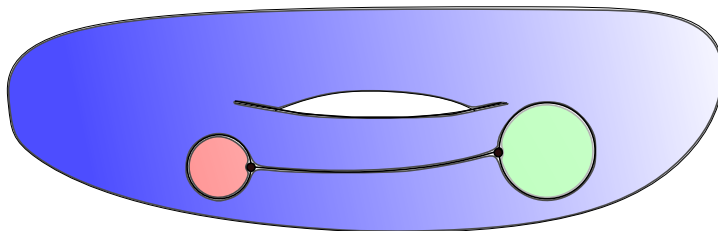


Figure 8.2: An example of a stuffed map. The green and red faces are regular 2-cells as they are discs (1-punctured sphere). The blue face however is a non-trivial 2-cell as it is a once punctured torus.

8.3.4 The six dimensional case

This case already appeared to be special before, in the chapter on the double scaling limit. It appears to be special again when considering the recursion solving process. In fact after the shift one obtains a new matrix model whose $1/N$ expansion matches a *topological expansion*.

Let us make the following remark. Consider the potential term of the shifted theory

$$\text{Tr} \sum_{p \geq 2} \frac{\alpha^p}{N^{\frac{d-2}{2}p}} \left(\sum_c \mathcal{M}_c \right)^p. \quad (8.3.64)$$

Expanding the $(\sum_c \mathcal{M}_c)^p$ we obtain a potential that for each value of p writes as a product of traces of \mathcal{M}_c at some power q_c . The q_c are greater than 0 and their sum must equal p . Consider $1 \leq n = \text{number of non-zero } q_c \leq d$. Then the global N scaling in front of the interaction is $N^{-\frac{d-2}{2}p+d-n}$ and p can be written $p = 2 + h$ for some $h \geq 0$, so that the N scaling is $N^{2-\frac{d-2}{2}h-n}$. Now, if the value of $\beta = \frac{d-2}{2}$ is even, we obtain a model that is a generating series of colored *stuffed maps* as described³ by Gaetan Borot in [Bor13]. These maps are a generalization of the usual $2d$ maps in the sense that their 2-cells may not only be discs (*i.e.* surfaces of genus 0 with one boundary) but also surfaces of genus g with n boundaries. They have then a non-trivial effect on the Euler characteristic of the associated ribbon graphs. See an example of a stuffed map on Fig. 8.2. In our case, the 2-cells of non trivial topology have Euler characteristic $\chi_{\frac{\beta h}{2}, n} = 2 - 2\frac{\beta}{2}h - n$. Moreover, the color condition intervenes in the fact that the boundary components carry a color index and can only be glued to faces of the ribbon graph that are of the same color. The scaling of such models thus corresponds to a topological scaling of orientable surfaces built out of

³Actually, Gaetan Borot explored the case of non-colored stuffed maps, but was at the origin of the stuffing of maps idea. He described a matrix model formulation of their generating series.

8.3. LOOP EQUATIONS FOR THE T^4 MODEL

ribbon graphs with 2-cells of non trivial topology. Now we notice that β is even for a series of dimensions

$$\beta = \frac{d-2}{2} = 2k \quad \text{for some } k \in \mathbb{N} \quad \Leftrightarrow \quad d = 4k + 2, \quad k \in \mathbb{N}. \quad (8.3.65)$$

This of course includes the two dimensional case, but also dimensions $d = 6, 10, 14, 18, 22, 26, \dots$. There is no available interpretation, either geometric or combinatorial, of this fact. So it may be pure “numerology”. However it is striking that the double scaling “wall” also appear in six dimensions, and that, it is also well known that the double scaling limit is also not summable in the two dimensional situation. One speculates⁴ that it may be related to several known facts. First the fact that this period of 4 reminds us about Bott periodicity for homotopy groups of $U(\infty)$. Moreover there may be some combinatorial interpretation as the symmetric groups \mathfrak{S}_n of degree $n = 2, 6$ are special since they are the only non complete symmetric groups. This is because \mathfrak{S}_2 has a non trivial center, while for \mathfrak{S}_6 the outer automorphism group is non trivial $\text{Out}(\mathfrak{S}_6) = \mathfrak{S}_2$. One should investigate the consequences of these facts on tensor models⁵.

As we have seen in the previous section, in the three dimensional case the term $W_{2,1}^0(z_1, z_2)$ did not appear in the computation of the NLO term of the shifted model. This was a very different feature from the Hermitian matrix model case and due to the specific non-topological scaling. In the six dimensional case this term appears again already from the NLO term of the shifted model, and will be present in the same way than for a Hermitian matrix model. This translates in a particular manner when studying the loop equations. In fact if the leading order is unchanged, it has consequences on all the subsequent orders of the shifted model. First one sees that the term $W_{2,1}(x, x)$ of (8.3.33) is not suppressed at the NLO order. But it also changes the behaviour of the potential term, as the splitting into partition of the set of ζ_j variables allows the appearance of some more terms in the topological scaling case. From what we have said, in six dimensions,

$$W_{\mathbf{k}}(x_{\mathbf{k}}) = \sum_{g \geq 0} N^{2-2g-|\mathbf{k}|} W_{\mathbf{k}}^g(x_{\mathbf{k}}). \quad (8.3.66)$$

⁴These are speculations, so one should not take them too seriously.

⁵The relation to Bott periodicity, if existent, is not clear at all even though there exists relation between matrix models and homotopy invariants of the sphere and these relations are likely to extend to other dimensions. One should also point out the work of Ben Geloun and Ramgoolam [BGR13a], that establishes connection with permutation TFT and homotopy of the sphere when it comes to counting tensor invariants. The relation to properties of symmetric groups may seem more natural. In fact the loop equations solutions for the d dimensional T^4 melonic tensor model are symmetric under a certain action of \mathfrak{S}_d . However I do not think this is the real point here since this symmetry is just the trace of the re-coloring symmetry of the observables and one can consider models that are not symmetric in colors but that still have this specific topological scaling. I would rather guess that one has to work with the permutation formulation of d -combinatorial maps to investigate such possible connections. In any case I think these are possibly very important problems and they should really be investigated further.

8.3. LOOP EQUATIONS FOR THE T^4 MODEL

The next-to-leading order equation in the six dimensional case writes

$$\begin{aligned}
0 = & 2W_{1,1}^0(x)W_{1,1}^1(x) + W_{2,1}^0(x, x) \\
& - \oint \frac{d\zeta_1}{2i\pi} \frac{\zeta_1}{x - \zeta_1} W_{1,1}^1(\zeta_1) + \frac{\alpha^2}{2} \left(2 \oint \left(\prod_j \frac{d\zeta_j}{2i\pi} \right) \frac{\zeta_1}{x - \zeta_1} \sum_{J \vdash \mathcal{C}} \prod_{J_i} W_{J_i}^0(\zeta_{J_i}) \right. \\
& + 2 \sum_{k \neq 1} \oint \left(\prod_j \frac{d\zeta_j}{2i\pi} \frac{1}{x - \zeta_1} \zeta_k \sum_{J \vdash \mathcal{C}} \prod_{J_i} W_{J_i}^0(\zeta_{J_i}) \right) + \frac{\alpha^2}{2} \left(2 \oint \left(\prod_j \frac{d\zeta_j}{2i\pi} \right) \frac{\zeta_1}{x - \zeta_1} \right. \\
& \left. \sum_{\substack{\{s_i\}_{i \in \llbracket 1, 6 \rrbracket} \\ \sum_i s_i = 1}} \prod_i W_{1,1}^{s_i}(\zeta_i) + 2 \sum_{k \neq 1} \oint \left(\prod_j \frac{d\zeta_j}{2i\pi} \right) \frac{\zeta_k}{x - \zeta_1} \sum_{\substack{\{s_i\}_{i \in \llbracket 1, 6 \rrbracket} \\ \sum_i s_i = 1}} \prod_i W_{1,1}^{s_i}(\zeta_i) \right) \\
& + \frac{\alpha^3}{3} \left(3 \oint \prod_j \frac{d\zeta_j}{2i\pi} \frac{\zeta_1^2}{x - \zeta_1} W_{1,1}^0(\zeta_1) \prod_{i \neq 1} W_{1,1}^0(\zeta_i) + 6 \sum_{k \neq 1} \oint \left(\prod_j \frac{d\zeta_j}{2i\pi} \right) \frac{\zeta_1}{x - \zeta_1} \right. \\
& W_{1,1}^0(\zeta_1) \zeta_k W_{1,1}^0(\zeta_k) \prod_{i \neq 1, k} W_{1,1}^0(\zeta_i) + 3 \sum_{k \neq 1} \oint \left(\prod_j \frac{d\zeta_j}{2i\pi} \right) \frac{W_{1,1}^0(\zeta_1)}{x - \zeta_1} \zeta_k^2 W_{1,1}^0(\zeta_k) \\
& \prod_{i \neq 1, j} W_{1,1}^0(\zeta_i) + 6 \sum_{\substack{k, m \neq 1 \\ k \neq m}} \oint \left(\prod_j \frac{d\zeta_j}{2i\pi} \right) \frac{W_{1,1}^0(\zeta_1)}{x - \zeta_1} \zeta_k W_{1,1}^0(\zeta_k) \zeta_m W_{1,1}^0(\zeta_m) \\
& \left. \prod_{i \neq 1, k, m} W_{1,1}^0(\zeta_i) \right). \tag{8.3.67}
\end{aligned}$$

The partitions $J = \{J_i\}$ are here the partitions with four sets with one element of the form $J_i = \{\zeta_i\}$ and one set with two elements of the form $\{\zeta_k, \zeta_m\}$. One can compute $W_{1,1}^1(x)$ by brute force, in the same way than what has been done in the three dimensional case. It is a bit more tedious since the topological scaling allows some more terms. This reduces to

Direct computation

$$\begin{aligned}
0 = & -(1 - \alpha^2) \sqrt{\sigma_x} W_{1,1}^1(x) + W_{2,1}^0(x, x) + \frac{5\alpha^5}{(1 - \alpha^2)(1 - 11\alpha^2)} W_{1,1}^0(x) \\
& + 5\alpha^2 \oint \frac{d\zeta_2}{2i\pi} \zeta_2 W_{(11\bar{0})}^0(x, \zeta_2) + \alpha^3 x^2 W_{1,1}^0(x) - \alpha^3 x. \tag{8.3.68}
\end{aligned}$$

Also by using the equation (8.3.55), we deduce that

$$W_{2,1}^0(x, x) dx \otimes dx = -B_{l^* z_2}(z, z) + h(z, z). \tag{8.3.69}$$

From this one obtains $W_{2,1}^0(x, x) dx$ by taking the interior product of the second variable with the vector field $\frac{\partial}{\partial x}$ from now on denoted ∂_x ,

$$W_{2,1}^0(x, x) dx = W_{2,1}^0(x, x) dx(\cdot) \otimes dx(\partial_x) = [-B_{l^* z_2}(z, z) + h_{2,1}^0(z, z)](\cdot, \partial_x). \tag{8.3.70}$$

8.3. LOOP EQUATIONS FOR THE T^4 MODEL

From $dz(\partial_x) = \frac{dz}{dx}$ it follows

$$\frac{dz}{dx} = \sqrt{1 - \alpha^2} \frac{z}{(z - 1/z)}, \quad (8.3.71)$$

$$W_{2,1}^0(x, x)dx = \frac{\sqrt{1 - \alpha^2}}{z - 1/z} \left[\frac{z}{(z^2 - 1)^2} - \frac{\alpha^2(d - 1)}{d(2\alpha^2 - \alpha^4) + \alpha^4 - \alpha^2 - 1} \frac{1}{z^3} \right] dz. \quad (8.3.72)$$

This is sufficient to obtain the exact expression for $\omega_{1,1}^1$,

$$\begin{aligned} \omega_{1,1}^1 &= \frac{z}{(z - 1/z)^2} \left[\frac{1}{(z^2 - 1)^2} - \frac{5\alpha^2}{11\alpha^2 - 5\alpha^4 - 1} \frac{1}{z^4} \right] dz \\ &+ \frac{5\alpha^2}{(1 - \alpha^2)^{3/2}(1 - 11\alpha^2)} \frac{dz}{z^2} + \frac{\alpha^3}{(1 - \alpha^2)^{3/2}} (z + 1/z)^2 \frac{dz}{z^2} \\ &- \frac{\alpha^3}{(1 - \alpha^2)^{3/2}} (z + 1/z) \frac{dz}{z} - \frac{\alpha^2 \sqrt{1 - \alpha^2}}{11\alpha^2 - 5\alpha^4 - 1} \frac{dz}{z^2}. \end{aligned} \quad (8.3.73)$$

This confirms our assertion. After the computation of $\omega_{1,1}^{1/2}$, the poles at ± 1 really come from the $W_{2,1}^0$ term of the loop equations. There are still poles at 0 as in the case of $\omega_{1,1}^{1/2}$. So $\omega_{1,1}^1$ really writes as a meromorphic form in a neighbourhood Ω_ϵ of the cut Γ plus a form holomorphic on Ω_ϵ . In fact it is exactly the result stated in [Bor13]. One could try to extend the residue formula by stating that

$$\begin{aligned} \omega_{1,1}^1(z) &= \frac{1}{2i\pi} \oint \frac{\omega_{1,1}^1(z')}{z' - z} = \frac{1}{2i\pi} \sum_{p \in \{\text{poles}=P\}} \oint_{C_p} \frac{\omega_{1,1}^1(z')}{z - z'} \\ &= \frac{1}{2i\pi} \sum_{\{\pm 1\}} \oint_{\pm} \frac{\omega_{1,1}^1(z')}{z - z'} + \frac{1}{2i\pi} \sum_{p' \in P'} \oint_{C_{p'}} \frac{\omega_{1,1}^1(z')}{z - z'}. \end{aligned} \quad (8.3.74)$$

In the last line of (8.3.74), the holomorphic part on Ω_ϵ of $\omega_{1,1}^1$ does not contribute to the first term and is contained in the second term. So one is tempted to split $\omega_{1,1}^1$ in two parts. One *polar* part $\omega_{1,1}^{1,P}$ on Ω_ϵ which has poles on Ω_ϵ and one *holomorphic* part $\omega_{1,1}^{1,\mathcal{H}}$ on Ω_ϵ which is regular on Ω_ϵ . We denote them respectively $\omega_{1,1}^{1,P}$ and $\omega_{1,1}^{1,\mathcal{H}}$. This very much look like the setting used in [BS15]. Without mastering enough these ideas to apply them concretely in this specific case yet, we are quite convinced that it should extend to at least all the topological scaling cases, hence in dimensions $d = 4k + 2$.

8.4 Remarks

In this chapter we have explained the Schwinger-Dyson equations of the generic 1-tensor model. We have then particularized to a specific model and shown how, at least in this

8.4. REMARKS

case, some of the information they contain can be recast in a set of loop equations that mimic the set of Virasoro constraints of the Hermitian one matrix model. Also we have briefly presented the topological recursion technique, and tried to show that it is likely that we can extend this technique in the case of the shifted quartic melonic tensor models, at least for the specific family of dimensions $d = 4k + 2$.

Of course, this deserves much more study, and there is still much work to do in this direction. Some of the mathematical apparatus presented in [Bor13] and [BS15] has to be applied to this context. This is why this part of this thesis is still an ongoing research project.

However the program is pretty clear, one should first investigate the topological scaling case as it behaves very much like the case described in [Bor13]. After that one should understand how the non-topological part of the scaling perturbs the topological part of the loop equations in the non-topological case. In fact the non topological terms seem to behave as source terms for the topological terms. As we have seen in the example explicitly computed in this chapter this perturbs the poles structure of the combinatorial solutions of loop equations in a different way than in [Bor13]. But the recurrence type structure is still there, so one should be able to recast this computation in terms of residue formula. This could be done by forcing the non-topological term to enter the definition of the $W_{\mathbf{k}}^g$, allowing the $W_{\mathbf{k}}^g$ to keep a dependence in N . In this way $W_{\mathbf{k},N}^g$ would be a sub-formal series in N of $W_{\mathbf{k},N}$. Or one could explore the recurrence equations on N , but with no guarantee that the poles structure can be worked out in sufficient detail so as to recast everything in term of concise residue formulas.

Moreover, if this can be achieved one should investigate whether or not the algebraic geometry framework of the topological recursion is conserved in this model. One should relate the $W_{\mathbf{k}}^s$ to geometric data of the spectral curve. This is certainly the case for the topological cases $d = 6, 10, 14, \dots$, and one is tempted to refer to a quartic melonic tensor model with only two interactions terms for that. In fact in that case one can consider a kind of $O(n)$ model but with two Hermitian matrices instead of one. The associated spectral curve is a torus. Then by rescaling the coupling constant by a factor $N^{(2-d)/2}$ one would reinterpret the spectral curve obtained in this way as a pinched torus leading to a collection of punctured spheres. In that way the $W_{\mathbf{k}}^s$ should be connected to geometric data of the resulting pinched torus. Also one can think of the work of [BS15], which connects the observable of multi-trace Hermitian one matrix models to integrals over moduli spaces of curves. However, the non-topological cases are not understood at all.

The loop equations of the Hermitian one matrix models are often called Virasoro constraints as they are reminiscent of its Schwinger-Dyson equations. They can be rewritten in term of the action of a family of differential operators that together with the commutator form the half positive of a Virasoro (Witt) algebra. These constraints appear in almost all

8.4. REMARKS

(if not all) the problems that can be treated with the topological recursion. The Schwinger-Dyson equations of the generic 1-tensor model can also be rephrased in terms of differential operators. Moreover these differential operators also form a Lie algebra with their commutator. Consequently, one shall point out that this Lie algebra contains numerous sub-Witt algebras⁶ that should be translated in terms of loop equations⁷. One then should explore the consequences of the existence of these many sets of loop equations, and in particular whether they are redundant or independent. Can they be used to write recursion formulas on subsets of observables? The question of independence of the corresponding *several* sets of loop equations may well be related to the questions of independence of the set of tensor invariants. In fact the tensor invariants represented by graphs are known to generate all the invariants of the tensor but one is not able to tell whether or not they form a basis of the tensor invariants (*i.e.* are they independent?). This is the case when considering matrices, a basis of the invariants of a square matrix of size N is provided by the family $\{\text{Tr}(M^p)\}_{p \in \llbracket 0, N \rrbracket}$. But we have no such results yet about tensor invariants.

⁶the number of which depends on the dimensions.

⁷This is possible in this case since the set indexing the operators of these sub-Witt algebras can be mapped one-to one with \mathbb{N} .

8.4. REMARKS

Bibliography

- [ADJ91] Jan Ambjorn, Bergfinnur Durhuus, and Thordur. Jonsson. Three-dimensional simplicial quantum gravity and generalized matrix models. *Modern Physics Letters A*, 06(12):1133–1146, 1991.
- [AJL06] J. Ambjorn, J. Jurkiewicz, and R. Loll. The universe from scratch. *Contemp. Phys.*, 47:103–117, 2006.
- [AK96] Jorge Alfaro and Ivan K. Kostov. Generalized hirota equations in models of 2-d quantum gravity. 1996.
- [Ald91] David Aldous. The continuum random tree. i. *Ann. Probab.*, 19(1):1–28, 01 1991.
- [Ald93] David Aldous. The continuum random tree iii. *Ann. Probab.*, 21(1):248–289, 01 1993.
- [Bae96] John C. Baez. Spin network states in gauge theory. *Adv. Math.*, 117:253–272, 1996.
- [Bae00] J. C. Baez. An introduction to spin foam models of quantum gravity and bf theory. *Lect. Notes Phys.*, 543:25–94, 2000.
- [Ber73] Claude Berge. *Graphs and Hypergraphs*. North Holland Publisher, 1973.
- [BGKMR10] Joseph Ben Geloun, Thomas Krajewski, Jacques Magnen, and Vincent Rivasseau. Linearized group field theory and power counting theorems. *Class. Quant. Grav.*, 27:155012, 2010.
- [BGR12] Valentin Bonzom, Razvan Gurau, and Vincent Rivasseau. Random tensor models in the large n limit: Uncoloring the colored tensor models. *Phys. Rev.*, D85:084037, 2012.
- [BGR13a] Joseph Ben Geloun and Sanjaye Ramgoolam. Counting Tensor Model Observables and Branched Covers of the 2-Sphere. 2013.

- [BGR13b] Joseph Ben Geloun and Vincent Rivasseau. A renormalizable 4-dimensional tensor field theory. *Commun.Math.Phys.*, 318:69–109, 2013.
- [BGRR11] Valentin Bonzom, Razvan Gurau, Aldo Riello, and Vincent Rivasseau. Critical behavior of colored tensor models in the large n limit. *Nucl.Phys.*, B853:174–195, 2011.
- [BI02] P. Bleher and A. Its. Double scaling limit in the random matrix model: the riemann-hilbert approach. *ArXiv Mathematical Physics e-prints*, 2002.
- [BM94] John Baez and J.P. Muniain. *Gauge Fields, Knots and Gravity*. World Scientific, 1994.
- [Bor13] Gaetan Borot. Formal multidimensional integrals, stuffed maps, and topological recursion. 2013.
- [Bou92] D.V. Boulatov. A model of three-dimensional lattice gravity. *Mod.Phys.Lett.*, A7:1629–1646, 1992.
- [BS12a] V. Bonzom and M. Smerlak. Bubble divergences from twisted cohomology. *Communications in Mathematical Physics*, 312:399–426, June 2012.
- [BS12b] Valentin Bonzom and Matteo Smerlak. Bubble divergences: sorting out topology from cell structure. *Annales Henri Poincare*, 13:185–208, 2012.
- [BS15] G. Borot and S. Shadrin. Blobbed topological recursion: properties and applications. *ArXiv e-prints*, February 2015.
- [CC12] Ali H. Chamseddine and Alain Connes. Resilience of the spectral standard model. *JHEP*, 1209:104, 2012.
- [CK00] Alain Connes and Dirk Kreimer. Renormalization in quantum field theory and the riemann-hilbert problem i: The hopf algebra structure of graphs and the main theorem. *Communications in Mathematical Physics*, 210(1):249–273, 2000.
- [Con94] Alain Connes. *Noncommutative Geometry*. Academic Press, 1994.
- [Dar14] S. Dartois. A givental-like formula and bilinear identities for tensor models. *ArXiv e-prints*, September 2014.
- [DE13] F. David and B. Eynard. Planar maps, circle patterns and 2d gravity. *ArXiv e-prints*, July 2013.
- [DFGZJ95] P. Di Francesco, Paul H. Ginsparg, and Jean Zinn-Justin. 2-d gravity and random matrices. *Phys.Rept.*, 254:1–133, 1995.

BIBLIOGRAPHY

- [DGR13] Stephane Dartois, Razvan Gurau, and Vincent Rivasseau. Double scaling in tensor models with a quartic interaction. *JHEP*, 1309:088, 2013.
- [Di 04] P. Di Francesco. 2d quantum gravity, matrix models and graph combinatorics. *ArXiv Mathematical Physics e-prints*, June 2004.
- [Di 12] P. Di Francesco. Integrable combinatorics. *ArXiv e-prints*, October 2012.
- [Dis03] V. Disertori, M.; Rivasseau. Random matrices and the anderson model. *ArXiv e-prints*, 2003.
- [DMS14] B. Duplantier, J. Miller, and S. Sheffield. Liouville quantum gravity as a mating of trees. *ArXiv e-prints*, September 2014.
- [DRT14] Stéphane Dartois, Vincent Rivasseau, and Adrian Tanasa. The $1/n$ expansion of multi-orientable random tensor models. *Annales Henri Poincaré*, 15(5):965–984, 2014.
- [Dup11] B. Duplantier. The hausdorff dimension of two-dimensional quantum gravity. *ArXiv e-prints*, August 2011.
- [Dys49] F. J. Dyson. The radiation theories of tomonaga, schwinger, and feynman. *Phys. Rev.*, 75:486–502, Feb 1949.
- [EH13] David Eisenbud and Joe Harris. *3264 and All That Intersection Theory in Algebraic Geometry*. 2013.
- [EHLN14] C. Even-Zohar, J. Hass, N. Linial, and T. Nowik. Invariants of random knots and links. *ArXiv e-prints*, November 2014.
- [Ein14a] Albert Einstein. Covariance properties of the field equations of the theory of gravitation based on the generalized theory of relativity. *Z.Math.Phys.*, 63:215–225, 1914.
- [Ein14b] Albert Einstein. On the foundations of the generalized theory of relativity and the theory of gravitation. *Phys. Z.*, 15:176–180, 1914.
- [Ein15] Albert Einstein. The field equations of gravitation. *Sitzungsber.Preuss.Akad.Wiss.Berlin*, 1915.
- [EKPM14] Bertrand Eynard, Amir-Kian Kashani-Poor, and Olivier Marchal. A matrix model for the topological string i: Deriving the matrix model. *Annales Henri Poincare*, 15:1867–1901, 2014.
- [Emo06] Hiroki Emoto. Quantum gravity through non-perturbative renormalization group and improved black hole. pages 116–129, 2006.

- [EO08] B. Eynard and N. Orantin. Algebraic methods in random matrices and enumerative geometry. *ArXiv e-prints*, 2008.
- [Eyn04] B. Eynard. Topological expansion for the 1-hermitian matrix model correlation functions. *JHEP*, 0411:031, 2004.
- [Eyn06] B. Eynard. Formal matrix integrals and combinatorics of maps. *ArXiv Mathematical Physics e-prints*, November 2006.
- [Eyn09] B. Eynard. A matrix model for plane partitions. *Journal of Statistical Mechanics: Theory and Experiment*, 10:11, October 2009.
- [Eyn15a] B. Eynard. Random matrices. *IPhT theoretical physics course lecture notes*, 2015.
- [Eyn15b] Bertrand Eynard. *Counting surfaces*. Birkhauser Basel, 2015.
- [Fer82] M. ; Gagliardi C. Ferri. The only genus zero n -manifold is S^n . *Proc. Amer. Math. Soc.*, 85:638–642, 1982.
- [Fey49] R. P. Feynman. Space-time approach to quantum electrodynamics. *Phys. Rev.*, 76:769–789, Sep 1949.
- [Fey50] R. P. Feynman. Mathematical formulation of the quantum theory of electromagnetic interaction. *Phys. Rev.*, 80:440–457, Nov 1950.
- [Fey63] R.P. Feynman. Quantum theory of gravitation. *Acta Phys. Polon.*, Vol: 24, Dec 1963.
- [FG82] M. Ferri and C. Gagliardi. Crystallisation moves. *Pacific J. Math.*, 100(1):85–103, 1982.
- [Fre05] Laurent Freidel. Group field theory: An overview. *Int.J.Theor.Phys.*, 44:1769–1783, 2005.
- [FT14] E. Fusy and A. Tanasa. Asymptotic expansion of the multi-orientable random tensor model. *ArXiv e-prints*, August 2014.
- [Gla61] Sheldon L. Glashow. Partial-symmetries of weak interactions. *Nuclear Physics*, 22(4):579 – 588, 1961.
- [GR11] Razvan Gurau and Vincent Rivasseau. The $1/n$ expansion of colored tensor models in arbitrary dimension. *Europhys.Lett.*, 95:50004, 2011.
- [GR12] Razvan Gurau and James P. Ryan. Colored tensor models - a review. *SIGMA*, 8:020, 2012.

BIBLIOGRAPHY

- [GR14] R. Gurau and J. P. Ryan. Melons are branched polymers. *Annales Henri Poincaré*, 15:2085–2131, November 2014.
- [GS13] R. Gurau and G. Schaeffer. Regular colored graphs of positive degree. *ArXiv e-prints*, July 2013.
- [GSW62] Jeffrey Goldstone, Abdus Salam, and Steven Weinberg. Broken symmetries. *Phys. Rev.*, 127:965–970, Aug 1962.
- [GTY15] Razvan Gurau, Adrian Tanasa, and Donald R. Youmans. The double scaling limit of the multi-orientable tensor model. 2015.
- [Gur10] Razvan Gurau. Lost in translation: Topological singularities in group field theory. *Class.Quant.Grav.*, 27:235023, 2010.
- [Gur11a] R. Gurau. Universality for random tensors. *ArXiv e-prints*, November 2011.
- [Gur11b] Razvan Gurau. The $1/n$ expansion of colored tensor models. *Annales Henri Poincare*, 12:829–847, 2011.
- [Gur11c] Razvan Gurau. Colored group field theory. *Commun.Math.Phys.*, 304:69–93, 2011.
- [Gur11d] Razvan Gurau. Reply to comment on ‘lost in translation: topological singularities in group field theory’. *Class.Quant.Grav.*, 28:178002, 2011.
- [Gur12a] Razvan Gurau. The complete $1/n$ expansion of colored tensor models in arbitrary dimension. *Annales Henri Poincare*, 13:399–423, 2012.
- [Gur12b] Razvan Gurau. The schwinger dyson equations and the algebra of constraints of random tensor models at all orders. *Nucl.Phys.*, B865:133–147, 2012.
- [Gur14] R. Gurau. The $1/n$ expansion of tensor models beyond perturbation theory. *Communications in Mathematical Physics*, 330:973–1019, September 2014.
- [Gursh] Razvan Gurau. *Random Tensors*. Oxford University Press, (To Publish).
- [Har92] Joe Harris. *Algebraic Geometry*. Springer-Verlag New York, 1992.
- [IZ80] C. Itzykson and J.B. Zuber. The planar approximation. ii. *Journal of Mathematical Physics*, 21(3):411–421, 1980.
- [JM85] Michio Jimbo and Tetsuji Miwa. Monodromy, solitons and infinite dimensional lie algebras. In J. Lepowsky, S. Mandelstam, and I.M. Singer, editors, *Vertex Operators in Mathematics and Physics*, volume 3 of *Mathematical Sciences Research Institute Publications*, pages 275–290. Springer US, 1985.

- [Kak93] Michio Kaku. *Quantum Field Theory: A Modern Introduction*. 1993.
- [Kon92] Maxim Kontsevich. Intersection theory on the moduli space of curves and the matrix airy function. *Comm. Math. Phys.*, 147(1):1–23, 1992.
- [KOR14a] Wojciech Kaminski, Daniele Oriti, and James P. Ryan. Towards a double-scaling limit for tensor models: probing sub-dominant orders. *New J.Phys.*, 16:063048, 2014.
- [KOR14b] Wojciech Kaminskiski, Daniele Oriti, and James P. Ryan. Towards a double-scaling limit for tensor models: probing sub-dominant orders. *New J.Phys.*, 16:063048, 2014.
- [KW10] Joanna L. Karczmarek and Daoyan Wang. Into the bulk: Reconstructing spacetime from the $c=1$ matrix model. *Phys.Rev.*, D82:126004, 2010.
- [Lan04] Alexander K. Lando, Sergei K. ; Zvonkin. *Graphs on Surfaces and Their Applications*. Springer-Verlag Berlin Heidelberg, 2004.
- [Le 14] J.-F. Le Gall. Random geometry on the sphere. *ArXiv e-prints*, March 2014.
- [LM85] Sostenes Lins and Arnaldo Mandel. Graph-encoded 3-manifolds. *Discrete Mathematics*, 57(3):261 – 284, 1985.
- [LM04] Madan Lal Mehta. *Random Matrices*. Academic Press, 2004.
- [LMW14] A. Lubotzky, J. Maher, and C. Wu. Random methods in 3-manifold theory. *ArXiv e-prints*, May 2014.
- [Mat90] S.V. Matveev. Complexity theory of three-dimensional manifolds. *Acta Applicandae Mathematica*, 19(2):101–130, 1990.
- [Muk06] Sunil Mukhi. Matrix models of moduli space. In Edouard Brezin, Vladimir Kazakov, Didina Serban, Paul Wiegmann, and Anton Zabrodin, editors, *Applications of Random Matrices in Physics*, volume 221 of *NATO Science Series II: Mathematics, Physics and Chemistry*, pages 379–401. Springer Netherlands, 2006.
- [NDE15] VietAnh Nguyen, Stéphane Dartois, and Bertrand Eynard. An analysis of the intermediate field theory of t4 tensor model. *Journal of High Energy Physics*, 2015(1), 2015.
- [Ori06] Daniele Oriti. The group field theory approach to quantum gravity. 2006.
- [Pen88] R. C. Penner. Perturbative series and the moduli space of riemann surfaces. *J. Differential Geom.*, 27(1):35–53, 1988.

BIBLIOGRAPHY

- [Pol98] Joseph Polchinski. *String Theory*, volume 1. Cambridge University Press, 1998. Cambridge Books Online.
- [Riv11] Vincent Rivasseau. Quantum gravity and renormalization: The tensor track. *AIP Conf.Proc.*, 1444:18–29, 2011.
- [Riv14] Vincent Rivasseau. The tensor track iii. *Fortsch.Phys.*, 62:81–107, 2014.
- [Rov07] Carlo Rovelli. *Quantum Gravity*. Cambridge University Press, 2007.
- [RT15] Matti Raasakka and Adrian Tanasa. Next-to-leading order in the large n expansion of the multi-orientable random tensor model. *Annales Henri Poincaré*, 16(5):1267–1281, 2015.
- [RW10] V. Rivasseau and Z. Wang. Loop vertex expansion for Φ^{2k} theory in zero dimension. *Journal of Mathematical Physics*, 51(9):092304, September 2010.
- [Rya12] James P. Ryan. Tensor models and embedded riemann surfaces. *Phys.Rev.*, D85:024010, 2012.
- [Sal68] Abdus Salam. Weak and electromagnetic interactions. *Conf.Proc.*, C680519:367–377, 1968.
- [Sch98] Gilles Schaeffer. *Conjugaison d’arbres et cartes combinatoires aléatoires*. Phd thesis, 1998. in French.
- [Sch07] Martin Schlichenmaier. *An Introduction to Riemann Surfaces, Algebraic Curves and Moduli Spaces*. Springer-Verlag Berlin Heidelberg, 2007.
- [Sch11] Christoph Schweigert. *Mathematical Structures in Physics*. 2011.
- [Sme11] Matteo Smerlak. Comment on ‘lost in translation: Topological singularities in group field theory’. *Class.Quant.Grav.*, 28:178001, 2011.
- [SW64] A. Salam and J.C. Ward. Electromagnetic and weak interactions. *Physics Letters*, 13(2):168 – 171, 1964.
- [SZ03] G. Schaeffer and P. Zinn-Justin. On the asymptotic number of plane curves and alternating knots. *ArXiv Mathematical Physics e-prints*, April 2003.
- [Tan11] Adrian Tanasa. Some combinatorial aspects of quantum field theory. 2011.
- [Tan12] Adrian Tanasa. Multi-orientable group field theory. *J.Phys.*, A45:165401, 2012.
- [tH93] Gerard ’t Hooft. Dimensional reduction in quantum gravity. pages 0284–296, 1993.

- [tH02] Gerard 't Hoof. *Perturbative Quantum Gravity*. 2002.
- [Thi07] Thomas Thiemann. *Modern Canonical Quantum General Relativity*. Cambridge Monographs on Mathematical Physics. Cambridge University Press, October 2007.
- [Wee03] J. R. Weeks. Computation of hyperbolic structures in knot theory. *ArXiv Mathematics e-prints*, September 2003. To be published in Handbook of Knot Theory.
- [Wei67] Steven Weinberg. A model of leptons. *Phys. Rev. Lett.*, 19:1264–1266, Nov 1967.
- [Wit91] Edward Witten. Two-dimensional gravity and intersection theory on moduli space. *Surveys Diff. Geom.*, 1:243–310, 1991.
- [Zvo97] A. Zvonkin. Matrix integrals and map enumeration: An accessible introduction. *Math. Comput. Model.*, 26(8-10):281–304, October 1997.
- [Zvo02] D. Zvonkine. Strebel differentials on stable curves and kontsevich's proof of witten's conjecture. *ArXiv Mathematics e-prints*, September 2002.
- [ZZ99] P. Zinn-Justin and J. . Zuber. Matrix integrals and the counting of tangles and links. *ArXiv Mathematical Physics e-prints*, April 1999.

Titre : Modèles de Tenseurs Aléatoires : Combinatoire, Géométrie, Gravité Quantique et Intégrabilité.

Résumé :

Dans cette thèse nous explorons différentes facettes des modèles de tenseurs aléatoires. Les modèles de tenseurs aléatoires ont été introduits en physique dans le cadre de l'étude de la gravité quantique. En effet les modèles de matrices aléatoires, qui sont un cas particuliers de modèles de tenseurs, en sont une des origines. Ces modèles de matrices sont connus pour leur riche combinatoire et l'incroyable diversité de leurs propriétés qui les font toucher tous les domaines de l'analyse, la géométrie et des probabilités. De plus leur étude par les physiciens ont prouvé leur efficacité en ce qui concerne l'étude de la gravité quantique à deux dimensions.

Les modèles de tenseurs aléatoires incarnent une généralisation possible des modèles de matrices. Comme leurs cousins, les modèles de matrices, ils posent questions dans les domaines de la combinatoire (comment traiter les cartes combinatoires d dimensionnelles ?), de la géométrie (comment contrôler la géométrie des triangulations générées ?) et de la physique (quelle type d'espace-temps produisent-ils ? Quels sont leurs différentes phases ?). Cette thèse espère établir des pistes ainsi que des techniques d'études de ces modèles.

Dans une première partie nous donnons une vue d'ensemble des modèles de matrices. Puis, nous discutons la combinatoire des triangulations en dimensions supérieures ou égales à trois en nous concentrant sur le cas tri-dimensionnelle (lequel est plus simple à visualiser). Nous définissons ces modèles et étudions certaines de leurs propriétés à l'aide de techniques combinatoires permettant de traiter les cartes d dimensionnelles. Enfin nous nous concentrons sur la généralisation de techniques issues des modèles de matrices dans le cas d'une famille particulières de modèles de tenseurs aléatoires. Ceci culmine avec le dernier chapitre de la thèse donnant des résultats partiels concernant la généralisation de la récurrence topologique de Eynard et Orantin à cette famille de modèles de tenseurs.

Title: Random Tensor Models: Combinatorics, Geometry, Quantum Gravity and Integrability.

Abstract: In this thesis manuscript we explore different facets of random tensor models. These models have been introduced to mimic the incredible successes of random matrix models in physics, mathematics and combinatorics. After giving a very short introduction to few aspects of random matrix models and recalling a physical motivation called Group Field Theory, we start exploring the world of random tensor models and its relation to geometry, quantum gravity and combinatorics. We first define these models in a natural way and discuss their geometry and combinatorics. After these first explorations we start generalizing random matrix methods to random tensors in order to describes the mathematical and physical properties of random tensor models, at least in some specific cases.